UMI University Microfilms International

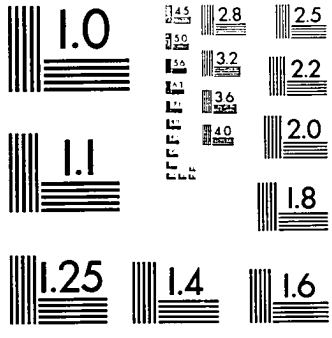

MICROCOPY RESOLUTION TEST CHART
NATIONAL BUREAU OF STANDARDS
STANDARD REFERENCE MATERIAL 1010a
(ANSI and ISO TEST CHART No. 2)

University Microfilms Inc.
300 N. Zeeb Road, Ann Arbor, MI 48106

INFORMATION TO USERS

This reproduction was made from a copy of a manuscript sent to us for publication and microfilming. While the most advanced technology has been used to photograph and reproduce this manuscript, the quality of the reproduction is heavily dependent upon the quality of the material submitted. Pages in any manuscript may have indistinct print. In all cases the best available copy has been filmed.

The following explanation of techniques is provided to help clarify notations which may appear on this reproduction.

1. Manuscripts may not always be complete. When it is not possible to obtain missing pages, a note appears to indicate this.

2. When copyrighted materials are removed from the manuscript, a note appears to indicate this.

3. Oversize materials (maps, drawings, and charts) are photographed by sectioning the original, beginning at the upper left hand corner and continuing from left to right in equal sections with small overlaps. Each oversize page is also filmed as one exposure and is available, for an additional charge, as a standard 35mm slide or in black and white paper format.*

4. Most photographs reproduce acceptably on positive microfilm or microfiche but lack clarity on xerographic copies made from the microfilm. For an additional charge, all photographs are available in black and white standard 35mm slide format.*

***For more information about black and white slides or enlarged paper reproductions, please contact the Dissertations Customer Services Department.**

UMI University Microfilms International

8603516

Nguyen, Nhung Tuyet

ELECTROCHEMICAL AND ENZYMATIC OXIDATION OF TRYPTOPHAN AND 7-METHYLURIC ACID AND SPECTROELECTROCHEMICAL SEARCH FOR A TERTIARY ALCOHOL INTERMEDIATE IN THE ELECTROCHEMICAL OXIDATION OF URIC ACID

The University of Oklahoma PH.D. 1985

University
Microfilms
International 300 N. Zeeb Road, Ann Arbor, MI 48106

THE UNIVERSITY OF OKLAHOMA

GRADUATE COLLEGE

ELECTROCHEMICAL AND ENZYMATIC OXIDATION OF TRYPTOPHAN AND 7-METHYLURIC ACID

AND

SPECTROELECTROCHEMICAL SEARCH FOR A TERTIARY ALCOHOL INTERMEDIATE IN THE ELECTROCHEMICAL OXIDATION OF URIC ACID

A DISSERTATION

SUBMITTED TO THE GRADUATE FACULTY

in partial fulfillment of the requirements for the degree of

DOCTOR OF PHILOSOPHY

BY

NHUNG TUYET NGUYEN

Norman, Oklahoma

1985

ELECTROCHEMICAL AND ENZYMATIC OXIDATION OF TRYPTOPHAN AND 7-METHYLURIC ACID

AND

SPECTROELECTROCHEMICAL SEARCH FOR A TERTIARY ALCOHOL INTERMEDIATE IN THE ELECTROCHEMICAL OXIDATION OF URIC ACID

APPROVED BY

DISSERTATION COMMITTEE

To my parents, Mr. and Mrs. Sau Van Nguyen.

ACKNOWLEDGEMENTS

I would like to express my gratitude to Dr. Glenn Dryhurst for his guidance and financial support in the form of research assistantships during the course of study.

Special thanks go to Dr. C. LeRoy Blank for his encouragement and support and for many helpful discussions.

Financial assistance from the University of Oklahoma Chemistry Department in the form of teaching assistantships is greatly acknowledged. Special thanks must go to Graduate and Professional Opportunities Program (G*POP) for financial support in the form of a three year fellowship and in the preparation of this manuscript.

My appreciation especially goes out to Deniz Ege for her friendship and patience in helping me during my early electrochemistry days. Thanks also go out for the friendship I found among the postdoc's and graduate students in Dr. Dryhurst's lab.

I would like to thank the entire staff of the Chemistry Department for their support, especially the secretaries, Mr. Fred Dillon, Mr. Ron Stermer, Dr. Israel Bonnell and

Dr. Tom Karns.

It is not possible to adequately thank my parents and all of my brothers and sisters for their love, encouragement and support throughout my education.

TABLE OF CONTENTS

CHAPTER

LIST OF TABLES

LIST OF TABLES (continued)

LIST OF ILLUSTRATIONS

LIST OF ILLUSTRATIONS (continued)

LIST OF ILLUSTRATIONS (continued)

LIST OF ILLUSTRATIONS (continued)

LIST OF ILLUSTRATIONS (continued)

LIST OF ILLUSTRATIONS (continued)

LIST OF ILLUSTRATIONS (continued)

LIST OF ILLUSTRATIONS (continued)

LIST OF ILLUSTRATIONS (continued)

ELECTROCHEMICAL AND ENZYMATIC OXIDATION OF TRYPTOPHAN AND 7-METHYLURIC ACID

AND

SPECTROELECTROCHEMICAL SEARCH FOR A TERTIARY ALCOHOL INTERMEDIATE IN THE ELECTROCHEMICAL OXIDATION OF URIC ACID

PART I

ELECTROCHEMICAL AND ENZYMATIC OXIDATION OF TRYPTOPHAN

CHAPTER 1

INTRODUCTION

Benzopyrrole, commonly known as "indole", is a nitrogen heterocycle in which a benzene ring is fused to the 2- and

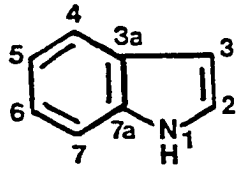

3- positions of the pyrrole ring. The numbering of the atoms in the indole starts with the nitrogen atom next to

the ring junction in the pyrrole ring and continues around the nucleus as shown above[1].

The intensive research on the dye "indigo" in the mid-nineteenth century led to the development of indole chemistry. Indole chemistry continued to progress until newer dyes replaced the indoles in the early twentieth century[1]. After a brief decline, the discovery of alkaloids (containing the indole nucleus), the recognition of tryptophan as an essential amino acid[2], and indole-3-acetic acid as the plant growth hormone[3] in the 1930's increased the importance of indole chemistry. Since then it has become an intriguing research area for chemists and biochemists. In more recent years indoles have achieved increased significance in medicinal chemistry. Serotonin (5-hydroxytryptamine) has been identified as an important metabolite in brain chemistry. Several indoles such as 5,6-dihydroxytryptamine, 5,7-dihydroxytryptamine have been found to be neurotoxins[4-10]. Several important pigments such as melamine[11] and adrenochromes[12] are indole derivatives. Indole derivatives are found in many natural products. Indole itself has been obtained from many naturally occurring materials by decomposing its derivatives[13]. Indole has been found in the jasmines[14], certain citrus plants[15], in orange blossoms[16], in the wood of Celtis reticulosa[17], in coal tar[18], and in molasses tar[19].

Indoles are nitrogen heterocyclic compounds having 10

delocalized (π) electrons. These compounds are good candidates for electrochemical study and electron transfer reactions because of the presence of the delocalized (π) electrons. Electrochemical studies can be used to determine the number of electrons involved in the electron transfer step, to detect intermediates formed during or after the electron transfer reaction, kinetic data for the formation and the decay of the intermediates and much more useful information[20,21].

A number of indole compounds possess fundamental biological importance in both the animal and plant kingdoms. Much of the chemistry of indoles in biological system involves rather complex oxidation reactions. Tryptophan, a naturally occurring and biologically important indole, undergoes a wide range of oxidative biological transformations. In general, these reactions are not well understood in terms of mechanisms or even the products formed.

Tryptophan (TPP) was first detected in a protein and named in 1890[22]; however, it was first isolated in 1901[23]. L-Tryptophan is one of the essential amino acids[24], and normal growth is impossible on diets deficient in it. Nevertheless, it may be replaced by its D-isomer, as well as a number of derivatives and related products[25].

Hydroxylation of tryptophan followed by decarboxylation gives serotonin (5-hydroxytryptamine). Defects in trypto-

phan metabolism and the resulting disruption in serotonin levels might be the cause of certain mental disorders[26].

The metabolism of tryptophan has been studied quite extensively[27-30] and a number of generalized schemes for the metabolic interconversions of tryptophan and related substances have been proposed by Mason[31].

In 1936, Kotake and Masayama described the conversion of L-TPP to L-kynurenine *in vitro* by crude extracts of rabbit liver and named the enzyme involved in the cleavage of the pyrrole ring of TPP as "TPP pyrrolase"[32].

According to Knox and coworkers, two enzymes are involved in the oxidation of L-TPP to L-kynurenine[33]. The first, L-tryptophan pyrrolase, also known as L-tryptophan oxygenase or tryptophan-2,3-dioxygenase, catalyzes the conversion of L-TPP to formylkynurenine and the second enzyme catalyzes the hydrolysis of the latter to L-kynurenine and formic acid (Fig. 1). The kynurenine pathway[32-35] represents the first step in a biosynthetic route to nicotinic acid and hence the pyridine nucleotides[36-39]. Much work has been carried out to identify the possible chemical intermediates in the conversion of TPP to formylkynurenine[40,41].

Kotake and coworkers[42] originally suggested that oxindolylalanine (2, Fig.2) is the first chemically distinct indole intermediate formed upon oxidation of L-tryptophan with TPP-2,3-dioxygenase and O_2. According to Julian *et*

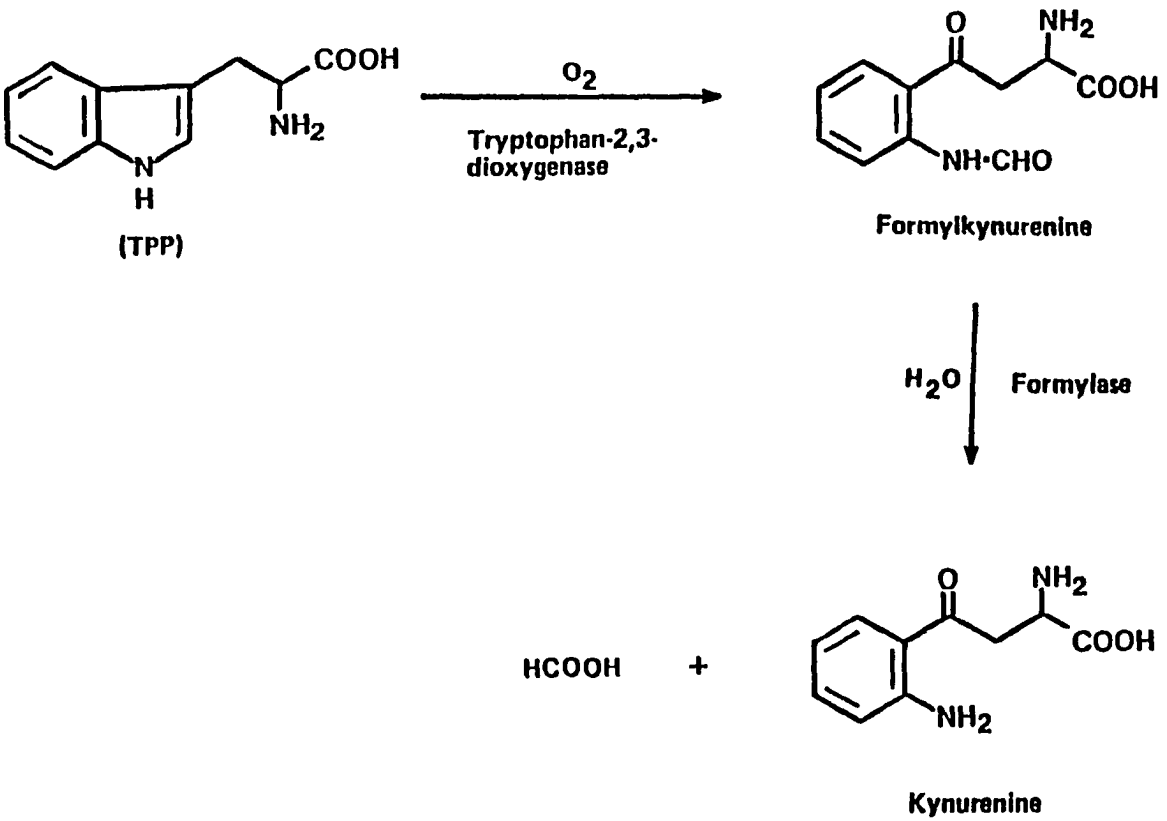

Fig. 1 Outline of the enzymatic conversion of tryptophan (TPP) to kynurenine.

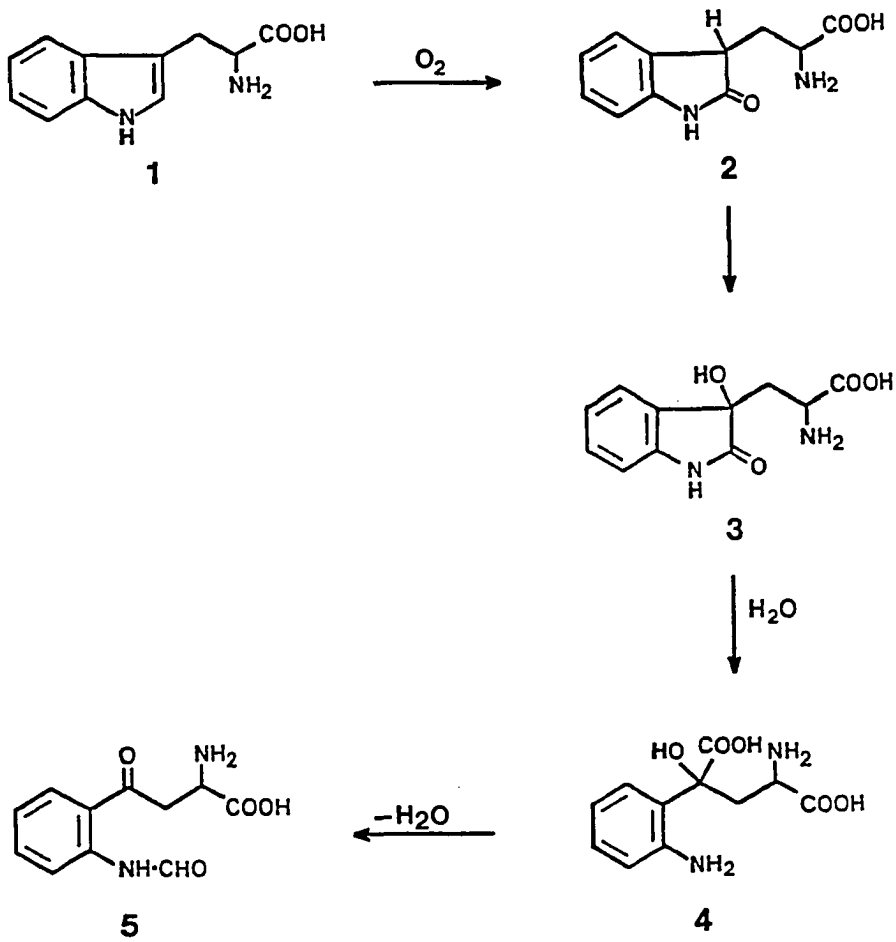

Fig. 2 Reaction scheme of the enzymatic conversion of tryptophan to formylkynurenine proposed by Julian *et al.*[41]

al.[41], the reaction could proceed via dioxindolylalanine (3, Fig. 2). Then, a hydrolyzing enzyme might convert dioxindolylalanine into the hydroxycarboxylic acid (4, Fig. 2) which would yield formylkynurenine (5, Fig.2) by losing water. However, oxindolylalanine is shown to be an unlikely intermediate between TPP and formylkynurenine because it is metabolized differently than TPP[43-45].

Knox and Mehler[33,46] have suggested that peroxide could add to L-TPP to give 2,3-dihydro-2,3-dihydroxytryptophan (6) which upon dehydrogenation and ring opening could give formylkynurenine (Fig. 3). However, there has been no direct

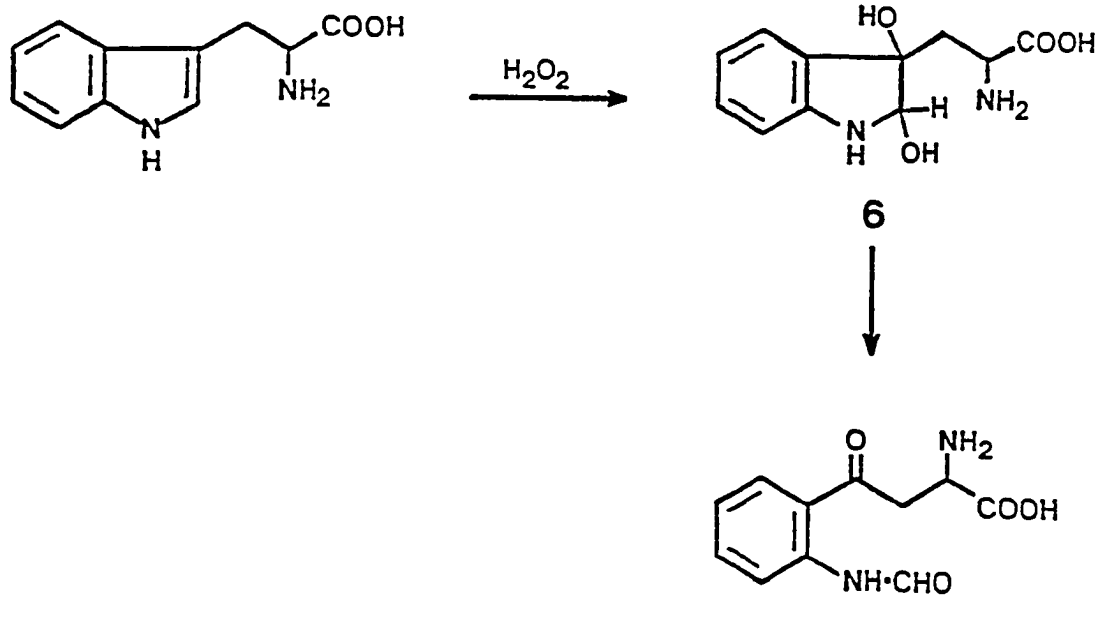

Fig. 3 Reaction scheme of the conversion of tryptophan to formylkynurenine proposed by Knox and Mehler[33,46].

evidence of this scheme. A hydroperoxide (7) intermediate has been suggested by Witkop and coworkers[47-51].

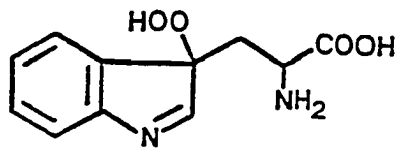

7

Nakagawa et al.[52-57] have proposed that the dye-sensitized photooxidation of TPP involves initial formation of a 3-hydroperoxy (II) intermediate which undergoes facile intramolecular addition to form 3a-hydroperoxyhexahydro-pyrroleindole (III) which rearranges to formylkynurenine (IV) on warming (Fig. 4). They believe that this scheme (Fig. 4) establishes and characterizes intermediates which provide a rational pathway for the TPP-2,3-dioxygenase catalyzed oxi-

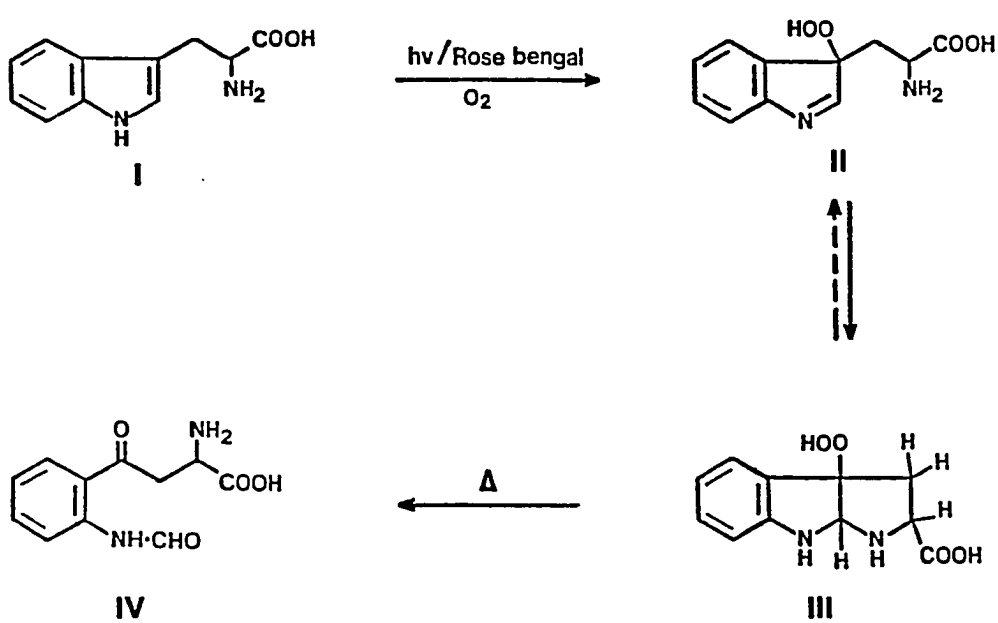

Fig. 4 Reaction scheme proposed for the rose bengal-sensitized photooxidation of tryptophan to formylkynurenine.

dation of TPP[56]. However, this has not been definitively shown to be followed in the biochemical process.

Apart from kynurenine and its precursor formylkynurenine, there are a large number of other known or suspected oxidative metabolites of TPP[28,30,31,58,59]. In addition, new enzymes continue to be discovered which catalyze other oxidation reactions of TPP. For example, a group of pyrrolooxygenases from wheat germ and rat liver oxidize the pyrrole ring of D- and L-TPP and other indoles giving kynurenine, formylkynurenine and oxindolylalanine as products[60]. Takai et al.[61,62] recently found an enzyme that catalyzes the oxidation of the side chain of tryptophan and other indole derivatives. In the case of L-TPP the primary product of the reaction appeared to be 3-indolylglyoxal (8).

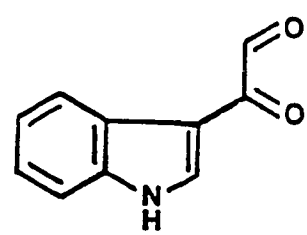

8

Similarly, Noda et al.[63] have isolated a crystalline hemeprotein from Pseudomonas which catalyzes the oxidation of the side chain of TPP containing peptides forming an α,β-dehydrotryptophan product. The mechanisms of these various oxidative processes are not known in any detail.

Chemical oxidations of TPP have been studied quite

extensively[1,13,64]. However, because of the bewildering range of oxidants and experimental conditions used it is very difficult to obtain fundamental information about the redox chemistry of TPP or real insights into biological oxidation reactions.

Very little information on the electrochemistry of TPP is presented in the chemical literature. Takayama[65] found that tryptophan could be electrooxidized giving only ammonia and CO_2 as identified products. However, these experiments were carried out under essentially uncontrolled conditions. Recently, Brabec and Mornstein [66] have shown that TPP is electrochemically oxidized at a graphite electrode. A 2e electrooxidation reaction was proposed giving an unstable and unidentified intermediate which reacted to give unidentified products. Malfoy and Reynaud[67] have also reported that TPP is electrochemically oxidized at gold and carbon electrodes in a 2e reaction to give oxindolylalanine. However, no report is presented either on the mechanistic details or the intermediates.

The specific aim and scope of this work involved the use of electrochemical techniques such as linear sweep voltammetry (LSV), cyclic voltammetry (CV), controlled potential coulometry and thin-layer spectroelectrochemistry to investigate the oxidation chemistry of tryptophan. For comparative purposes various enzymatic oxidation reactions were also studied. The major products obtained from electroche-

mical and enzymatic oxidation were separated by liquid chromatography (LC) and high pressure liquid chromatography (HPLC). Subsequently, the separated products were characterized by melting point, electronic spectra, mass spectra, gas chromatography (GC), and gas chromatography-mass spectrometry (GC-MS). A systematic scheme for understanding the electrooxidation chemistry of TPP has been developed which helps to understand the biochemical (enzymatic) oxidation of this compound.

CHAPTER 2

EXPERIMENTAL

2. A. CHEMICALS

L-tryptophan, L-kynurenine, and mercaptoethanol were obtained from Sigma (St. Louis, MO) and were used without further purification. Three isoperoxidases isolated from horseradish (EC 1.11.1.7) were used: peroxidase type VI (R_Z ~3.0, probably consisting of two basic isoenzymes), peroxidase type VIII (R_Z ~ 3.0, acidic isoenzyme), and peroxidase type IX (R_Z ~ 3.2, basic isoenzyme). Chloroperoxidase (EC 1.11.1.10) isolated from Caldariomyces fumago was also used. All enzymes were obtained from Sigma (St. Louis, MO). Enzymes were stored at -5°C when not in use. N-Formyl-L-kynurenine (ring monoformyl) was obtained from Calbiochem-Behring (La Jolla, CA). N,O-Bis(Trimethylsilyl) acetamide (BSA), N,O-Bis(Trimethylsilyl) trifluoroacetamide (BSTFA), and N-Methyl-N-(tertbutyldimethylsilyl) trifluoroacetamide (MTBSTFA) were obtained from Pierce Chemical Co., (Rockford, IL). Deuterated BSA (BSA-d_9) was obtained from Merck (St. Louis, MO). Silylation grade pyridine, N,N-

dimethylformamide (DMF) and acetonitrile were obtained from Supelco (Houston, TX).

Phosphate buffers were prepared as described by Christian and Purdy[68] and had an ionic strength of 0.5 M, unless otherwise specified.

Synthesis:

Tricyclic pyrroloindole (2-carboxy-3a-hydroxy-1,2,3,3a,8,8a-hexahydropyrrolo-(2,3b)-indole) was synthesized by the method of Savige[69], with slight modification. Tryptophan (0.05 mol) was mixed with 2.75 M peroxyacetic acid[69,70] (0.05 mol) and kept at 0-5°C. After ca. 18 hrs, the resulting deep yellow solution was freeze-dried. The resulting solid was redissolved in water (160 ml). 10 ml aliquots were injected onto a column of Sephadex G-10 (90 x 2.5 cm) using water as the eluent (34 mlh^{-1}). The eluent was monitored at 290 nm and 4 ml fractions were collected using a fraction collector. The fractions which exhibited U. V. absorption bands at λ_{max} = 203, 235, and 290 nm were collected together and freeze-dried. The crude product was further purified by reinjecting onto the same column 3 to 4 additional times. The total yield of tricyclic pyrroloindole was 15% (0.0075 mol).

Oxindolylalanine was synthesized by the method of Savige and Fontana[71]. Dioxindolylalanine was synthesized as described by Savige[69].

2. B. APPARATUS

Linear sweep voltammetry and cyclic voltammetry were performed with a Polarographic Analyzer having a conventional operational amplifier design[72,73] and a Princeton Applied Research Corporation Model 175 Universal Programmer. Voltammograms were recorded on a Hewlett-Packard Model 7001A or a Houston Instruments Model 2000 X-Y recorder. Voltammograms at fast sweep rates ($>500 mVs^{-1}$) were recorded on a Tektronix Model 5031 Dual Beam Storage Oscilloscope, equipped with a Tektronix Model C-70 Camera or Tektronix Model 5111 Dual Beam Storage Oscilloscope equipped with a Tektronix Model C-5B Camera.

Voltammetry was carried out in a single compartment cell, which had a capacity of 5ml, at room temperature ($25^{o} \pm 1^{o}C$). A platinum (Pt) wire sealed at the bottom of the cell served as the counter electrode and a saturated calomel electrode (SCE) served as the reference electrode. A pyrolytic graphite electrode or a glassy carbon electrode served as the working electrode. Electrical contact with the reference electrode was made through a double salt bridge with a Luggin capillary. All the potentials reported in this thesis are referred to the SCE at $25^{o}C$.

Pyrolytic graphite electrodes (PGE) were made by sealing a small rod of pyrolytic graphite (Pfizer minerals, Pigments,and Metals Division, Easton, PA) ca. 2mm X 2mm X

10mm in a glass tube with Hysol Epoxi-Patch 1C White (Hysol Division, The Dexter Corp., Olean, N. Y.). The PGE was resurfaced before running each voltammogram by grinding on a 600-grit silicon carbide disc (Fisher Scientific Company, Pittsburgh, PA) mounted on a metallographic polishing wheel, washed with double-distilled water to remove the graphite powder from the surface, dried by wiping the body of the electrode and gently touching the surface with a soft paper tissue.

The glassy carbon electrode (GCE, Princeton Applied Research Corp., Princeton, N. J.) having a surface area of 0.33 cm^2 was polished on 0.5 um alumina (Buehler LTD, Evanston, IL.) impregnated in a piece of soft felt, rinsed thoroughly with double-distilled water and dried with a soft paper tissue before running each voltammogram.

Controlled potential electrolyses were carried out either in a thin-layer reticulated vitreous carbon (RVC) cell (*vide infra*), or in a three compartment cell with a working compartment capacity of *ca.* 25 ml or 100 ml. The compartments of the electrochemical cell were separated by a Nafion membrane (Du Pont) or an agar salt bridge which was prepared by dissolving 4g of agar in 90 ml of phosphate buffer pH 7.0 (u = 0.5M) or dilute HCl pH 2.4 with heating[74]. The counter and reference electrode compartments contained the same buffer solution as the working compartment. A Pt gauze or Pt foil served as a counter elec-

trode and a SCE (Fisher Scientific Co., Pittsburgh, PA.) served as the reference electrode. Several plates of pyrolytic graphite having a total surface area of ca. 60 cm^2 or 360 cm^2 served as the working electrode. The solutions were stirred magnetically with a teflon covered magnetic stirrer and bubbled with nitrogen during the electrolysis. The potential was controlled by a potentiostat (Princeton Applied Research Corporation Model 173 or a Wenking Model LT 73). A coulometer (Koslow Scientific Model 541) was used to integrate the current during electrolyses in both the bulk electrolysis cell and the thin-layer cell.

The U.V. spectra were recorded on a Hitachi 100-80 computerized spectrophotometer. All pH measurements were carried out with an Orion Model 501 digital pH meter using the Polymer Body Liquid-Filled combination Electrode having an Ag/AgCl reference electrode (Fisher Scientific Co., Pittsburgh, PA).

Optically transparent thin-layer electrochemical cells were constructed similar to the design described by Norvell and Mamantov[79] except that optical quality quartz plates 2 in X 1 in X 1/16 in (Esco Optics Products, Oak Ridge, N. J.) were used. A thin slice of reticulated vitreous carbon (RVC) (100 ppi porosity 12 mm X 40 mm Fluorocarbon Co., Anaheim, CA) with the thickness of 0.1 - 0.5 mm was sandwiched between the slides and the edges of the slides were

sealed with Hysol Epoxi-Patch 1C White (Hysol Division , The Dexter Corp., Olean, N. Y.). Openings were left at the bottom and one spot at the top of the cell for cleaning and filling with the test solution. Thin-layer spectroelectrochemical studies were carried out using a Rapid Scanning Spectrometer (Harrick Scientific Co., Ossining, N. Y.) interfaced to a Cromemco Systems Three Computer or a CompuPro System 8/16.

A Hewlett-Packard Model 5880 gas chromatograph with a flame ionization detector (FID) (Hewlett-Packard Co , Avondale, PA.) was used for gas chromatographic (GC) studies. A Hewlett-Packard Model 5985B GC-MS was used for gas chromatography-mass spectrometry (GC-MS) studies. An electron beam voltage of 70 eV was used to obtain electron impact (EI) mass spectra and methane was used as a reactant gas (2×10^{-4} torr) in the source chamber to obtain chemical ionization (CI) mass spectra. An electron beam energy of 150 eV was used for all CI-MS studies.

Fast atom bombardment (FAB)-MS was carried out with a VG Instruments Model ZAB-SE spectrometer.

A glass column (1.8 m x 2 mm i.d.) packed with 3% SE - 30 on Chromasorb W (Supelco, Inc. , Bellefonte, PA.) was used for all GC and GC-MS separations. The carrier gas was helium at the flow rate of 30 $ml min^{-1}$.

Liquid chromatography was carried out using a Pharmacia

Model SR 25/100 (2.5 cm X 100 cm) column with 90 cm of Sephadex G-10 gel permeation resin. Water was used as the eluent. A Holochrome variable wavelength detector (Gilson Medical Electronics, Inc., Middleton, WI.) was used. A Houston Instruments Omniscribe Stripchart recorder was used to record the detector output. An ISCO Model 328 fraction collector (Instrumentation Specialties Co., Lincoln, NE.) was used to collect effluent in 4ml fractions.

High Performance Liquid Chromatography (HPLC) was carried out with a Bio-Rad system (Richmond, CA) using a Shodex OH-Pak column (50 x 2 cm) with water as the eluent (3 $mlmin^{-1}$). Water Associates Model 440 Absorbance Detector (Millipore Water Associates, Milford, Mass.) was used. A Houston Instruments Omniscribe Stripchart Recorder was used to record the detector output.

2. C. PROCEDURES

2. C. 1. Procedure for silylation

Silylation was accomplished using ca. 100 ul of silylating reagent and 100 ul of solvent (generally pyridine, acetonitrile or DMF) in a 3 ml reacti-vial. With MTBSTFA, the silylation was carried out at room temperature for ca. 30 minutes or overnight. With BSA or BSTFA the derivatization was carried out overnight at room temperature or at 120°C for ca. 20-30 minutes. The above conditions were

employed in all cases, unless otherwise specified.

For all GC studies, 5 ul aliquots of the cooled, derivatized sample were injected. The GC rentention times (t_R) reported were obtained under the following conditions: initial temperature 100°C for 12 min followed by a linear temperature gradient (6°C per min) to 280°C. The final temperature was held constant for 30 min.

2. C. 2. Procedure for enzymatic oxidation

Stock solutions of type VI, VIII, IX peroxidase (0.4 uM, molecular weight ~ 40,000), H_2O_2 (600 uM) and TPP solution (600 uM) were prepared fresh in an appropriate buffer. Normally, 0.7 ml each of the TPP and peroxidase solutions were mixed in a 1.0 cm quartz spectrophotometer cell. After the addition of 0.7 ml of the H_2O_2 stock solution to the above mixture, the enzymatic oxidation reaction was monitored by repetitively scanning the spectra in the U.V. region (400-190 nm). The reference cell for spectrophotometric studies contained the same amount of buffer, H_2O_2, and enzyme as was in the sample cell except that no TPP was present.

CHAPTER 3

RESULTS AND DISCUSSION

3. A ELECTROCHEMICAL OXIDATION OF TRYPTOPHAN

3.A. 1. Stability of tryptophan

Tryptophan is stable in solution even if it is exposed to air and light at room temperature in the pH range 2.0 to 11.0 for 10 days.

The pK_a values of TPP have been determined[81,82] and are given below. These values refer, respectively, to the α-carboxyl and the α-amino group of the aliphatic side chain and the NH group of the heterocyclic ring.

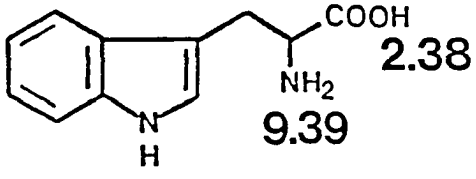

Tryptophan (TPP)

3. A. 2. Linear sweep and Cyclic Voltammetry

pH study.

A series of linear sweep voltammograms of TPP recorded at a sweep rate of 5 mVs^{-1} between pH 2.0 and 11.0 using a pyrolytic graphite electrode (PGE) is given in Fig. 5. At slow sweep rates ($\leq$ 10 mVs^{-1}) two closely spaced oxidation peaks (I'_a and I_a) are observed. Between pH 3.0 and 7.0 peaks I'_a and I_a are easily distinguishable, but at higher and lower pH values peak I'_a is observed as an indistinct inflection on the rising portion of peak I_a. An indistinct inflection (peak II_a) is observed at potentials more positive than peak I_a in the pH range 2.0-9.0. Because of its indistinct shape, accurate measurement of E_p for peak II_a was not possible.

The variation of E_p with pH for oxidation peaks I'_a and I_a of TPP (1 m<u>M</u>), measured at a sweep rate of 5 mVs^{-1} are given in Eqns. (1) and (2) and in Fig. 6.

Peak I'_a: $E_p(\text{pH } 2.0 - 11.0) = [0.948 - 0.045\ \text{pH}]$ V (1)

Peak I_a : $E_p(\text{pH } 2.0 - 11.0) = [1.018 - 0.043\ \text{pH}]$ V (2)

At sweep rates > 10 mVs^{-1} peak I'_a and I_a merge to give a single peak which will be referred to as peak I_a (Fig. 7). Equation (3) and Fig. 8 illustrate the pH dependence of E_p for oxidation peak I_a at a sweep rate of 200 mVs^{-1}.

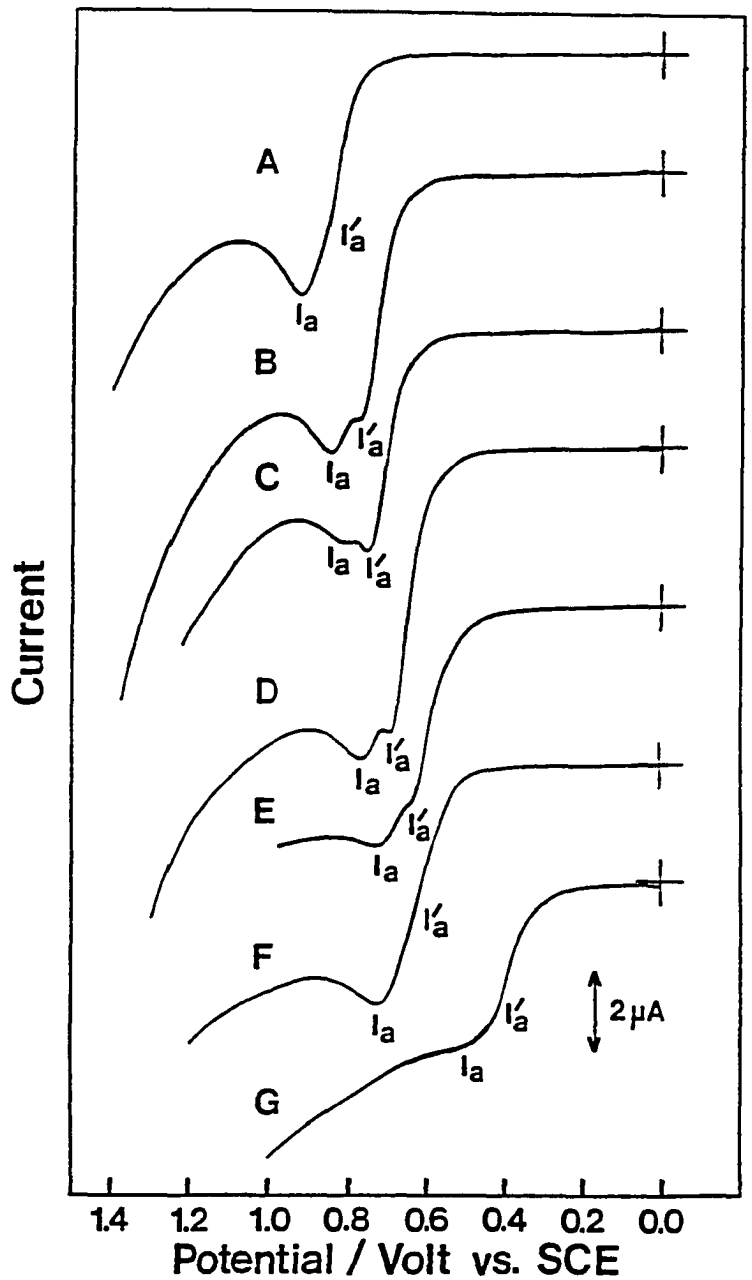

Fig. 5 Linear sweep voltammograms obtained at the PGE of 1 mM tryptophan in phosphate buffers (u = 0.5 M) at pH (A) 2.28, (B) 3.30, (C) 4.36, (D) 5.72, (E) 6.92, (F) 7.30 and (G) 9.82. Sweep rate: $5 mV s^{-1}$.

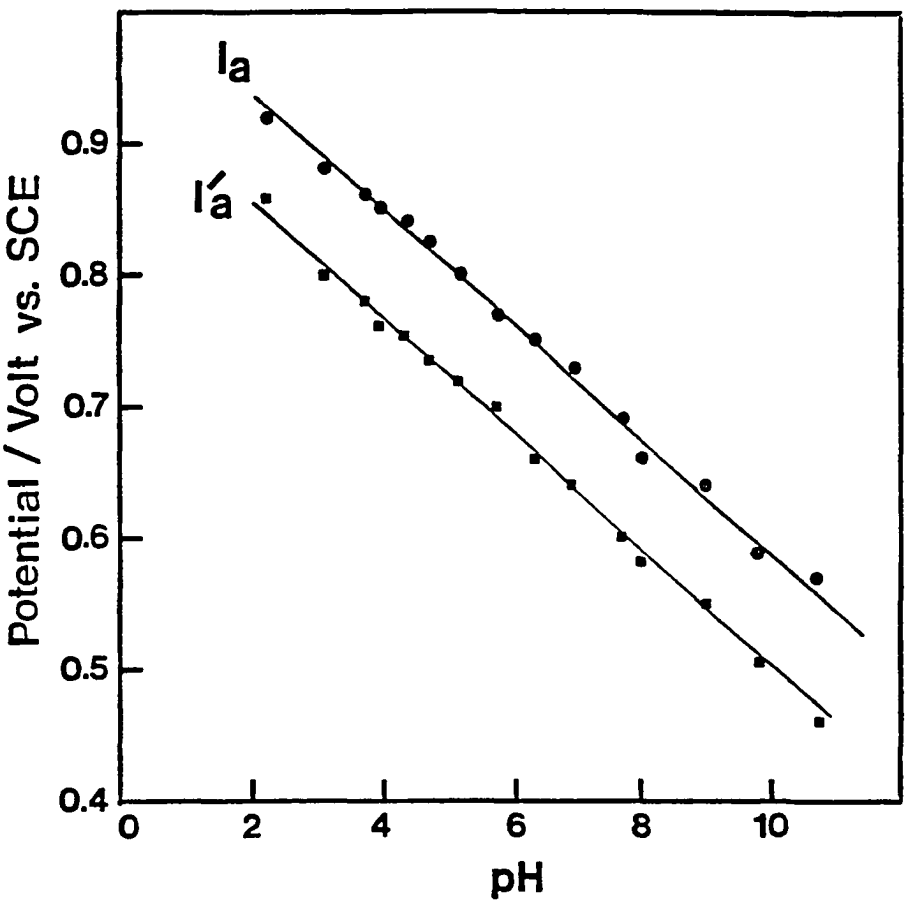

Fig. 6 The peak potential (E_p) vs. pH curve obtained at the PGE of 1 mM TPP in phosphate buffers (u = 0.5M) at a sweep rate of 5 mVs^{-1} for oxidation peak I_a and I'_a.

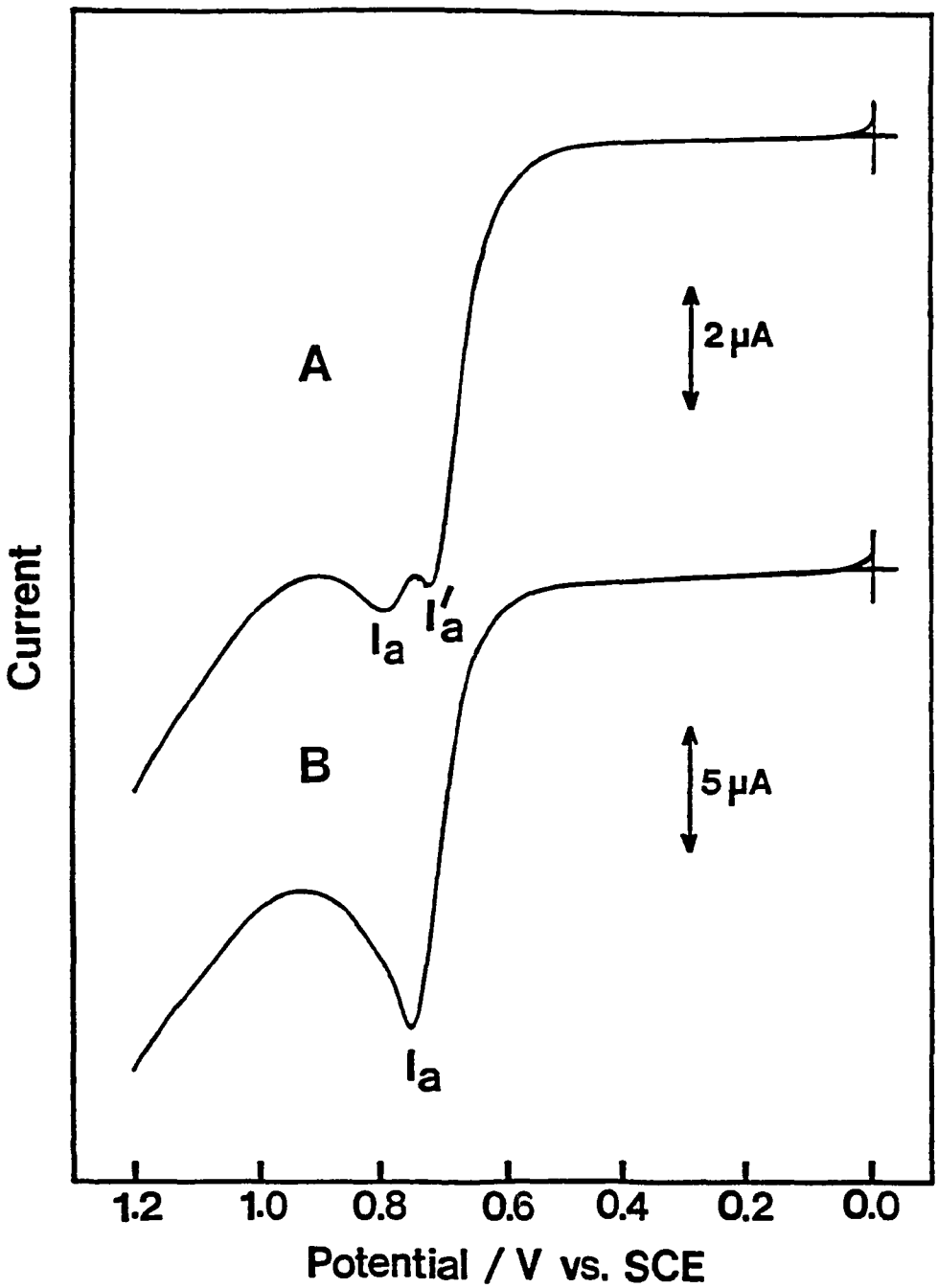

Fig. 7 Linear sweep voltammograms obtained at the PGE of 1mM tryptophan in phosphate buffer pH 5.30 (u = 0.5). Sweep rate: (A) 5 mVs^{-1}; (B) 20 mVs^{-1}.

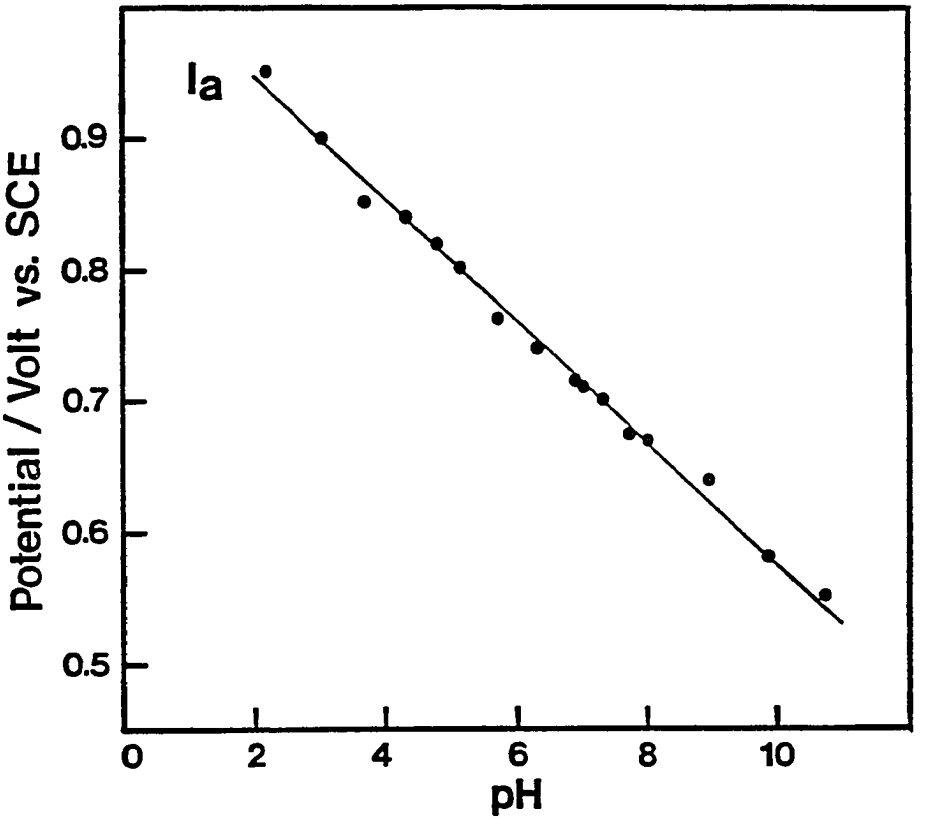

Fig. 8 The peak potential (E_p) vs. pH curve obtained at the PGE of 1 mM TPP in phosphate buffers (u = 0.5) at a sweep rate of 200 mVs^{-1} for oxidation peak I_a.

Peak I_a : E_p (pH 2.0 - 11.0) = [1.04 - 0.047 pH] V (3)

The E_p *vs.* pH plots shown in Fig. 6 and Fig. 8 show no break points in pH regions corresponding to the pK_a values reported for TPP (2.38, 6.23 and 9.39)[81,82]. This indicates that the electrochemical oxidation of TPP does not change drastically in the pH range 2.0-11.0.

For a reversible redox reaction the slope of the E_p *vs.* pH plot at 25°C can be calculated using Eqn. (4)[83], where p is the number of protons and n is the number of electrons involved in the electrode process. In a reversible or a quasi-reversible reaction, if the slope of the E_p

$$\frac{dE_p}{dpH} = \frac{-\ 0.059\ p}{n} \qquad (4)$$

vs. pH plot is *ca.* 59 mV then the number of electrons and protons involved in the electrode process is equal.

For an irreversible redox reaction Eqn.(4) becomes more complex and the slope is defined by Eqn. (5)[83], where α is the electron transfer coefficient and n_a is

$$\frac{dE_p}{dpH} = \frac{-\ 0.059\ p}{\alpha n_a} \qquad (5)$$

the number of electrons involved in the rate limiting

reaction at the electrode.

At a given pH the E_p and the i_p values for peaks I'_a and I_a are independent of the ionic strength (u) of the phosphate buffer used (u = 0.1-1.0 M). At sweep rates >10 mVs^{-1}, the peak current (i_p) for peak I_a measured at both the PGE and GCE decreases with increasing pH (ca. a 40-50% decrease was observed in the pH range 2.0-11.0). A series of cyclic voltammograms of TPP at a PGE over the pH range 2.0-11.0 is shown in Fig. 9. If the first sweep is directed towards positive potentials, oxidation peak I_a appears and on the reverse sweep at pH < 7.0, three reduction peaks (I_c, II_c, and III_c) appear (Fig. 9A,B). At pH > 7.0 reduction peak III_c disappears (Fig. 9D,E). If the first sweep is initiated at 0.0 V towards negative potentials, TPP shows no voltammetric reduction peaks. Also, reduction peaks I_c and II_c increase in height relative to the oxidation peak I_a with increasing sweep rate. The calculated ratios I_c/I_a and II_c/I_a are given in Table 1. However, at a given sweep rate peak I_c decreases in height relative to peak I_a with increasing pH whereas peak II_c increases in height (Fig. 9). On the second cycle towards positive potentials three new oxidation peaks (II'_a, III'_a, and IV'_a, Fig. 9) appear. Switching potential experiments reveal that it is necessary to sweep only through reduction peak I_c in order to observe these three new oxidation peaks (Fig. 9C). When the potential sweep is reversed immediately after scan-

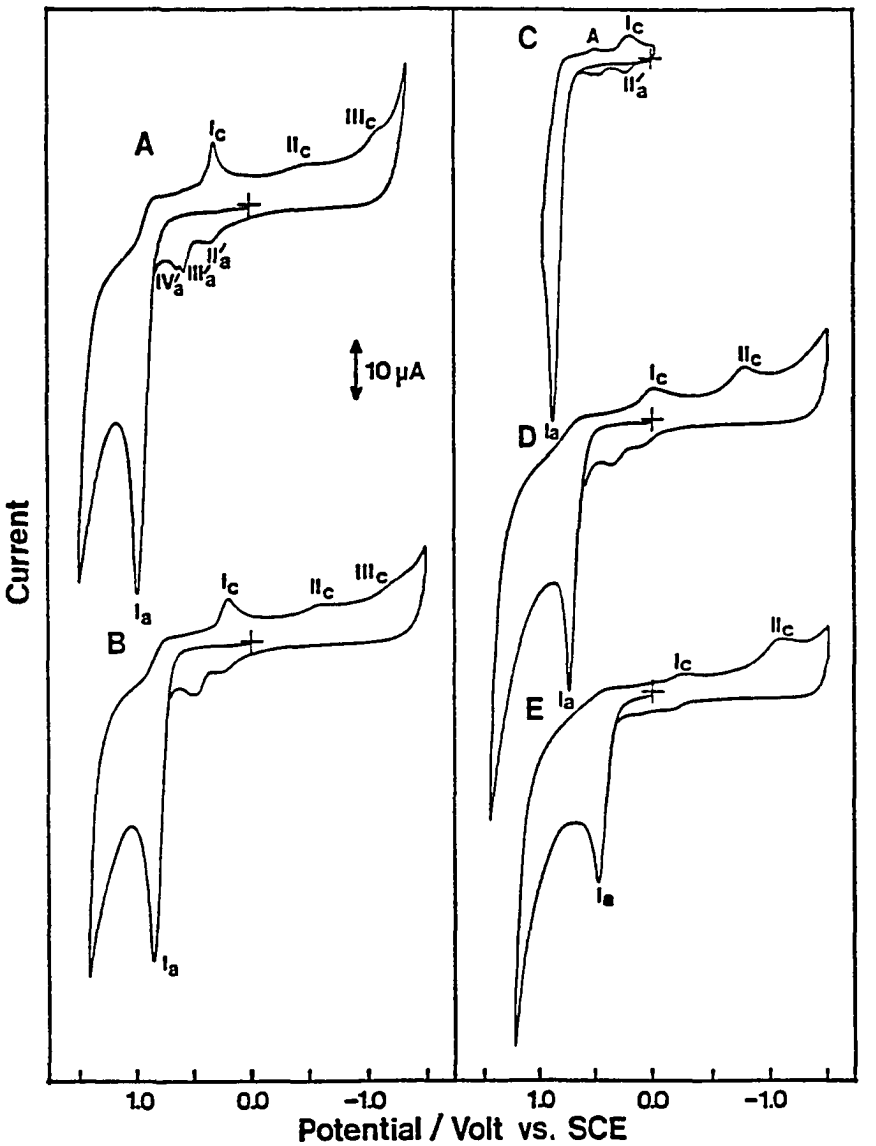

Fig. 9 Cyclic voltammograms at the PGE of 1 mM tryptophan in phosphate buffers (u = 0.5) at pH (A) 2.28, (B,C) 4.36, (D) 7.00 and (E) 10.55. Sweep rate: 200 mVs^{-1}.

Table 1

The current ratios, I_c/I_a and II_c/I_a, of 1 m$\underline{M}$ tryptophan as a function of sweep rate in pH 4.4 phosphate buffer (u = 0.5 M) at the PGE electrode (A = 2 mm^2).

v (Vs^{-1})	i_p (uA)				
	I_c	II_c	I_a	I_c/I_a	II_c/I_a
0.2	8.0	2.0	46.0	0.17	0.04
1	28.6	12.5	131.1	0.21	0.09
2	71.4	28.6	285.7	0.25	0.10
5	100.0	51.4	342.9	0.29	0.15
10	214.3	107.1	500.0	0.43	0.21
20	375.0	178.6	714.3	0.52	0.25

ning through oxidation peak I_a a new, small reduction peak A appears at 0.5 V, which is shown in Fig. 9C. Peaks I_c and II'_a seem to form a quasi-reversible couple. E_p values for all of the oxidation and reduction peaks observed in cyclic voltammetry are dependent on pH and are shown in Fig.9. As noted earlier, the height of reduction peak II_c increases with increasing pH, relative to that of peak I_a, but all other peaks (I_c, II_c, II'_a, III'_a, and IV'_a) become smaller. With increasing sweep rate peaks A, I_c, II_c, III_c, II'_a, III'_a, and IV'_a increase in height relative to oxidation peak I_a. Such cyclic voltammetric behavior indicates that the oxidation peak I_a of TPP leads to formation of reducible intermediates or products responsible for peaks I_c, II_c, and III_c. One of the intermediates, responsible for peak I_c, is reduced and may give product(s) which are subsequently oxidized via peak II'_a, III'_a, and IV'_a during the second cycle towards the positive potentials.

Cyclic voltammetry of TPP at slow and fast sweep rates (5 mVs^{-1} up to $100Vs^{-1}$) does not show a reversible reduction peak coupled to oxidation peak I_a. Furthermore, peak I_a potential is shifted in positive direction by ca. 44 mV at pH 4.36 for each tenfold increase in sweep rate. This value is approximately that expected for irreversible oxidation reaction ($30\ mV/\alpha n_a = 40$ mV at 25^oC)[84]. Thus, it must be concluded that the oxidation reaction shown by peak I_a is electrochemically irreversible.

Concentration study

At the pyrolytic graphite electrode (PGE), a peak current (i_p) vs. concentration studies for the oxidation peak I_a of TPP was carried out at a sweep rate of 5 mVs^{-1} between pH 3.0-7.0. This pH range was chosen because oxidation peak I'_a and I_a are easily distinguishable. This study can be used to determine the type of process controlling the electrode reaction. If the electrode process is diffusion controlled then the peak current, i_p, is directly proportional to the bulk concentration of the electroactive species in the solution. However, if the electroactive compound is adsorbed on the electrode surface then the peak current will increase in a linear fashion only at low concentration.

At low concentrations, oxidation peak I'_a is the dominant peak (Fig. 10A). However, with increasing concentrations of TPP peak current for oxidation peak I'_a reaches a limiting height (Fig. 10A) and peak I_a becomes the dominant peak (Fig. 10E). Such behavior indicates that peak I'_a is probably an adsorption prepeak, i. e., adsorption is due to the electrooxidation product(s)[85]. However, i_p for oxidation peak I_a (the sum of i_p for peaks I'_a and I_a was measured, Fig. 10B) does not show a linear relationship with bulk concentration of TPP but also reaches a limiting value (Fig. 11). This effect is probably due to a product or products of the electrooxidation reaction blocking the electrode surface(see later discussion). Cyclic voltammograms of

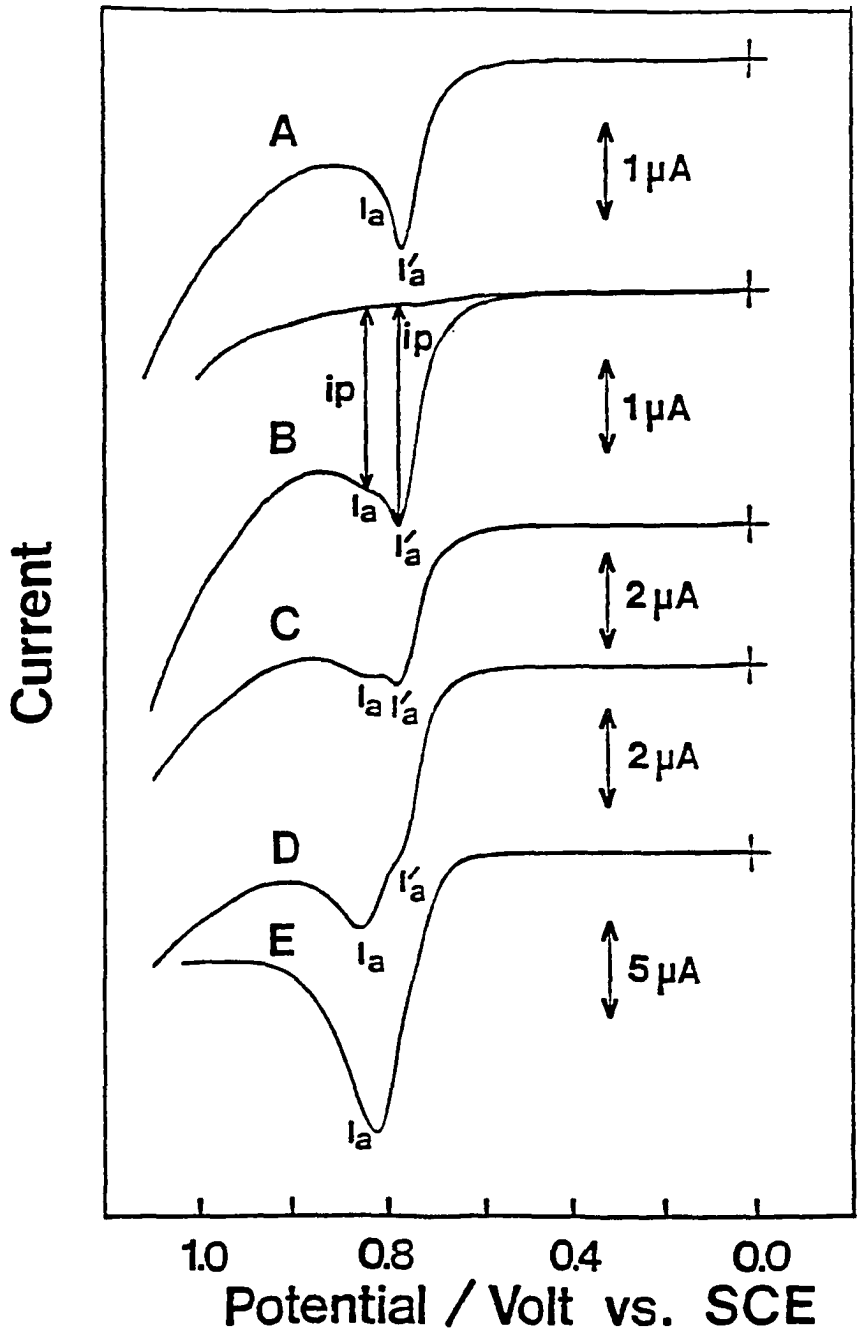

Fig. 10 Linear sweep voltammograms obtained at the PGE of tryptophan in pH 4.39 phosphate buffer (u =0.5). TPP concentrations: (A) 0.125 mM,(B) 0.25 mM, (C) 0.5 mM, (D) 1.0 mM and (E) 7.5 mM. Sweep rate: 5 mVs^{-1}.

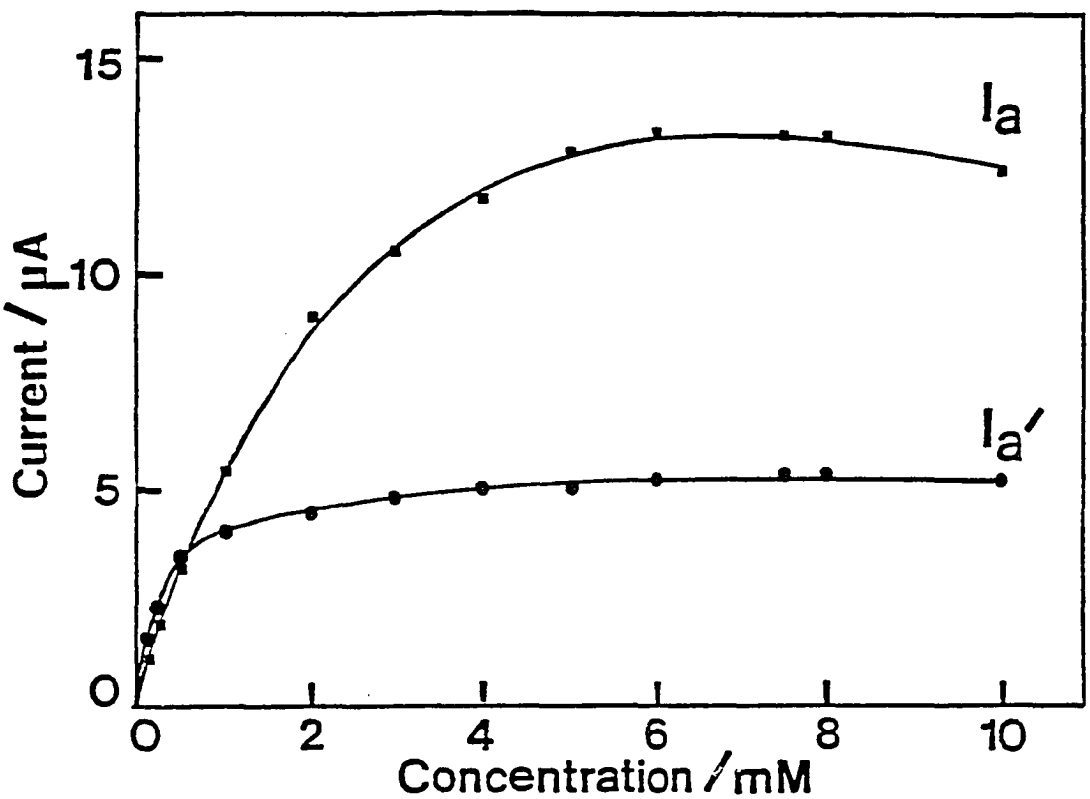

Fig. 11 Peak current (i_p) *vs.* concentration curves for oxidation peaks I'_a and I_a of 1 mM TPP in phosphate buffer pH 4.4 measured at a sweep rate of 5 mVs^{-1}.

TPP at different concentrations and current vs. concentration curves at pH 4.39 are shown in Fig. 10 and Fig. 11, respectively. Similar electrochemical behavior was observed between pH 3.0 and 7.0 where it was possible to obtain approximate i_p values for peak I'_a and I_a.

Sweep rate study

Sweep rate studies can also be used to determine whether an electrooxidation process is diffusion or adsorption controlled. In such a study the experimental parameter i_p is measured as a function of sweep rate. From i_p vs. v data the peak current function, $i_p/C_o\, v^{1/2}A$, is calculated (where i_p is the peak current in uA, C_o is the bulk solution concentration of electroactive species in mole/l, v is the sweep rate in Vs^{-1}, and A is the surface area of the electrode in cm^2). For a diffusion controlled process the peak current function should remain constant as the sweep rate is varied. If the electroactive compound is adsorbed at the electrode surface, then the peak current function increases with increasing sweep rate[85].

It was not possible to study the effect of sweep rate on the relative heights of peaks I'_a and I_a because these peaks merge together at a sweep rate > 10 mV^{-1} (vide supra). However, the experimental peak current function for peak I_a measured at sweep rates between 10 mVs^{-1} and 20 Vs^{-1} increased significantly with increasing sweep rate (Table 2).

Table 2

Change in i_p for peak I_a of 1 m$\underline{M}$ tryptophan as a function of sweep rate in pH 4.4 phosphate buffer at the PGE electrode ($A = 2\ mm^2$).

v (Vs^{-1})	$v^{1/2}$ ($V^{1/2}s^{-1}$)	i_p (uA)	$i_p/ACv^{1/2}$ (uA/mm^2 mmole $V^{1/2}s^{-1/2}$)
0.01	0.1	10	50.0
0.02	0.14	15	53.5
0.05	0.22	30	68.2
0.1	0.32	46	73.0
0.2	0.45	71	79.4
1.0	1.0	210	105.0
2.0	1.4	350	125.0
5.0	2.24	720	160.7
10.0	3.16	1180	186.7
20.0	4.47	1800	201.3

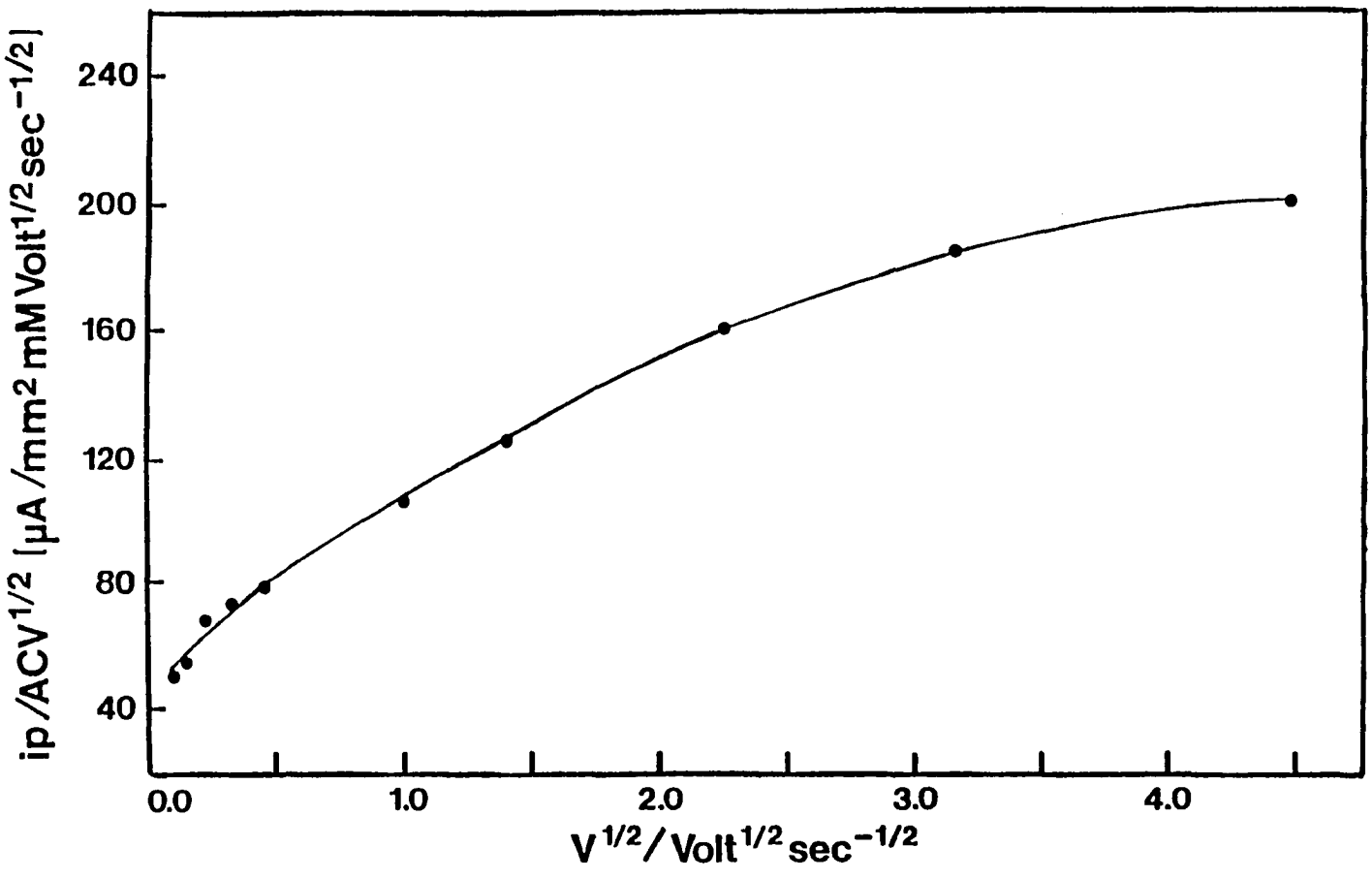

Fig. 12 Peak current function vs. the square root of the sweep rate for the voltammetric oxidation peaks I'_a and I_a of 1 mM TPP in pH 4.36 phosphate buffer ($u \cong 0.5$ M).

Fig. 12 shows that the peak current function for peak I_a increases rapidly with increasing sweep rate at pH 4.36. Similar behavior was also observed in both neutral (pH 7.0) and basic (pH 10.65) solutions. This behavior suggests that TPP is adsorbed at the PGE surface[85].

3. A. 3. Voltammetric n-values.

Attempts to measure reliable values for the number of electrons transferred per molecule of TPP oxidized at voltammetric peak Ia using a PGE were not very successful because of the rather irreproducible surface of this electrode which results in variable i_p values. However, a highly polished GCE gave quite reproducible i_p values ($\pm$ 5%) and data obtained with this electrode were used to calculate the voltammetric n-values using Eqn. (6)[21].

$$n = i_p/2.99 \times 10^5 (\alpha n_a)^{1/2} A C_o D^{1/2} v^{1/2} \qquad (6)$$

where

ip : peak current in A

C_o : initial concentration of electroactive species in the bulk solution in M

A : area of the electrode in cm^2

v : sweep rate of the applied linear voltage in volts sec^{-1}

D : diffusion coefficient of the electroactive species in $cm^2\ sec^{-1}$

n_a : number of electrons involved in the rate determining

step

α: electron transfer coefficient

This equation was used to calculate the voltammetric n-values because TPP is electrochemically oxidized in an irreversible process (vide supra). The diffusion coefficient, D, for TPP was assumed to be 10^{-5} cm^2s^{-1}. Values of αn_a were obtained using Eqn. (7)[21,84,86].

$$\alpha n_a = \frac{0.048\ V}{E_p - E_{p/2}} \qquad (7)$$

Voltammograms of TPP were recorded in phosphate buffers (u = 0.5) at pH 3.92, 6.92 and 10.55 at sweep rates between 5 mVs^{-1} and 20 Vs^{-1} with TPP concentrations of 0.55 mM and 1.10mM (Table 3). At pH 3.92 the experimental αn_a value was 0.65 ± 0.15 (mean ± maximum deviation) and the experimental n value (n_{exp}) was 2.2 ± 0.49. At pH 6.92, αn_a = 0.59 ± 0.12 ; n_{exp} = 1.89 ± 0.13. At pH 10.55, αn_a = 0.30 ± 0.13 ; n_{exp} = 1.52 ± 0.33. On the basis of the above results, it was concluded that under voltammetric conditions TPP is electrochemically oxidized in an irreversible 2e process. The systematic decrease of the αn_a value with increasing pH appears to account for the observed decrease in experimental i_p values with increasing pH. However, no rational explanation is attempted for the decreasing of αn_a with increasing pH.

Table 3

Voltammetric n-values observed upon electrolysis of L-tryptophan at peak I_a potential at a GCE electrode (A = 0.33 cm^2) in pH 3.9 phosphate buffer (u = 0.5 M).

C (mM)	i_p (uA)	v (Vs^{-1})	αn_a	n
0.55	24.4	0.005	0.74	2.33
0.55	72.7	0.05	0.80	2.11
0.55	107.0	0.1	0.69	2.38
0.55	144.3	0.2	0.60	2.43
1.1	48.8	0.005	0.68	2.43
1.1	153.3	0.05	0.64	2.50
1.1	222.0	0.1	0.60	2.65
1.1	304.0	0.2	0.60	2.56
1.1	460.0	0.5	0.67	2.45
1.1	552.0	1.0	0.80	1.80
1.1	773.6	2.0	0.80	1.79
1.1	957.2	5.0	0.53	1.72
1.1	1326.3	10.0	0.51	1.71
1.1	1565.5	20.0	0.51	1.43

3. A. 4. Controlled potential coulometry

Controlled potential coulometry of TPP at peak I_a potentials was carried out in phosphate buffers (u = 0.1M) between pH 2.3 and 10.6 and in dilute HCl (pH 2.4). Using a conventional three electrode compartment cell (20 cm^2 PGE, 25 ml stirred solution) experimental n-values of 4.0 ± 0.2 were measured when very dilute solutions of TPP (10-50 uM) were electrolyzed. Such electrolyses were completed in ca. 2 h. Electrolyses using TPP concentrations of 0.50-2.0 mM took 8-10 h to reach completion if the electrodes were periodically resurfaced. Without resurfacing, completion of these electrolyses took ca. 6-7 days. Experimental n-values obtained were rather variable and ranged from 4.6-5.7 (Table 4). These coulometric results suggest that using relatively high concentrations of TPP (≥ 0.5 mM) and prolonged electrolysis, a slow chemical reaction follows a relatively rapid overall 4e process forming products which can undergo further electrooxidation. Fig. 13 shows a series of cyclic voltammograms of TPP before, during and after electrolysis. After the completion of electrolysis, a cyclic voltammogram at the sweep rate of 200 mVs^{-1} shows a well defined oxidation peak at 1.0 V (Fig. 13E). E_p for this peak at pH 4.7 and 7.34 are 1.15 V and 0.95 V, respectively. These E_p values agree with the potentials observed for the indistinct oxidation peak II_a of TPP.

During the controlled potential electrooxidations the

Table 4

Coulometric *n*-values for the controlled potential electro-oxidation of L-tryptophan at peak I_a potential.

pH	C (m*M*)	Applied Potential/V *vs.* SCE	*n*-value
Phosphate buffers (u = 0.5 M)			
2.3	0.64	1.1	4.0
2.3	0.95	1.1	5.6
4.7	0.17	0.8	4.0
4.7	0.60	0.8	4.6
4.7	0.52	1.0	4.9
7.3	0.50	0.75	5.6
7.3	0.53	1.1	6.2
10.6	0.50	0.7	5.7
Dilute HCl			
2.4	0.15	1.2	4.0
2.4	0.50	1.2	4.6
2.4	0.95	1.2	5.6

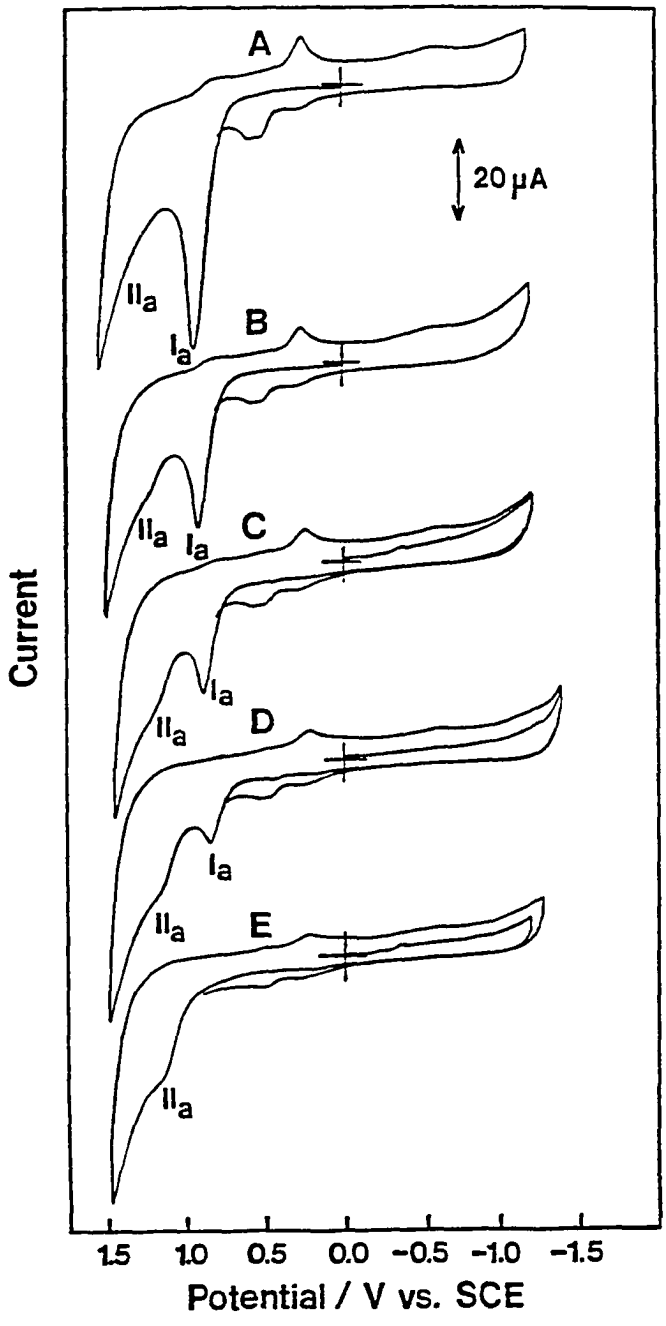

Fig. 13 Cyclic voltammograms at the PGE taken throughout the course of a controlled potential oxidation of 0.5 mM TPP in pH 4.7 phosphate buffer (u = 0.1M) at 0.9 V. (A) Before electrolysis, (B), (C), (D) and (E) were recorded after 1.5, 19, 43, and 56 h of electrolysis. Sweep rate: 200 mVs^{-1}.

colorless TPP solution turns yellow . If the concentration of TPP used is above 0.5 m*M* then a yellow film is deposited on the electrode surface. This coating probably blocks the electrode surface and leads to very long electrolysis time. Spectral changes observed during the electrooxidation of TPP at peak Ia potentials at pH 4.78 are shown in Fig. 14. As the electrolysis proceeds the characteristic U.V. bands of TPP (λ_{max} = 275 and 215 nm) disappear and new bands appear at λ_{max} = 350-294, 244, and 203 nm. The band centered at 244 nm increases throughout the electrolysis but over the last 1-2 h it decreases somewhat.

3. A. 5. Thin-layer spectroelectrochemistry

Thin-layer spectroelectrochemistry is a useful technique to identify and to characterize the rapidly generated intermediates in electrode reactions[87,88].

Thin-layer spectroelectrochemical studies of TPP at pH 4.8 and pH 7.0 were carried out using an optically transparent reticulated vitreous carbon (RVC) electrode. Curve 1 in Fig. 15A is the spectrum of TPP at pH 4.8. When a potential corresponding to peak Ia (0.9 V) is applied, virtually no spectral changes were observed for the first *ca*. 80 s. This period will be described as a "lag period". Then, the characteristic absorption bands of TPP (λ_{max} = 275, 215 nm) begin to decrease and the former absorption band shifts to higher wavelength (*ca*. 285 nm) and the latter

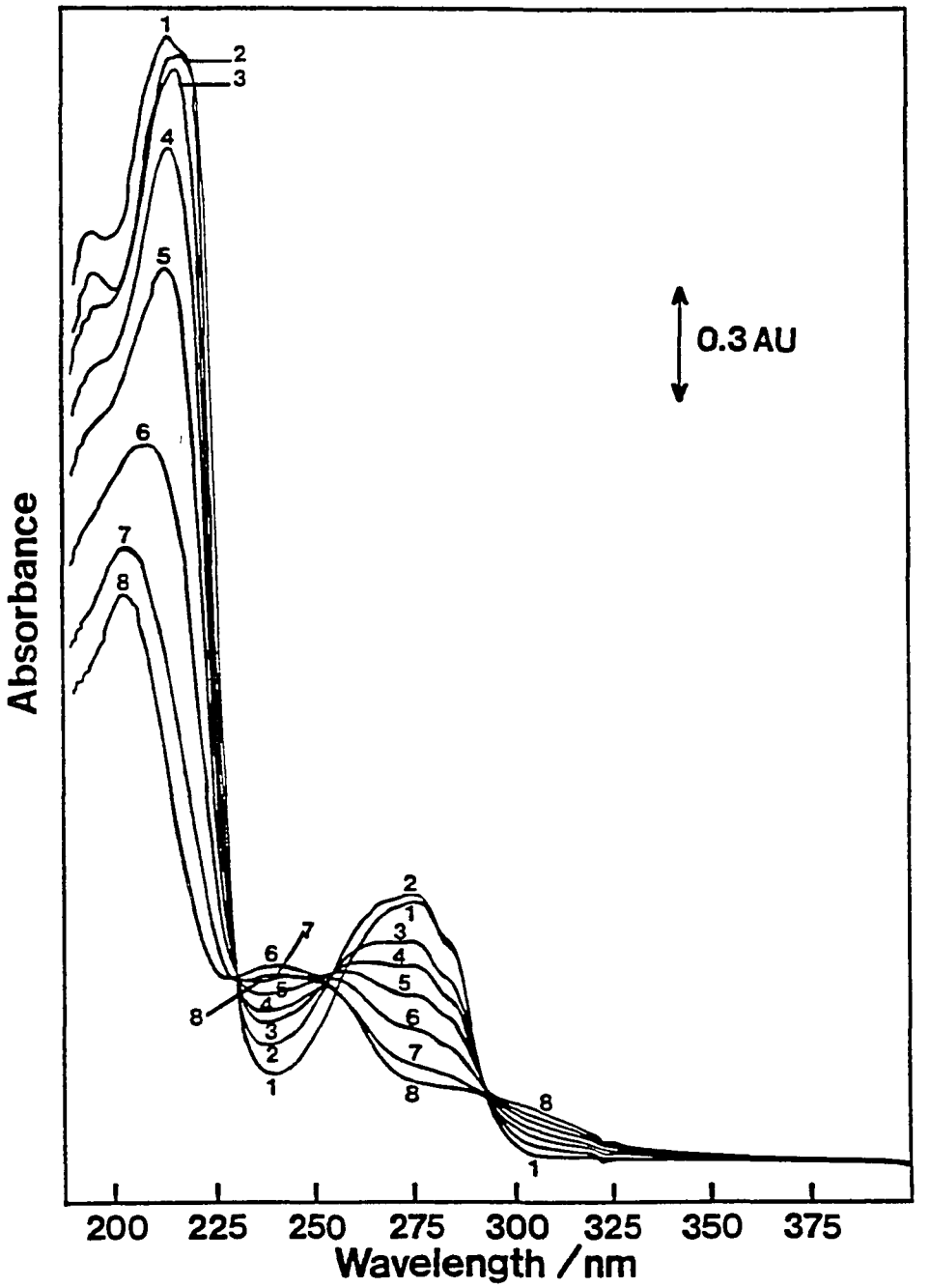

Fig. 14 Spectral changes observed during the controlled potential electrooxidation of 1.6 mM tryptophan in pH 4.78 phosphate buffer (u = 0.1M) at 0.9 V. Curve (1) is the spectrum of TPP. Spectra were recorded after (2) 1 h, (3) 2 h, (4) 3 h, (5) 4 h, (6) 5 h, (7) 6 h and (8) 8 h electrolysis.

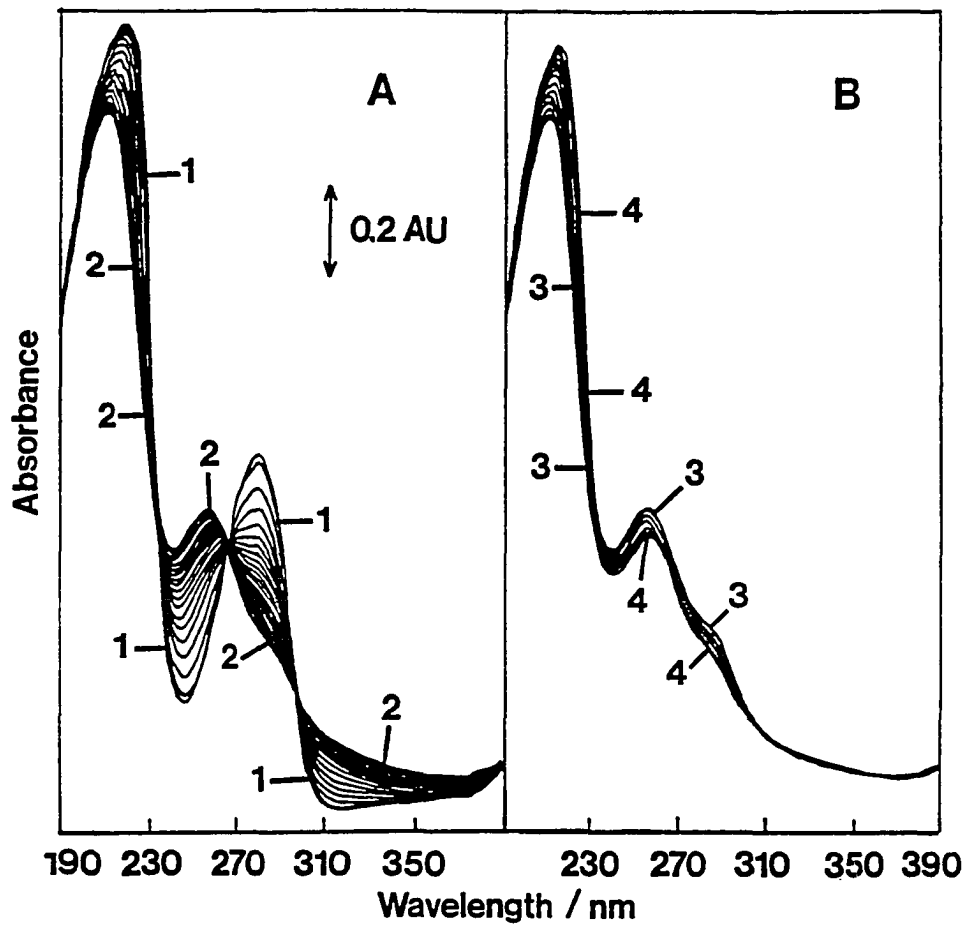

Fig. 15 (A) Spectra of 2 mM tryptophan in pH 4.8 phosphate buffer (u = 0.5M) undergoing oxidation at 0.9V in a thin-layer cell containing a RVC electrode. Curve (1) is the spectrum of TPP. After recording curve (2) the RVC electrode was open circuited and the spectral changes between curves (3) and (4) in (B) were observed. Repetitive spectral sweeps of 18.9 s with no interval between sweeps are shown in (A). The time lapsed between curves (3) and (4) in (B) is 15 min.

to shorter wavelengths (ca. 205 nm). Simultaneously a new absorption band grows in at ca. 244 nm and shifts to longer wavelength (ca. 250 nm) and the absorbance between about 355-290 nm also increases. After the TPP solution is oxidized for 18 min, curve 2 in Fig. 15A was recorded. At this point the RVC electrode was open-circuited . The spectral changes observed after the electrolysis are shown between curves 3 and 4 in Fig. 15B. After the electrolysis, the absorbance decreases at wavelengths centered at 285 nm and 250 nm and increases at shorter wavelengths (ca. 205 nm) and shifts to longer wavelengths(ca. 215 nm). Such spectroelectrochemical behavior indicates that the electrooxidation of TPP at peak Ia potentials probably generates intermediate species at 215, 250, and 275 nm which undergo further chemical follow up reactions. Selected absorbance vs. time curves, recorded at 215, 250, and 285 nm, are shown in Fig. 16. No lag period was observed at pH 7.0. Otherwise, the general spectroelectrochemical behavior observed at pH 7.0 was almost identical to that at pH 4.8 (Fig. 17).

A first order rate law can be written for the change in concentration of the intermediate with time as shown in the Eqn. (8).

$$-\frac{d[C]}{dt} = k\,[C] \qquad (8)$$

where

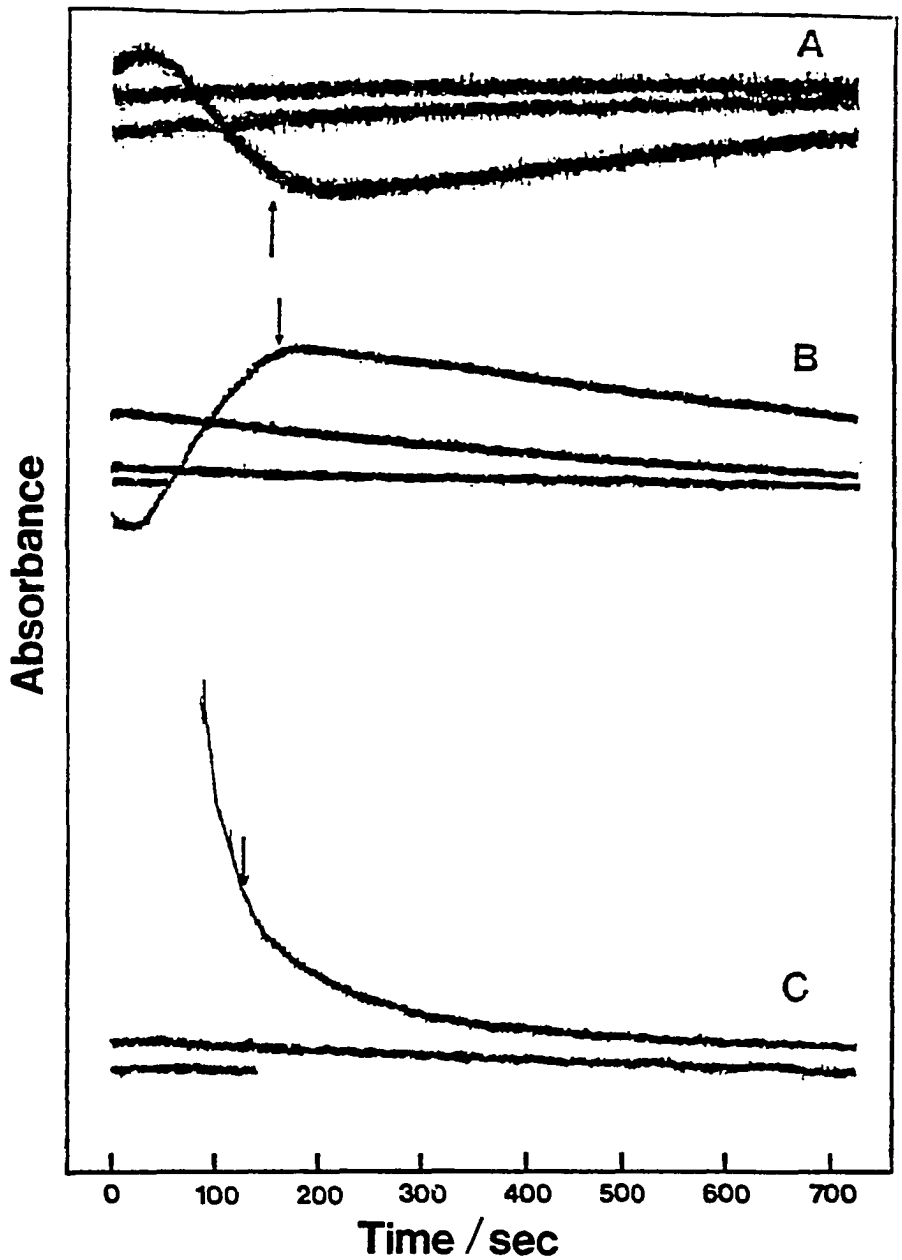

Fig. 16 Absorbance vs. time curve for the decay of the intermediate species generated upon electrolysis of 2.0 mM TPP at 0.8 V in pH 7.0 phosphate buffer. Arrow indicates time when electrode was open circuited. At wavelength (A) 215 nm, (B) 245 nm and (C) 274 nm.

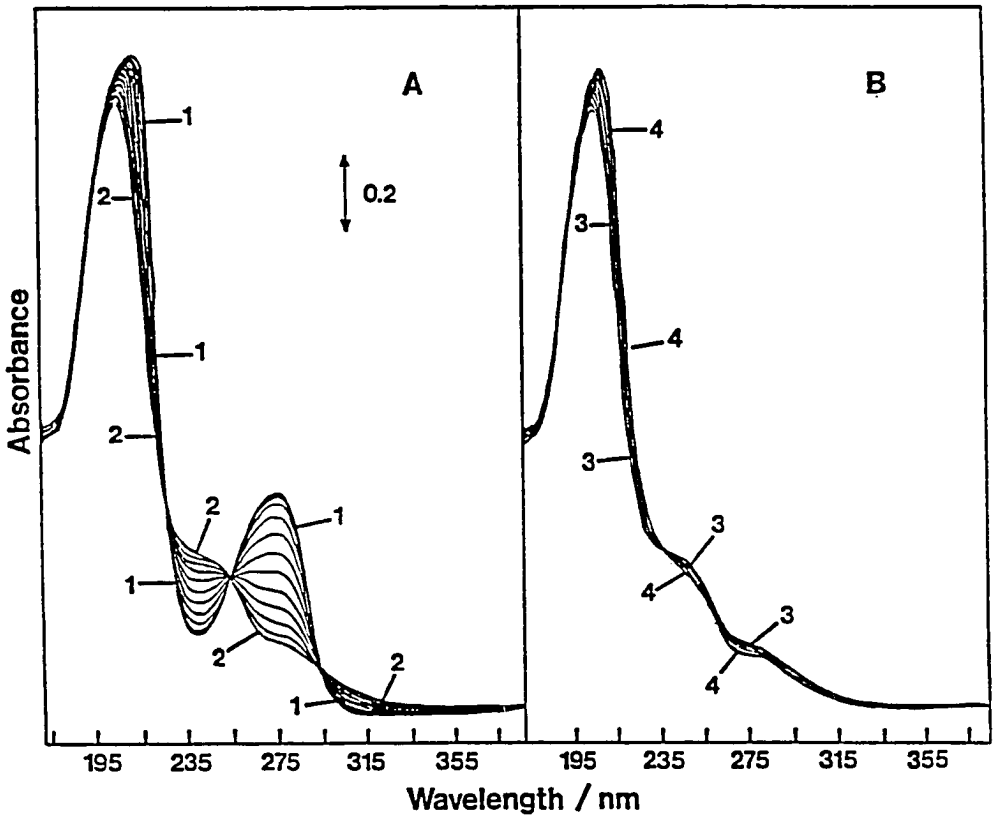

Fig. 17 (A) Spectra of 2 mM TPP in pH 7.0 phosphate buffer (u = 0.1M) undergoing oxidation at 0.8 V in a thin-layer cell containing the RVC electrode. Curve (1) is the spectrum of TPP. After recording curve (2) the RVC electrode was open circuited and the spectral changes between curves (3) and (4) in (B) were recorded. Repetitive spectral sweeps of 75.2 s with no interval between sweeps are shown in (A). The time lapsed between curves (3) and (4) is 15 min.

[C]: concentration of the intermediate

k : the first order rate constant in s^{-1}

Assuming that absorbance is directly proportional to concentration, the first order rate law can be rewritten as shown in the Eqn. (9)

$$\frac{-dA}{dt} = kA \qquad (9)$$

If A_0 represents the absorbance of the intermediate at time t=0, and A represents the absorbance of the intermediate at time t, integration of Eqn. (9), i. e., Eqn. (10).

$$\int_{A_0}^{A} \frac{-dA}{A} = k \int_{0}^{t} dt \qquad (10)$$

leads to

$$-\ln \frac{A}{A_0} = \ln \frac{A_0}{A} = kt \qquad (11)$$

or

$$\ln A = \ln A_0 - kt \qquad (12)$$

If a plot of ln A <u>vs</u>. t gives a straight line, then the reaction is first order. The slope of this line can be used to calculate k. With the first order rate constant, k, the half-life time, $t_{1/2}$ can be calculated using Eqn. (13).

$$t_{1/2} = \frac{\ln 2}{k} = \frac{0.693}{k} \qquad (13)$$

The absorbance changes of TPP in both pH 4.8 and 7.0 are quite small, but analysis of absorbance vs. time curve at 215, 250, and 285 nm revealed that first order kinetics are followed. The experimental rate constants are shown in Table 5. The rate constant at 215 and 250 nm are the same but the rate constant at 285 nm is different. Hence, it may be concluded that the decay of two intermediates is observed. It seems that the intermediate species monitored at around 285 nm is less stable at pH 7 than at pH 4.8. The lag period observed at pH 4.8 suggests that an intermediate at around 285 nm which has an U.V. spectrum similar to TPP is formed during that period. The greater instability of the intermediate absorbing at around 285 nm at pH 7.0 compared to pH 4.8 appears to be related to the absence of the lag period at pH 7.0. It must be noted here that it was exceedingly difficult to obtain reproducible thin-layer spectroelectrochemical behavior. Often, the electrooxidation of TPP in the thin-layer cell proceeded extremely slow so that it was impossible to observe intermediate species. It seems that this effect is due to filming of the RVC electrode surface by one or more products. Accordingly, conclusions based on such thin-layer spectroelectrochemical results must be regarded as somewhat tentative. Nevertheless, it does seem that under thin-layer spectroelectro-

Table 5

Observed first-order rate constants for reaction of intermediates generated upon electrochemical oxidation of L-tryptophan in a RVC thin-layer cell.

pH	(nm)	$k_{obs}(s^{-1})^a$
4.8	215	0.0031 ± 0.0003
4.8	250	0.0030 ± 0.0004
4.8	285	0.0019 ± 0.002
7.0	213	0.0019 ± 0.0002
7.0	245	0.0017 ± 0.0001
7.0	280	0.0142 ± 0.001

[a] The average of at least three replicate measurements is reported ± standard deviation.

chemical conditions the decay of two intermediates can be observed. One exhibits an absorption band at around 250 nm and its decomposition can be followed by the decrease in absorbance at this wavelength or a corresponding increase in absorbance at 215nm. This intermediate is more stable at neutral pH than at lower pH and, therefore, it might be concluded that this intermediate is responsible for the reduction peak II_c observed in cyclic voltammograms of TPP (Fig. 9). The second intermediate absorbs at ca. 285 nm and its decomposition can be followed by the decrease of absorbance at this wavelength and it seems to be more unstable at neutral pH than at acid pH. Such behavior suggests that this intermediate might be responsible for the reduction peak I_c observed in cyclic voltammograms of TPP (Fig. 9).

3. A. 6. Isolation and identification of electrochemical oxidation products

Isolation of electrochemical oxidation products

Controlled potential electrooxidations of TPP were carried out in phosphate buffers at pH 2.33, 4.70, 7.36 and 10.65 and in dilute HCl (pH 2.4). In all cases the electrolyzed solutions were deep yellow. Product solutions were freeze-dried and the resulting solid mass was redissolved in ca. 2ml of water and injected on to a column of sephadex G-10 gel permeation resin using water as the eluent. The resulting liquid chromatograms were dependent on the pH of

the phosphate buffer used for the electrolysis, the applied potential, the initial concentration of TPP and whether or not electrolyses were allowed to proceed to completion (i.e., until all TPP was oxidized). Representative liquid chomatograms are shown in Figs. 18 and 19*. Figure 18 shows liquid chromatograms obtained for the product mixtures formed by the electrooxidation of TPP at pH 2.4. After complete electrolysis of 1m$\underline{M}$ TPP in phosphate buffer pH 2.4 (u = 0.1M) liquid chromatograms of the resulting products show four liquid chromatographic (LC) peaks (A, B, E and F, Fig. 18A). LC peaks A and B are partially due to inorganic phosphate. Following complete electrolysis of 1m$\underline{M}$ TPP in dilute HCl (pH 2.4), the liquid chromatogram of the products is essentially identical to that shown in Fig. 18A indicating that organic products are eluted along with phosphate under LC peaks A and B. If, however, the electrooxidation of 1m$\underline{M}$ TPP is not taken to completion then the liquid chromatogram of the products shows that LC peak F is much larger than LC peak E and two new small LC peaks (C and D) appear (Fig. 18B). LC peak I in Fig. 18B is due to unoxidized TPP. When a much higher concentration of TPP (10 m$\underline{M}$) is electrolyzed in dilute HCl (pH 2.4), liquid chromatograms of the

*These chromatograms were obtained over a time period of 1-2 years using columns having slightly different dimensions. Thus, there are some variations noted in experimental retention volumes.

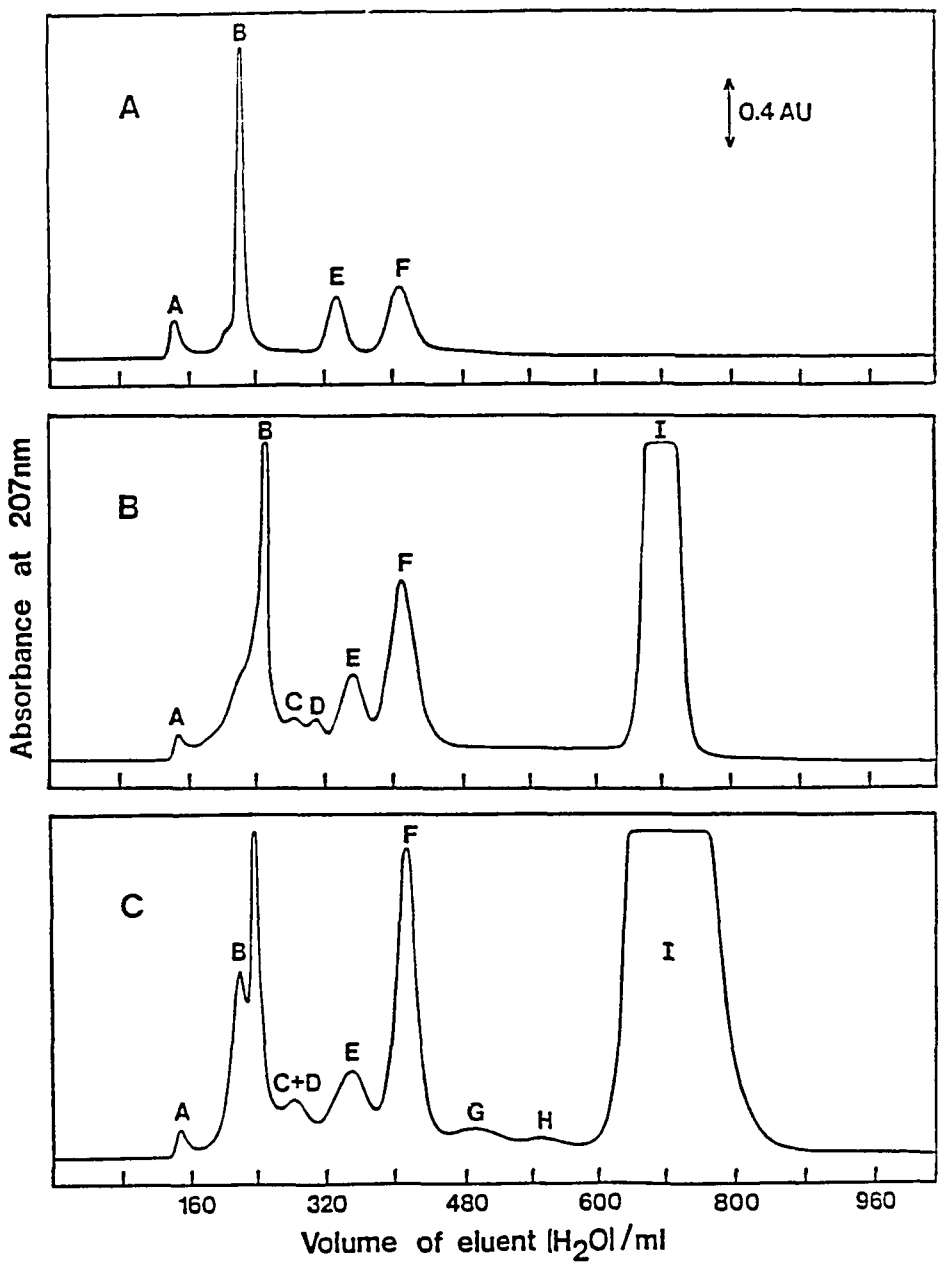

Fig. 18 Liquid chromatograms of the products of electrochemical oxidation of tryptophan at pH 2.4. (A) 1 mM TPP oxidized at 1.1 V in phosphate buffer (u = 0.1); complete oxidation. (B) 1 mM TPP oxidized at 1.2 V in dilute HCl; partial oxidation. (C) 10 mM TPP oxidized at 1.2 V in dilute HCl; partial oxidation. Chromatography done on Sephadex G-10 (90 x 2.5 cm) using water as the eluent (32 $ml h^{-1}$).

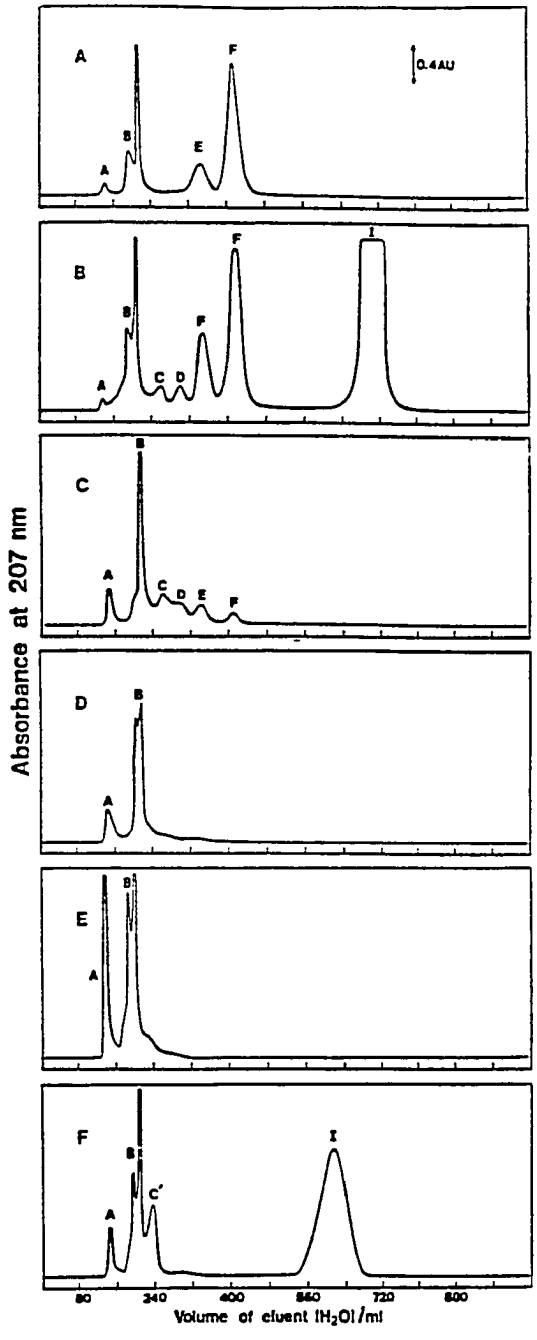

Fig. 19 Liquid chromatograms of the products of electrochemical oxidation of tryptophan in phosphate buffers (u = 0.1M). (A) 2 mM TPP oxidized at 0.9 V at pH 4.7; complete oxidation. (B) 2 mM TPP oxidized at 0.9 V at pH 4.7; partial oxidation. (C) 0.5 mM TPP oxidized at 0.75 V at PH 7.36; complete oxidation. (D) 0.5 mM TPP oxidized at 1.1 V at pH 7.36; complete oxidation. (E) 0.5 mM TPP oxidized at 0.7 V at pH 10.65; complete oxidation. (F) 0.5 mM TPP oxidized at 0.7 V at pH 10.65; partial oxidation. Chromatography done on Sephadex G-10 (90 x 2.5 cm) using water as the eluent (32 mlh^{-1}).

products show two additional peaks (G and H, Fig. 18C). Electrolysis of TPP in phosphate buffer at pH 2.4 under the condition outlined in Fig. 18B and C gave similar liquid chromatograms.

The liquid chromatograms shown in Fig. 18 suggest that complete electrooxidation of TPP leads to four products responsible for LC peaks A, B, E and F. When relatively low initial concentrations of TPP (ca. 1 mM) are only partially oxidized the relative yield of the product responsible for LC peak F increases. This suggests that the component responsible for LC peak F is slowly oxidized at the potentials used to oxidize TPP. Similarly, LC peaks C and D appear if TPP is partially oxidized indicating that they are due to compounds which can be oxidized at peak Ia potentials. LC peaks G and H (Fig. 18C) appear only when high initial concentrations of TPP (ca. 10mM) are used and the electrooxidation is not taken to completion. This again suggests that the components responsible for LC peaks G and H are electrochemically oxidizable.

Figure 19 shows liquid chromatograms of product mixture obtained by electrooxidation of TPP in phosphate buffers at pH 4.7, 7.36 and 10.65. In all cases LC peaks A and B are partially due to inorganic phosphate. The liquid chromatograms obtained for the product mixtures formed at pH 4.7 and 7.36 (Fig. 19A, B, C) are similar to those obtained for

product mixtures formed at pH 2.4 (Fig. 18). The liquid chromatogram shown in Fig. 19D demonstrates that complete electrooxidation of TPP at a potential 350 mV more positive than peak I_a results in the disappearance of LC peaks C-H. This effect was noted at all pH values studied. After complete electrolysis of TPP at pH 10.65 liquid chromatogram of the products shows only LC peaks A and B (Fig. 19E). However, the products of partial electrolysis show a large peak (C') which has a retention volume similar to that of LC peaks C and D.

The above liquid chromatographic studies indicate that incomplete electrolysis of relatively low concentrations of TPP (< 2 m$\underline{M}$) at pH < 7.0 leads to products responsible for LC peaks A, B, C, D, E, and F. Partial electrolysis of higher concentrations of TPP (ca. 10 m$\underline{M}$) gives LC peaks G and H (Fig.18), in addition to LC peaks A, B, C, D, E, and F. Complete electrolysis of TPP at pH 2.4 and 4.7 causes elimination of the products responsible for LC peaks C and D and a significant decrease in the yield of the product responsible for LC peak F. At pH 10.65 the products of complete electrolysis leads to the appearance of only LC peaks A and B.

The decrease or disappearance of LC peaks C-H following complete electrolysis of TPP shows that the compounds responsible for these peaks are electrochemically oxidizable at peak I_a potentials. The total elimination of LC peaks C-H

is observed when TPP is electrolyzed at very high positive potentials (ca. 1.3 V). These observations indicate that the products eluted under LC peaks C-H are further oxidized at such potentials to give species which are responsible for LC peaks A and B.

Identification of electrooxidation products

Liquid chromatographic component A

The component eluted under LC peak A was a pale yellow solid. Its U.V. spectrum in water exhibited a shoulder at ca. 205 nm. This component gave no voltammetric oxidation or reduction peaks at the PGE in aqueous phosphate buffers between pH 2.0-11.0 or in dilute HCl pH 2.4. Mass spectrometry of the solid material did not give useful mass spectral data. FAB-MS using glycerol or thioglycerol as the liquid matrix was also unsuccessful. Attempts to derivatize the solid with a variety of silylating agents under many different experimental conditions were unsuccessful in the sense that the product solutions did not give any GC peaks.

The component responsible for LC peak A emerges very rapidly from a column of Sephadex G-10 gel permeation resin (retention volume ca. 150 ml, Figs. 18 and 19). This information and the failure to obtain a mass spectrum or a volatile trimethylsilyl derivative suggests that LC component A is probably an oligomeric or polymeric material.

Liquid chromatographic component B

The component eluted under LC peak B was a bright yellow solid. In water its U. V. spectrum exhibited shoulders at 290, 235 and 205 nm. The shoulder at 290 nm extended beyond 380 nm resulting in the yellow color of the solution. This product gave no voltammetric oxidation or reduction peaks at the PGE between pH 2.0-11.0. MS and FAB-MS (glycerol or thioglycerol matrix) failed to give useful mass spectral information. Similarly silylation with BSA, BSTFA and MTBSTFA in various solvents (pyridine, DMF, acetonitrile) did not give a volatile derivative which could be analyzed by gas chromatography. Thus, it is tentatively concluded that LC component B is probably an oligomeric or polymeric compound.

Liquid chromatographic components C and D*

The components eluted under LC peaks C and D were a very pale yellow solids. In water components C and D showed identical U.V. spectra (λmax = 293, 233, and 205 nm, Fig. 20). The yields of LC components C and D were extremely small (<< 1mg following about 60% electrooxidation of 10 mg of TPP). The yield of components C and D is approximately < 5% of TPP oxidized. Components C and D are electrochemi-

*In many liquid chromatograms LC peak C and D emerged as a single peak.

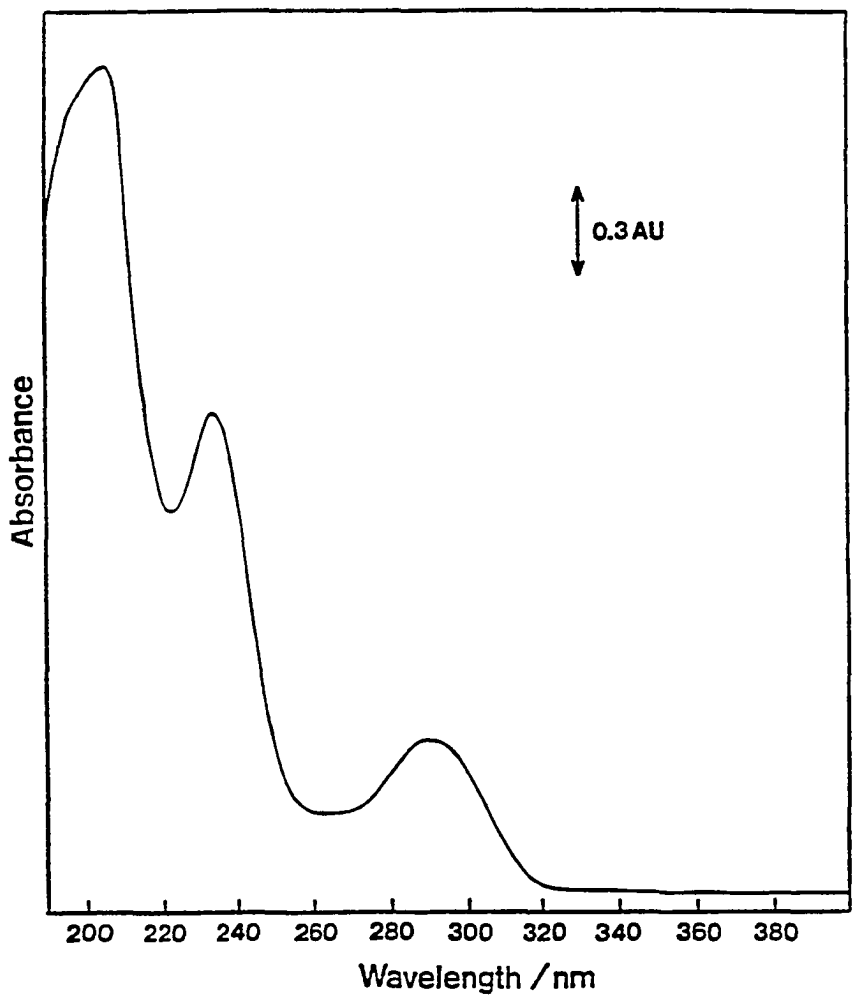

Fig. 20 U.V. spectrum of LC components C and D in water.

cally active. At a slow sweep rate (ca. 5 mVs^{-1}), a single voltammetric oxidation peak was observed at the PGE (Fig. 21A). The linear E_p vs. pH relationship for this peak at a sweep rate of 5 mVs^{-1} is given by Eqn. (14).

$$E_p \text{ (pH 2.0 - 11.0)} = [0.99 - 0.052 \text{ pH}] \text{ V} \quad (14)$$

At faster sweep rates (ca. 200 mVs^{-1}), this peak resolves into two overlapping peaks and an indistinct third oxidation peak appears at potentials close to the background discharge (Fig. 21B). A typical cyclic voltammogram of components C and D at pH 7.0 is shown in Fig. 22. Comparison of this cyclic voltammogram with that of TPP at the same pH (Fig. 9D) shows remarkable similarities suggesting that components C and D are electrochemically oxidized to the similar intermediates and products as TPP. Furthermore, the peak potential for oxidation of components C and D are very close to that of TPP. MS on component C (70 eV, 200°C) gave the following results, m/e (relative abundance): 222 (1.0%), 221 (9.2%), 220 (M^+, 56.9%), 204 (0.3%), 203 (1.0%), 202 (M^+-H_2O, 4.3%), 177 (23.7%), 176 (11.5%), 175 (M^+-COOH, 22.2%), 159 (4.9%), 158 (M^+-COOH-H_2O, 24.2%), 148 (17.5%), 147 (69.9%), 146 ($M^+-CH_2CH(NH_2)COOH$, 100.0%), 120 (25.3%), 119 (16.4%), 118 (20.1%). Component D under the same conditions gave a virtually identical mass spectrum. Components C and D (ca. 100ug) could be derivatized by reacting with BSA or BSTFA (100 ul) in pyridine (50 ul) and dimethylsulfoxide (50 ul) in a sealed vial at room temperature for 24

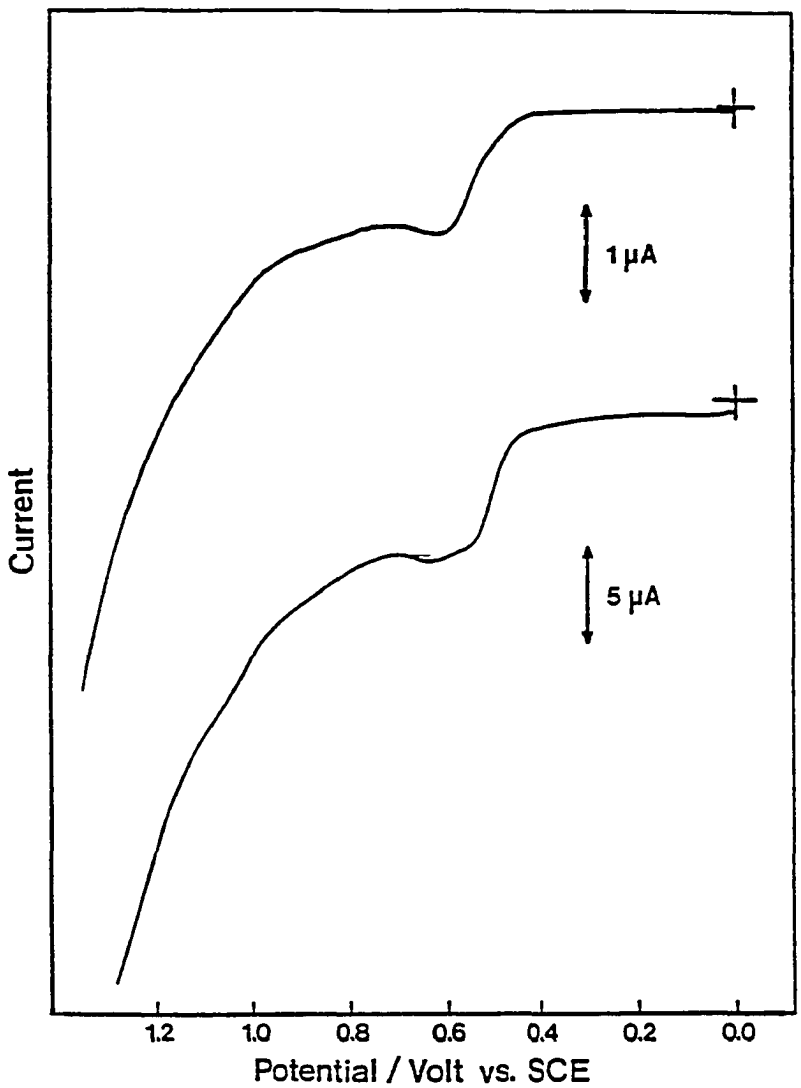

Fig. 21 Linear sweep voltammograms obtained at the PGE of LC components C and D in phosphate buffer pH 7.0 (μ = 0.5 M). Sweep rate: (A) 5 mVs^{-1}, (B) 200 mVs^{-1}.

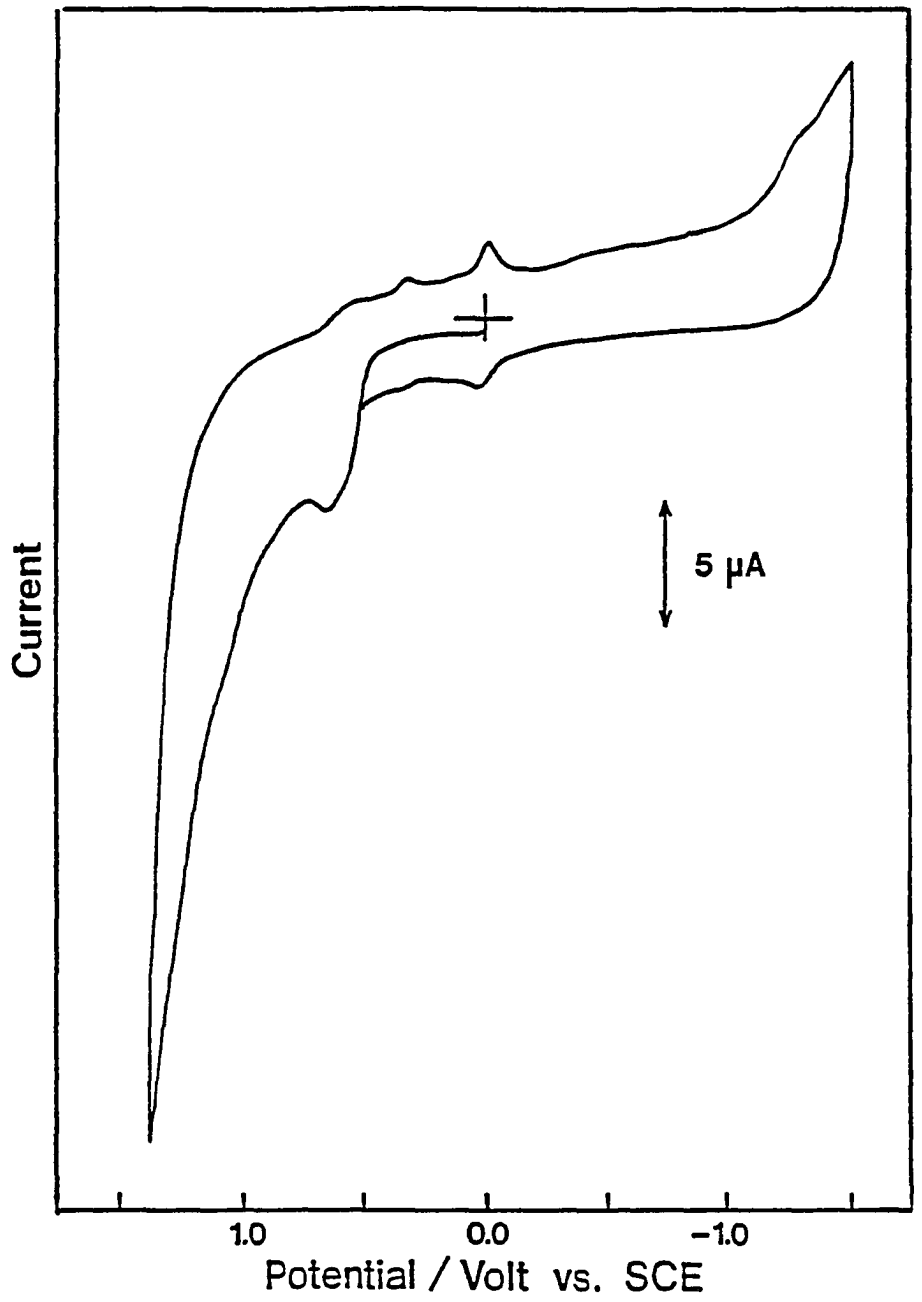

Fig. 22 Cyclic voltammogram of LC components C and D obtained at the PGE in pH 7.0 phosphate buffer (u = 0.5 M).

hr. The trimethylsilyl derivative of component C gave a large GC peak at t_R = 30.9 min while that of component D gave a GC peak at t_R = 31.4 min (Fig. 23). EI- and CI-MS of the products eluted under these peaks showed that the trimethylsilyl derivatives of components C and D both had a molar mass of 436 g and similar GC-mass spectra (Tables 6 and 7). Since the molecular weight of both components C and D is 220 they must both form tri-trimethylsilyl derivatives.

The tricyclic pyrroloindole, 2-carboxy-3a-hydroxy-1,2,3,3a,8,8a-hexahydropyrrolo-(2,3b)-indole (3), shows identical U.V. and mass spectra and electrochemical behavior to that reported above for components C and D. Furthermore, chemically synthesized 3 was resolved into two peaks by liquid chromatography on Sephadex G-10 using water as the eluent. These two LC peaks had the same retention volumes as LC components C and D, respectively. Similarly high pressure liquid chromatography using a column of Shodex OH-Pak (50 x 2 cm) using water as the eluent (3 ml min^{-1}) gave two peaks (t_R = 16.4 and 18.1 min) (Fig.24). Both HPLC

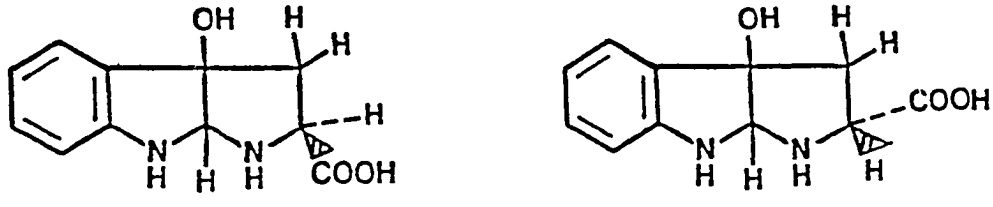

3

fractions gave a trimethylsilyl derivative (GC and GC-MS)

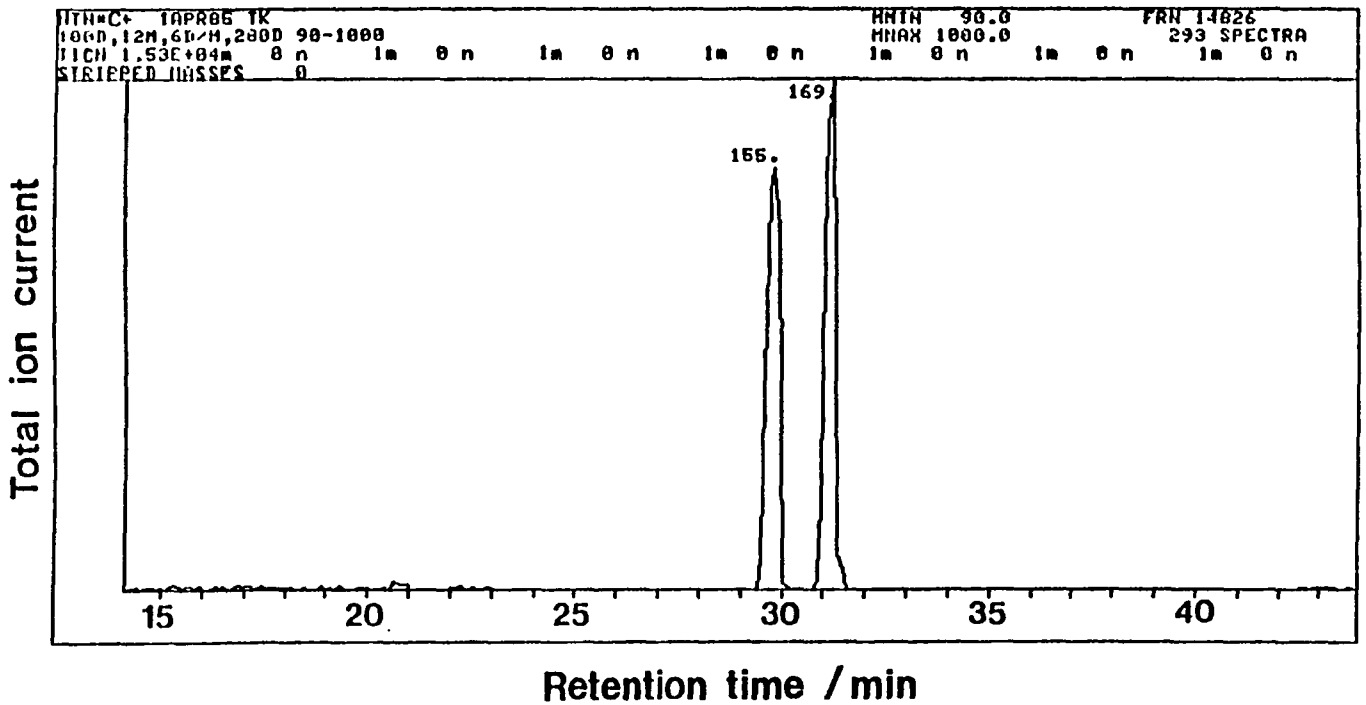

Fig. 23 Total ion current chromatogram of LC components C and D silylated with BSA at room temperature for 24 h.

Table 6. GC-MS data for liquid chromatographic component C formed by electrochemical oxidation of tryptophan

Derivative	Retention time/min	Ionization type	Major MS Peak/ m/e (relative abundance)	Compound
BSA	30.9	EI	437 (1.1%); 436 (M^+, 2.3%); 421 (M^+-CH_3, 1.2%); 366 (3.7%); 365 (9.0%); 364 (M^+-72, 31.4%); 351 (1.6%); 350 (3.3%); 349 ($M^+-72-CH_3$, 12.2%); 321 (14.7%); 320 (13.2%); 319 ($M^+-COOSi(CH_3)_3$, 31%); 249 (9.5%); 248 (27.5%); 247 ($M^+-COOSi-(CH_3)_3-72$, 100%); 220 (24.7%); 219 (31.4%); 218 (77.9%); 206 (9.7%); 205 (18.8%); 204 (25%); 159 (6.4%); 158 (48.9%); 157 (95.8%); 149 (4%); 148 (6.9%); 147 (25.3%); 132 (10.7%); 131 (17.1%); 130 (72.2%).	
BSA	30.4	CI	465 ($M+C_2H_5^+$, 7.8%); 439 (6.5%); 438 (19%); 437 ($M+H^+$, 56.4%); 436 (M^+, 33.8%); 423 (13.9%); 422 (30.7%); 421 (M^+-CH_3, 87.9%); 366 (10.7%); 365 (27.9%); 364 (M^+-72, 28.7%); 351 (5.6%); 350 (11.2%); 349 ($M^+-72-CH_3$, 47.4%); 321 (18.1%); 320 (51.6%); 319 (34.9%); 249 (8.7%); 248 (24.1%); 247 (29.8%); 220 (14.3%); 219 (17.6%); 218 (47.4%); 206 (30.1%); 205 (16.4%); 204 (19.6%); 176 (20.1%); 175 (21%); 174 (100%).	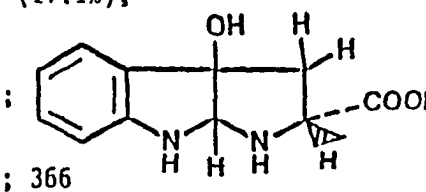 3

Table 7. GC-MS data for liquid chromatographic component D formed by electrochemical oxidation of tryptophan

Derivative	Retention time/min	Ionization type	Major MS Peak/ m/e (relative abundant)	Compound
BSA	31.4	EI	438 (6.6%); 437 (14.5%); 436 (M^+, 39.4%); 423 (2%); 422 (4.5%); 421 (M^+-CH_3, 11.7%); 366 (1.7%); 365 (3.9%); 364 (M^+-72, 13.8%); 351 (0.8%); 350 (2%); 349(M^+-72-CH_3, 6.6%); 321 (18.1%); 320 (36.1%); 319 (M^+-$COOSi(CH_3)_3$, 100%); 249(3.4%); 248 (9.8%); 247 (M^+-$COOSi(CH_3)_3$-72, 40.7%); 220 (19.5%); 219 (18.9%); 218 (39.4%); 206 (7.2%); 205 (16.5%); 204 (48.4%); 159 (2.5%); 158 (18.9%); 157 (37.7%); 149 (5.4%); 148 (5.2%); 147 (23.9%); 132 (5.5%); 131 (13.3%); 130 (74.6%)	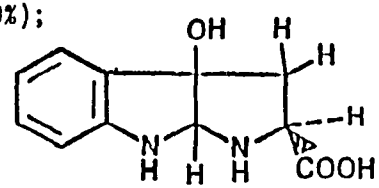 3
BSA	31.4	CI	477.2 (M+C_3H_5, 1.6%); 467 (1.2%); 466 (3.3%); 465 (M+C_2H_5, 10.6%); 43 9 (8%); 438 (23.9%); 437 (M+H^+, 62.8%); 436 (M^+,45.9%); 423 (17.1%); 422 (36.5%); 421 (M^+-CH_3, 100%); 349 (19.7%); 348 (21.5%); 347 (M^+-$OSi(CH_3)_3$, 62.1%); 321 (3.1%); 320 (9.0%); 319 (M^+-$COOSi(CH_3)_3$, 13.7%); 249 (1.8%); 248 (5.2%); 247 (6.8%); 220 (4%); 219 (45%); 218 (17.1%); 206 (7.4%); 205 (8.7%); 204 (8.5%); 176 (3.4%); 175 (5.5%); 174 (18.9%).	

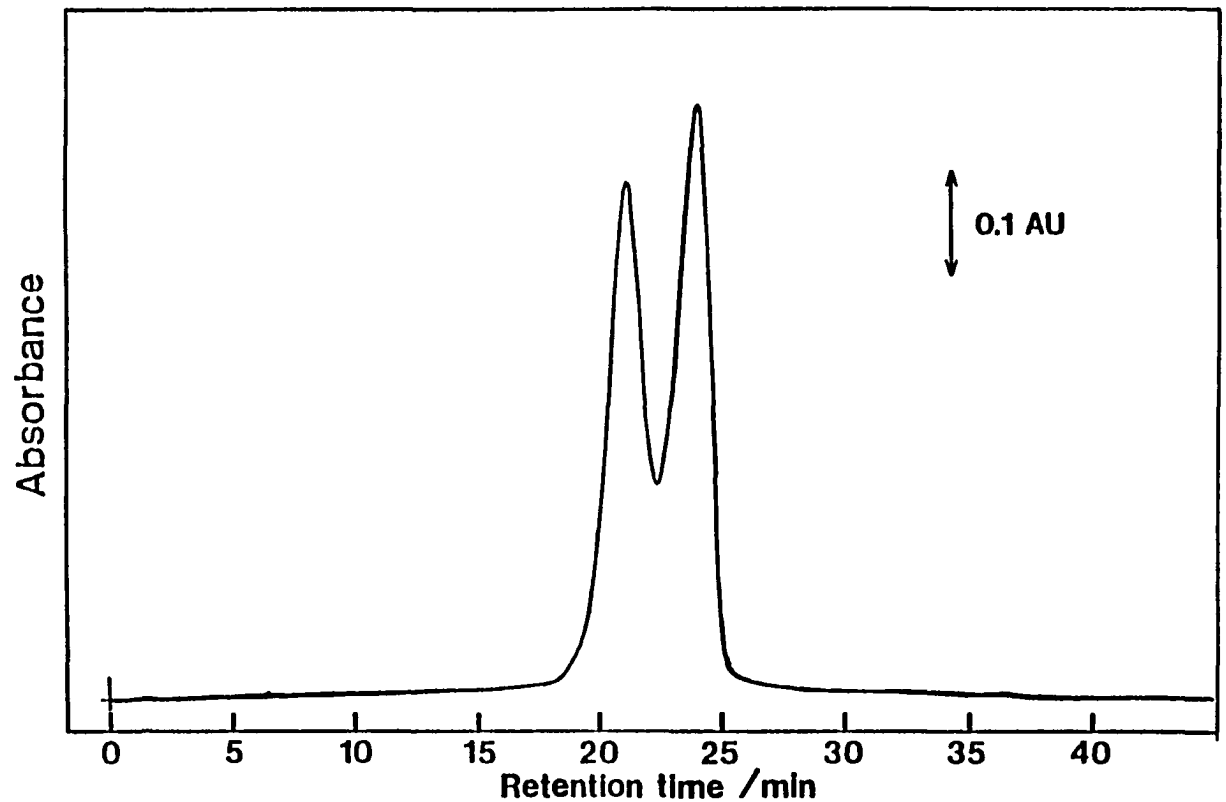

Fig. 24 HPLC chromatogram of chemically synthesized tricyclic pyrroloindole on a column of Shodex OH-Pak (50 x 2 cm) using water as the eluent (3 $ml min^{-1}$).

identical to that formed with components C and D. Hence, it is highly probable that LC components C and D are stereoisomers of the tricyclic pyrroloindole 3 as shown above.

Liquid chromatographic peak C'

The component eluted under LC peak C' (Fig. 19F) was a white solid. Its U.V. spectrum in water exhibited characteristic absorption bands at λ_{max} = 288, 229 (sh), and 200 nm (Fig. 25). This spectrum is similar to that of the tricyclic pyrroloindole (3). At pH 10.6 LC component C' exhibits very well-defined bands at λ_{max} = 282, 231, and 212 nm (Fig. 26). It has been found that dioxindolylalanine (8) immediately after dissolving in pH 10.6 phosphate buffer (u = 0.5M) shows absorption bands at λ_{max} = 280, 258 (sh), 239, and 214 nm. However, this spectrum totally changes over the period of 30 minutes to give new absorption bands at λ_{max} 282, 231, and 212 nm (Fig. 27). At pH 10.65 the tricyclic pyrroloindole 3 shows bands at λ_{max} = 289, 234 and 209 nm. These data indicate that at high pH (ca. pH 10.6) dioxindolyalanine (8) reacts to give LC component C' and that the latter compound must have a similar structure to tricyclic pyrroloindole (3). One rational explanation is that dioxindolylalanine (8) cyclizes at high pH (ca. pH 10.65) to give 2-carboxy-3a,8a-dihydroxy-1,2,3,3a,8,8a-hexahydro-pyrrolo-(2,3b)-indole (13) as shown in Eqn.15. The latter compound would be expected to have a very similar U.V. spectrum to that of the tricyclic pyrroloindole 3 and

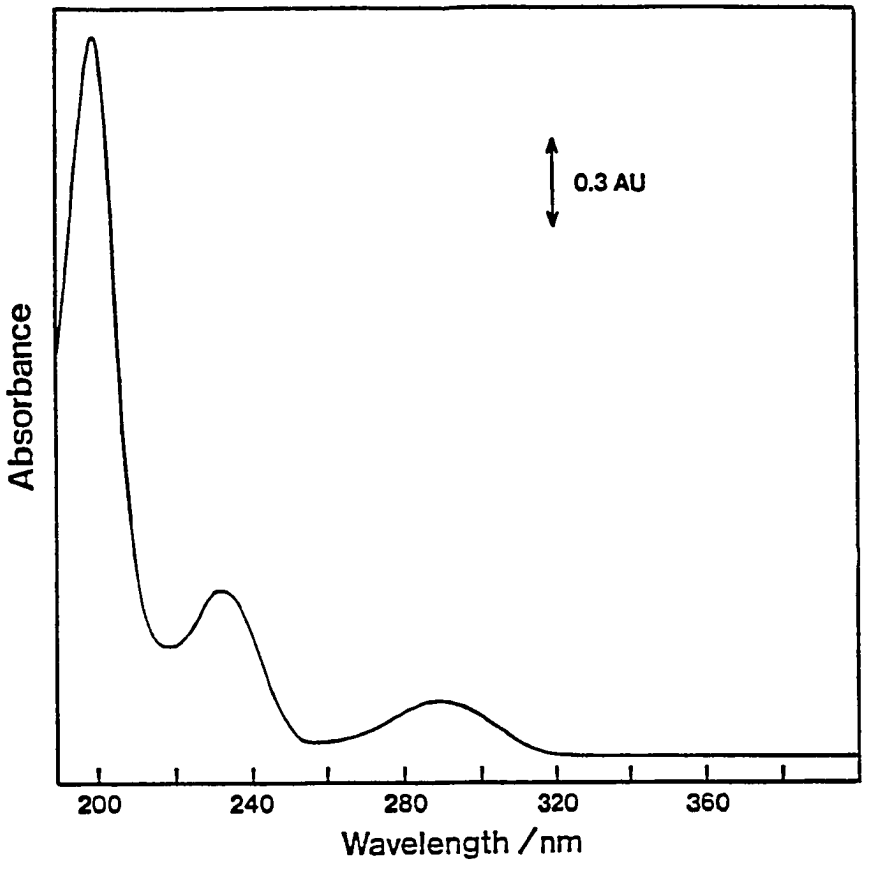

Fig. 25 U.V. spectrum of LC component C' in water.

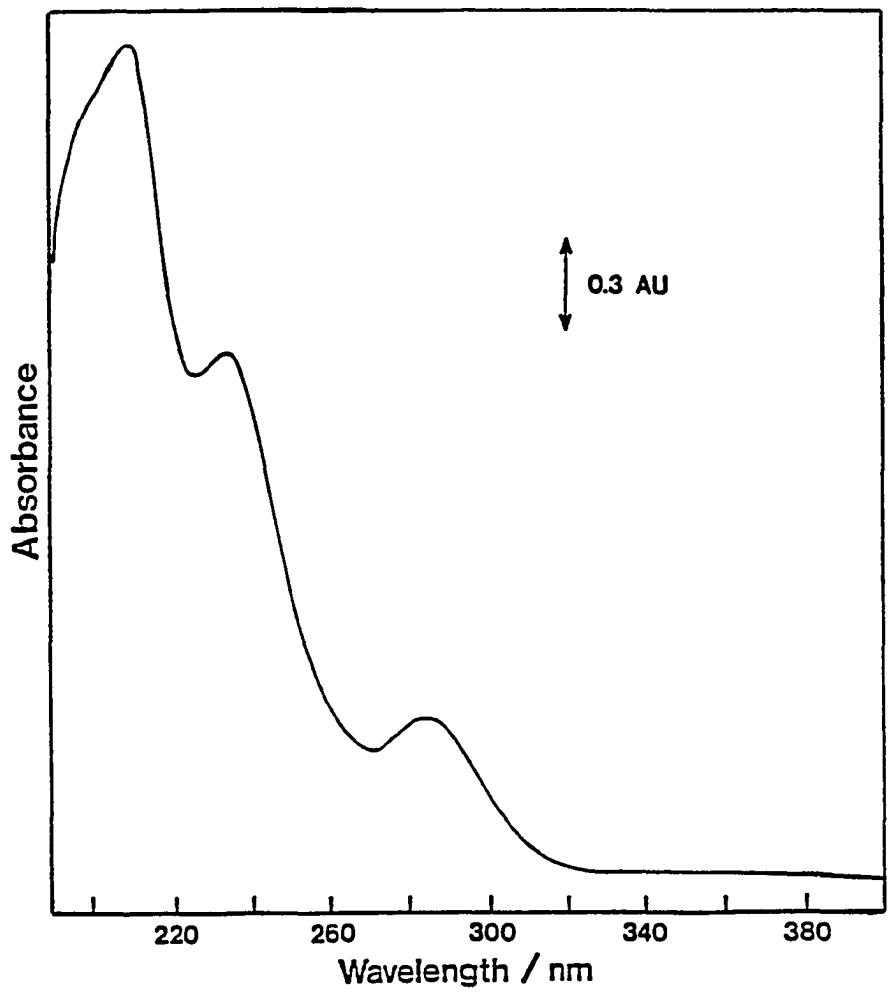

Fig. 26 U.V. spectrum of LC component C' in pH 10.65 phosphate buffer (u = 0.5 M).

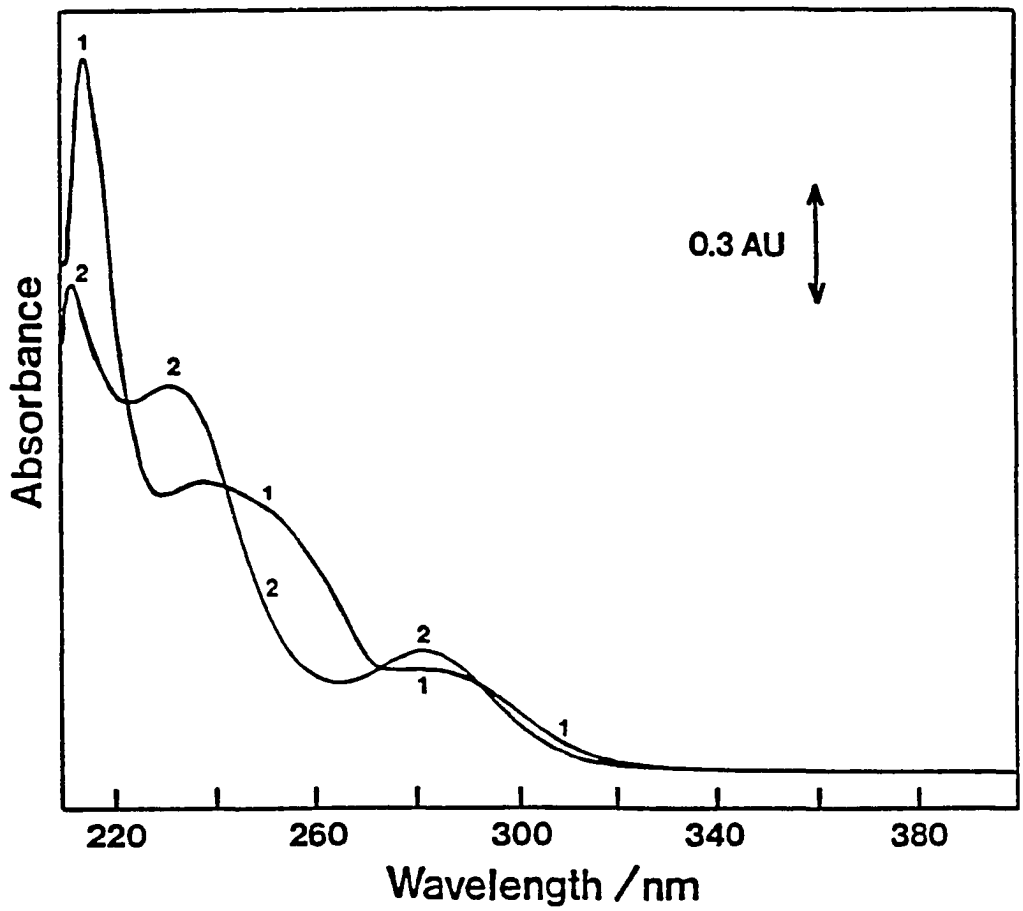

Fig. 27 U.V. spectra of dioxindolylalanine in pH 10.65 phosphate buffer (u = 0.5 M). (1) immediately after dissolving, (2) after 30 min.

the intramolecular cyclization of 8 would be greatly enhanced at high pH (ca. 10.65) owing to complete deprotonation of the exocyclic amino group. LC component C' gave a trimethylsilyl derivative identical (GC and GC-MS) to that formed with dioxindolylalanine. This suggests that LC component C' converts back to dioxindolylalanine during the silylation reaction. Thus, it is clear that LC component C' is 2-carboxy-3a,8a-dihydroxy-1,2,3,3a,8,8a-hexa-hydropyrrolo-(2,3b)-indole which at high pH is formed by cyclization of dioxindolylalanine.

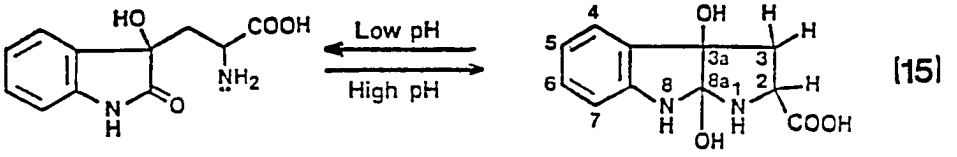

8 13 [15]

Liquid chromatographic component E

LC component E was a white solid. In water component E showed very well-defined U.V. absorption bands at λ_{max} 287, 253 and 205 nm (Fig. 28). LC component E was electrochemically active. At a sweep rate of 5 mVs^{-1}, LC component E shows a single voltammetric oxidation peak at the PGE (Fig. 29A). The linear E_p vs. pH relationship for this peak at a sweep rate of 5 mVs^{-1} is shown in Eqn. 16. Thus, LC

$$E_p(\text{pH } 2.0 - 11.0) = [1.37 - 0.065\ \text{pH}]\ V \qquad (16)$$

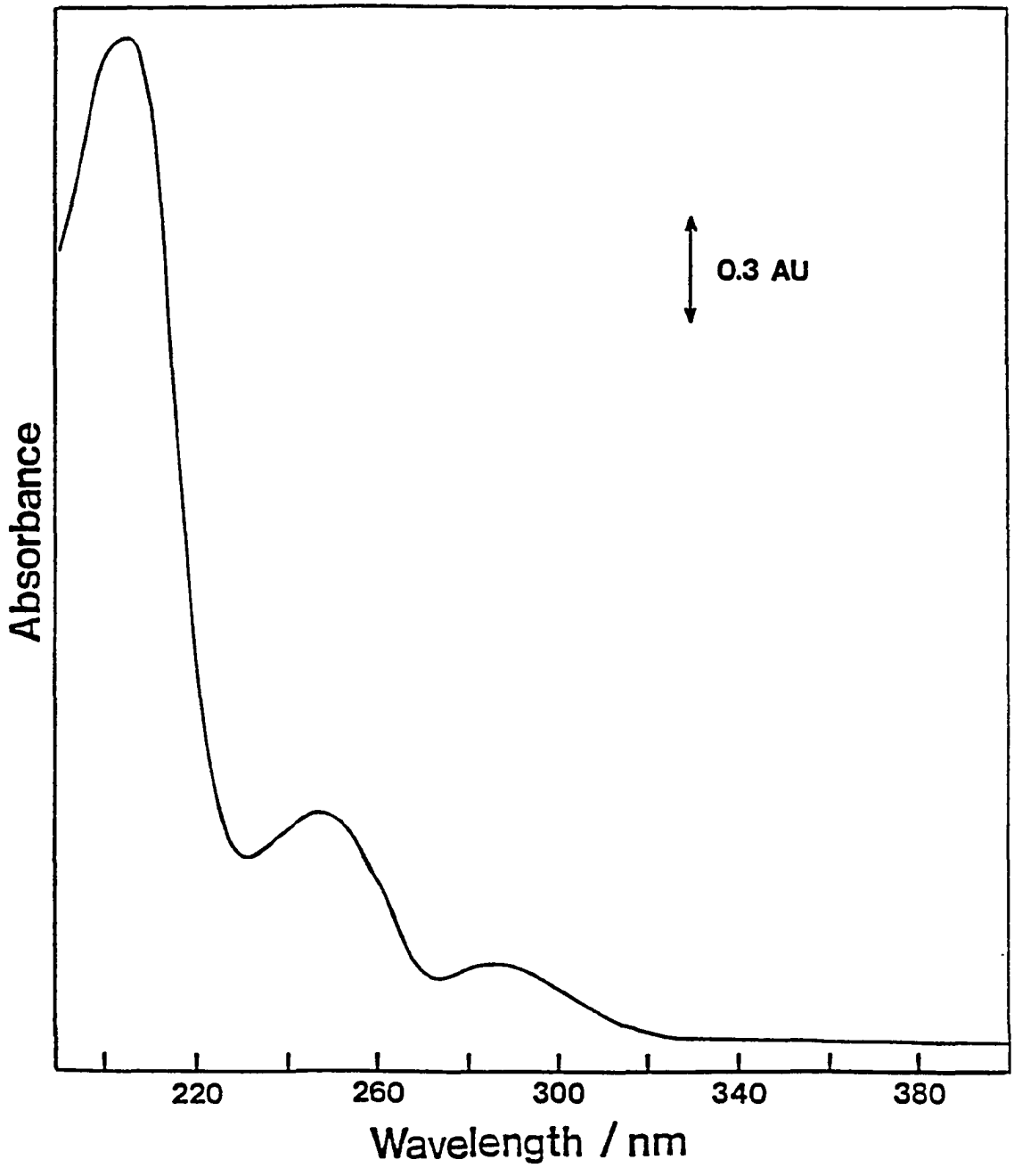

Fig. 28 U.V. spectrum of LC component E in water.

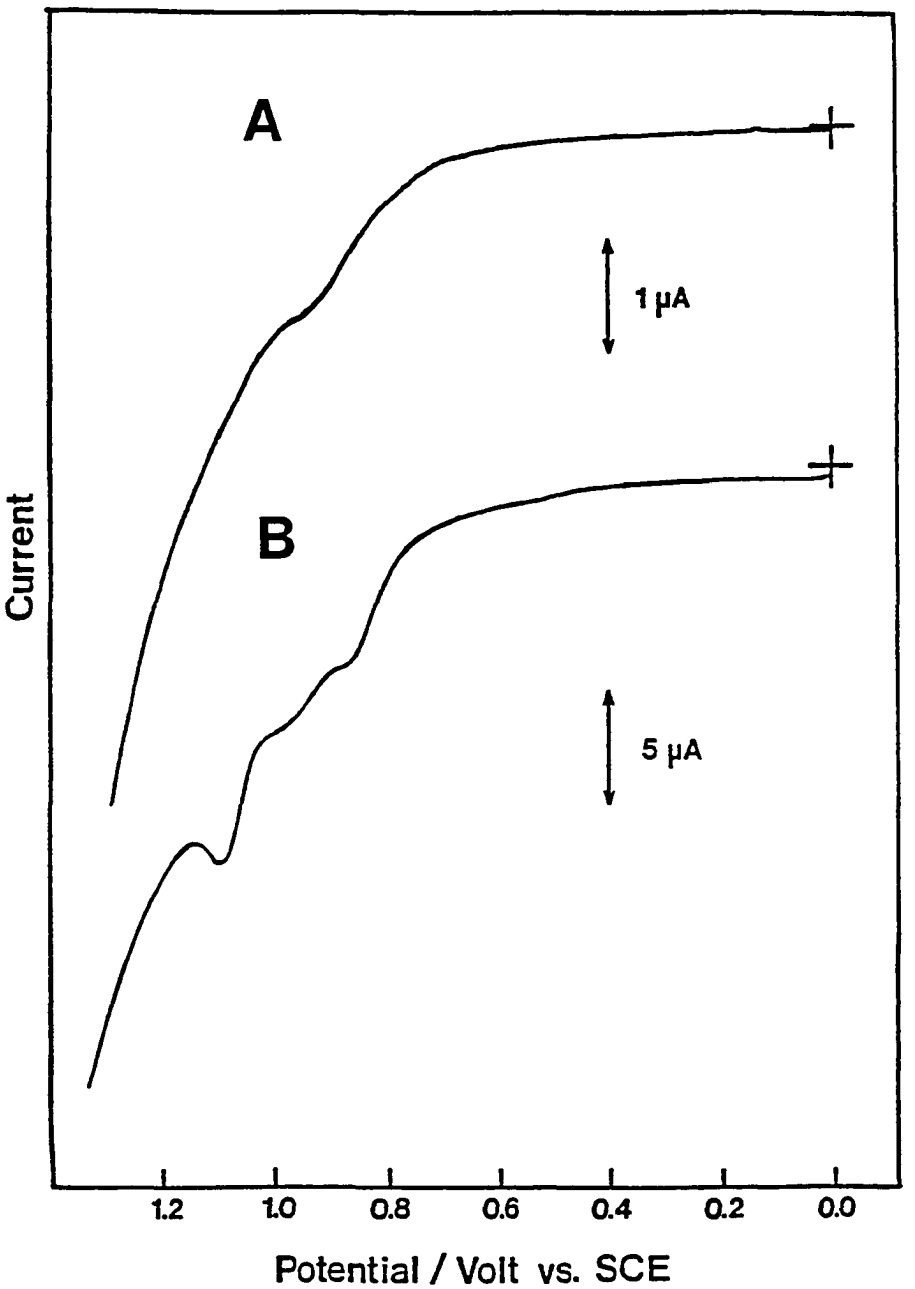

Fig. 29 Linear sweep voltammograms obtained at the PGE of LC component E in pH 7.0 phosphate buffer ($u = 0.5$ M). Sweep rate: (A) 5 mVs^{-1} and (B) 200 mVs^{-1}.

component E is electrochemically oxidized at more positive potentials than is TPP. At faster sweep rates LC component E gives three closely spaced oxidation peaks(Fig. 29B). A typical cyclic voltammogram of LC component E at pH 7.0 is shown in Fig. 30. On the second cycle no well defined reduction or oxidation peaks appear. Mass spectrometry of the solid (70 eV, 200°C) gave the following results, m/e (relative abundance): 237 (0.7%), 236 (M^+, 7.3%), 220 (1.6%), 219 (1.1%), 218 (M^+-H_2O, 9.2%), 202 (0.9%), 201 (2.3%), 200 (6.7%), 176 (1.1%), 175 (10.7%), 174 (62.1%), 173 (29.4%), 147 (17.1%), 146 (100%), 145 (47.9%), 144 (11.1%), 131 (11.2%), 130 (62.7%), 129 (22.4%), 128 (21.9%), 121 (10.6%), 120 (71.5%), 119 (21.7%), 118 (23.9%), 117 (29.1%), 104 (11.8%), 103 (13.3%), 102 (11.0%).

Component E (ca. 500 ug) was derivatized with BSA (70 ul) in acetonitrile (70 ul) in a sealed vial at room temperature overnight or at 120°C for 30 min. EI- and CI-MS on the resulting trimethylsilyl derivative gave a single GC peak at t_R = 36.2 min (Fig. 31). The compound eluted under this peak had a molar mass of 524 g (Table 8). Derivatization with BSA-d_9 under the same conditions gave a single GC peak (t_R = 34.2 min). CI-MS of this derivative showed it to have a molar mass of 560 g (Table 8). These mass spectral data indicate that LC component E has a molecular weight of 236 and that it forms a tetra-trimethylsilyl derivative. Authentic dioxindolylalanine (8) shows identical U.V., mass

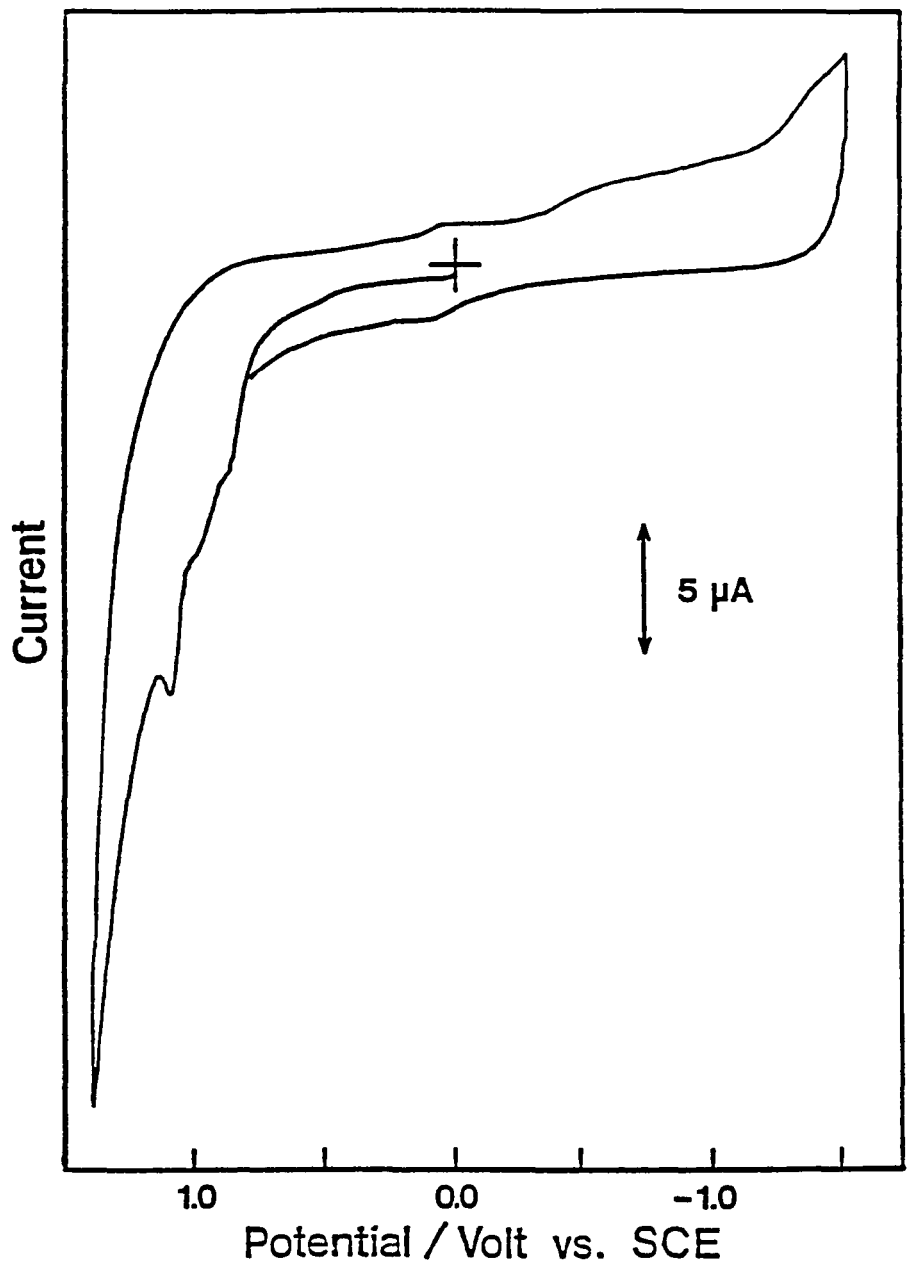

Fig. 30 Cyclic voltammogram of LC component E obtained at the PGE in pH 7.0 phosphate buffer (u = 0.5 M).

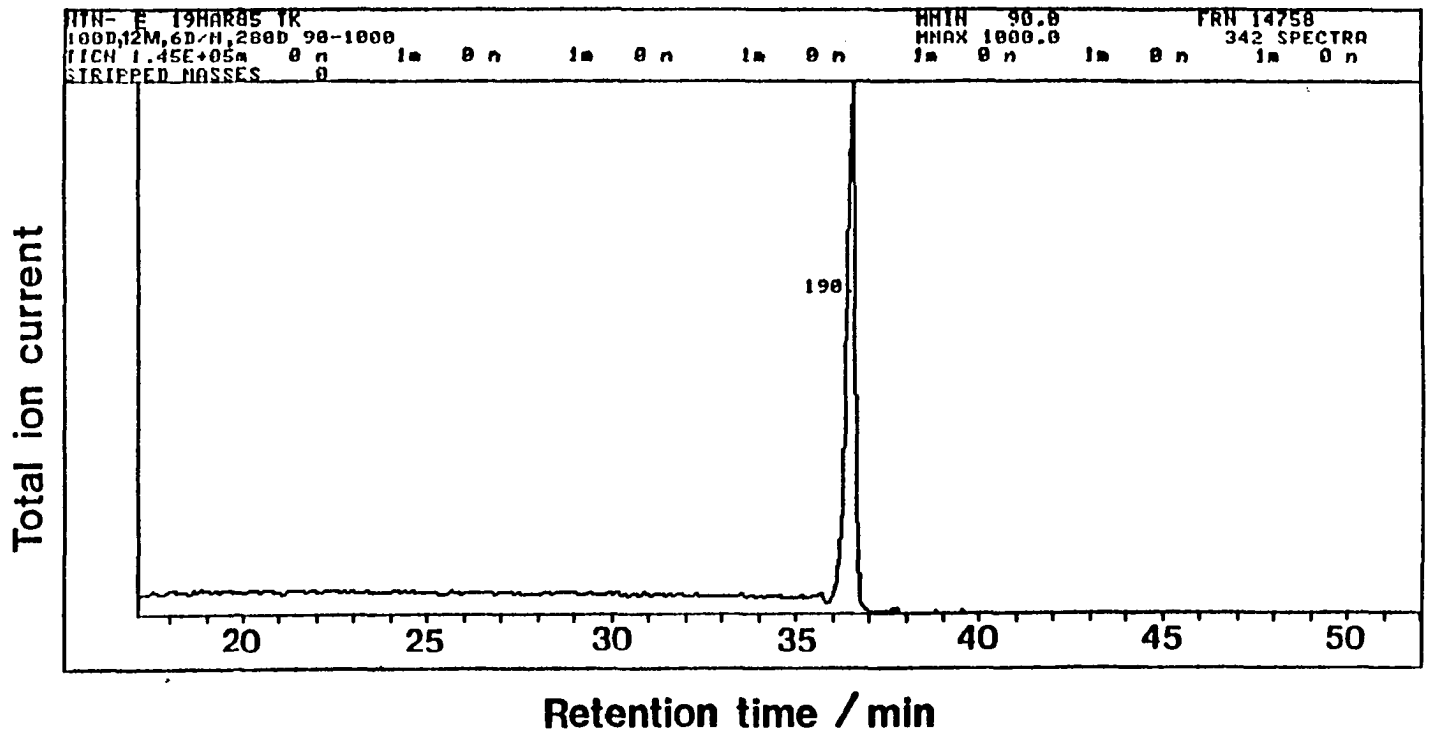

Fig. 31 Total ion current chromatogram of LC component E silylated with BSA at 120°C for 30 min.

Table 8. GC-MS data for liquid chromatographic component E formed by electrochemical oxidation of tryptophan

Derivative	Retention time/min	Ionization type	Major MS peak/ m/e (relative abundance)	Compound
BSA	36.2	EI	524 (M^+, 0.5%); 509 (M^+-CH_3, 0.4%); 419 (0.2%); 403 (0.2%); 365 (0.7%); 336 (0.2%); 294 (1.8%); 293 (5.9%); 292 (4.3%); 279 (1.6%); 278 (0.7%); 277 (1.9%); 247 (0.8%); 246 (1.1%); 245 (3.3%); 222 (0.5%); 221 (1.8%); 220 (2.6%); 206 (1.5%); 205 (2.6%); 204 (1.7%); 192 (1.3%); 191 (1.2%); 190 (1.6%); 185 (5.3%); 184 (14.9%); 183 (100%); 149 (2.2%); 148 (2.5%); 147 (12.6%).	
BSA	36.2	CI	567 (0.4%); 566 (0.6%); 565 ($M+C_3H_5^+$, 1.0%); 555 (2.5%); 554 (4%); 553 ($M+C_2H_5$, 9.1%); 527 (10%); 526 (24.5%); 525 ($M+H^+$, 52.8%); 524 (M^+, 35.7%); 511 (23.7%); 510 (44.9%); 509 (M^+-CH_3, 100%); 454 (5.9%); 453 (14.9%); 452 (M^+-72, 6.8%); 437 (27.6%); 436 (10.5%); 435 ($M^+-OSi(CH_3)_3$, 21.3%); 365 (6.2%); 364 (6.2%); 363 (M^+-NH-2x$Si(CH_3)_3$, 17.3%); 320 (1.2%); 319 (3.9%); 318 (1.1%); 294 (1.3%); 293 (2.5%); 292 (3.7%); 279 (1.7%); 278 (0.8%); 277 (1.0%); 247 (3.3%); 246 (3.8%); 245 (3.2%).	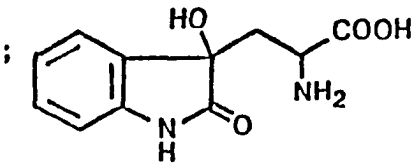 8

Table 8(continued)

Derivative	Retention time/min	Ionization type	Major MS peaks/ m/e (relative abundance)	Compound
d_9-BSA	34.2	CI	603 (0.7%); 602 (1.2%); 601 ($M+C_3H_5^+$, 2.3%); 591 (3.5%); 590 (6.7%); ($M+C_2H_5^+$, 14.1%); 563 (12.8%); 562 (27.0%); 561 ($M+H^+$, 57.6%); 560 (M^+, 38.1%); 544 (25.8%); 543 (50%); 542 (M^+-CD_3, 100%); 482 (0.4%); 481 (1.2%); 480(3.6%); 464 (6.0%); 463 (11.5%); 462 (M^+-$OSi(CD_3)_3$, 31%); 445 (1.0%); 444 (1.6%); 443 (2.2%); 389 (1.0%); 388 (2.2%); 387 (6.3%); 364 (0.9%); 363 (1.9%); 362 (1.0%); 311 (0.7%); 310 (1.0%); 229 (0.6%); 228 (0.7%); 227 (2.4%); 210 (0.7%); 209 (0.8%); 208 (1.0%); 183 (0.5%); 182 (0.6%); 181 (1.0%); 164 (0.8%); 163 (1.7%); 162 (8.5%); 156 (1.1%); 155 (1.3%); 154 (1.7%).	

and GC-MS properties and electrochemical behavior to those reported for LC component E.

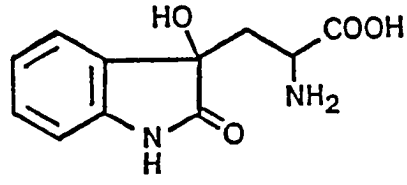

8

Liquid chromatographic component F

LC component F was a pale yellow solid. In water it exhibited three U.V. absorption bands at λ_{max} = 280 (sh), 250, and 200 nm (Fig. 32). LC component F is electrochemically active and shows a single voltammetric oxidation peak at the PGE (Fig.33). The linear E_p *vs.* pH relationship for this peak at a sweep rate 5 mVs^{-1} is given in Eqn. (17).

$$E_p(\text{pH } 2.0 - 11.0) = [1.34 - 0.065\ \text{pH}]\ V \qquad (17)$$

A typical cyclic voltammogram of component F at pH 7.0 is shown in Fig. 34. After scanning through the oxidation peak, two small reduction peaks appear at approximately the same potential as peaks I_c and II_c of TPP (Fig. 9D) and, on the second sweep towards positive potentials two oxidation peaks appear at approximately the same potentials as peaks II'_a and III'_a of TPP, respectively. The mass spectrum of LC component F (70 eV, 200°C) was as follows, m/e (relative abundance): 221 (1.0%), 220 (M^+, 6.0%), 203 (0.2%), 202 (M^+-

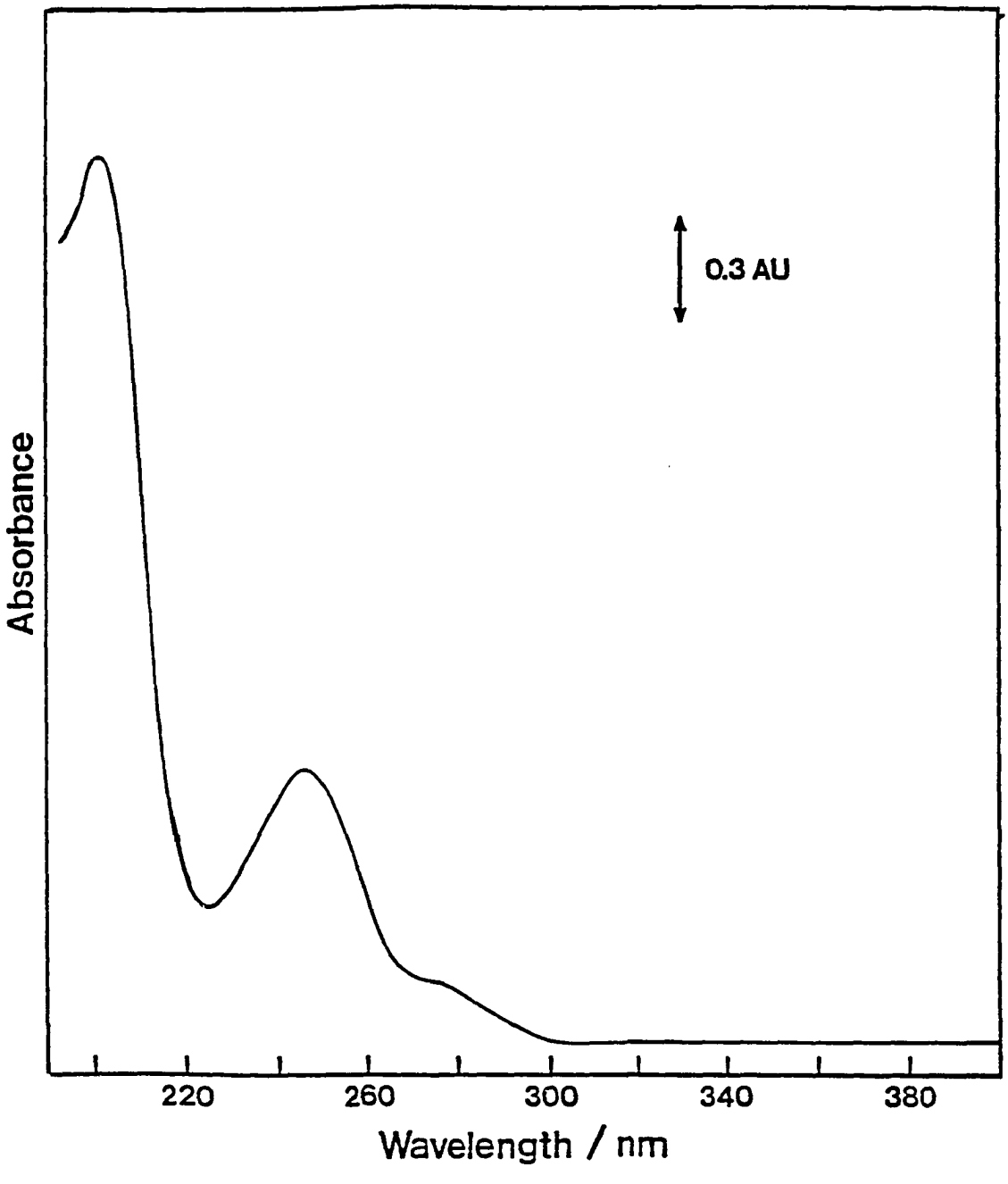

Fig. 32 U.V. spectrum of LC component F in water.

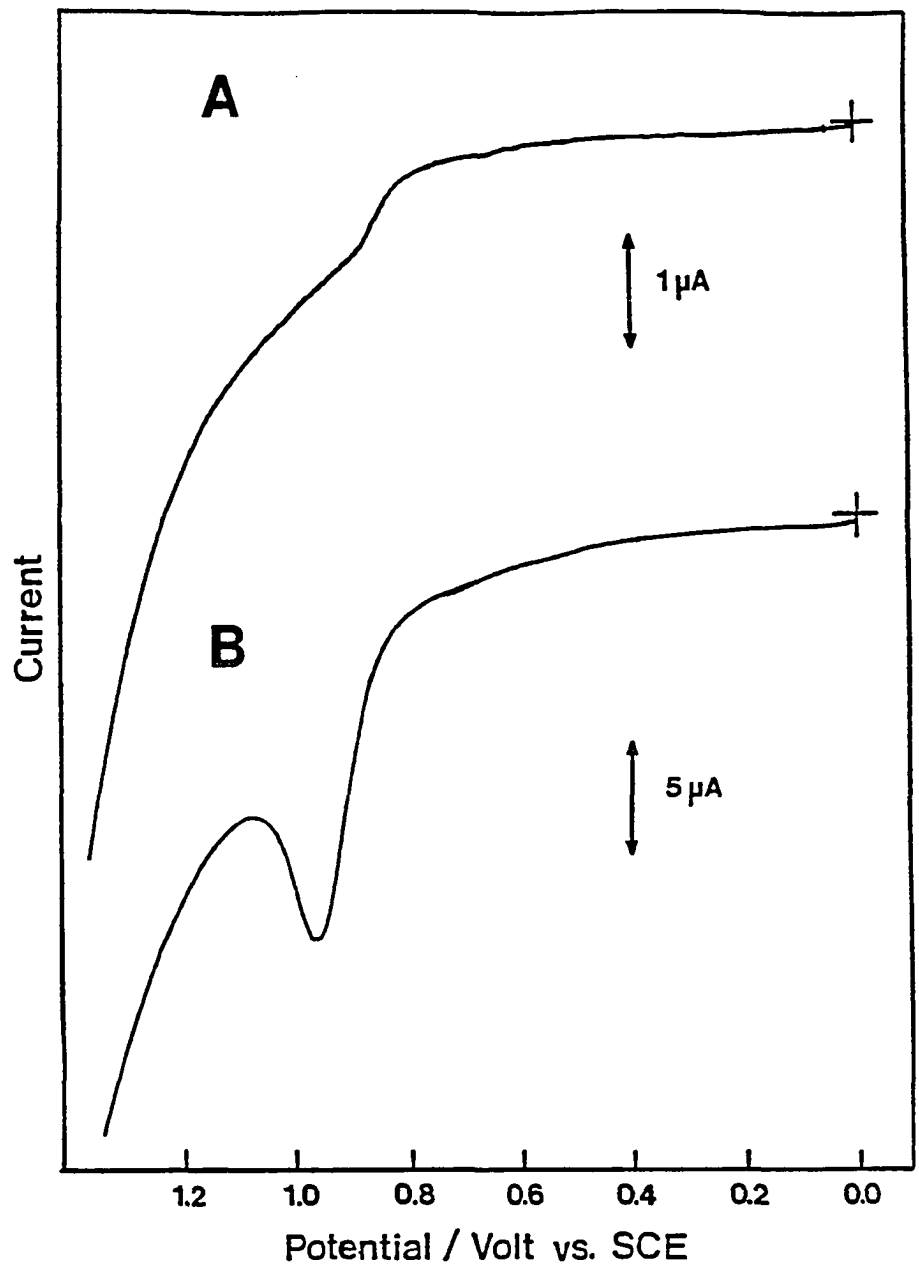

Fig. 33 Linear sweep voltammograms obtained at the PGE of LC component F in pH 7.0 phosphate buffer (u = 0.5 M). Sweep rate: (A) 5 mVs^{-1}, (B) 200 mVs^{-1}.

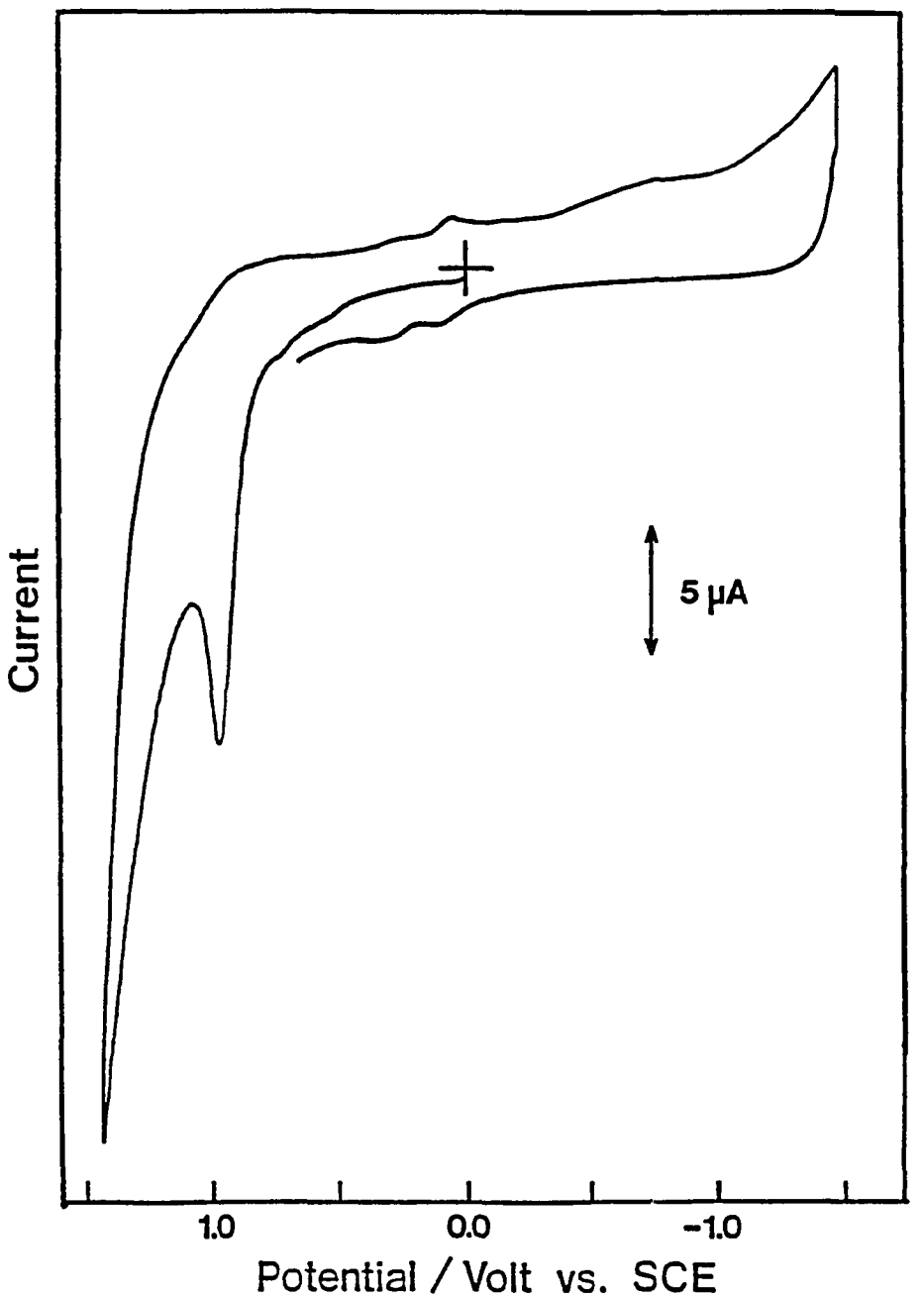

Fig. 34 Cyclic voltammogram of LC component F obtained at the PGE in pH 7.0 phosphate buffer (u = 0.5 M).

H_2O, 1.6%), 175 (3.0%), 174 (2.5%), 173 (1.5%), 159 (1.0%), 158 (3.8%), 157 (3.0%), 148 (0.9%), 147 (9.7%), 146 (100%), 134 (1.6%), 133 (16.9%), 132 (20.1%), 119 (2.0%), 118 (5.6%), 117 (5.7%), 105 (2.2%), 104 (7.5%), 103 (2.6%).

Component F (ca. 500 ug) could be silylated with BSTFA (70 ul) in acetonitrile (70 ul) at room temperature for 24h. GC of the resulting derivative showed a single peak at t_R = 32.8 min (Fig. 35). EI- and CI-MS of this derivative indicated it had a molar mass of 436 g (Table 9). Derivatization of component F (ca. 500 ug) with MTBSTFA (70 ul) in acetonitrile (70 ul) at room temperature for 24 h gave a tert-butyldimethylsilyl derivative which showed a single GC peak at t_R = 38.6 min. EI- and CI-MS of this derivative indicated it had a molar mass of 562 g. Hence, component F has a molecular weight of 220 and can be silylated at three

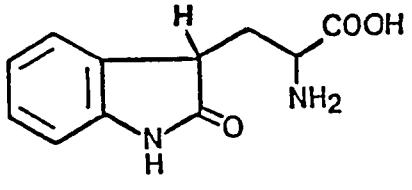

6

positions. Authentic oxindolylalanine (6) showed identical GC, GC-MS and electrochemical properties to that reported above for component F.

Controlled potential coulometry of oxindolylalanine (6) at 1.1 V in dilute HCL (pH 2.4) gives n-values of 2 ± 0.2.

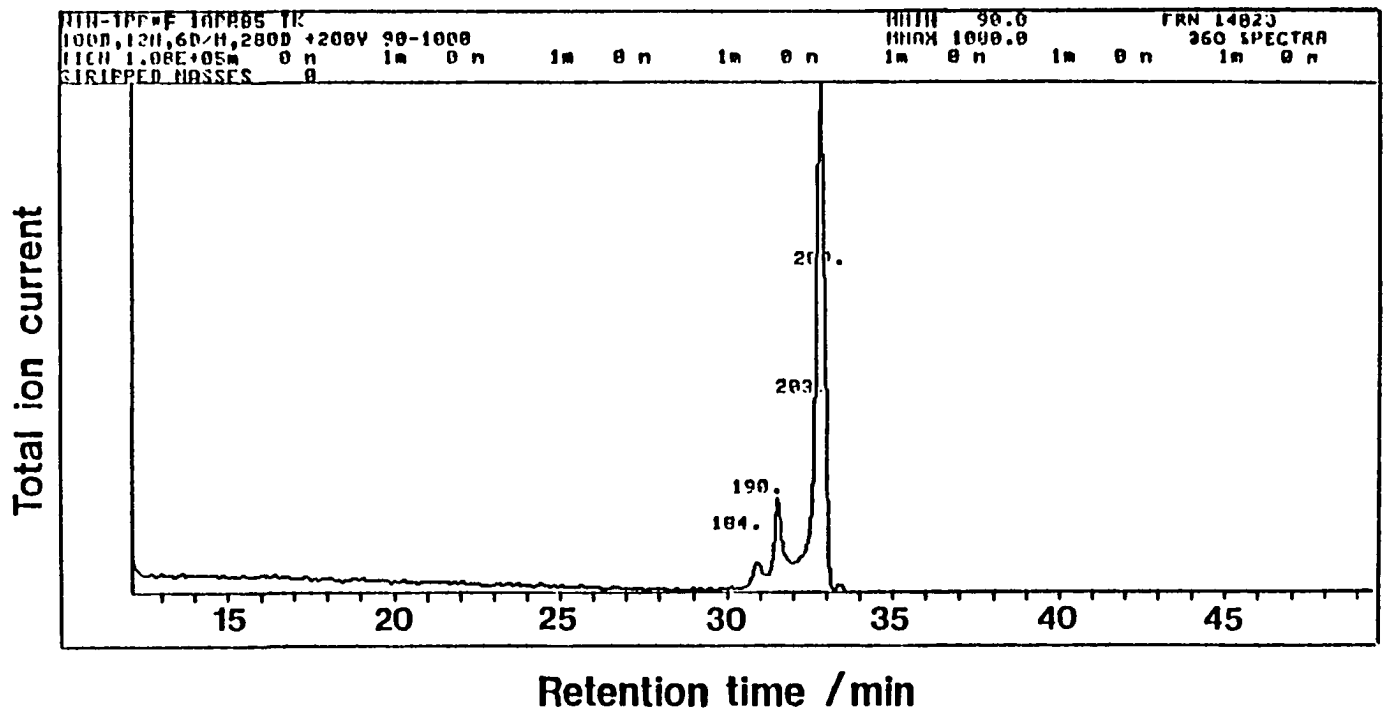

Fig. 35 Total ion current chromatogram of LC component F silylated with BSTFA at room temperature for 24 h.

Table 9. GC-MS data for liquid chromatographic component F formed by electrochemical oxidation of tryptophan

Derivative	Retention time/min	Ionization type	Major MS peak/ m/e (relative abundance)	Compound
BSTFA	32.8	EI	436 (M^+, 0.1%); 422 (0.0%); 421 (M^+-CH_3, 0.2%); 320 (0.6%); 319 (1.5%); 318 (1.4%); 292 (12.9%); 291 (35%); 290 (100%); 276 (1.1%); 275 (0.7%); 274 (1.7%); 230 (1.5%); 229 (1.0%); 228(0.2%); 220 (0.8%); 219 (34%); 218 (7.9%); 204 (1.7%); 203 (4.9%); 202 (17.7%); 149 (0.7%); 148 (1.6%); 174 (8.2%); 132 (2.6%); 131 (2.6%); 130 (2.9%); 102 (0.8%); 101 (1.7%); 100 (3.5%).	
BSTFA	32.8	CI	538 (0.2%); 537 ($M+C_2H_5^+$, 0.3%); 511 (1.6%); 510 (2.5%); 509 (M^+H^+, 6.0%); 495 (0.8%); 494 (1.8%); 493 (M^+-CH_3, 3.6%); 478 (0.1%); 477 (0.1%); 467 (0.3%); 466 (0.8%); 465 (1.6%); 439 (0.8%); 438 (1.9%); 437 (5.3%); 423 (0.8%); 422 (1.7%); 421 (4.6%); 407 (0.2%); 406 (0.4%); 405 (1.2%); 395 (0.2%); 394 (0.4%); 393 (1.1%); 367 (0.3%); 366 (0.7%); 365 (2.7%); 349 (1.8%); 348 (1.2%); 347 (2.3%); 320 (0.8%); 319 (2.0%); 318 (2.7%); 292 (20.3%); 291 (59.5%); 290 (100%); 278 (1.0%); 277 (2.0%); 276 (5.7%); 248 (0.8%); 247 (1.1%); 246 (2.7%).	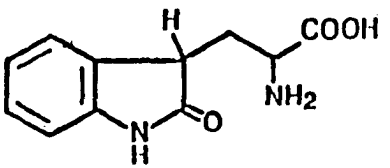 6

Table 9 (continued)

Derivative	Retention time/min	Ionization type	Major MS peak/ m/e (relative abundance)	Compound
MTBSTFA	38.6	EI	562 (M^+, 0.2%); 507 (0.4%); 506 (1.0%); 505 (M^+-$C(CH_3)_3$, 2.3%); 405 (0.4%); 404 (1.1%); 403 (M^+-$COOSiC(CH_3)_5$, 2.7%); 305 (0.9%); 304 (1.6%); 303 (5.8%); 262 (5.9%); 261 (21.5%); 260 (100%); 247 (1.3%); 246 (4.4%); 245 (2.3%); 204 (1.1%); 203 (2.7%); 202 (10.7%); 162 (1.0%); 161 (1.1%); 160 (3.4%); 149 (1.6%); 148 (2.3%); 147 (9.0%).	

The electrolyzed solution was yellow. Product solution was freeze-dried and the resulting solid mass was dissolved in water and separated by high pressure liquid chromatography using a column of Shodex OH-pak (50 cm x 2 cm) and water as the eluent (2 ml min^{-1}). After complete electrolysis of 1 m$\underline{M}$ oxindolylalanine at 1.1 V in dilute HCl pH 2.4 liquid chromatogram of the resulting product showed two HPLC peaks (I and II). The components eluted under HPLC peaks I and II have the same U.V. spectra and HPLC retention volumes that obtained for components A and B (Figs. 18 and 19). If, however, the electrooxidation was not taken to completion then chromatography on the products showed two new HPLC

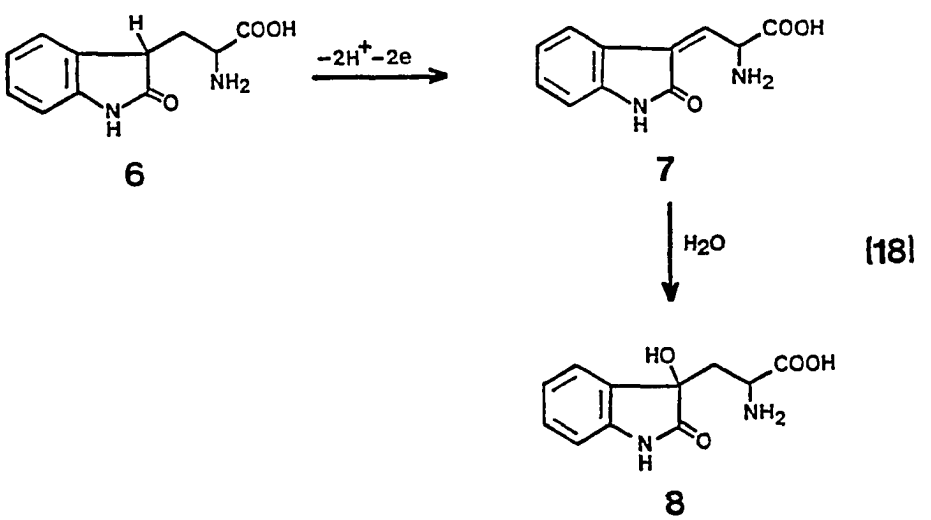

[18]

peaks III and IV (Fig. 36). The U.V. and mass spectra of component eluted under LC peak III were identical to that of authentic dioxindolylalanine (8). LC peak IV is due to unoxidized oxindolylalanine (6). The proposed scheme for the electrochemical oxidation of oxindolylalanine is shown

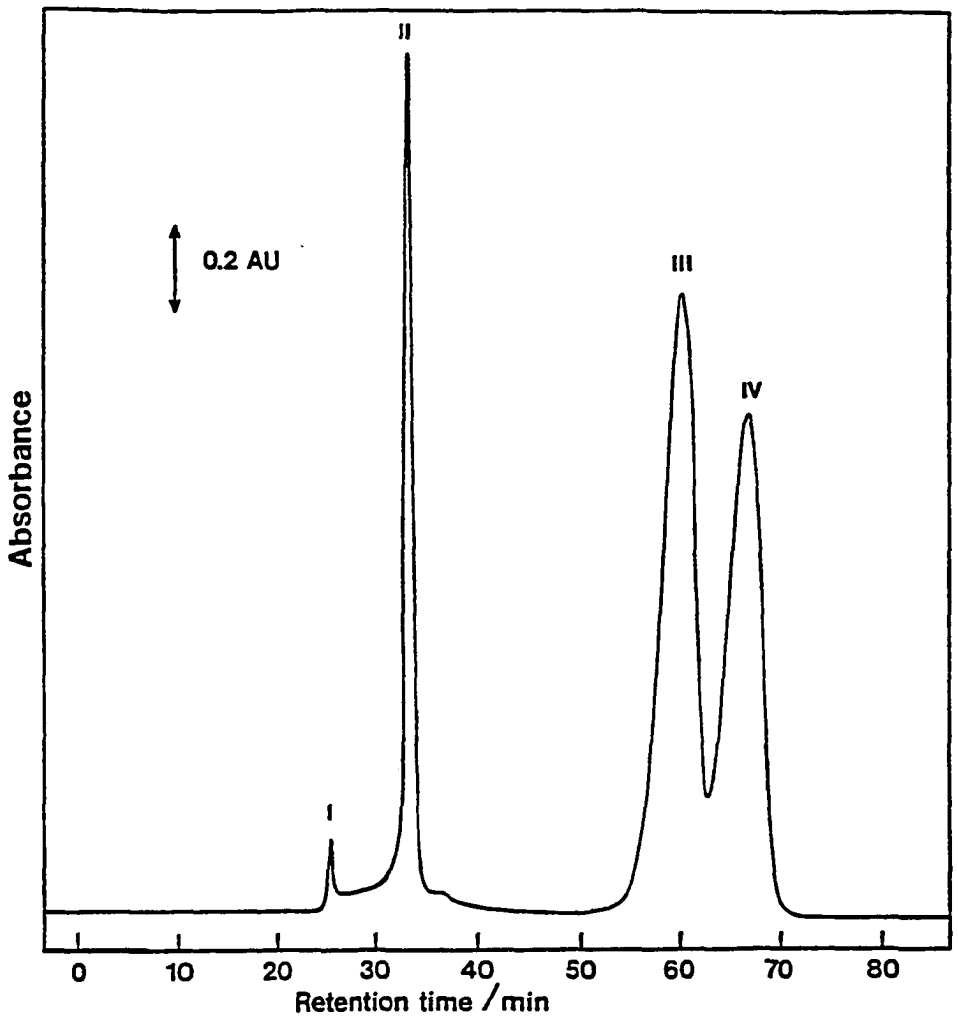

Fig. 36 HPLC chromatogram of oxindolylalanine oxidized at 1.1 V in dilute HCl (pH 2.4) using a column of Shodex OH-Pak (50 x 2 cm) and water as the eluent (2 $ml\,min^{-1}$).

in Eqn. 18. Initial two electron oxidation ($2\underline{e}$-$2H^+$) of oxindolylalanine (6) leads to the 3-methylene-2-oxindole derivative (7). Then, 7 undergoes nucleophilic attack by water and gives dioxindolylalanine (8).

Liquid chromatographic component G

LC component G was a yellow solid . It was formed in exceedingly small amounts (< 1% yield). In phosphate buffer (pH 1.98) component G exhibited characteristic U.V. absorption bands at λ_{max} = 360, 285 (sh), 255, 220, and 200 nm (Fig. 37). This spectrum is very similar to that of authentic kynurenine (λ_{max} at pH 1.98 = 360, 285 (sh), 250, 226, and 197 nm). In addition, the retention volume of LC component G and authentic kynurenine were the same on a

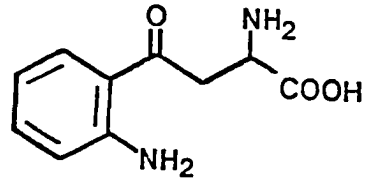

11

Sephadex G-10 column using water as the eluent. The product G had same cyclic voltammetric behavior as that of kynurenine at pH 7.0. Thus, it was concluded that LC component G is kynurenine (11). As the product G is obtained in very small amount, no mass spectral studies were carried out to compare with authentic kynurenine.

However, the voltammetry of authentic kynurenine (11)

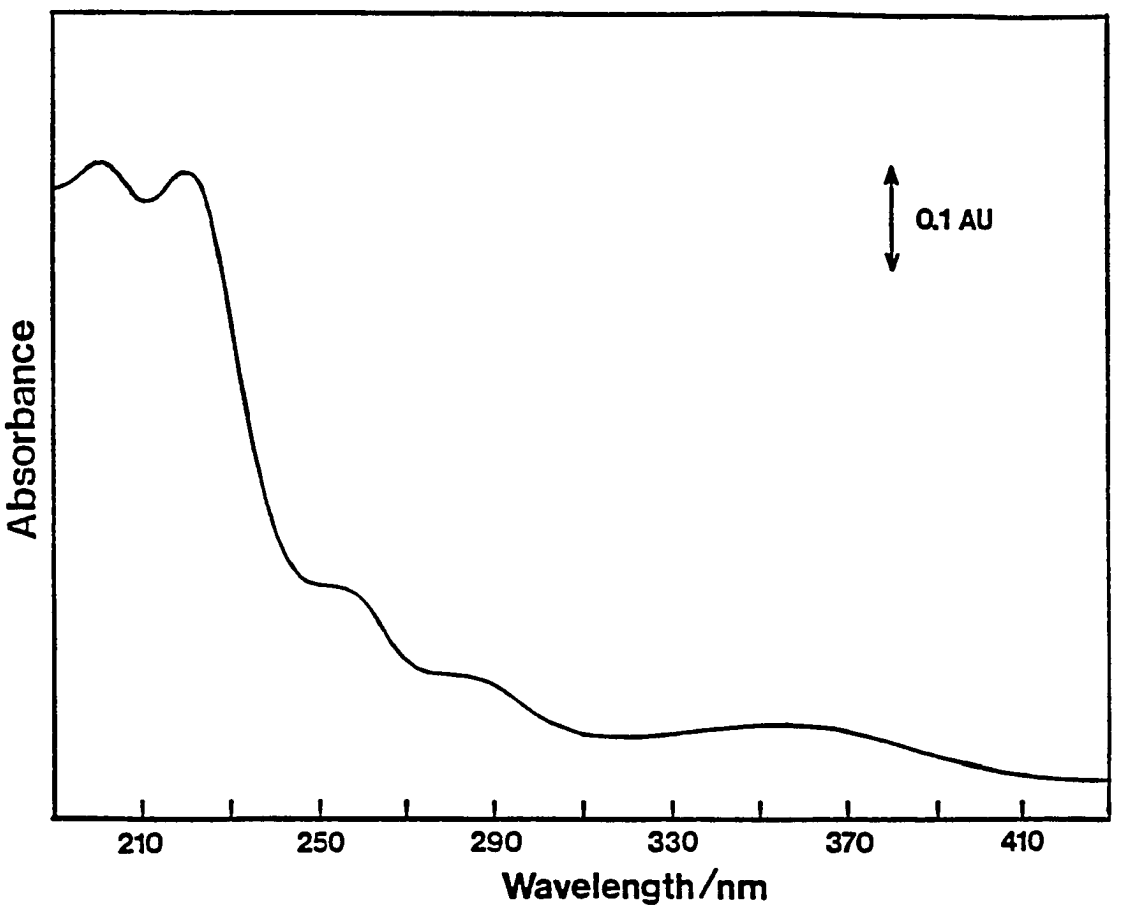

Fig. 37 U.V. spectrum of LC component G in pH 1.98 phosphate buffer (u = 0.5 M).

was studied. At a sweep rate of 5 mVs^{-1} at the PGE, kynurenine shows four oxidation peaks (O_1, O_2, O_3, and O_4). The E_p *vs.* pH relationships for these peaks are shown in Eqns. 19-22.

$$\text{Peak } O_1 : E_p(\text{pH } 2.0 - 5.8) = 0.8 \text{ V} \qquad (19)$$
$$E_p(\text{pH } 5.8 - 11.00) = [1.07 - 0.049 \text{ pH}] \text{ V}$$

$$\text{Peak } O_2 : E_p(\text{pH } 2.0 - 5.8) = [0.93 - 0.015 \text{ pH}] \text{ V} \qquad (20)$$

$$\text{Peak } O_3 : E_p(\text{pH } 2.0 - 5.8) = [1.0 - 0.002 \text{ pH}] \text{ V} \qquad (21)$$
$$E_p(\text{pH } 5.8 - 11.0) = [1.29 - 0.055 \text{ pH}] \text{ V}$$

$$\text{Peak } O_4 : E_p(\text{pH } 2.0 - 3.7) = [1.15 - 0.023 \text{ pH}] \text{ V} \qquad (22)$$

A cyclic voltammogram of kynurenine (11) is shown in Fig. 38. The initial sweep towards negative potentials showed a reduction peak at *ca.* -1.4 V (pH 6.88). Hence, kynurenine is electrochemically reducible. At a sweep rate of 200 mVs^{-1} E_p values for the voltammetric reduction peak of 11 at pH 1.98, 3.68, 5.11, 5.78 and 6.88 are -1.05, -1.17, -1.27, -1.32, and -1.4 V, respectively. At pH $\geq$ 7.0 this reduction peak disappears.

Liquid chromatographic component H

LC component H was formed in even lower yield than component G. In water it showed a well-defined U.V. spectrum, λ_{max} = 285, 223 (sh), and 200 nm (Fig. 39). Insufficient material could be obtained to study the mass or GC-MS

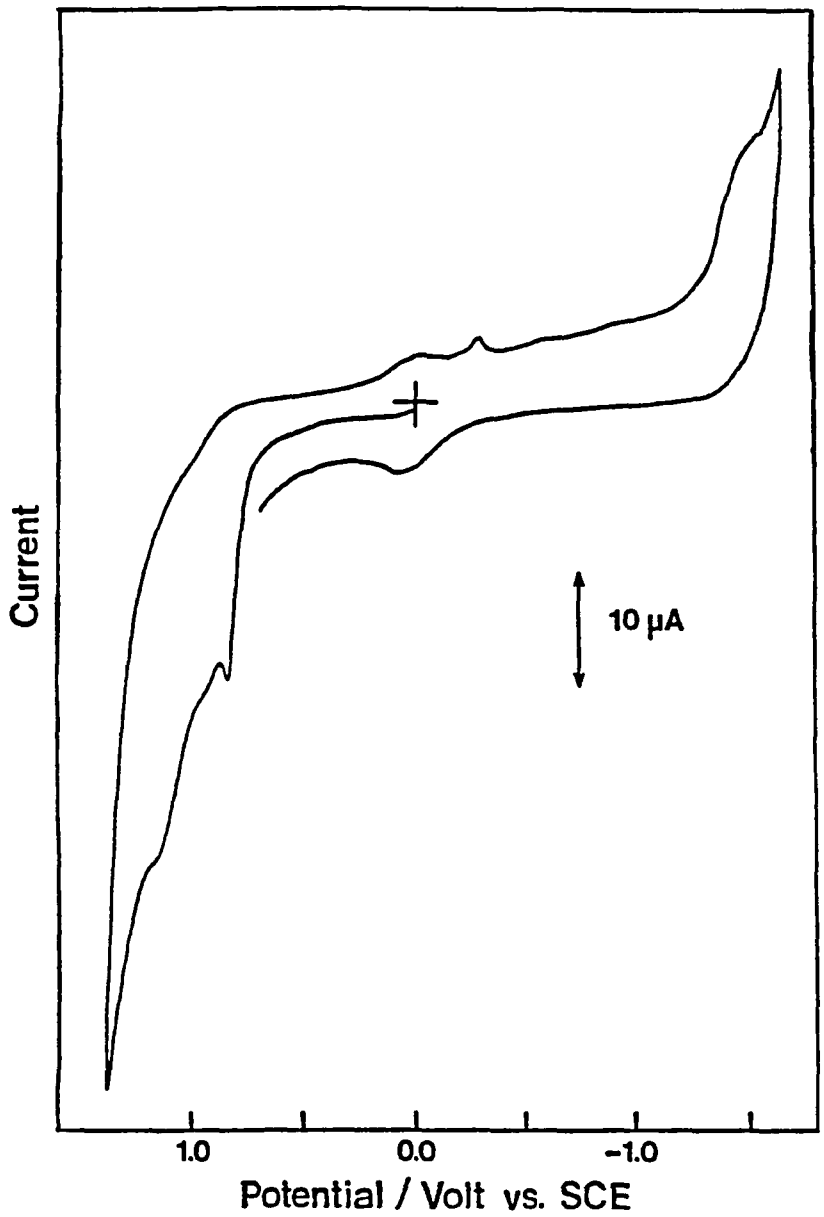

Fig. 38 Cyclic voltammogram of Kynurenine obtained at the PGE in pH 7.0 phosphate buffer (u = 0.5 M).

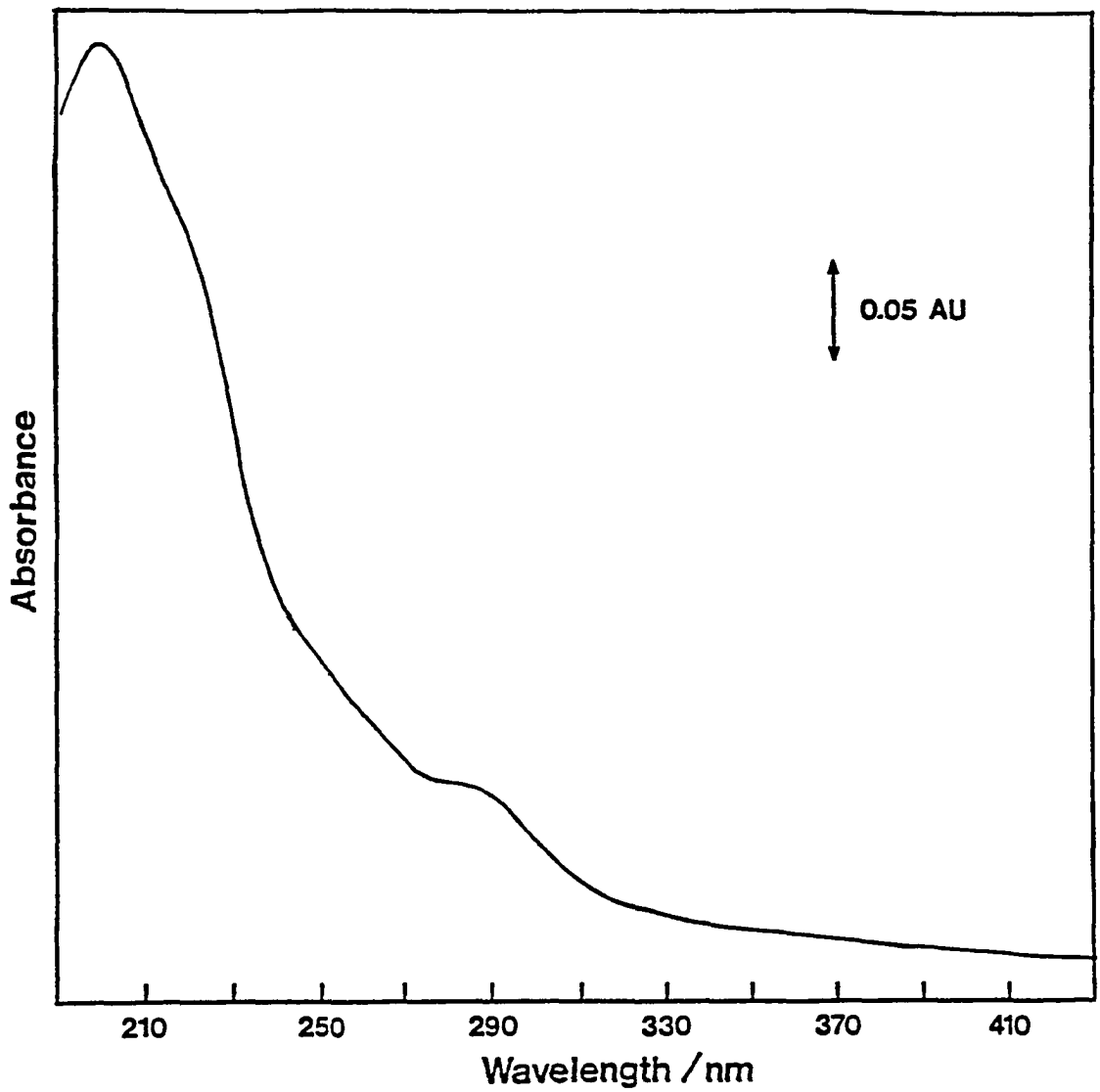

Fig. 39 U.V. spectrum of LC component H in water.

of this compound. However, the LC retention volume and U.V. spectrum of LC component H is quite different to an anticipated product, formylkynurenine.

Liquid chromatographic component I

The U. V. and mass spectra of component I were identical to that of authentic tryptophan.

3. A. 6. Mechanistic pathway for the electrochemical oxidation of L-tryptophan

The important experimental observations concerning the electrochemical oxidation of TPP will first be summarized. Both TPP and its primary electrooxidation product are adsorbed at the PGE. Formation of a prepeak (peak I'_a) at slow sweep rates ($\leq$ 10 mVs^{-1}) suggests that the primary product is more strongly adsorbed than TPP. Voltammetric peak I_a is due to an irreversible, pH-dependent, 2e reaction between pH 2.0-11.0. However, for the prolonged controlled potential electrolysis experimental n-values were $\geq$ 4. This supports the conclusion that the primary 2e product disappears by way of one or more follow up chemical reactions to give products which can be further oxidized. The spectroelectrochemistry of TPP (Fig. 14) indicates that at least one product is formed which absorbs at ca. 240 - 250 nm and which is further oxidized at the same potential as TPP. Thin-layer spectroelectrochemistry suggests that two intermediate

species are generated. Also, cyclic voltammetry indicates that two or more electroactive (reducible) intermediates are generated in the electrooxidation of TPP.

Identified products include oxindolylalanine (6), dioxindolylalanine (8), two stereoisomers of the tricyclic pyrroloindole 3 and kynurenine (11). It also seems probable that two or more oligomeric/polymeric species, responsible for LC peaks A and B, are formed. At high pH (ca. pH 10.65) the dihydroxypyrroloindole 13 is formed by the cyclization of dioxindolylalanine (8).

It is proposed, therefore, that the primary peak I_a electrooxidation step for TPP is a 2e reaction giving the 3-methylene-imine 1 (Fig. 40). Since fast sweep cyclic voltammetry of TPP does not show a reversible reduction peak coupled to oxidation peak I_a it must be concluded that the

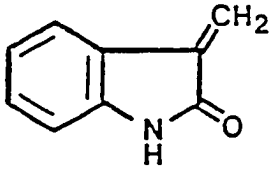

14

3-methylene-imine 1 is extremely reactive. The 3-methylene-imine 1 has not previously been proposed as an intermediate in the oxidation of TPP. It is also believed that compounds such as 3-methyleneoxindole (14), which has a similar structure to 1, are extremely reactive particularly towards dimerization or polymerization[89,90]. Thus, it seems reasonable

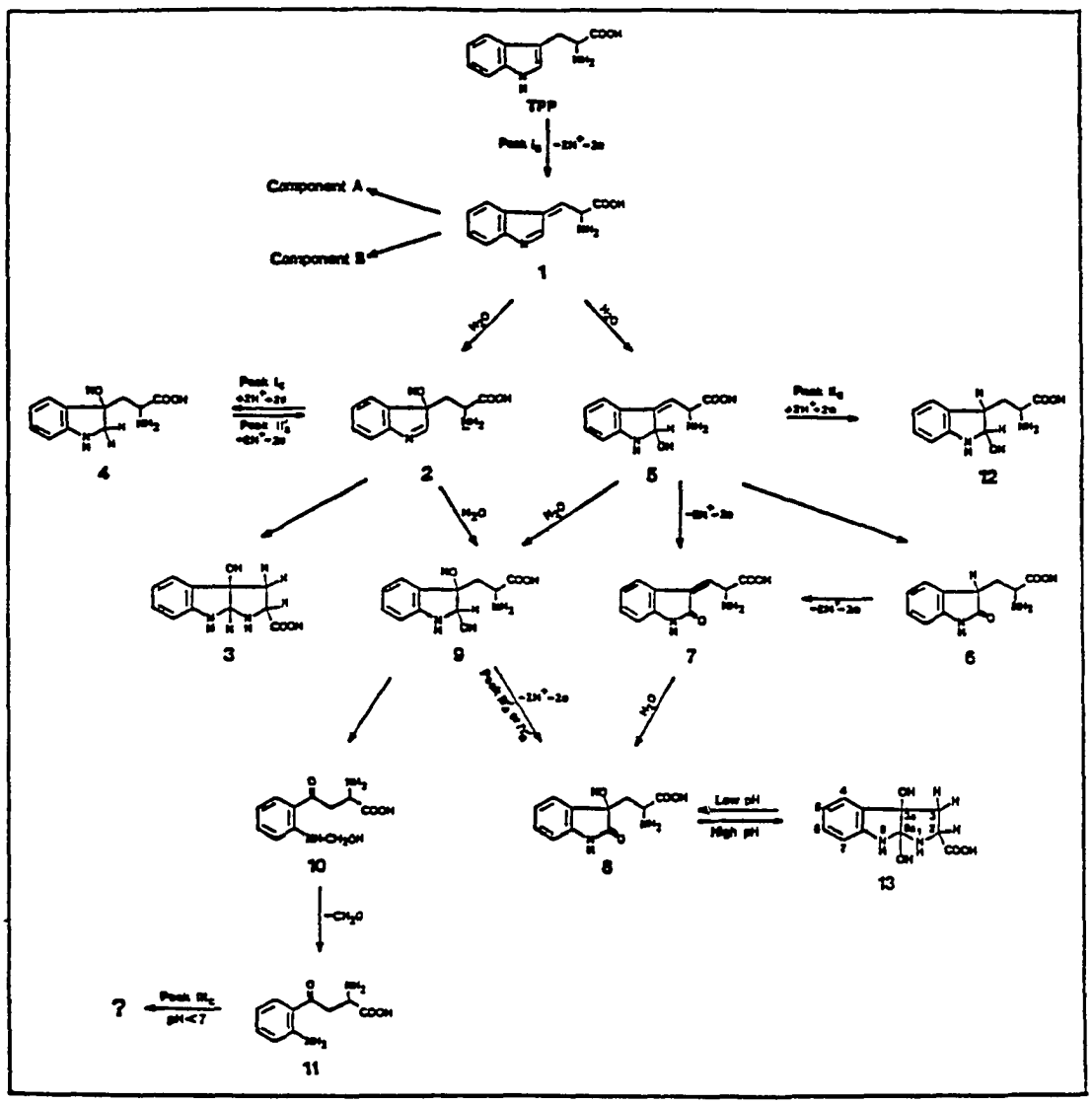

Fig. 40 Reaction scheme proposed for the electrochemical oxidation of tryptophan.

to conclude that one or more reaction pathways for 1 involve formation of oligomers or polymers. The TPP electrooxidation products responsible for LC peaks A and B appear to be due to oligomeric or polymeric materials. Unfortunately, at this time we have been unable to obtain structural information on these products.

The 3-methylene-imine 1 must be a strong electrophile which is highly susceptible towards attack by nucleophiles present in the reaction solution. TPP, water, and probably, even 1 are nucleophiles present in the bulk solution. Reaction of 1 with TPP or even with the exocyclic amino group of 1 no doubt leads to oligomeric or, ultimately, to polymeric products. Nucleophilic attack by water would lead to the formation of indolenine 2 and 5 (Fig. 40). Intracyclization of indolenine 2 gives the stereoisomers of the tricyclic pyrroloindole 3. It will be recalled that cyclic voltammograms of TPP show that several reducible intermediates are formed as a result of the peak I_a oxidation (Fig. 9). The indolenine 2 would be expected to be an electrochemically reducible species. A $2e\text{-}2H^+$ reduction of 2 across the N(1)=C(2) imine double bond would give the indoline 4 (i.e., 2,3-dihydro-3-hydroxytryptophan, Fig. 40). The latter compound has been speculated to be an intermediate in the peroxidase-catalyzed oxidation of TPP[91]. Since indolenine 2 is an unstable compound and is only one of several intermediates formed in the electrooxidation of TPP it is difficult

to specify the exact reduction peak in cyclic voltammograms of TPP which is responsible for indolenine 2. Thin-layer spectroelectrochemical experiments, however, show that one intermediate is generated in the peak I_a oxidation which absorbs at about 275 nm and is probably responsible for cyclic voltammetric reduction peak I_c (vide supra). Furthermore, it is known that indolenines having structures similar to 2 absorb at about 275 nm, particularly when protonated at N(1)[1,92]. Thus, it is probable that intermediate 2 has a very similar U.V. spectrum to TPP particularly in acidic solutions. Hence, rapid formation of intermediate 2 upon electrochemical oxidation of TPP would account for the lag period observed in thin-layer spectroelectrochemical experiments at pH 4.8 (see Fig. 14 and associated discussion). Cyclic voltammetry of TPP indicates that the product of reduction peak I_c may be quasi-reversibly oxidized in the oxidation peak II'_a reaction. It seems reasonable to conclude that the peak II'_a reaction involves the $2e$-$2H^+$ oxidation of 4 to 2 (Fig. 40). Cyclic voltammetric peak I_c decreases in height relative to oxidation peak I_a with increasing pH. This is expected if the tricyclic pyrroloindole 3 is formed by intramolecular cyclization of indolenine 2 as shown in Eqn. 23. This is so because with increasing pH protonation of the exocyclic amino function of intermediate 2 would decrease which in turn would facilitate the intramolecular cyclization reaction. With increasing pH the reaction of indolenine 2 to tricyclic pyrroloindole 3 should

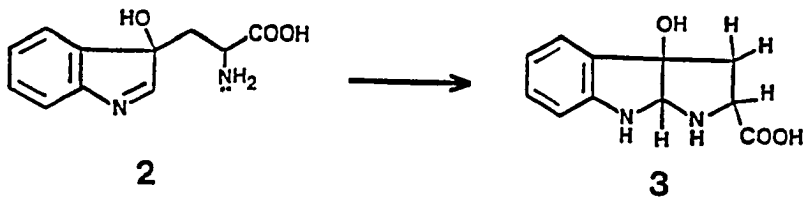

2 3 [23]

occur more rapidly such that less of indolenine 2 would be available for electrochemical reduction.

The yield of the tricyclic pyrroloindole 3 formed by the peak I_a oxidation of TPP is very small. Indeed, the stereoisomers of 3 are only observed as products of incomplete oxidations of TPP. The E_p data reported earlier for TPP and 3, summarized in Table 10, show that the latter compound should be electrochemically oxidized at the potentials used to electrolyze TPP. Thus, the appearance of 3 as a product by the partial oxidation of TPP is due to rather slow intramolecular cyclization of intermediate 2 ($t_{1/2}$ = 7 min at pH 4.8 and 1 min at pH 7.0). In complete electrolyses the latter reaction proceeds to completion and all 3 formed is electrochemically oxidized.

The alternative product of nucleophilic attack on the intermediate 1 by water is 5 (Fig. 40). Formation of oxindolylalanine (6) provides strong evidence for the existence of 5. The expected chemistry of 5 can be used to rationalize the formation of three electrooxidation products of TPP as shown below. Rearrangement of 5 leads to oxindolylala-

Table 10

Peak potentials (E_p) for voltammetric oxidation of tryptophan and its electrooxidation products at the PGE.

Compound	pH[a]	E_p/Volt *vs.* SCE[b]
Trytptophan	2.33	0.92
	4.70	0.82
	7.36	0.7
	10.65	0.56
Tricyclic pyrroloindole, *3*	2.33	0.87
	4.70	0.75
	7.36	0.62
	10.65	0.45
Dioxindolylalanine, *8*	2.33	1.22
	4.70	1.07
	7.36	0.89
	10.65	0.65
Oxindolylalanine, *6*	2.33	1.19
	4.70	1.04
	7.36	0.86
	10.65	0.65
Kynurenine, *11*	2.33	0.80
	4.70	0.80
	7.36	0.71
	10.65	0.55

[a] Phosphate buffers, u = 0.5 *M*

[b] E_p values were measured at a sweep rate of 5 mV s^{-1}

nine (6). The yield of oxindolylalanine however, relative to that of dioxindolylalanine depends upon whether TPP is partially or completely electrolyzed. Partial oxidations of TPP give a larger yield of oxindolylalanine relative to dioxindolylalanine than do complete electrolyses (e.g., compare Fig. 19A and Fig. 19B). This suggests that at the potentials used to electrochemically oxidize TPP, oxindolylalanine is also slowly electrolyzed. E_p values for oxindolylalanine (Table 10) occur at somewhat more positive potentials than for TPP. However, a comparison of the voltammograms for 6 and TPP reveals that E_p for TPP corresponds to the rising portion of the voltammogram of oxindolylalanine. Thus, electrolysis of TPP at E_p for peak I_a should also bring about the slow oxidation of oxindolylalanine. Accordingly, the longer the electrolysis of TPP is allowed to proceed the more extensive will be the oxidation of oxindolylalanine . Experiments have shown that controlled potential electrooxidation of oxindolylalanine at the potentials used to electrolyze TPP at peak I_a leads to the formation of dioxindolylalanine. The latter reaction has not been studied in detail but it seems reasonable to propose that oxindolylalanine is initially oxidized in a $2e\text{-}2H^+$ process to the 3-methylene-2-oxindole derivative (7, Fig. 40) which upon nucleophilic attack by water gives dioxindolylalanine. The small decrease in U.V. absorbance at ca. 240-250 nm noted towards the end of controlled potential oxidations of TPP (Fig. 14) is probably related to the slow oxidation of

oxindolylalanine to dioxindolylalanine. It might also be noted that oxidation peak II_a which is observed as a very indistinct peak in voltammograms of TPP (Fig. 13) occurs at the potential expected for oxindolylalanine (Table 10).

Another route for the formation of dioxindolylalanine involves attack of water on 5 giving the 2,3-dihydroxyindoline (9) followed by electrochemical oxidation (Fig. 40). Alternatively, electrochemical oxidation of 5 to 7 followed by addition of water would also give dioxindolylalanine (Fig. 40).

Thin-layer spectroelectrochemical experiments indicate that an intermediate is generated by the peak I_a oxidation of TPP which absorbs at ca. 245 nm and , as it decays, gives products which absorb strongly at 213 nm. Furthermore, this intermediate is responsible for cyclic voltammetric reduction peak II_c. It is suggested that 5 is the intermediate responsible for these observations since its rearrangement product, oxindolylalanine, absorbs very strongly at short wavelengths and it would also be expected to be electrochemically reducible. The simplest and most probable reduction route for 5 would involve a $2e\text{-}2H^+$ reaction giving the 2-hydroxyindoline (12, Fig. 40).

Based on the information available it is very difficult to decide which species are responsible for peaks III_a' and IV_a' observed in cyclic voltammograms of TPP. It is possi-

ble that the 2,3-dihydroxyindoline (9) formed by the rather slow hydration of intermediates 2 or 5 could be responsible for at least one of these peaks leading to dioxindolylalanine.

Previously it was concluded that neither oxindolylalanine nor dioxindolylalanine are likely intermediates in the oxidation of TPP to kynurenine[13,40,41,90]. However, ring opening of intermediate 9 should readily lead to kynurenine via 10 (Fig. 40). The yield of 11 from incomplete controlled potential electrooxidation of TPP is extremely small. Any kynurenine formed during the electrolyses of TPP would be immediately oxidized (Table 10). Thus, it must be concluded that the small amount of kynurenine detected among the products of partially oxidized TPP must be due to its formation from intermediates 2, 5 and 9, the former two of which appear to have lifetimes of a few minutes. In other words, at the instant that the partial electrolysis of TPP is terminated some 2, 5 and 9 remains and decomposes to kynurenine and oxindolylalanine. Cyclic voltammograms of TPP at pH < 7.0 show a small reduction peak III_c (Fig. 9). This peak can only be observed after scanning through oxidation peak I_a. E_p values for peak III_c are virtually the same as those observed for the single reduction peak of kynurenine. Furthermore, reduction peak III_c observed in cyclic voltammograms of TPP at pH < 7.0 is not observed at pH $\geq$ 7.0. The reduction peak of 11 also disappears at pH $\geq$

7.0.

Controlled potential electrooxidation of TPP at potentials much more positive than oxidation peak I_a results in the elimination of the tricyclic pyrroloindole 3, oxindolylalanine, dioxindolylalanine and kynurenine as products. Indeed, only products responsible for liquid chromatographic peaks A and B remain after such electrolyses (e.g., Fig. 19E). However, E_p data shown in Table 10 indicates that at potentials about 350 mV more positive than the potential of peak I_a of TPP most identified oxidation products are oxidized. Detailed studies of these oxidations have not been carried out. However, it has been found that following the controlled potential electrolyses of the tricyclic pyrroloindole 3, oxindolylalanine and dioxindolylalanine, liquid chromatograms of the resulting product mixtures are similar to those obtained after oxidation of TPP at very positive potentials (i.e., LC peaks A and B appear).

The reaction pathways shown in Fig. 40 provide a reasonable basis for understanding the oxidation chemistry of TPP particularly between pH 2.0-7.4. However, liquid chromatograms of the products formed upon incomplete electrolysis of TPP at pH 10.65 show only LC peaks A, B, and C' (Fig. 19F). LC peaks A and B appear to be due to the same or similar oligomeric or polymeric products as are formed at lower pH values. However, LC peak C' is due to 2-carboxy-3a,8a-dihydroxy-1,2,3,3a,8,8a-hexahydropyrrolo-(2,3b)-indole

(13) formed by intracyclization of dioxindolylalanine. The absence of oxindolylalanine as a major product at higher pH is probably related to the closeness of its oxidation potential to that of TPP. For example, E_p values for these two compounds are closer at higher pH than at lower pH values. Furthermore, the voltammetric peaks for TPP and 6 are broader at higher pH. Hence, at the potentials used to oxidize TPP, 6 is also oxidized to dioxindolylalanine which rearranges to the dihydroxy pyrroloindole (13) at high pH. While it is probable that small amounts of tricyclic pyrroloindole 3 are co-eluted under LC peak C' (Fig. 19F), this compound 3 could not be detected in the presence of dihydroxy pyrroloindole (13) which has a very similar U.V. spectrum.

It is improtant to note that the products such as the tricyclic pyrroloindole, oxindolylalanine and kynurenine are the end products of 2e oxidations of TPP while dioxindolylalanine requires a 4e oxidation. Coulometric n-values were always $\geq$ 4.0. It is known that the tricyclic pyrroloindole and kynurenine are oxidized at peak I_a potentials and therefore are only detected in small yields in incomplete oxidations of TPP. Oxindolylalanine and to a lesser extent dioxindolylalanine can also be oxidized at peak I_a potentials. All of these secondary electrooxidations contribute to a greater or lesser extent to experimental n-values.

3. B. ENZYMATIC OXIDATION OF TRYPTOPHAN

3. B. 1. Spectral study

The oxidation of L-tryptophan by type VI, VIII and IX peroxidases and chloroperoxidase were studied in phosphate buffers (u = 0.5) pH 4.29 and pH 7.0. These pHs were chosen because they were the same pHs as those carried out in the electrochemical studies.

Type VI peroxidase.

U.V. spectra were recorded throughout the course of the oxidation of L-tryptophan by type VI peroxidase at pH 4.29 and are shown in Figure 41A. Curve 0 in Fig. 41A is the spectrum of tryptophan (λ_{max} = 273, and 218 nm at pH 4.29). Upon initiation of the enzymatic oxidation with type VI peroxidase (Fig. 41A) both U.V. absorption bands of L-tryptophan begin to decrease. Simultaneously, the absorbance between 230-265 nm and 285-390 nm increases. Curve 12 in Fig. 41A is the spectrum observed when L-tryptophan has been largely oxidized and the product mixture shows U.V. absorption bands at λ_{max} = 295(sh), 280(sh), 275, 255, and 216 nm. Spectral changes during the oxidation of L-tryptophan with type VI peroxidase at pH 7.0 were recorded and are shown in Fig. 41B. These spectral results are similar to those observed at pH 4.29 except that the reaction was slower than at pH 4.29.

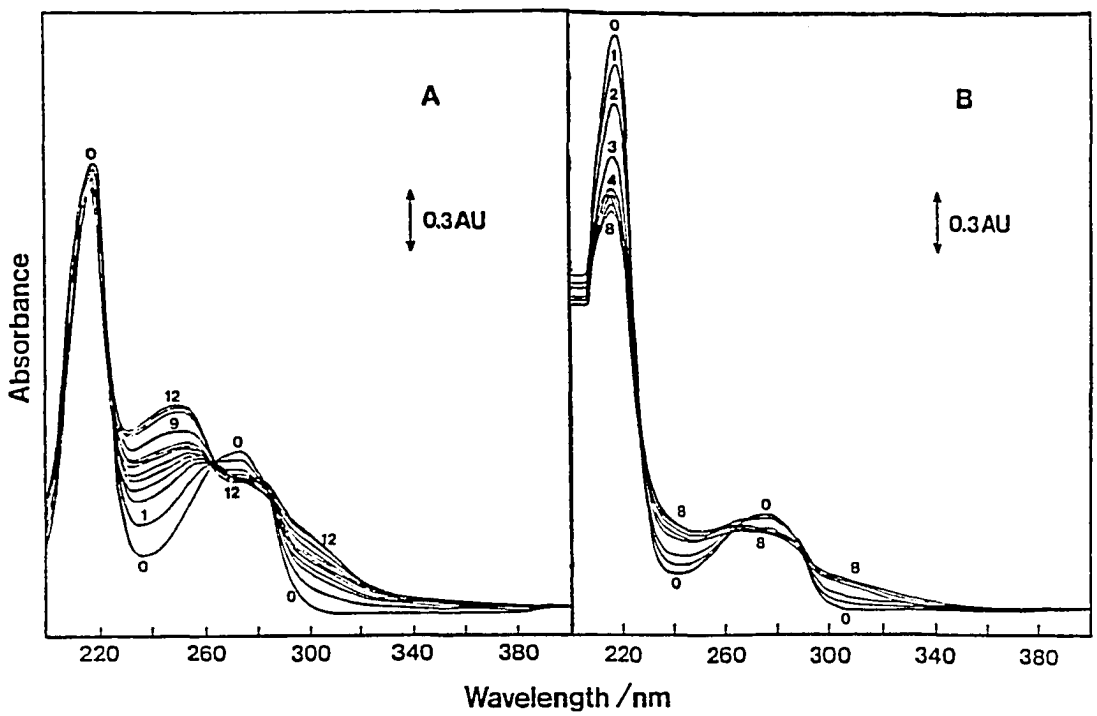

Fig. 41 Spectra taken during the course of the oxidation of L-TPP (66.7 uM) by H_2O_2 (66.7 uM) catalyzed by the type VI peroxidase (1.13 uM) in phosphate buffer (A) pH 4.29 (B) pH 7.0. Curves 0 are the initial spectra of L-TPP. Spectra were recorded at the following times after initiation of the oxidations:

(A): (1) 15 min (2) 30 min (3) 1 h (4) 11/2 h (5) 2 h (6) 3 h (7) 31/2 h (8) 4 h (9) 6 h (10) 8 h (11) 9 h (12) 10 h.

(B): (1) 20 min (2) 40 min (3) 1 h (4) 1.5 h (5) 2 h 40 min (6) 4 h (7) 6 h (8) 12 h.

Type VIII peroxidase

The oxidation reaction of L-tryptophan catalyzed by type VIII peroxidase showed slightly different spectral changes (Fig. 42A) to those observed with type VI (Fig. 41A) and type IX (Fig. 43A) peroxidases. Curve 0 in Fig. 42A is the initial spectrum of L-tryptophan. Upon initiation of the enzymatic oxidation with type VIII peroxidase, a much larger decrease of the U.V. absorption band at 218 nm is observed and this absorption band is replaced by a smaller U.V. absorption band at 214 nm during the course of the oxidation. In addition, the well-defined U.V. absorption bands at λ_{max} = 296 and 242 nm increased in absorbance (curve 11. Fig. 42A). The oxidation reaction catalyzed by type VIII peroxidase is much slower than that catalyzed by type VI peroxidase. Spectra recorded during the oxidation of L-TPP with type VIII peroxidase at pH 7.0 are shown in Figure 42B. The general trends of spectral changes at pH 7.0 are quite similar to those reported at pH 4.29 except the reaction was slower than at pH 4.29.

Type IX peroxidase

The oxidation reaction catalyzed by type IX peroxidase at pH 4.29 (Fig. 43A) and at pH 7.0 (Fig. 43B) showed similar changes with the oxidation reaction catalyzed by type VI peroxidase at pH 4.29 (Fig.41A) and at pH 7.0 (Fig. 41B), respectively, except the oxidation proceeded at much slower rate than with the type VI and type VIII peroxidases.

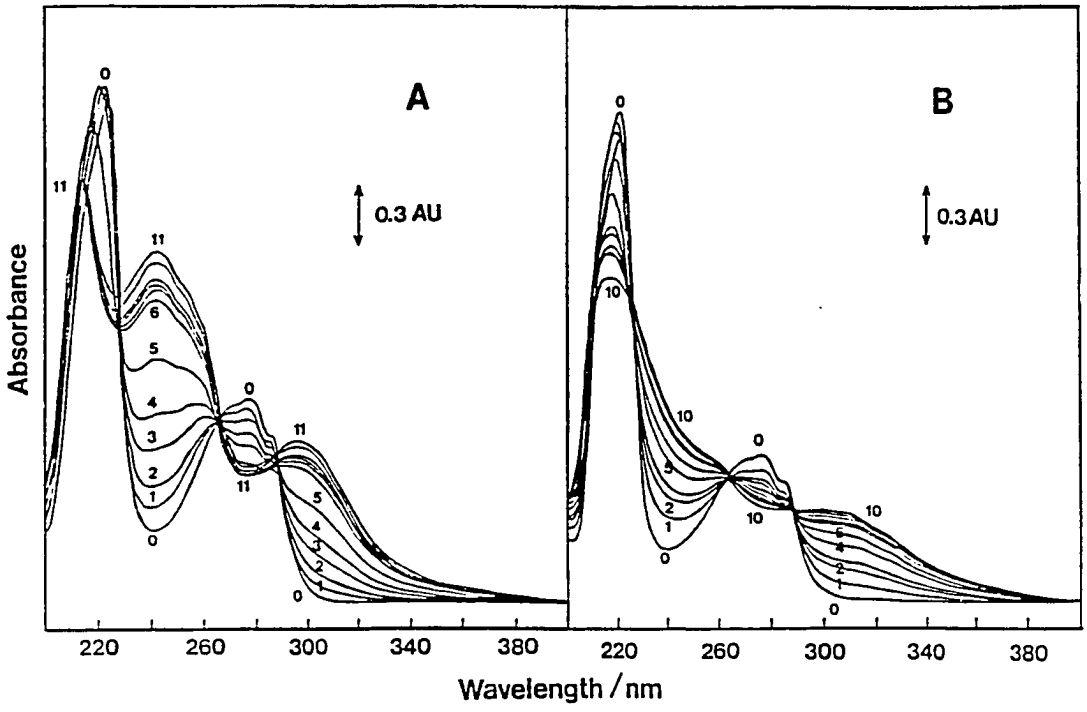

Fig. 42 Spectra taken during the course of the oxidation of L-TPP (66.7 uM) by H_2O_2 (66.7 uM) catalyzed by the type VIII peroxidase (1.13 uM) in phosphate buffer (A) pH 4.29 (B) pH 7.0. Curves 0 are the initial spectra of L-TPP. Spectra were recorded at the following times after initiation of the oxidations:

(A): (1) 25 min (2) 45 min (3) 75 min (4) 2.5 h (5) 4.5 h (6) 5.25 h (7) 6.33 h (8) 8.33 h (9) 8.5 h (10) 18 h (11) 36 h.

(B): (1) 1 h (2) 2 h (3) 2 h 45 min (4) 4 h (5) 5 h 30 min (6) 7.5 h (7) 8 h (8) 9 h 45 min (9) 12 h (10) 14 h.

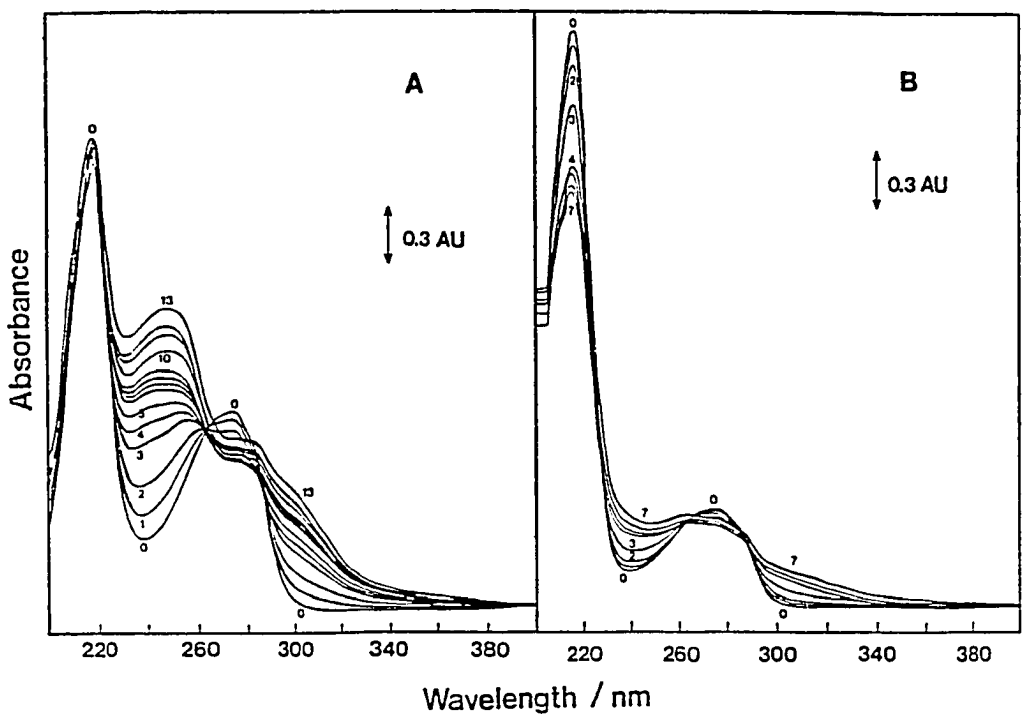

Fig. 43 Spectra taken during the course of the oxidation of L-TPP (66.7 uM) by H_2O_2 (66.7 uM) catalyzed by the type IX peroxidase (1.13 uM) in phosphate buffer (A) pH 4.29 (B) pH 7.0. Curves 0 are the initial spectra of L-TPP. Spectra were recorded at the following times after initiation of the oxidations:

(A): (1) 15 min (2) 30 min (3) 1 h (4) 1.5 h (5) 2 h (6) 3.5 h (7) 4.5 h (8) 5.5 h (9) 7 h (10) 13.5 h (11) 24 h (12) 30 h (13) 48 h.

(B): (1) 15 min (2) 30 min (3) 1 h (4) 2 h (5) 3 h (6) 5 h (7) 17 h.

Chloroperoxidase.

L-tryptophan was only slightly oxidized (< 5%) over the course of 12 h by chloroperoxidase under the same experimental conditions used for the other enzymes.

Based on the above results, it is clear that the oxidation of L-tryptophan by H_2O_2 in the presence of type VI, VIII, and IX peroxidases is rather slow. The enzymatic oxidation appears to proceed more rapidly at pH 4.29 than at pH 7.0. U.V. spectra of the final product solutions were similar for all three peroxidases used. The reaction with type VI peroxidase is representative because spectral changes similar to other enzymes. It was used because reaction is so much faster. Hence, the detailed studies were limited to the reaction catalyzed by the type VI peroxidase. Experiments were also carried out under the same conditions described above but without any enzyme. Under these conditions L-tryptophan was not oxidized by H_2O_2 over time periods up to one month.

3. B. 2. Isolation and Identification of enzymatic oxidation products.

No attempts were made in this study to investigate the stoichiometry, kinetics or related aspects of the peroxidase-catalyzed oxidations of L-tryptophan. It was of more interest to examine the products formed in the enzymatic reaction. In order to accomplish this it was necessary to

carry out oxidations on a large scale. Typically, 5-6 mg of L-tryptophan was dissolved in 30 ml of phosphate buffer pH 4.29 (u= 0.1M) or in very dilute HCl having the same pH. Then 5.0 ml of H_2O_2 solution (62 m$\underline{M}$) was added followed by 4.5 mg of type VI peroxidase. The resulting initial concentrations of L-tryptophan, H_2O_2 and peroxidase were thus 0.1 m$\underline{M}$, 8.8 m$\underline{M}$, and 3.75 u$\underline{M}$ (27: 2347: 1), respectively. The homogeneous reaction mixture was stirred at room temperature for 10 days. As the oxidation proceeded the solution became yellow. The spectral changes observed during the enzymatic oxidation were similar to those shown in Figs. 41A, 42A and 43A. Although a large excess of H_2O_2 was used over L-tryptophan under these conditions, the oxidation was not complete even after 10 days and only 40-50% of the L-tryptophan originally present was oxidized. At the end of 10 days the yellow product solution was freeze-dried. The resulting solid was redissolved in $\underline{ca}$. 2 ml of distilled water and injected onto a column of Sephadex G-10 using water as the eluent. Typical liquid chromatograms of product mixture formed in pH 4.29 phosphate buffer shows seven liquid chromatographic peaks (A, B, C, D, E, F, and I, Fig. 44A). Liquid chromatographic (LC) peak A is primarily due to peroxidase. LC peak B is partially due to inorganic phosphate and one of the products. Liquid chromatograms of the enzymatic products formed in dilute HCl at pH 4.2 (Fig. 44B) were similar to those obtained when the oxidation was carried out in phosphate buffer. Again, LC peak A is due to

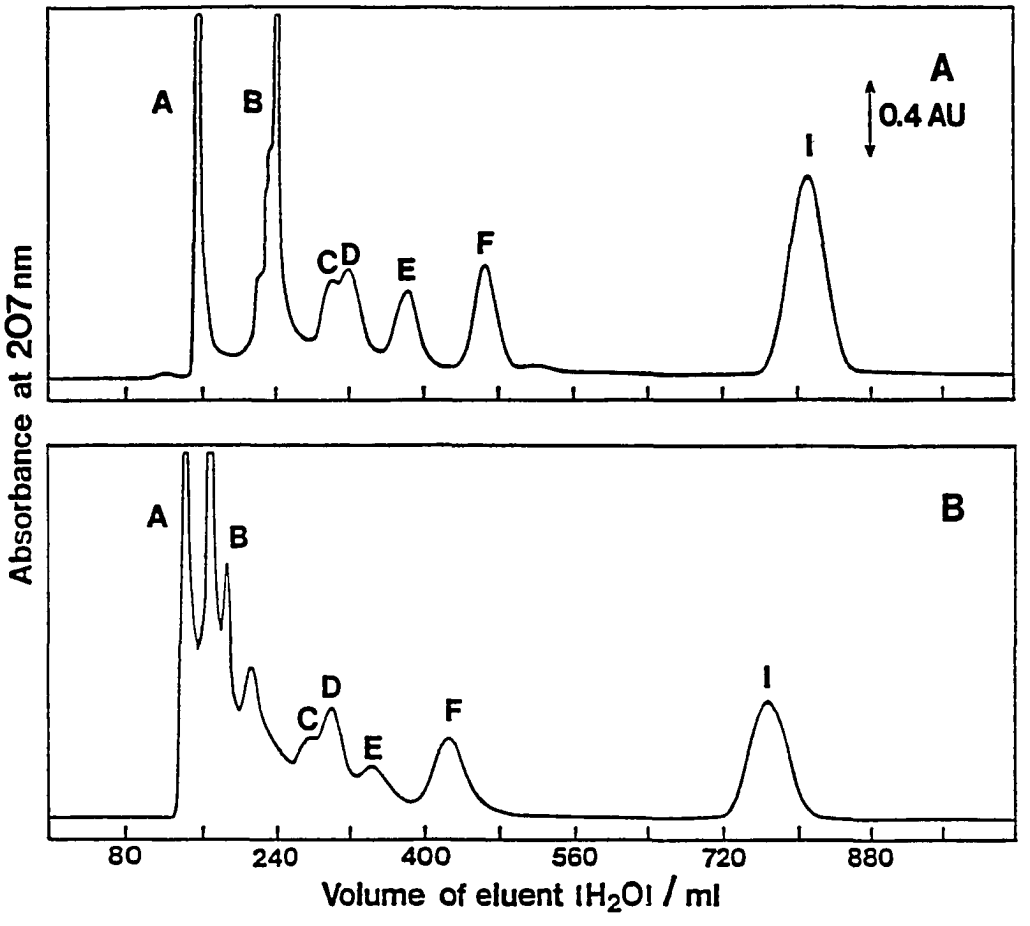

Fig. 44 Liquid chromatograms of the products formed by oxidation of L-TPP (ca. 0.1 mM) by H_2O_2 (8.8 mM) in the presence of type VI peroxidase (3.75 uM) in (A) pH 4.29 phosphate buffer (u = 0.1M) and (B) dilute HCl (pH 4.20). Chromatography was done on a column of Sephadex G-10 (90 x 2.5 cm) using water as the eluent (34 $ml h^{-1}$).

the peroxidase enzyme. However, LC peak B in Fig. 44A also consists of three or more overlapping peaks. These behaviors indicate that in both phosphate buffer and in dilute HCl solutions organic products derived from oxidation of L-tryptophan were eluted under LC peak B. The remaining LC peaks C-I are essentially the same for the products formed in both phosphate buffer and dilute HCL. The eluent corresponding to LC peaks B-I was collected and freeze-dried.

Liquid chromatographic component B

The solid material eluted under LC peak B was bright yellow solid. In water its U.V. spectrum exhibited shoulders at 290, 235, and 205 nm. The shoulder at 290 nm extented beyond 380 nm resulting in the yellow color of the solution. This product gave no voltammetric oxidation or reduction peaks at the PGE between pH 2.0 - 11.0. MS and FAB-MS (glycerol or thioglycerol matrix) failed to give useful mass spectral information. Similarly silylation with BSA, BSTFA and MTBSTFA in various solvents (pyridine, DMF, and acetonitrile) did not give a volatile derivative which could be analyzed by gas chromatography. Thus, it is tentatively concluded that LC component B is probably an oligomeric or polymeric compound. LC component B obtained from electrochemical oxidation shows identical U.V., mass, FAB-MS and GC-MS properties to those reported for LC component B obtained from enzymatic oxidation.

Liquid chromatographic components C and D.

The components eluted under LC peaks C and D were very pale yellow solids. In water they showed identical U.V. spectra (λ_{max} = 293, 233, and 205 nm, Fig. 20). The mass spectrum of component C (70 eV, 200°C) showed the following major peaks, m/e (relative abundance): 220 (M^+, 56.9%), 202 (M^+-H_2O, 4.3%), 177 (23.7%), 176 (11.5%), 175 (M^+-COOH, 22.2%), 158 (24.2%), 148 (17.5%), 147 (69.9%), 146 ($M^+-CH(NH_2)COOH$, 72.2%), 132 ($M^+-CH_2.CH(NH_2)COOH$, 100%), 120 (25.3%), 119 (16.4%), 118 (20.1%). Under the same conditions component D gave a virtually identical mass spectrum.

Components C and D were derivatized with BSA or BSTFA (100 ul) in pyridine (50 ul) and dimethylsulfoxide (50 ul) in a sealed vial at room temperature for 24 h. GC-MS (EI and CI) of the trimethylsilyl derivative of component C gave a GC peak at t_R = 30.9 min that had a molar mass of 436 g. The derivative of compound D gave a GC peak at t_R = 31.4 min which also had a molar mass of 436 g.

2-carboxy-3a-hydroxy-1,2,3,3a,8,8a-hexahydropyrrolo-(2,3b)-indole (3) shows identical U.V., mass and GC-MS to those observed for components C and D. Thus, LC components C and D must be stereoisomers of the tricyclic pyrroloindole (3). So, the components C and D obtained from enzymatic oxidation and the components C and D obtained from electrochemical oxidation are the same compound.

Liquid chromatographic component E.

LC component E was a white solid. In water component E showed very well-defined U.V. absorption bands at λ_{max} = 287, 253, and 205 nm (Fig. 28). Mass spectrometry of the solid (70 eV, 200°C) gave the following results, m/e (relative abundance): 237 (0.7%), 236 (M^+, 7.3%), 220 (1.6%), 219 (1.1%), 218 (M^+-H_2O, 9.2%), 202 (0.9%), 201 (2.3%), 200 (6.7%), 176 (1.1%), 175 (10.7%), 174 (62.1%), 173 (29.4%), 147 (17.1%), 146 (100%), 145 (47.9%), 144 (11.1 %), 131 (11.2%), 130 (62.7%), 129 (22.4%), 128 (21.9%), 121 (10.6%), 120 (71.5%), 119 (21.7%), 118 (23.9%), 117 (29.1%), 104 (11.8%), 103 (13.3%), 102 (11.0%).

LC component E was derivatized with BSA (70 ul) in acetonitrile (70 ul) in a sealed reacti-vial at room temperature for over night or at 120°C for 30 min. EI and CI-MS on the resulting trimethylsilyl derivative gave a single GC peak at t_R = 36.2 min which had a molar mass of 524 g. Derivatization with BSA-d_9 under the same condition gave a single GC peak at t_R = 34.2 min which had a molar mass of 560 g. These mass spectral data indicate that LC component E has a molecular weight of 236 and that it forms a tetra-trimethylsilyl derivative. Authentic dioxindolylalanine shows identical U.V., mass and GC-MS properties to those reported for LC component E. Thus, LC component E obtained from electrochemical oxidation and LC component E obtained from enzymatic oxidation are the same compound.

Liquid chromatographic component F

LC component F was a pale yellow solid. In water it exhibited three U.V. absorption bands at λ_{max} = 280(sh), 250, and 200 nm (Fig. 32). LC component F could be silylated with BSTFA (70 ul) at room temperature for 24 h. GC of the resulting derivative showed a single peak at t_R = 32.8 min. EI- and CI-MS of this derivative indicated it had a molar mass of 436 g. Derivatization of LC component F with MTBSTFA (70 ul) in acetonitrile (70 ul) at room temperature for 24 h have a tertbutyldimethylsilyl derivative which showed a single GC peak at t_R = 38.6 min. EI- and CI-MS of this derivative indicated it had a molar mass of 562 g. Hence, LC component F has a molecular weight of 220 and can be silylated at three positions. Authentic oxindolylalanine showed identical GC, GC-MS to that reported above for component F. Thus, LC component F obtained from electrochemical oxidation and LC component F obtained from enzymatic oxidation are the same compound.

Liquid chromatographic component I.

The U.V. and spectra of component I were identical to that of authentic tryptophan.

3. C. COMPARISION OF ELECTROCHEMICAL AND ENZYMATIC OXIDATION PATHWAYS.

The reaction pathway proposed for electrochemical oxi-

dation of L-tryptophan has been discussed in detail (Fig. 40).

Under the condition described above the products formed in the peroxidase-catalyzed oxidation of L-tryptophan are very similar to those formed in the electrochemical oxidation. Preliminary studies indicate that kynurenine is oxidized under the same conditions used to oxidize L-tryptophan by H_2O_2/peroxidase at pH 2.4 except that kynurenine oxidation is much slower than with L-tryptophan. As the peroxidase-catalyzed oxidation of kynurenine proceeds the reaction solution becomes yellow. Liquid chromatography of the resulting products shows a large LC peak having approximately the same retention volume as LC peak B observed in Figs. 18 and 44. No attempt has been made to identify this product, although its U.V. spectrum is very similar to that of LC component B obtained from electrochemical oxidation of TPP. Thus, the failure to observe kynurenine as a product of the peroxidase-catalyzed oxidation of L-tryptophan is probably because it is itself oxidized by peroxidase/H_2O_2.

Unfortunately, the rate of the enzymatic oxidation reaction is too slow to permit spectral observation of intermediates having half-lives of a few minutes (i.e., 2 and 5, Fig. 40). However, formation of a yellow polymeric material responsible for LC peak B, oxindolylalanine (6), dioxindolylanine (8), the isomers of tricyclic pyrroloindole 3 and trace amount of kynurenine (11) as products of both

the enzymatic and electrochemical oxidation reactions suggest that both process proceed by very similar mechanistic pathway.

It is, perhaps, worth noting that controlled potential electrooxidations of tricyclic pyrroloindole 3, oxindolylalanine (6), dioxindolylalanine (8) and kynurenine (11) give products which show LC peaks A and B. Except for LC component 8 (vide supra) detailed studies of these reactions, however, have not been carreid out. Experiments to investigate the peroxidase-catalyzed oxidation of 3 and 8 have not yet been performed. However, the relatively large scale enzymatic oxidations of L-tryptophan employed a very large excess of H_2O_2 and resulted in quite large yields of 3, 6 and 8 (vide supra). This suggests that if the latter compounds are oxidized by peroxidase, the reactions must proceed at a very significantly slower rate than does the oxidation of L-tryptophan. Thus, it is unlikely that dioxindolylalanine (8) is formed as a result of the peroxidase-catalyzed oxidation of oxindolylalanine (6). In some preliminary experiments it has been shown that under the conditions used to oxidized L-tryptophan by H_2O_2/peroxidase at pH 4.29 oxindolylalanine was not oxidized over the course of 12 h. Thus, it must be concluded that in the enzymatic reaction intermediates 5 and/or 9 are the species which are further oxidized leading ultimately to dioxindolylalanine (8) as shown in Fig. 40.

CHAPTER 4

CONCLUSION

The results reported above indicate that TPP is electrochemically oxidized by an initial, irreversible 2e reaction to give a very reactive 3-methylene-imine intermediate. This intermediate, being highly electrophilic, is attacked by nucleophiles such as TPP, water, and probably even the 3-methylene-imine intermediate present in the reaction solution. Nucleophilic attack by water leads to two different intermediates which can be detected by thin-layer spectroelectrochemistry and cyclic voltammetry. After the nucleophilic attack a rather complex series of chemical and electrochemical follow-up reactions then occur leading to formation of two stereoisomers of tricyclic pyrroloindole 3, dioxindolylalanine, oxindolylalanine and kynurenine as final products along with at least two oligomeric or polymeric products. The mechanistic pathway for the electrochemical oxidation has been proposed from the identified final products.

The oxidation of L-tryptophan by H_2O_2 catalyzed by type

VI peroxidase appears to be a rather complex reaction leading to at least one polymeric product and five well characterized monomeric products (i.e., the stereoisomers of the trycyclic pyrroloindole 3, oxindolylalanine, and dioxindolylalanine. This diversity of products suggests that a very reactive primary product is formed which can undergo a number of further reactions. Pyrroloindoles, oxindolylalanine and kynurenine may be formed by the chemical reactions shown in Fig. 40. Formation of dioxindolylalanine requires additional oxidation reactions. This could involve enzymatic oxidation of putative 5 and/or 9 intermediates. It seems unlikely that oxindolylalanine is a substrate for peroxidase since it is not oxidized by H_2O_2/peroxidase over the course of 12 hours under the conditions used to oxidize L-tryptophan.

The spectral changes which accompany the peroxidase-catalyzed oxidation of L-tryptophan and most of the products formed are very similar to those observed upon electrochemical oxidation. Electroanalytical techniques allow a more detailed mechanistic picture of the oxidation of L-tryptophan. In view of the noted similarities between the enzymatic and electrochemical oxidation reactions it seems reasonable to conclude that, in a chemical sense, the courses of the two reaction are essentially identical.

The reaction pathways presented in Fig. 40 provide a rational basis for understanding various aspects of the

oxidation chemistry of TPP, and the chemistry and electrochemisty of the various intermediate species.

PART II

ELECTROCHEMICAL AND ENZYMATIC OXIDATION OF 7-METHYLURIC ACID

CHAPTER 1

INTRODUCTION

The electrochemical and enzymatic oxidations of uric acid[78,80,93-98] and various N-methylated uric acids have been studied quite extensively by Dryhurst and coworkers[99-106]. These studies have been carried out in phosphate buffers between pH 2.0-11.0. In the case of all the uric acids studied at a pyrolytic graphite electrode, a single voltammetric oxidation peak I_a could be observed. Also, except in the case of 1,3,7,9-tetramethyluric acid, all other uric acids studied, show a second voltammetric oxidation peak II_a at more positive potentials. However, the latter voltammetric oxidation peak is observed only over certain pH ranges. For example, the second oxidation peak II_a can be observed at pH $\geq$ 5.7 for 7-methyluric acid, at pH > 6.0 for 3,7-dimethyluric acid[105], at pH > 3.0 for 7,9-dimethyluric acid[102] and at pH > 10.0 for 1,3,7-trimethyluric acid[101].

Even though N-methyluric acids have been studied quite extensively by Dryhurst and coworkers[100-106] in our laboratory, 7-methyluric acid has not previously been studied. Therefore, the specific aim and scope of this work will involve the use of electrochemical and analytical techniques to investigate the electrochemical and enzymatic oxidation chemistry of 7-methyluric acid. The mechanism of both electrochemical and enzymatic oxidation for 7-methyluric acid will be developed and compared. It was hoped that a systematic scheme for understanding the electrooxidation chemistry of 7-methyluric acid would help in understanding the mechanism of biological oxidation of this compound.

CHAPTER 2

EXPERIMENTAL

2. A. CHEMICALS

7-methyluric acid was obtained from Adams Chemical Co (Round Lake, IL) and was used without additional purification. Phosphate buffers were prepared as described by Christian and Purdy[68] and had an ionic strength of 0.5 M, unless otherwise specified. Other supporting electrolytes were prepared from 0.5 M NaCl plus 5 mM Na_2HPO_4 adjusted to the required pH by addition of HCl or NaOH. Other chemicals have been described in CHAPTER 2 (EXPERIMENT, PART I).

2. B. APPARTUS

Equipment used for electrochemical and thin-layer spectrochemical studies has been described in CHAPTER 2 (PART I).

2. C. PROCEDURES

Procedure for trapping the intermediates and products formed in thin-layer electrochemical oxidation of 7-methyluric acid.

Usually, 1 mM solutions of 7-methyluric acid were pre-

pared in low phosphate buffers. The sample was then electrolyzed in a thin-layer spectroelectrochemical cell for a time period of 30 sec to 2 min. After electrolysis the excess of unoxidized 7-methyluric acid solution located below the RVC minigrid electrode was removed by touching a dry paper tissue to the base of the cell. The remaining solution in the thin-layer cell (ca. 270 ul) was then carefully blown out of the cell into a cold (-78°C) screw-cap vial. The resulting frozen solution was then lyophilized. During lyophilization the sample was maintained below 0°C so that it remained in a frozen state.

A similar procedure was employed to obtain the products of the electrochemical oxidation except that the oxidation was allowed to proceed for 15-30 minutes. The solution was then frozen and dried by lyophilization.

Procedure for trapping the intermediates and identifying products formed by enzymatic oxidation of 7-methyluric acid.

In order to identify the intermediates and the major products formed upon enzymatic oxidation of 7-methyluric acid, low concentration phosphate buffers at pH 7.5 were used. The U.V.-absorbing intermediate was trapped in the following way: 0.04 ml of 3 mM 7-methyluric acid in low phosphate buffer was placed in a small beaker and to it was added 0.4 ml of 4 uM peroxidase in the same buffer. The

oxidation was initiated by addition of 0.05 ml of 6 m$\underline{M}$ H_2O_2 into the above solution. After time periods ranging from 30 s to 2 min the solution was transferred from the beaker into a small vial (3 ml volume) maintained at -78°C (dry ice-acetone). The sudden and rapid decrease in the temperature of the reaction mixture served to quench the oxidation reaction and to prevent extensive decomposition of the U.V.-absorbing intermediate. The frozen solution was then dried by lyophilization with the vial maintained at temperature below 0°C at all times.

A similar procedure was employed to obtain the products of the enzymatic oxidation except that the oxidation was allowed to proceed for 15-20 minutes. The solution was then frozen and dried by lyophilization.

Procedure for silylation

A procedure similar to the one described in CHAPTER 2 (PART I) was employed to identify the intermediates and products except that the silylation of the intermediates were carried out just before GC-MS analysis to avoid the decomposition of the intermediates.

CHAPTER 3

RESULTS AND DISCUSSION

3. A. Electrochemical oxidation of 7-methyluric acid

3. A. 1. Linear and Cyclic Sweep Voltammetry

7-methyluric acid gives a well-defined voltammetric oxidation peaks I_a at a PGE in phosphate buffers (u = 0.5 M) between pH 2.0-11.0. At pH $\geq$ 5.7 a well-defined second oxidation peak II_a is observed (Fig. 1).

The variation of E_p with pH for oxidation peaks I_a and II_a of 7-methyluric acid (1 mM) in phosphate buffers having an ionic strength of 0.5 M, measured at a sweep rate of $5 mVs^{-1}$, are given in Eqns. (1) and (2) and in Fig. 2.

$$\text{Peak } I_a : E_p(\text{pH } 2.0 - 11.0) = [0.73 - 0.049\ \text{pH}]\ \text{V} \quad (1)$$

$$\text{Peak } II_a: E_p(\text{pH } 5.7 - 11.0) = [1.61 - 0.090\ \text{pH}]\ \text{V} \quad (2)$$

A series of cyclic voltammograms recorded in phosphate buffers (u = 0.5 M) between pH 2.0 - 11.0 of 7-methyluric acid is shown in Fig. 1. At pH 5.7 oxidation peaks I_a and II_a are observed on the first sweep towards positive poten-

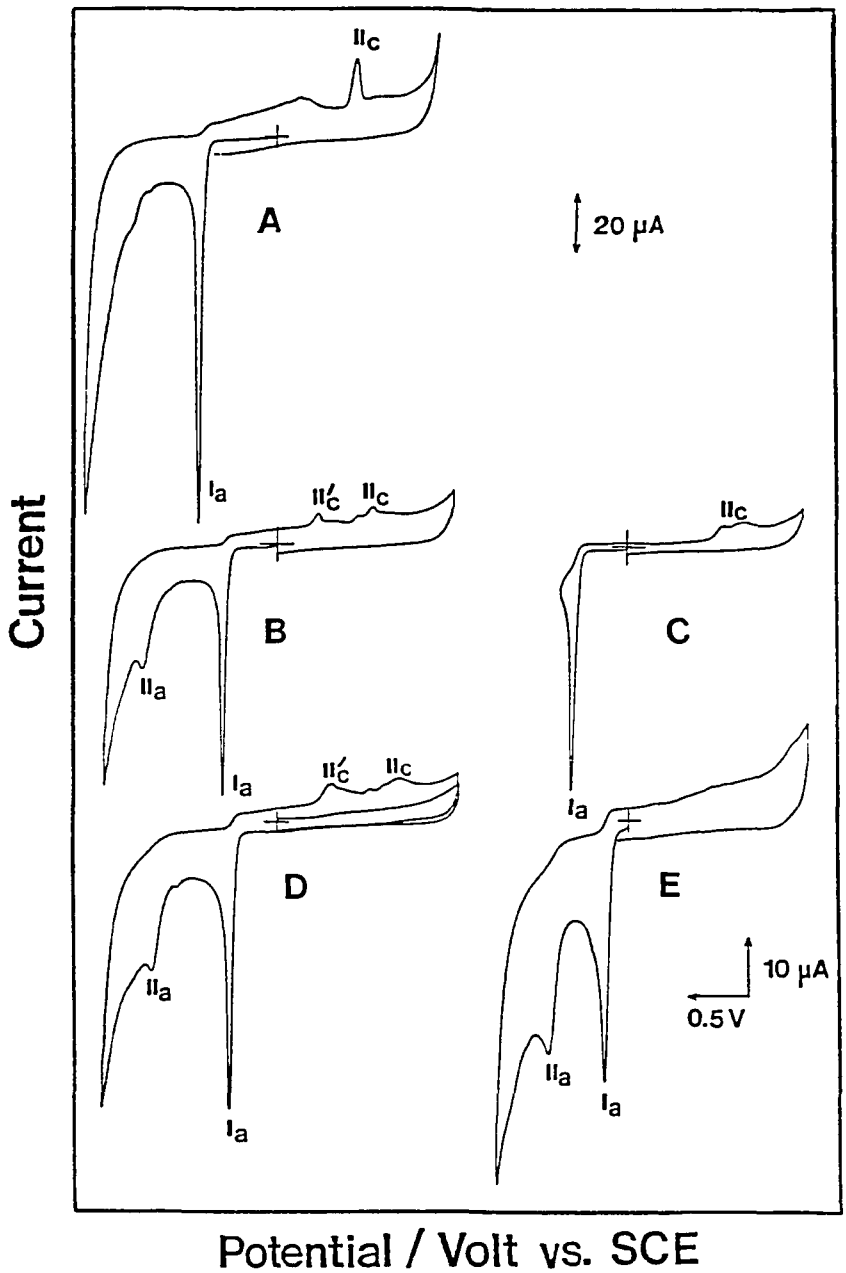

Fig. 1 Cyclic voltammograms at the PGE of 1 mM 7-methyluric acid at pH: (A) 1.98, (B) and (C) 5.72, (D) 7.0 and (E) 11.04 were obtained in phosphate buffers (u = 0.5 M). Sweep rate: 200 mVs^{-1}.

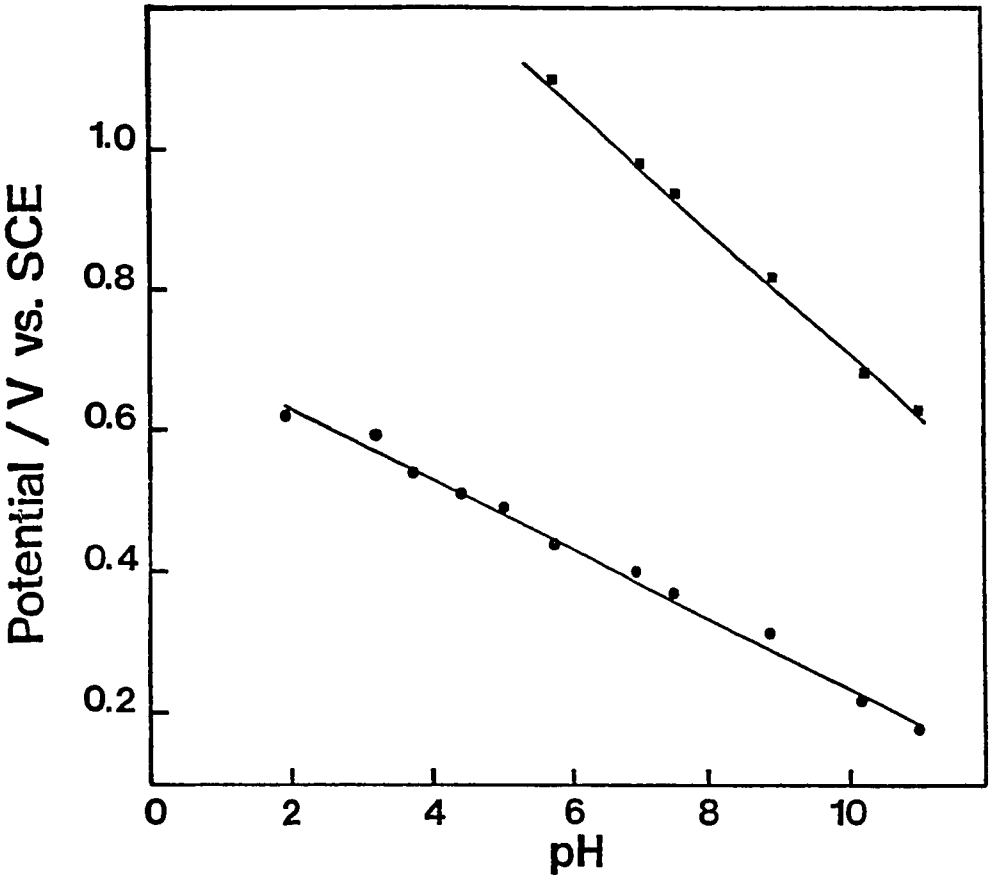

Fig. 2 The peak potential (E_p) vs. pH curve obtained at the PGE of 1 mM 7-methyluric acid in phosphate buffers (u = 0.5 M) at a sweep rate of 5 mVs^{-1}.

tials (Fig. 1B). On the reverse sweep reduction peaks II'_c and II_c appear. To observe the latter peak II_c, it is only necessary to scan up to oxidation peak I_a. However, it is necessary to scan up to peak II_a potentials to observe the reduction peak II'_c. Hence the species responsible for reduction peak II_c must be formed as a results of peak I_a oxidation of 7-methyluric acid and the species responsible for reduction peak II'_c must be formed as a result of peak II_a oxidation. At low pH, peak II_c becomes larger and well-defined, while peak II'_c becomes smaller (Fig. 1A). AT pH $\geq$ 11.0, peaks II'_c and II_c disappear (Fig. 1E).

Figure 3 shows a series of voltammograms of 7-methyluric acid in low phosphate buffers (0.5 M NaCl plus 5 mM Na_2HPO_4). At pH < 4.0 only the first oxidation peak I_a appears (Fig. 3A). At pH $\geq$ 4.0 oxidation peaks I_a and II_a may be observed on the first sweep towards positive potentials (Fig. 3B). On the reverse sweep, two reduction peaks II'_c and II_c appear. Peak II'_c can be observed only at pH $\geq$ 4.0 (Fig. 3B). Also peak II_c splits into two overlapping peaks at low pH (Fig. 3A).

Sweep rate studies in phosphate buffer pH 5.2 (u=0.5M) revealed that with increasing sweep rate the height of oxidation peak II_a decreased relative to peak I_a and at sufficiently fast sweep rate (ca. 20 Vs^{-1}) peak II_a disappeared. This indicates that the species responsible for peak II_a is formed slowly by chemical reactions of the

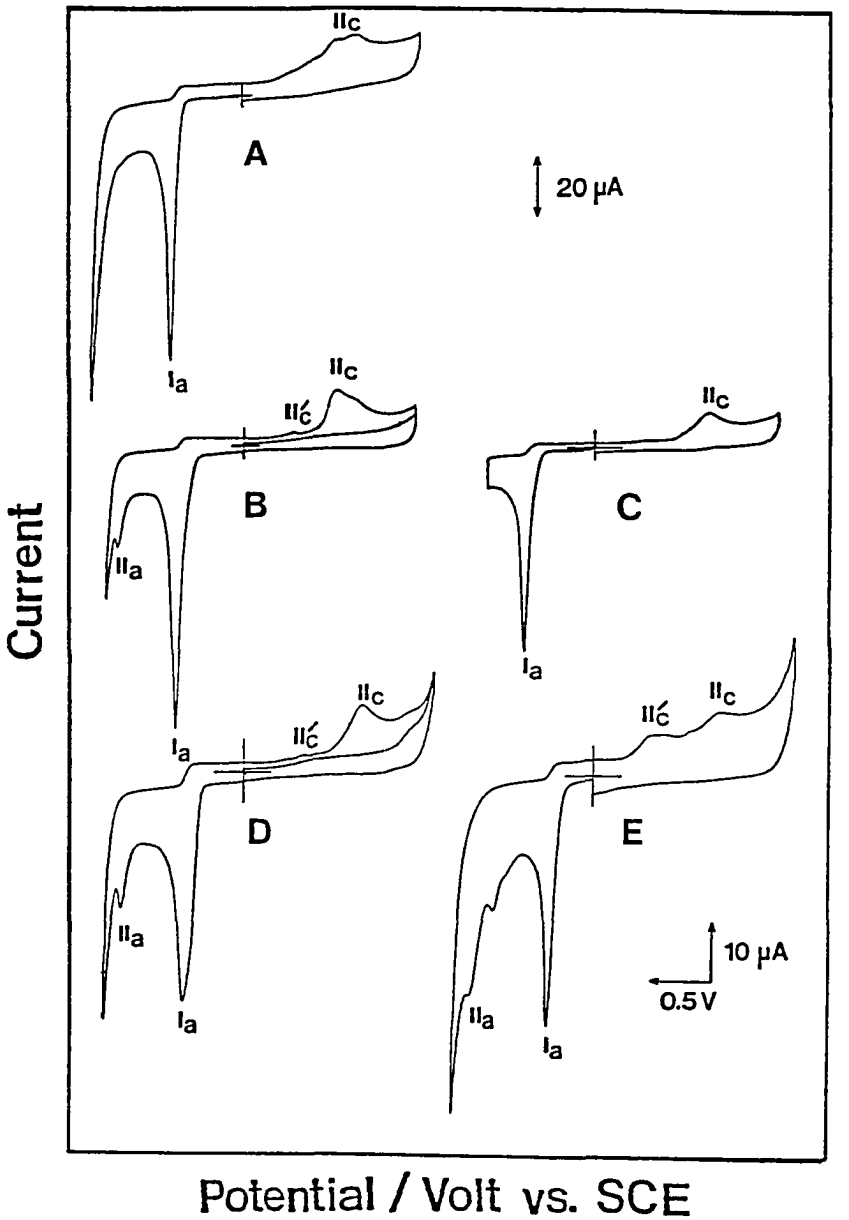

Fig. 3 Cyclic voltammograms at the PGE of 1 mM 7-methyluric acid at pH: (A) 3.0, (B) and (C) 4.0, (D) 6.0 and (F) 9.5 were obtained in 0.5 M NaCL plus 5 mM Na_2HPO_4. Sweep rate: 200 mVs^{-1}.

primary peak I_a product.

Cyclic voltammetry of 7-methyluric acid at slow and fast sweep rates (5 mVs^{-1} up to 100 Vs^{-1}) does not show a reversible reduction peak coupled to oxidation peak I_a. Thus, it must be concluded that oxidation reaction shown by peak I_a of 7-methyluric acid is electrochemically irreversible.

For an irreversible redox reaction, the slope of the E_p vs. pH is defined by Equation 3[83], where α is the electron transfer coefficient, p is the number of protons involved in

$$\frac{d(E_p)}{d(pH)} = \frac{- 0.059\ p}{\alpha n_a} \qquad (3)$$

the reaction and n_a is the number of electrons involved in the rate limiting reaction at the electrode. The electrone transfer coefficient, α, for 7-methyluric acid was assumed to be 0.5. The calculated number of protons involved in the reaction for 7-methyluric acid is 0.83. Thus, the initial peak I_a oxidation of 7-methyluric acid involves a $2e\text{-}H^+$ reaction.

3. A. 2. Thin-layer spectroelectrochemistry

Controlled potential electrooxidations of 7-methyluric acid were carried out in a fused quartz thin-layer cell containing an optically-transparent RVC electrode. Solu-

tions of 7-methyluric acid (ca. 1mM) in phosphate buffer or in 0.5 M NaCl plus 5mM Na_2HPO_4 adjusted to pH values ranging from 4.0 to 9.5 were studied. Complete electrolyses of 7-methyluricacid under these conditions at peak I_a potentials gave experimental n-values of 1.9 ± 0.2. It was not possible to observe oxidation peak II_a at a RVC electrode because of the limited positive potential window available at this electrode. Figure 4 shows linear and cyclic voltammograms of 7-methyluric acid in 0.5 M NaCl plus 5 mM Na_2HPO_4 adjusted to pH 7.5 in thin-layer cell.

The changes in the U.V. spectra observed during and after electrochemical oxidation of 7-methyluric acid at peak I_a potentials in a thin-layer cell in 0.5 M NaCl plus 5 mM Na_2HPO_4 between pH 4.0-9.0 were essentially identical. Typical thin-layer spectroelectrochemical behavior at pH 7.5 is shown in Fig. 5. Curve 1 in Fig. 5 shows the spectrum of 7-methyluric acid (λ_{max} = 294, 238 and 204 nm). Initiation of the peak I_a electrooxidation at 0.8 V causes the band at 294 nm to decrease while a new band grows in at 224 nm and the absorbance between about 352-310 nm also increases. If the electrolysis was terminated when the latter band had reached its maximal height (curve 11, Fig. 5A) then the spectral changes shown in Fig. 5B were observed. The absorbance decayed with time over the spectral region between about 352-190 nm (curve 12-23, Fig. 5B).

The above decompositions after the electrolysis indi-

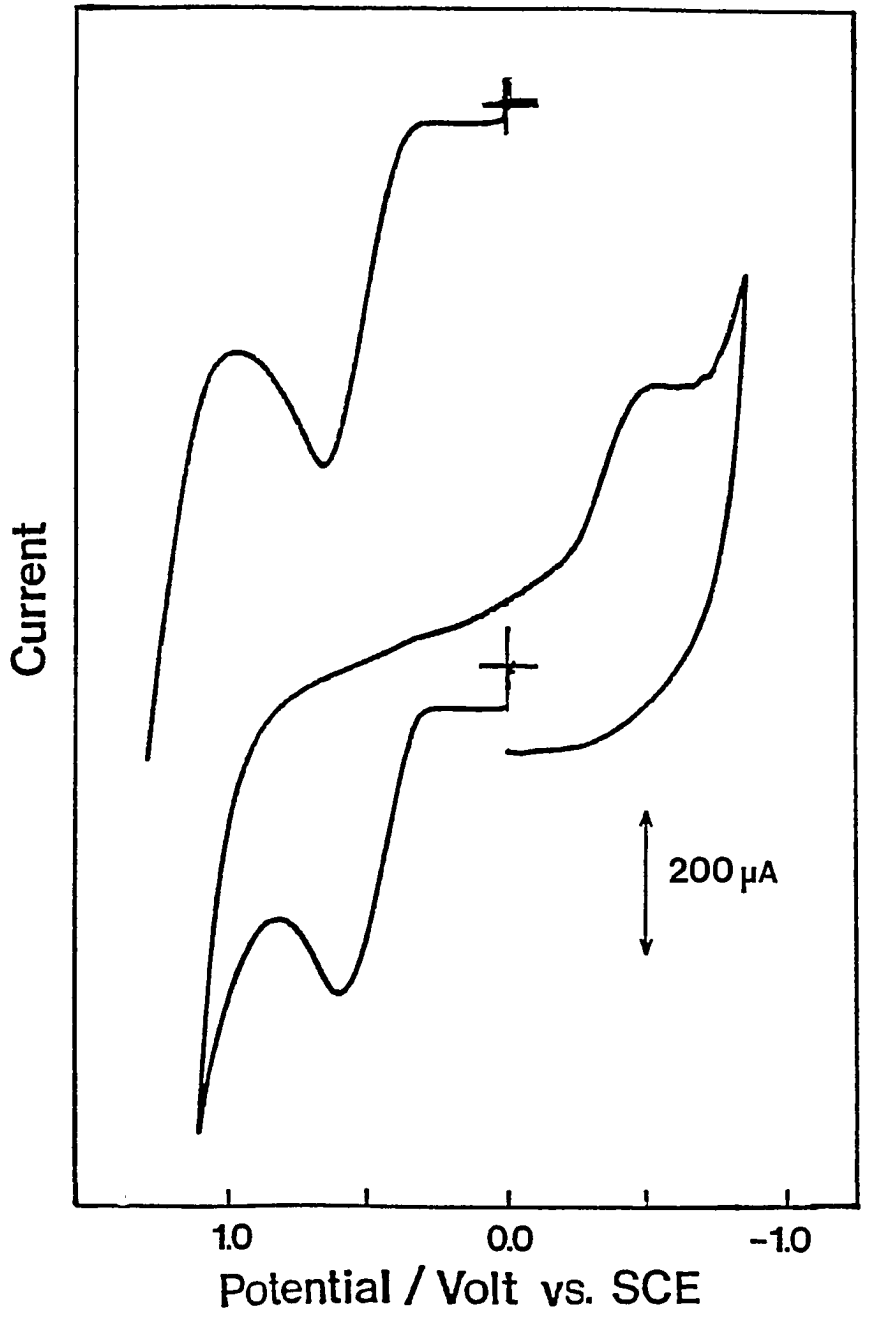

Fig. 4 Linear sweep and cyclic voltammograms at thin-layer cell containing a RVC electrode of 1 mM 7-methyluric acid at pH 9.5 in 0.5 M NaCl plus 5 mM Na_2HPO_4. Sweep rate: 200 mVs^{-1}.

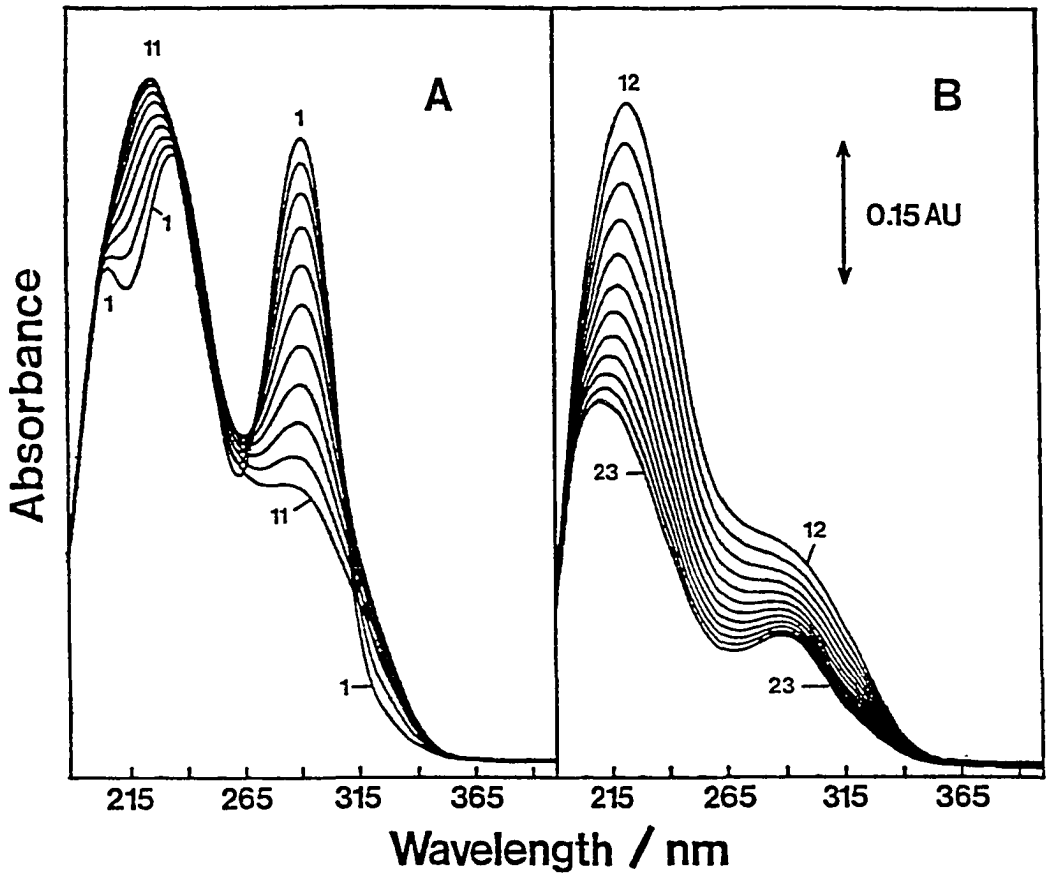

Fig. 5 (A) Spectra of 1 mM 7-methyluric acid in pH 7.5 (0.5 M NaCl plus 5 mM Na_2HPO_4) undergoing oxidation at 0.8 V in a thin-layer cell containing a RVC electrode. Curve 1 is the initial spectrum, curves 2-11 after initiation of the electrolysis. Each spectral sweep had a duration of 10 s with no time interval.

(B) After sweeping curve 11 in (A) the RVC electrode was open-circuited and curve 12-23 recorded. Each spectrum had a duration of 40 s.

cate that one or more U.V.-absorbing intermediate species are formed upon electrooxidation of 7-methyluric acid at peak I_a potentials. The A *vs.* t curves observed following electrochemical oxidation of 7-methyluric acid in 0.5 M NaCl plus 5 mM Na_2HPO_4 at pH 7.5 are shown in Fig. 6. The kinetics of decomposition of the intermediate species was studied by measuring the absorbance decay as a function of time at 220, 290 and 325 nm. The decomposition followed first order kinetics with the rate constants reported in Table 1.

Figure 7 shows the spectroelectrochemical behavior of 7-methyluric acid in 0.5 M NaCl plus 5 mM Na_2HPO_4 at pH 7.5. Curve 1 in Fig. 7A is the initial spectrum of 7-methyluric acid (λ_{max} = 294, 240 and 204 nm). Application of a potential to a RVC electrode of 0.6 V causes the long wavelength band at 294 nm to decrease while a new band grows in at short wavelengths (*ca.* 224 nm) and the absorbance between about 352-310 nm also increases. After about 93 s electrolysis curve 5 (Fig. 7A) may be observed which is the spectrum of intermediate species (λ_{max} = 300 and 224 nm). If, after sweeping curve 5 in Fig. 7A the RVC electrode was potentiostated at - 1.0 V the spectroelectrochemical behavior noted in Fig. 7B was observed. Thus, electroreduction of the intermediate (curve 6, Fig. 7B, λ_{max} = 300 and 224 nm) cause the long wavelength band to shift to shorter wavelength and grows while the shorter wavelength band de-

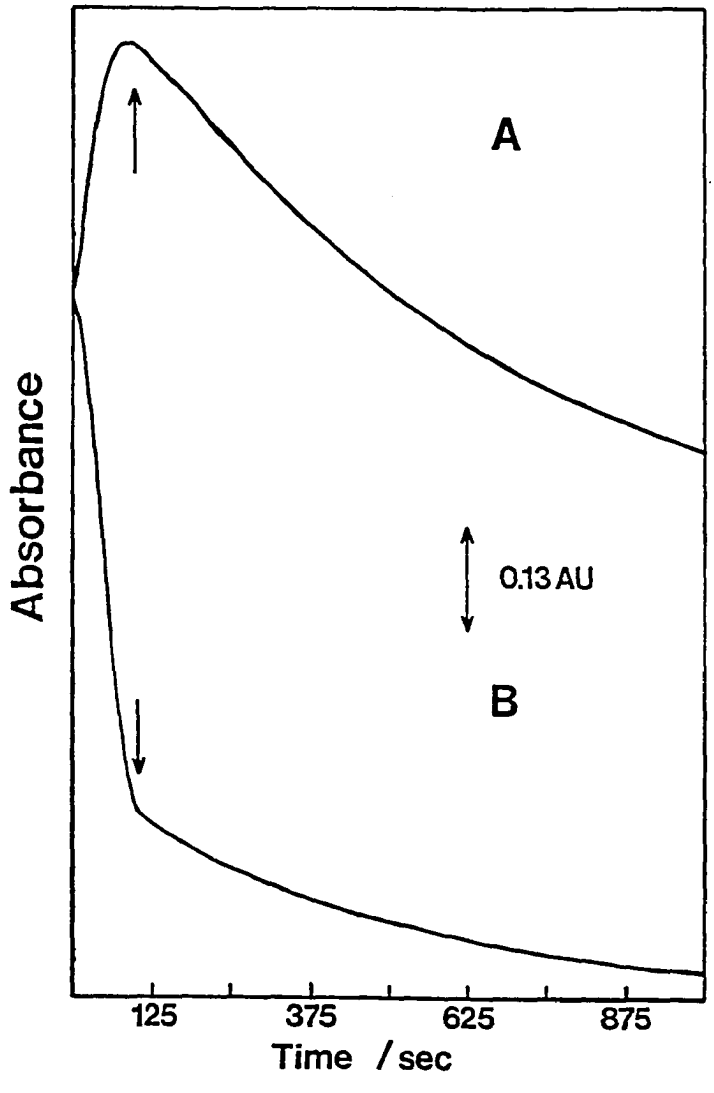

Fig. 6 Absorbance vs. time curve for the decay of the intermediate species generated upon electrochemical oxidation of 1 mM 7-methyluric acid at 0.8V in 0.5 M NaCl plus 5 mM Na_2HPO_4 pH 7.5. Arrow indicates time when electrode was open-circuited. At wavelength (A) 220 and (B) 290 nm.

Table 1

Observed first order rate constants for decomposition of the U.V.-absorbing intermediate generated upon peak I_a electro-oxidation of 7-methyluric acid at an optically-transparent RVC electrode in a thin-layer cell.

pH	Applied potential V *vs.* SCE	(nm)	$k_{obs}(s^{-1})^a$
0.5 M NaCl plus 5 mM Na_2HPO_4			
4.0	0.8	220	$7.5\times10^{-3} \pm 1.0\times10^{-5}$
		290	$1.9\times10^{-3} \pm 1.1\times10^{-5}$
5.6	0.8	220	$7.1\times10^{-3} \pm 1.1\times10^{-5}$
6.0	0.8	220	$4.7\times10^{-3} \pm 1.2\times10^{-5}$
		290	$3.7\times10^{-3} \pm 1.0\times10^{-5}$
7.5	0.8	220	$1.0\times10^{-3} \pm 1.0\times10^{-5}$
		290	$1.1\times10^{-3} \pm 1.1\times10^{-5}$
		325	$1.1\times10^{-3} \pm 1.0\times10^{-5}$
9.5	0.8	220	$2.6\times10^{-3} \pm 1.3\times10^{-5}$
		290	$2.2\times10^{-3} \pm 1.0\times10^{-5}$
		325	$2.4\times10^{-3} \pm 1.1\times10^{-5}$

[a] Calculated by analysis of A *vs.* t curves obtained at the wavelength noted. The average of at least three replicate measurements is reported ± standard deviation.

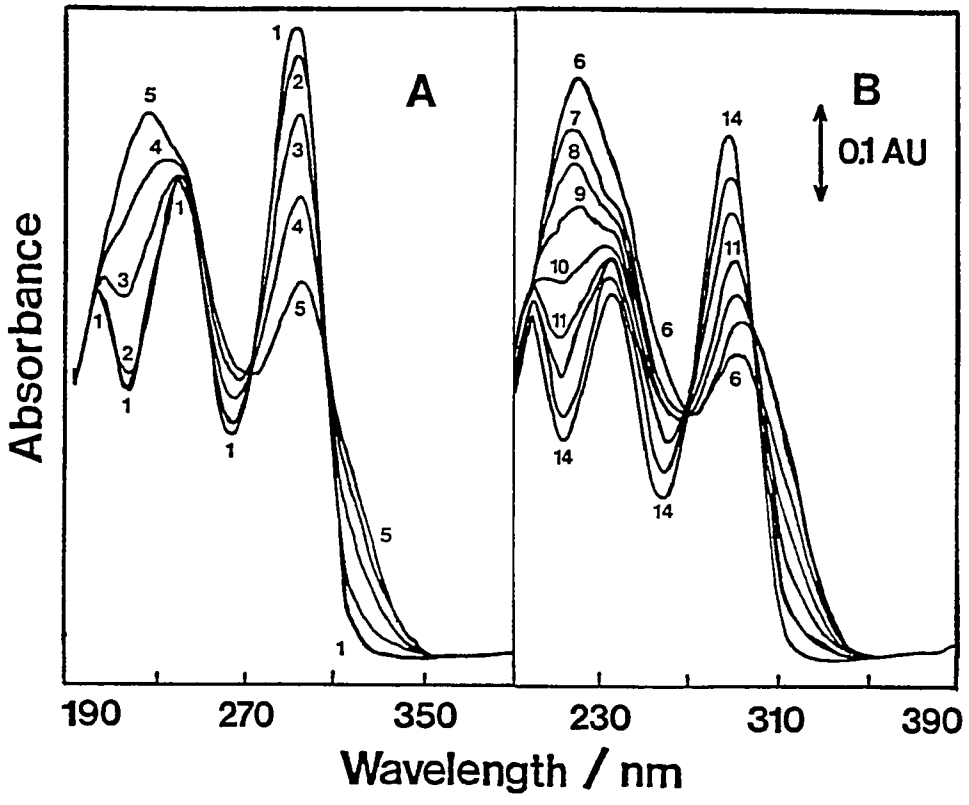

Fig. 7 (A) Spectra of 2mM 7-methyluric acid undergoing oxidation at 0.6V at a RVC electrode in a thin-layer cell in 0.5M NaCl plus 5mM Na_2HPO_4 pH 7.5. Curve 1 is the initial spectrum. Spectra were recorded at the following times after initiation of the oxidations: (2) 46, (3) 63, (4)80, and (5) 93 sec.

(B) After sweeping curve 5 in (A) the RVC electrode was potentiostated at -1.0V. Spectra were recorded at the following times: (6) 100, (7) 139, (8) 176, (9) 213, (10) 252, (11) 299, (12) 367, (13) 493 and (14) 1295 sec.

creases and splits into two. After about 5 min (curve 11, Fig. 7B) the spectrum observed is identical to that of 7-methyluric acid. Curve 14 in Fig. 7 is recorded after 21 min.

Spectroelectrochemical behavior of 7-methyluric acid in phosphate buffer (u = 0.5 M) at pH 7.0 is shown in Fig. 8. Curve 1 in Fig. 8A is the initial spectrum of 7-methyluric acid (λ_{max} = 293, 236 and 203 nm). Initiation of the peak I_a electrooxidation at 0.8 V causes the band at 293 nm to decrease while a new band grows in at 224 nm and the absorbance between about 352-300 nm also increases (curves 2-9, Fig. 8A). If, after scanning curve 9 in Fig. 8A the RVC electrode was open-circuited, the spectral changes shown between curves 10-20 in Fig. 8B were observed. Curve 20 in Fig. 8B is the spectrum due to some residual 7-methyluric acid and to the final reaction product. The A vs. t curves observed following electrochemical oxidation are shown in Fig. 9. The decay of the absorbance with time followed first order kinetics with the rate constants reported in Table 2. Experimental rate constants were linearly dependent on the ionic strength of phosphate buffers used (Fig. 10). However, if the U.V.-absorbing intermediate was first electrogenerated and then the RCV electrode was potentiostated at -1.4 V the spectroelectrochemical behavior noted in Fig. 8C was observed. Thus, the absorbance between about 352-190 nm decayed with time but no 7-methyluric acid was

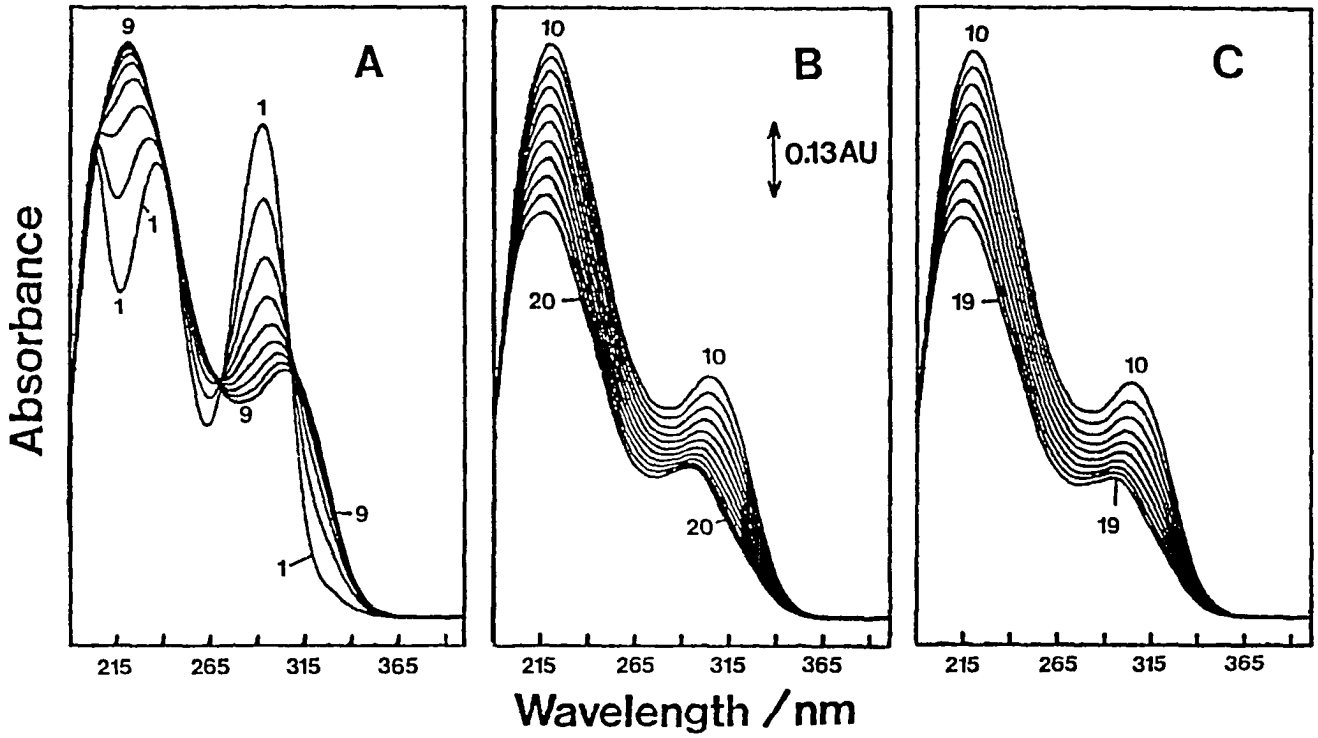

Fig. 8 (A) Spectra of 1mM of 7-methyluric acid in phosphate buffer (u = 0.5 M) pH 7.0 undergoing oxidation at 0.8 V in a thin-layer cell containing a RVC electrode. Curve 1 is the initial spectrum, curves 2-9 after initiation of the electrolysis. Each spectral sweep had a duration of 10 s with no time interval between sweeps. (B) After sweeping curve 9 in (A) the RVC electrode was open-circuited and curves 10-20 recorded, each sweep had a duration of 40 s. (C) After sweeping curve 9 in (A) the RVC electrode was potentiostated at -1.4 V and curves 10-19 recorded, each sweep had a duration of 40s.

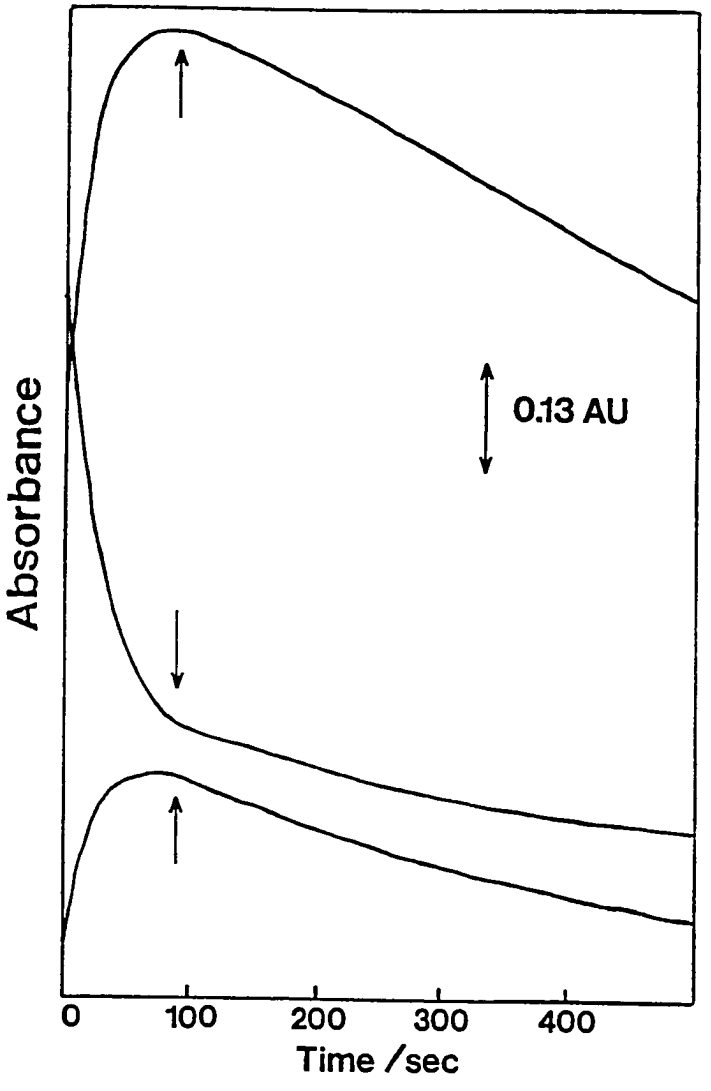

Fig. 9 Absorbance vs. time curve for the decay of the intermediate species generated upon electrolysis of 1 mM 7-methyluric acid at 0.8 V in pH 7.0 phosphate buffer (u = 0.5 M). Arrow indicates time when electrode was open-circuited. At wavelength (A) 220, (B) 290 and (C) 325 nm.

Table 2

Observed first order rate constant for decomposition of the U.V.-absorbing intermediate generated upon electrochemical oxidation of 1 mM 7-methyluric acid in phosphate buffer pH 7.0.

u	$k_{obs}(s^{-1})^a$ 220 nm	290 nm	325 nm
0.05	0.0002 ±0.00005	0.001 ±0.00005	0.0008 ±0.000006
0.01	0.0004 ±0.00003	0.002 ±0.00005	0.0009 ±0.000007
0.2	0.0006 ±0.00004	0.004 ± 0.0004	0.0013 ±0.000008
0.4	0.0007 ±0.00005	0.003 ± 0.0001	0.0019 ±0.000007
0.5	0.001 ± 0.00002	0.003 ± 0.0001	0.0024 ±0.000006
0.6	0.0012 ±0.00007	0.006 ±0.00003	0.0029 ± 0.00002
0.8	0.0013 ±0.00006	0.0065 ±0.0001	0.0034 ± 0.00001
1.0	0.0014 ±0.00005	0.0068 ±0.0001	0.0043 ± 0.00001

[a] Calculated by analysis of A vs. t obtained at the wavelength noted. The average of at least three replicate measurements is reported ± standard deviation.

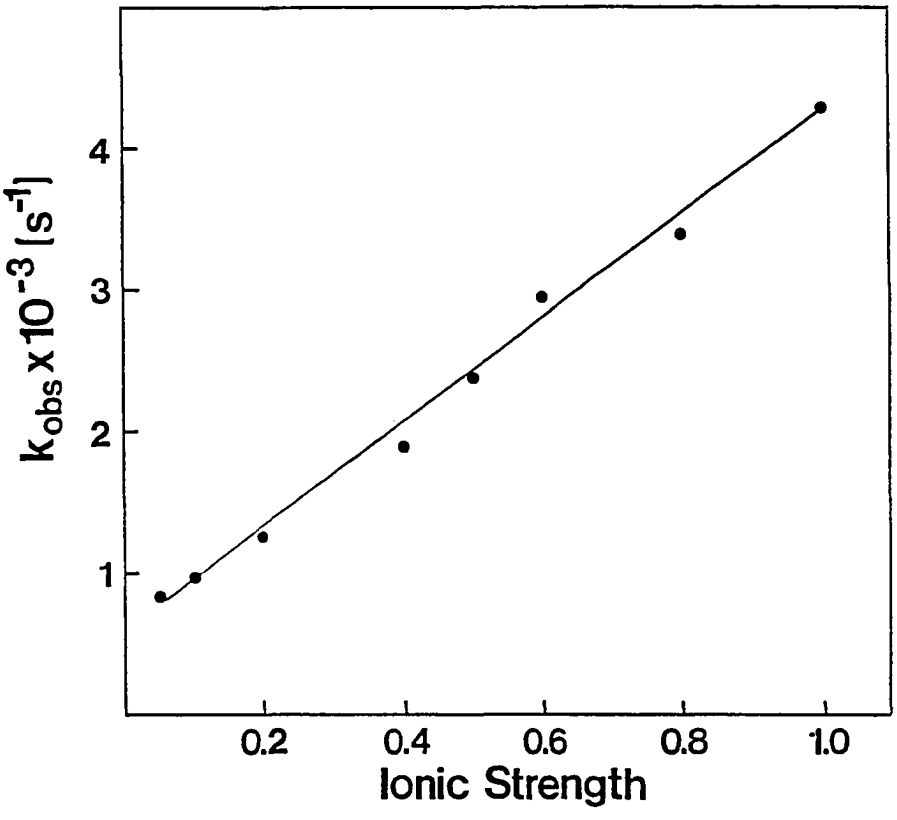

Fig. 10 Variation of the observed first order rate constant for decay of the U.V.-absorbing intermediate generated upon electrochemical oxidation of 7-methyluric acid at 0.8 V at a RVC electrode in a thin-layer cell as a function of the ionic strength of phosphate buffer pH 7.0. Absorbance monitored at 325 nm.

regenerated.

Spectroelectrochemical behavior of 7-methyluric acid under the same conditions mentioned above except that in phosphate buffer (u = 0.1 M) is shown in Fig. 11. Curve 1 in Fig. 11A is the initial spectrum of 7-methyluric acid (λ_{max} = 293, 236 and 203 nm). Application of a potential at 0.8 V to the RVC electrode causes the band at 293 nm to decrease while a new band grows in at 224 nm and the absorbance between about 352-300 nm also increase (curves 2-7, Fig. 11A). After about 140 sec electrolysis curve 7 is observed which is the spectrum of intermediate species (λ_{max} = 300 and 224 nm). If, after sweeping curve 7 in Fig. 11 the RVC electrode was opencricuited, the spectral changes shown between curves 8-12 in Fig. 11B were observed. Curve 12 in Fig. 11B is the spectrum due to some residual 7-methyluric acid and to the final reaction product. These behaviors are similar to those observed in phosphate buffer (u = 0.5 M) except that the rates of formation and decay of intermediate species are slower than in high ionic strength of phosphate buffer (u = 0.5 M). In addition, if the U.V.-absorbing intermediate was first electrogenerated and then the RVC electrode was potentiostated at -1.4 V the spectroelectrochemical behavior noted in Fig. 11C was observed. Thus, electroreduction of the intermediate (curve 8, Fig. 11C) causes the absorbance between about 352-190 nm to decrease for about 160 s (curve 9, Fig. 11C) then the long-

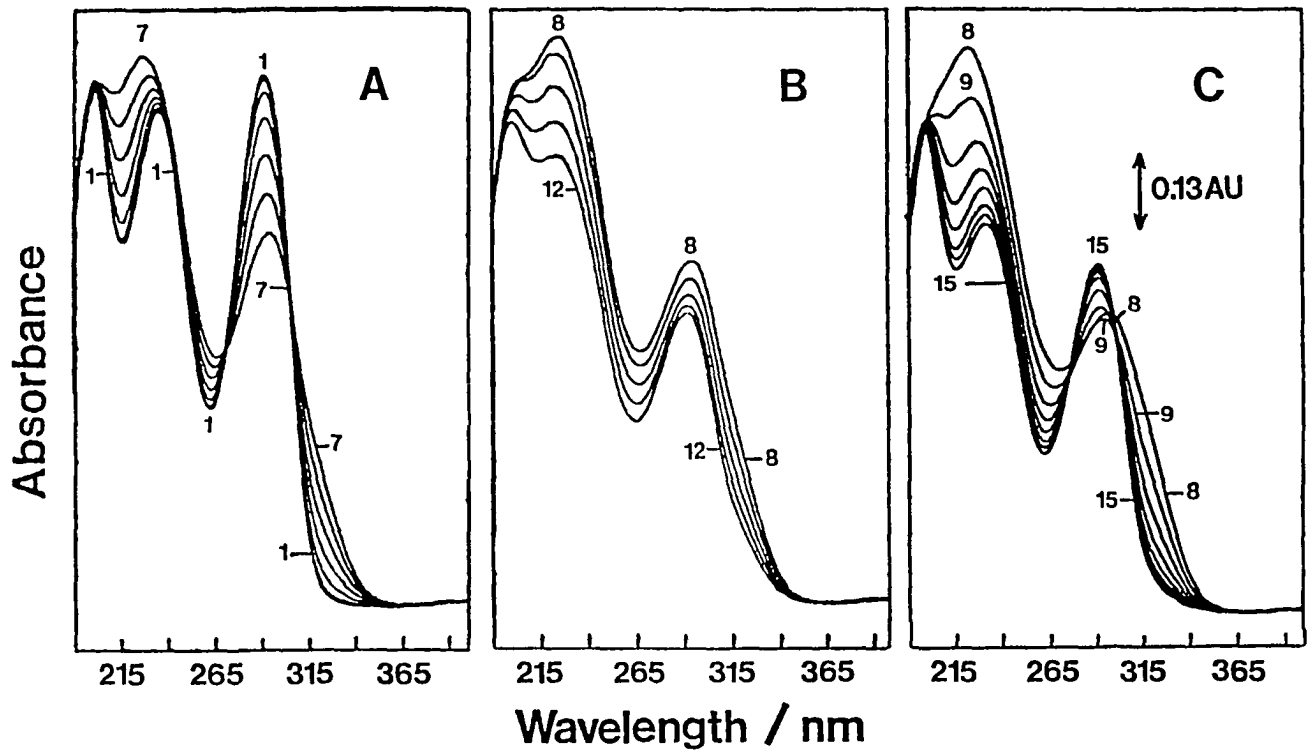

Fig. 11 (A) Spectra of 1 mM 7-methyluric acid in phosphate buffer (u = 0.1 M) pH 7.0 undergoing oxidation at 0.8 V in a thin-layer cell containing a RVC electrode. Curve 1 is the initial spectrum, curves 2-7 after initiation of the electrolysis. Each spectral sweep had a duration of 20 s. (B) After sweeping curve 7 in (A) the RVC electrode was open-circuited and curves 8-12 recorded. Each sweep had a duration of 160 s. (C) After sweeping curve 7 in (A) the RVC electrode was potentiostated at - 1.4 V and curves 8-15 recorded. Each sweep had a duration of 160s.

wavelength band shifts to shorter wavelength band decreases and splits into two. After about 14 min (curve 10, Fig. 11C) the spectrum observed is identical to that of 7-methyluric acid. Thus, it is clearly indicates that there are two intermediate species with the same U.V. spectra are involved in the spectroelectrochemical oxidation of 7-methyluric acid. It is proposed that these intermediates species are tertiary alcohol (III, Fig. 27) and the carboxylic acid (V, Fig. 27). However, reduction of the tertiary alcohol follows by dehydration to give 7-methyluric acid. On the other hand, the carboxylic acid undergoes further chemical reaction to give 4-methylallantoin. The results shown in Table 2 indicate that the rate constants for decomposition of the U.V.-absorbing intermediate generated upon spectroelectrochemical oxidation increased with increasing ionic strength of phosphate buffer used. This implies that the tertiary alcohol (III, Fig. 27) is a much shorter-lived intermediate in the presence of high concentrations of phosphate. This behavior agrees with the spectroelectrochemical behaviors observed in Figs. 8 and 11. Thus, the partial regeneration of 7-methyluric acid by reduction of the intermediate is observed only in low concentration of phosphate buffers (ca. $\leq$ 0.1 M).

Supporting electrolyte solutions of 0.5 M NaCl plus 5 mM Na_2HPO_4 were used because using such solution it was possible to trap and identify intermediates. In such ex-

periments the electrooxidation of 7-methyluric acid (ca. 1 mM) was carried out at a RVC electrode in a thin-layer cell for about 60-150 s until the maximal amount of intermediate species was present as shown from spectral measurements. The electrolysis was terminated and the solution containing the intermediate species was quickly transferred to a vial immersed in a bath of dry ice-acetone (-78°C). The frozen solution was freeze-dried. The resulting dry solid was silylated with BSA or BSA-d_9 in pyridine at 80°C for 30 min. The trimethylsilyl derivative of this intermediate gave GC peaks at retention times (t_R) Of 26.43 and 28.55 min having molar masses of 414 and 460 g, respectively. When silylation was carried out with BSA-d_9 GC peaks were observed at t_R = 26.5 and 29.2 min having molar masses of 441 and 496 g, respectively. These results indicate that the reaction mixture contains one compound having a molar mass of 198 g which possesses three silylatable sites and a second compound having a molar mass of 172 g possessing four silylatable sites. If the U.V.-absorbing intermediate species generated in the thin-layer cell was allowed to completely decompose for about 7 to 10 min, silylation of the product followed by GC-MS revealed that the compound having a molar mass of 198 g disappeared and the yield of the compound of molar mass of 172 g increased. Accordingly, it was concluded that the species having a molar mass of 198 g was the U.V.-absorbing intermediate and that of molecular weight 172 was a product.

On the basis of the kinetic analysis of A vs. t curves and the time required to generate and trap the intermediate, it is conluded that the intermediate identified is BCA (V, Fig. 27). However, BCA and its precursor tertiary alcohol have exactly the same molecular weight and molecular formula and possess four silylatable positions. Thus, it is possible that a mixture of tertiary alcohol and BCA are in fact trapped. These would be expected to exhibit very similar U.V. and mass spectra.

3. A. 3. Conventional electrolyses at peak I_a and peak II_a

The potential range available at a RVC electrode (in a thin-layer cell) does not extend to sufficiently positive potentials to permit peak II_a to be observed. Hence, it was necessary to perform conventional controlled potential electrolyses at pyrolytic graphite electrodes in order to compare the peak I_a and peak II_a oxidation reactions. Typically about 25 ml of 1 m$\underline{M}$ stirred solutions of 7-methyluric acid in phosphate buffer were electrolyzed at plates of pyrolytic graphite having a total surface area of 40 cm^2.

In pH 7.0 phosphate buffer having ionic strengths ranging from 0.1- 1.0 $\underline{M}$ experimental n-values of 1.9 $\pm$ 0.2 were observed when 7-methyluric acid was electrolyzed at peak I_a potentials (0.6 V). It is noted that following controlled potential electrooxidation of 7-methyluric acid at peak I_a

potentials, voltammogram of the product solution showed no evidence for oxidation peak II_a. Thus, the species responsible for peak II_a oxidation must be an unstable compound formed as a results of the peak I_a process. Coulometry at peak II_a potentials (1.2 V) gave experimental n-values which were depend on the ionic strength of the phosphate buffer as shown in Fig. 12. Thus, at a phosphate buffer ionic strength of 0.1 M the apparent n-value (n_{app}) was 2.3 ± 0.1 which increased to 3.1 ± 0.2 at an ionic strength of 0.5 M then slightly decreased to 2.7 ± 0.1 at an ionic strength of 1.0 M. The spectral changes observed during the electrooxidation of 7-methyluric acid at peak I_a potentials (ca. 0.8 V) in phosphate buffer (u = 0.1) at pH 7.0 are shown in Fig. 13. As the electrolysis proceeds the characteristic U.V. band of 7-methyluric acid (λ_{max} = 291 nm) decreases and a new bands appears at λ_{max} = 234 nm (curve 2, Fig. 13). After scanning curve 2, the U.V. bands at λ_{max} = 291 and 234 nm decrease throughout the electrolysis (curves 3-7, Fig. 13).

Figure 14 shows a series of cyclic voltammograms of 7-methyluric acid recorded during electrooxidation at peak I_a potentials (ca. 0.6V) in phosphate buffer (u = 0.1) at pH 7.0. Reduction peak II'_c split into two peaks (II'_c and II''_c) during the electrolysis (Figs. 14B, C, D and E). Oxidation peak I_a and peak II_a both decreased in height and disappeared at the end of electrolysis (Fig. 14F).

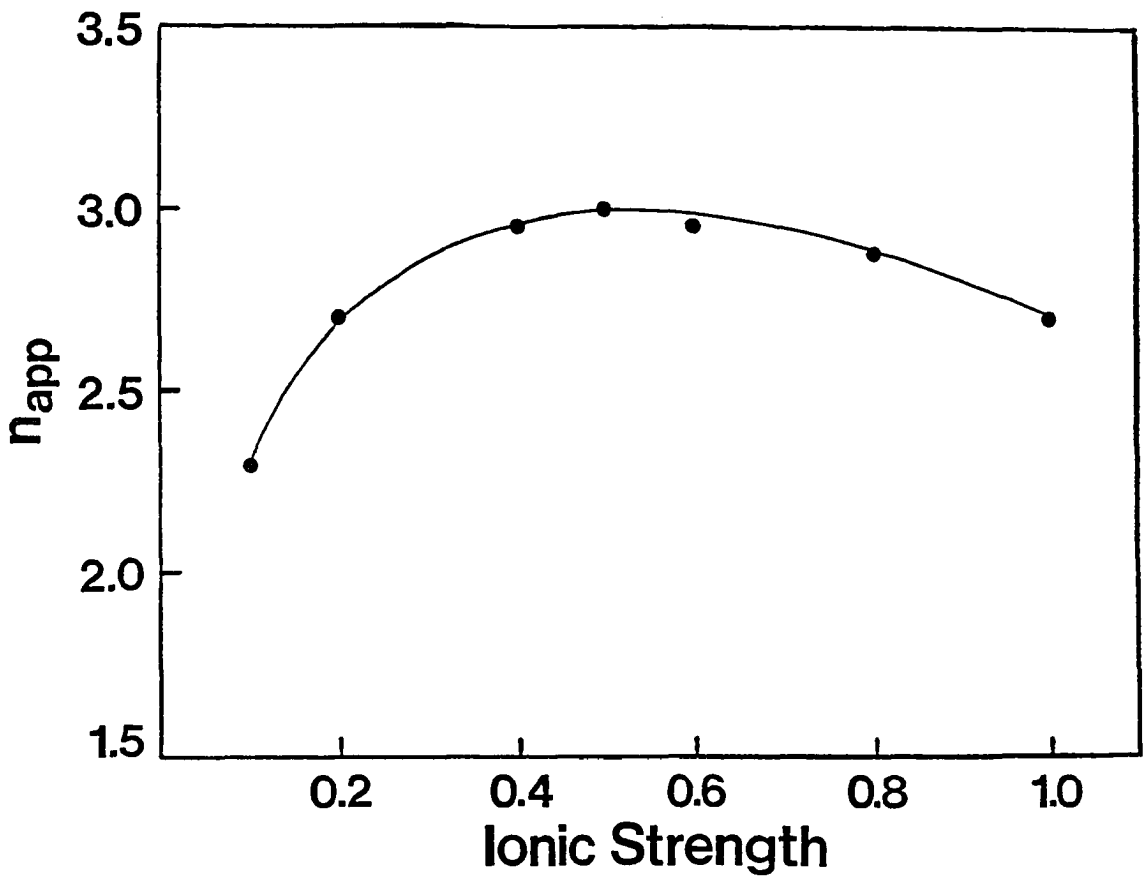

Fig. 12 Variation of n_{app} *vs.* the ionic strength of pH 7.0 phosphate buffer for the controlled potential electrooxidation of 7-methyluric acid at peak II_a potentials (1.2 V).

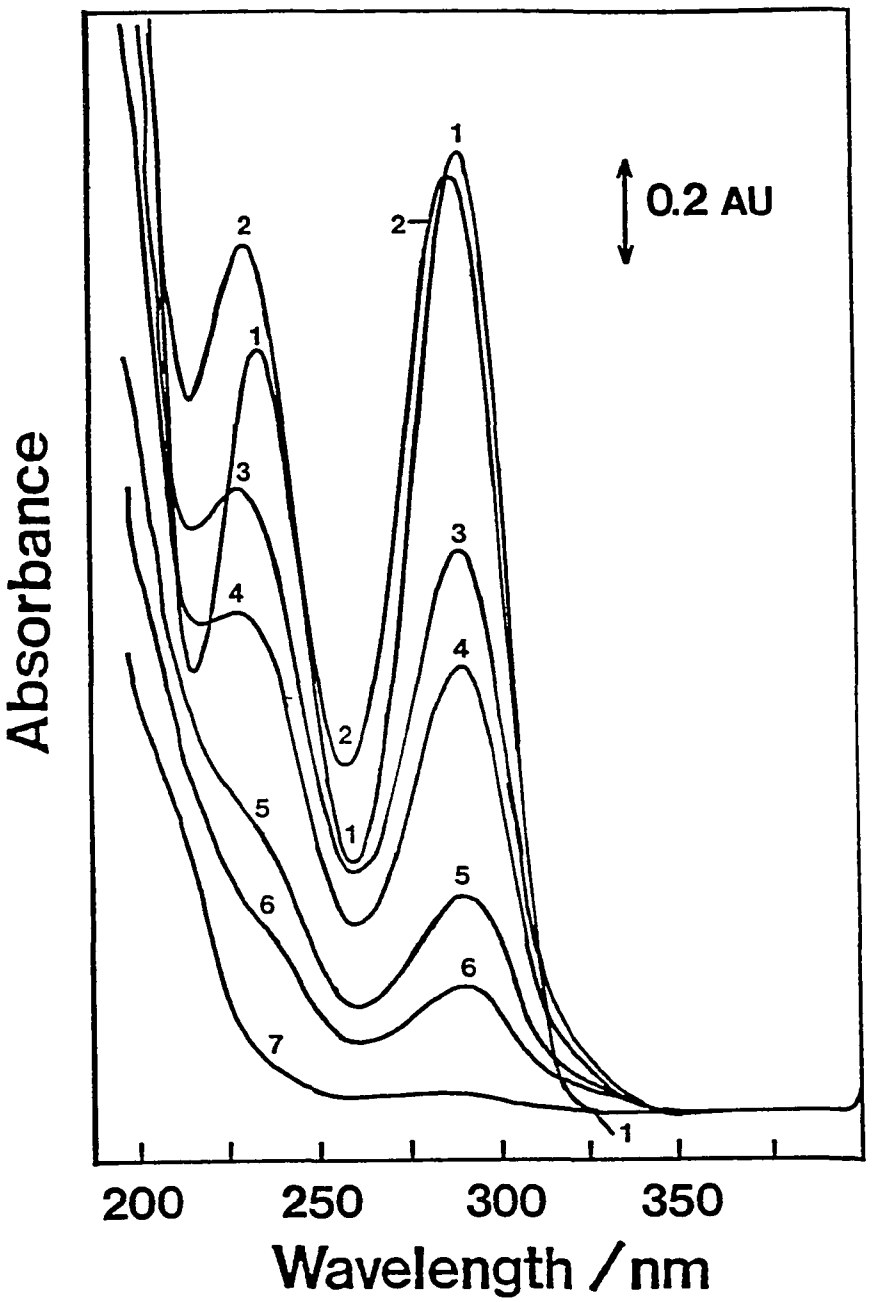

Fig. 13 Spectral changes observed during the controlled potential electrooxidation of 1.8mM 7-methyluric acid in pH 7.0 phosphate buffer (u = 0.1M) at 0.8V. Curve 1 is the U.V. spectrum of 7-methyluric acid. Spectra were recorded after (2) 15, (3) 25, (4) 33, (5) 50, (6) 66 and (7) 166 min.

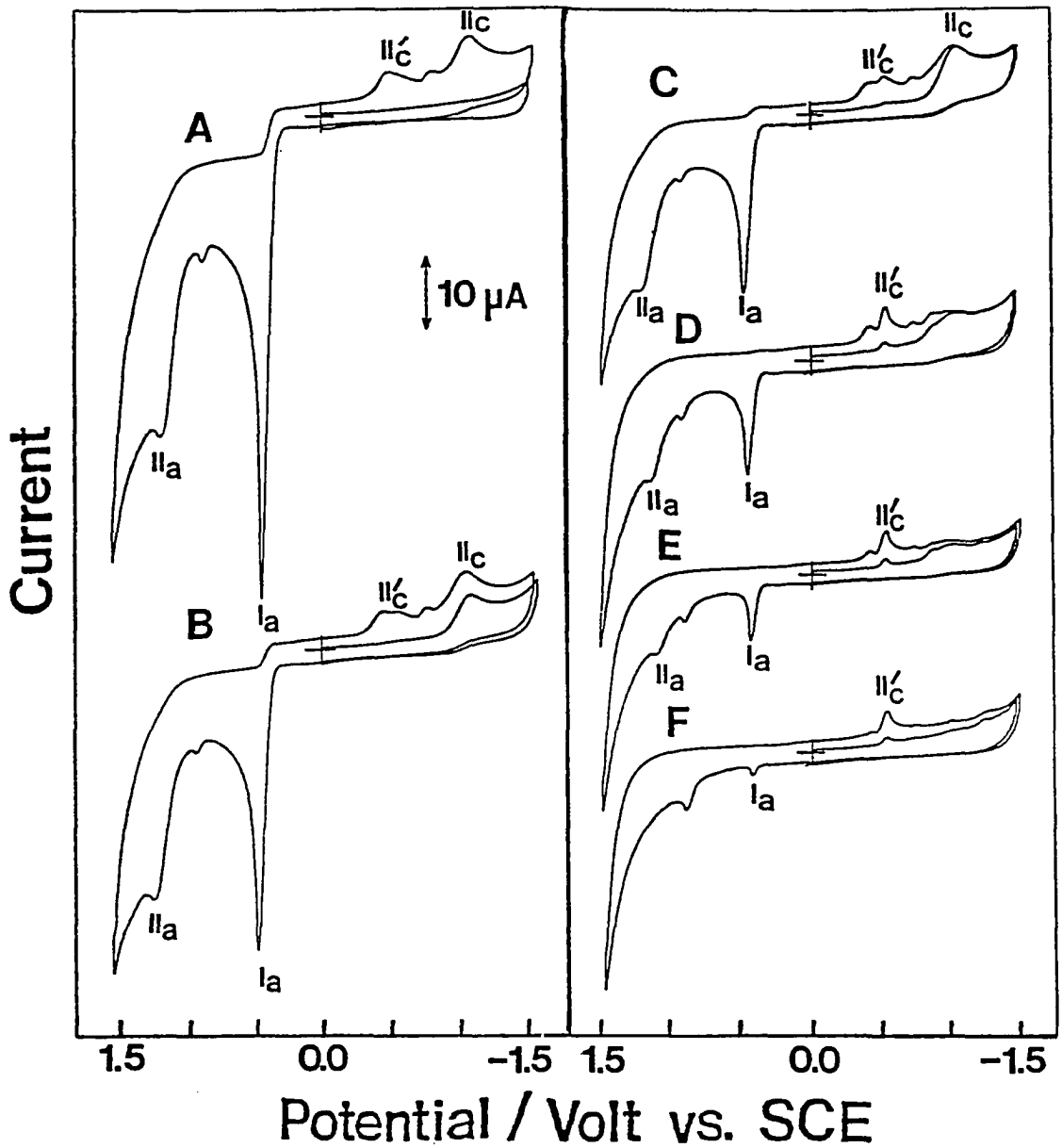

Fig. 14 Cyclic voltammograms at the PGE taken throughout the course of a controlled potential oxidation of 2mM 7-methyluric acid in pH 7.0 phosphate buffer (u = 0.1 M) at 0.6V. (A) Before electrolysis, (B), (C), (D), (E) and (F) were recorded after 15, 30, 45 min, 1 and 2 h of electrolysis. Sweep rate: 200 mVs-1.

Figure 15 shows a series of cyclic voltammograms of 7-methyluric acid recorded during electrooxidation at peak II_a potentials (ca. 1.2 V) in phosphate buffer (u = 0.1) at pH 7.0. Three new reduction peaks (II''_c, III_c and IV_c) appeared (Fig. 15E).

3. A. 4. Isolation and characterization of electrooxidation products

The product solutions obtained after controlled potential electrolyses of 7-methyluric acid were freeze-dried. The resulting solid was dissolved in about 2 ml of water and passed through a column of Sephadex G-10 gel permeation resin (80 x 1.5 cm) using water as the eluent (36 ml h^{-1} flow rate). The eluent was monitored at 207 nm (Gilson Holochrome U.V. detector) and 4 ml fractions were collected with a fraction collector. A liquid chromatogram of the products obtained from electrooxidation of 7-methyluric acid at peak I_a in phosphate buffer (u = 0.1) at pH 7.0 is shown in Fig. 16.

The component eluted under liquid chromatographic (LC) peak A was isolated after freeze-drying as a black syrup. In water it showed an U.V. absorption band at 230 nm (Fig. 17). Mass spectrometry of the solid material did not give an useful mass spectral data. Attempts to derivatize the solid with a variety of silylation agents under many different experimental conditions were unsuccessful.

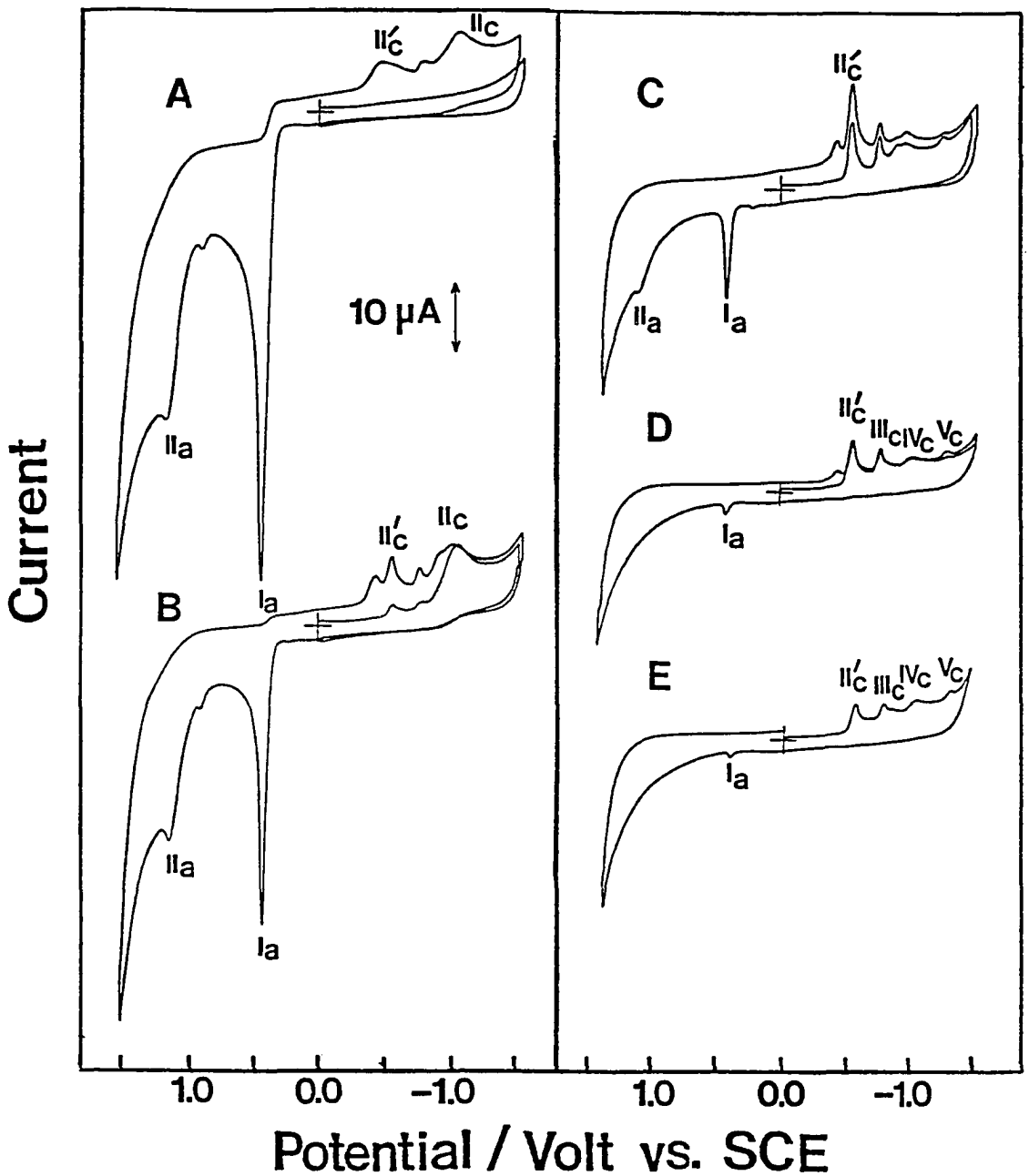

Fig. 15 Cyclic voltammograms at the PGE taken throughout the course of a controlled potential oxidation of 2mM 7-methyluric acid in pH 7.0 phosphate buffer (u = 0.1 M) at 1.2 V. (A) Before electrolysis, (B), (C), (D) and (E) were recorded after 15, 30, 45 and 75 min. Sweep rate: 200 mVs^{-1}.

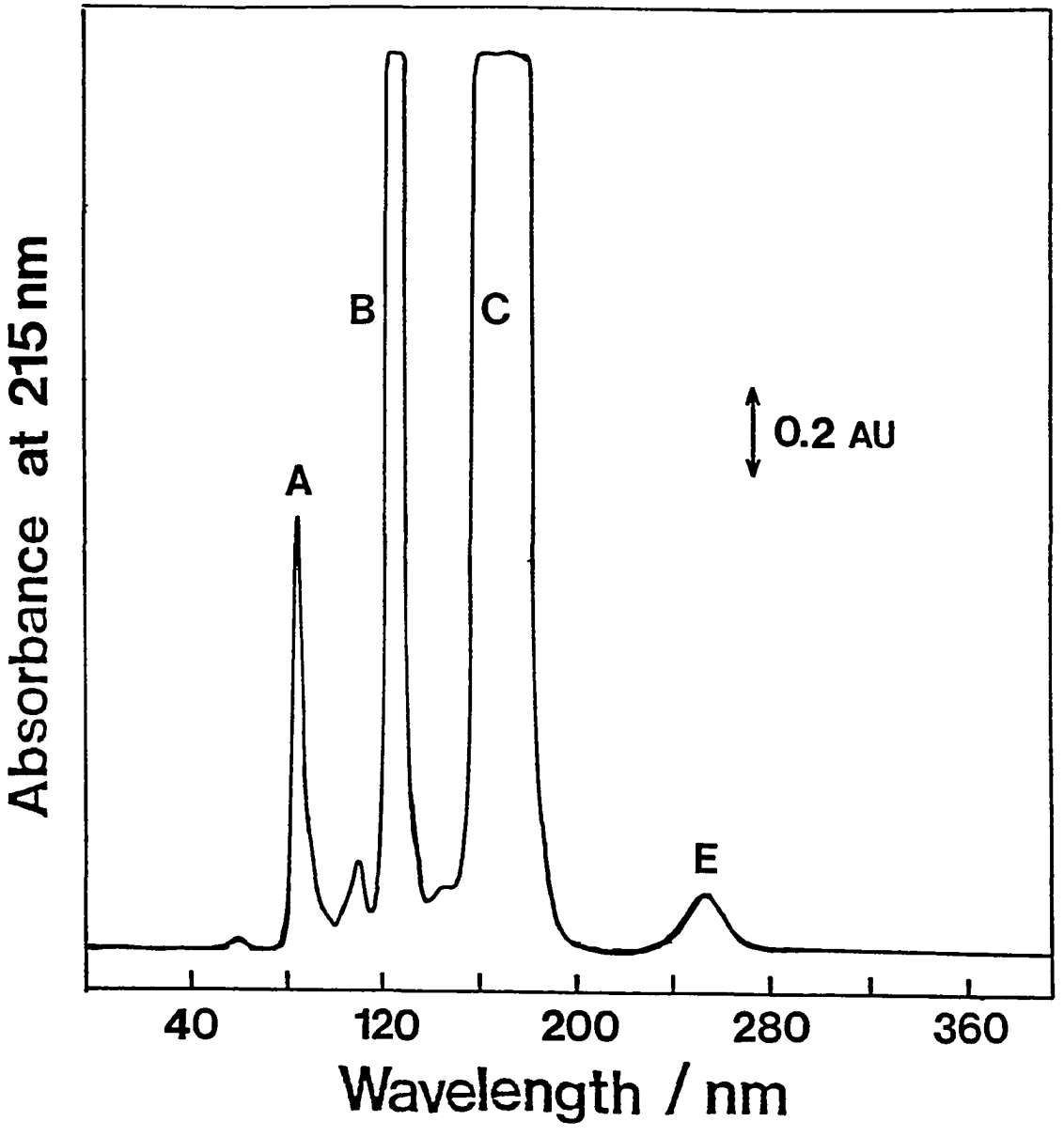

Fig. 16 Liquid chromatogram of the products of electrochemical oxidation of 2 mM 7-methyluric acid in pH 7.0 phosphate buffer (u = 0.1M) oxidized at 0.6 V. Chromatography done on Sephadex G-10 (80 x 2 cm) using water as the eluent (32 $ml h^{-1}$).

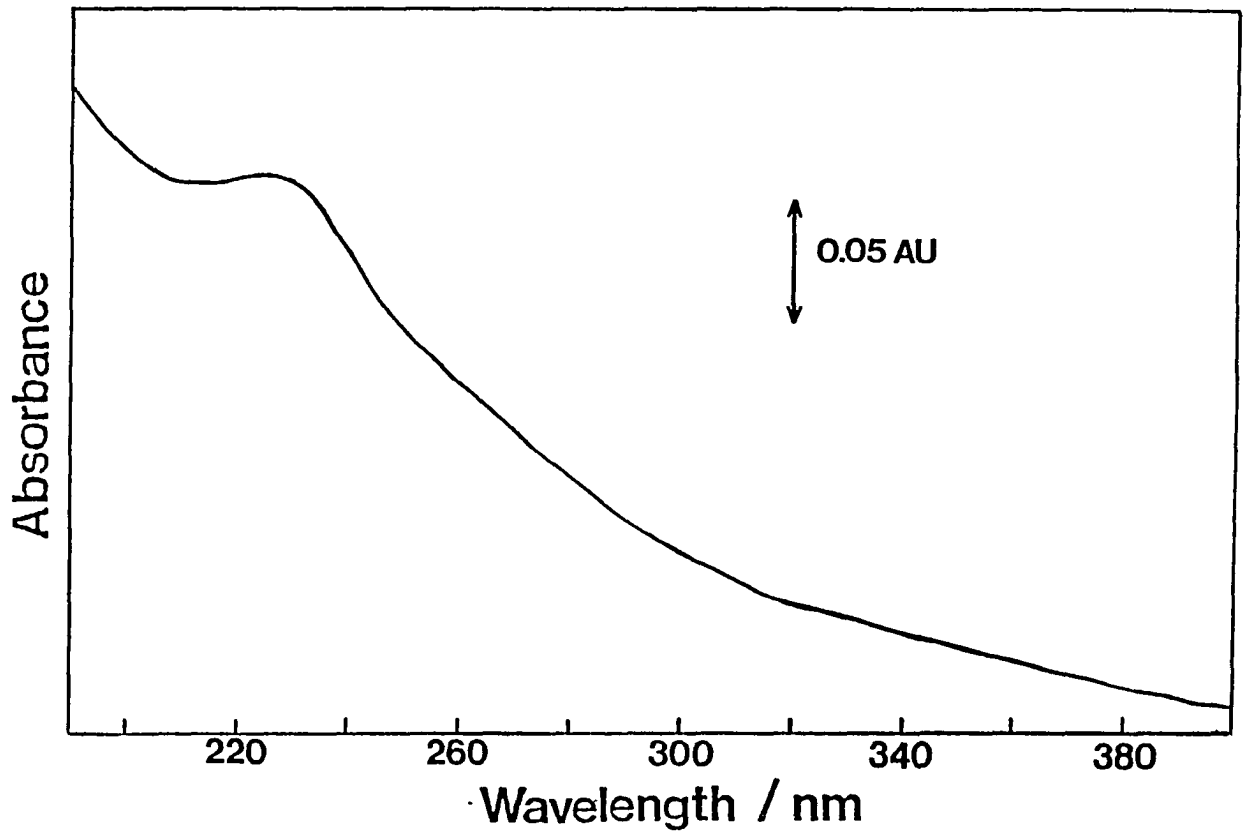

Fig. 17 U.V. spectrum of LC component A in water.

The component eluted under LC peak B is due to inorganic phosphate and partially due to a small amount of chloride ion from the reference electrode.

The component eluted under LC peak C was isolated after freeze-drying as a white powder. In water it showed a characteristic U.V. spectrum with λ_{max} = 207 nm (Fig. 18). The mass spectrum on solid sample gave the following results (70 eV, 200°C), m/e (relative abundance): 174 (1.3%), 173 (7.8%), 172 (M^+, 28.2%), 155 (32.1%), 145 (22.4%), 144 (100%), 129 (90.7%) and 128 (50.0%). Silylation with BSA in pyridine at 80°C for 30 min gave GC peaks at t_R = 28.75 min having molar mass of 460 g (based on EI and CI mass spectrometry). These results indicate that this major product had a molar mass of 172 g and in fact was the same product obtained following electrooxidation of 7-methyluric acid at peak I_a potentials in 0.5 M NaCl plus 5 mM Na_2HPO_4 at pH 7.5 in a thin-layer cell. Fragmentation data obtained from MS, EI- and CI-MS indicate that this product is 4-methylallantoin.

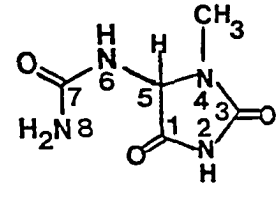

4-methylallantoin

An extremely small amount of product was eluted under LC peak E as shown in Fig. 16. It was not possible to

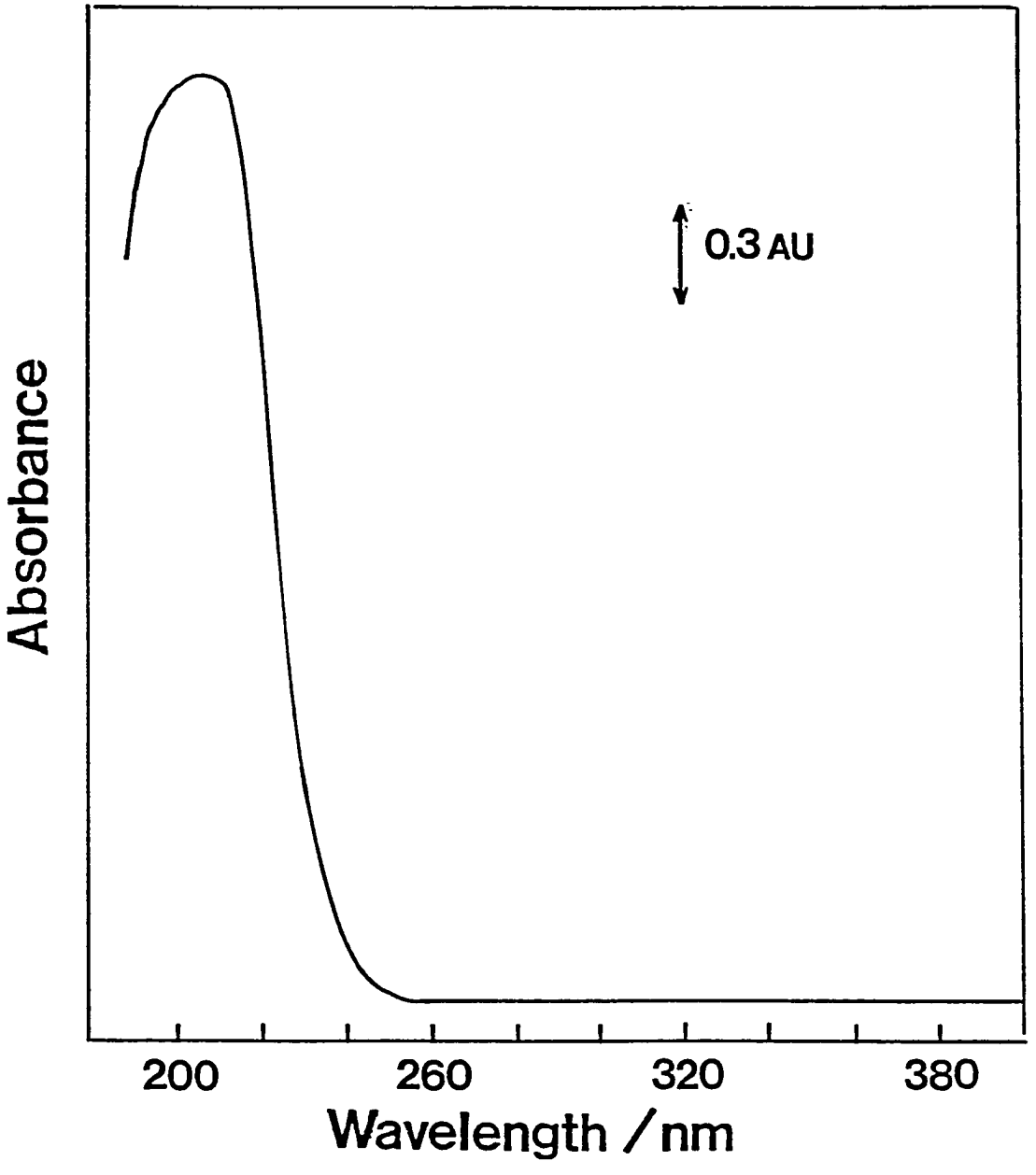

Fig. 18 U.V. spectrum of LC component C in water.

identify or characterize this compound.

It is also noted that at pH < 5.0 an additional peak I_a product appears. In water it showed an U.V. absorption band at 206 nm. This product was isolated after freeze drying as a white solid. EI- and CI/MS on the derivatized mixtures (BSTFA or MTBSTFA in acetonitrile at room temperature for 24 h) indicate that this product has a molar mass of 173 g and possesses only three of its four available sites.

Liquid chromatogram of the peak II_a products also showed two additional LC peaks D and F (Fig. 19). Comparison of the liquid chromatograms shown in Figs. 16 and 19 reveals that LC peaks A and E increase in height. However, these three LC peaks D, E and F are minor products comparing with component eluted under LC peak C (ca. < 5%). The product eluting under LC peak D was isolated after freeze drying as a white solid. In water this product exhibited an U.V. absorption band at 210 nm (Fig. 20). Silylation with BSTFA in acetonitrile at room temperature for 2 h gave GC peak at t_R = 18.88 min having a molar mass of 271 g (based on EI and CI mass spectrometry). Silylation with MTBSTFA in acetonitrile at room temperature for 2 h gave GC peak at t_R = 19.5 min having a molar mass of 355 g. These results indicate that the compound has a molar mass of 127 g and possesses 2 silylatable sites.

After removal of the eluent by freeze-drying, the com-

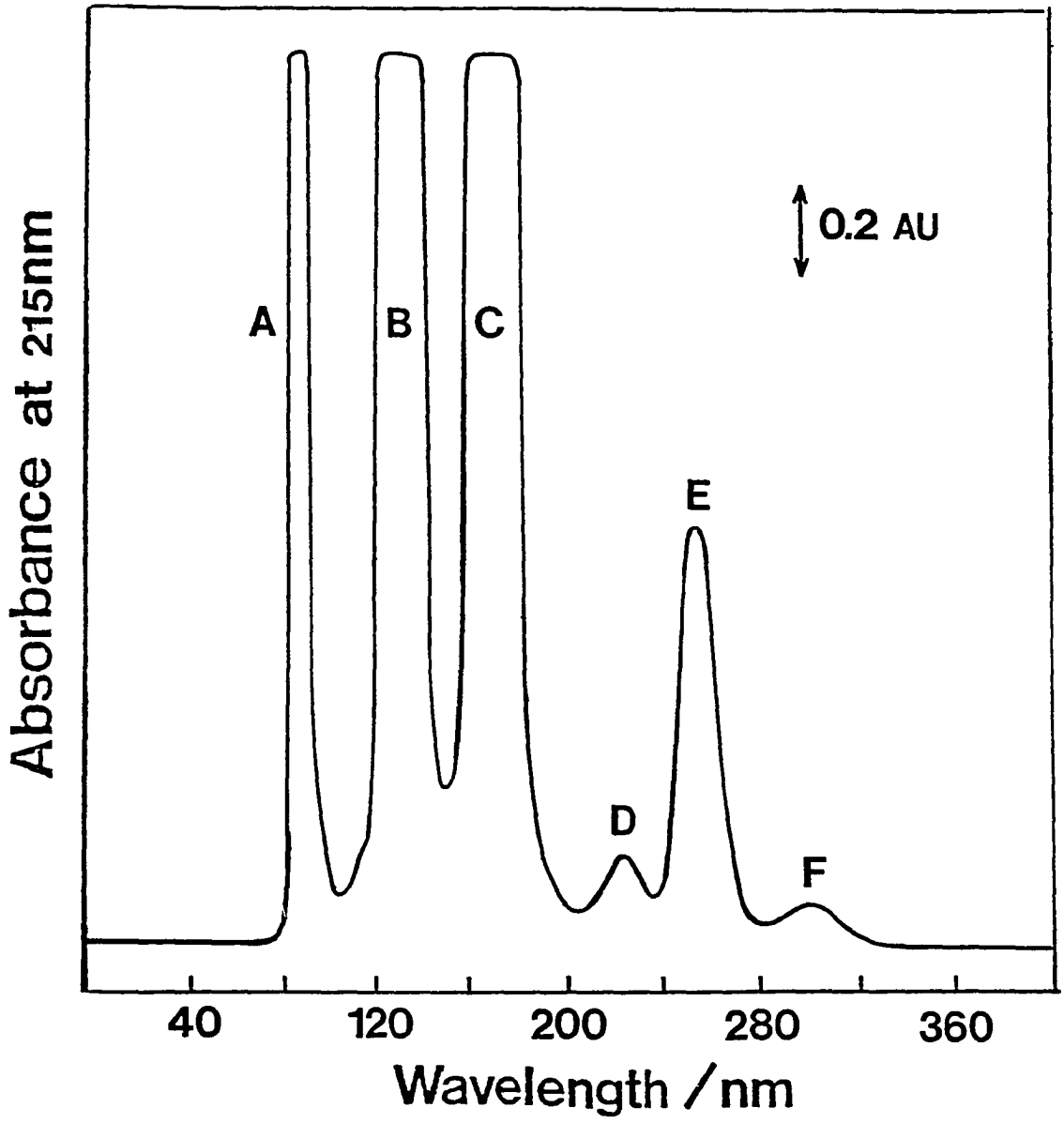

Fig. 19 Liquid chromatogram of the products of electrochemical oxidation of 2 mM 7-methyluric acid in pH 7.0 (u = 0.1M) at 1.2 V. Chromatography were done on Sephadex G-10 (80 x 2 cm) using water as the eluent (32 $ml h^{-1}$).

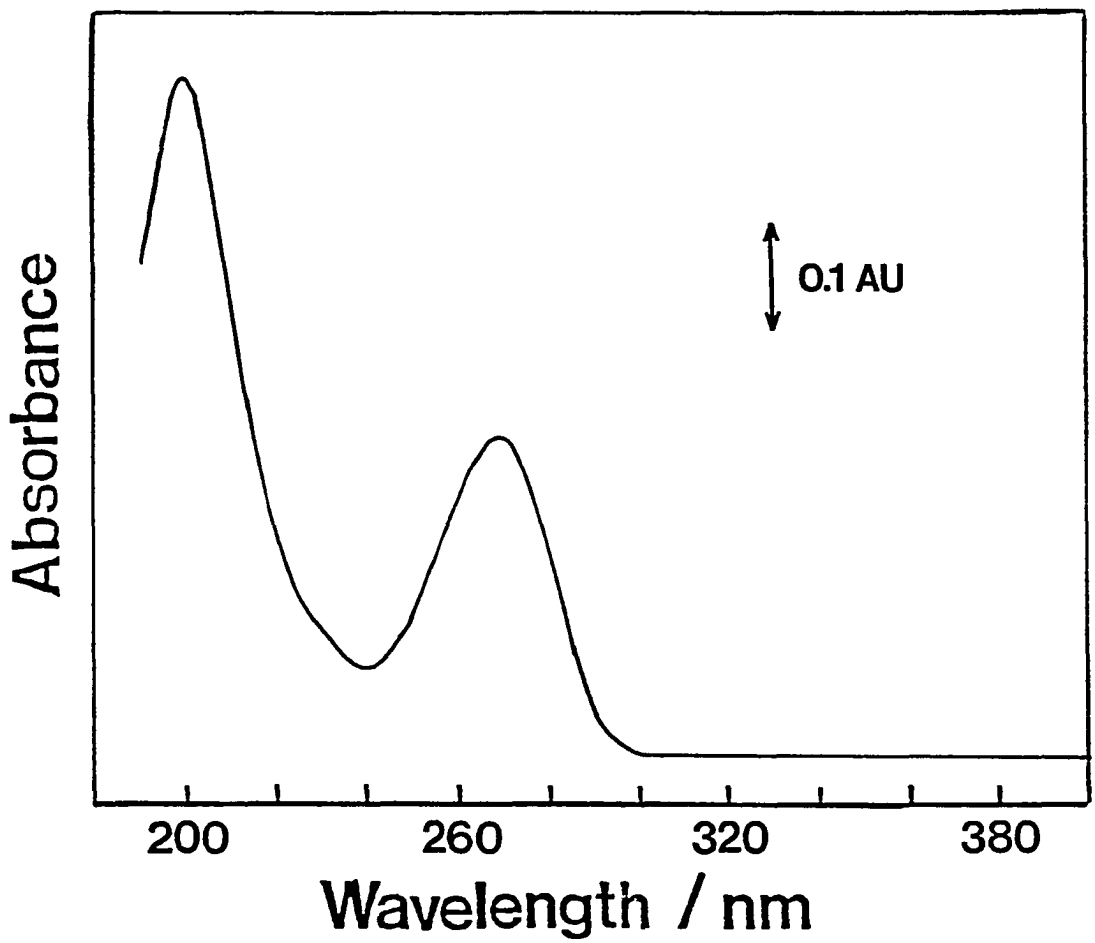

Fig. 20 U.V. spectrum of LC component D in water.

pound eluted under LC peak E was found to be a white solid. In water it showed U.V. absorption bands at $_{max}$ = 198 and 268 nm (Fig. 21). The U.V. spectrum and LC retention volume of this compound agree with those obtained for LC peak E in peak I_a product. Low resolution mass spectrometry (70 eV, 200°C) gave the following major peaks, m/e (relative abundance): 162 (0.2%), 161 (1.3%), 160 (M^+, 16.7%), 145 (0.9%), 144 (8.1%), 143 (M^+-OH, 68.5%), 132 (0.9%), 131 (5.7%), 130 (M^+-CH_3NH, 100%), 119 (0.3%), 118 (1.0%) and 117 (M^+-NHCO, 19.5%). A suggested fragmentation scheme to account for the major ions observed in the mass spectrum is shown in Fig. 22. Silylation with BSTFA in acetonitrile at room temperature for 24 h gave GC peak at t_R = 28.3 min having a molar mass of 358 g (based on EI and CI mass spectrometry). Silylation with MTBSTFA in acetonitrile at room temperature for 24 h gave a peak at t_R = 35.4 min having a molar mass of 484 g. These results indicate that the compound has a molar mass of 142 g and possesses three silylatable sites. The

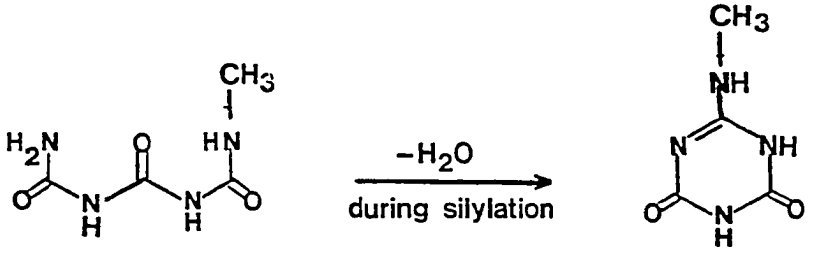

MW = 160 MW = 142

molar mass of this compound obtained from mass spectrometry and GC/MS is 18 g different. This can be explained that

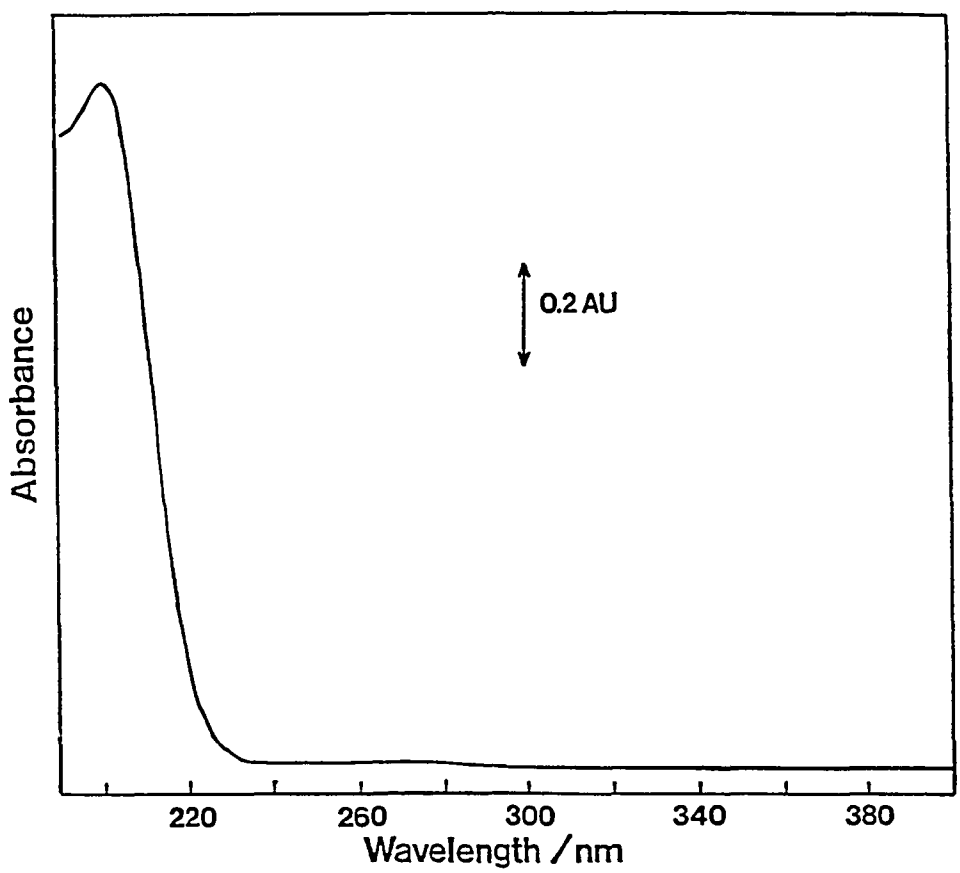

Fig. 21 U.V. spectrum of LC component E in water.

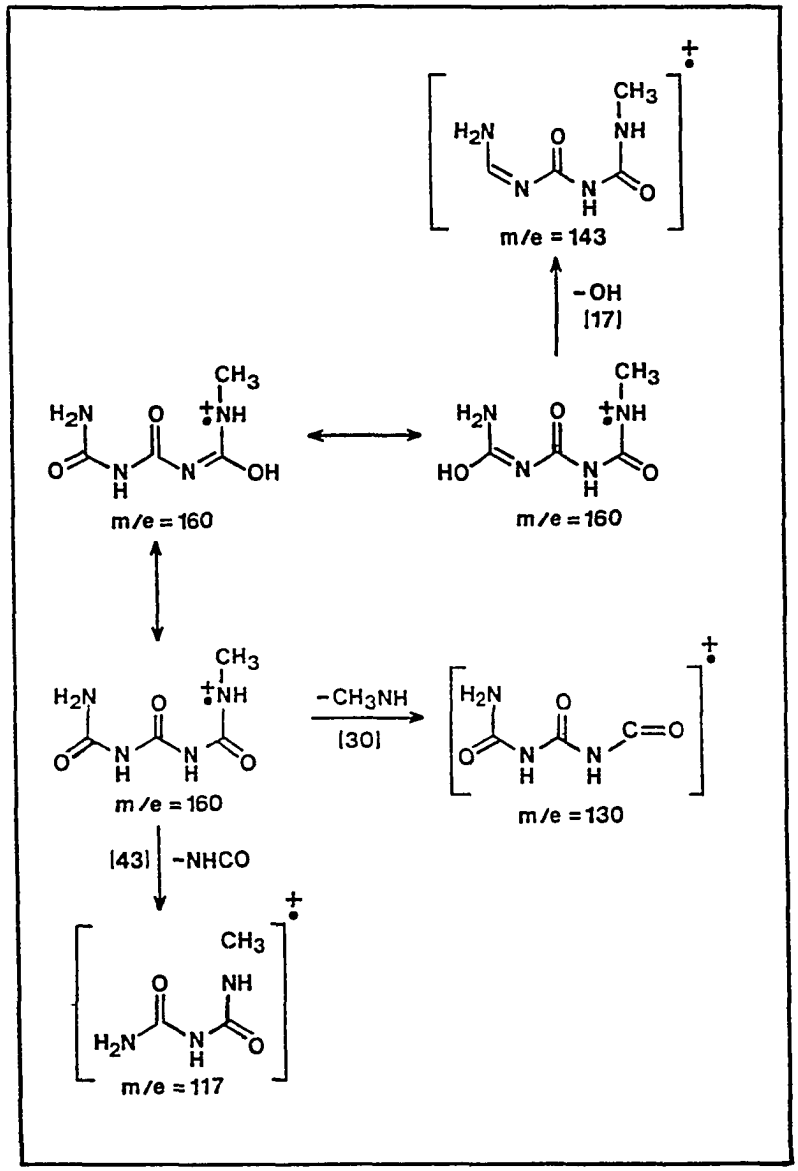

Fig. 22 Possible scheme to account for the major fragments observed in the low resolution mass spectrum of LC component E (the peak II_a product of electrooxidation of 7-methyluric acid).

during silylation water molecule is eliminated from this compound to give a six-membered ring compound(XXI).

The product eluted under LC peak F was isolated after freeze drying as a white solid. In water this product exhibited U.V. absorption bands at λ_{max} = 204 and 290 (sh) nm (Fig. 23). Silylation with BSTFA in acetonitrile at room temperature for 24 h gave GC peaks at t_R = 24.87 min having molar mass 344 g.

3. B. Enzymatic oxidation of 7-methyluric acid

3. B. 1. Spectral and kinetic studies

Stock solution of 7-methyluric acid, hydrogen peroxide and type VIII peroxidase were prepared fresh each day in an appropriate buffer. In order to spectrally monitor the enzyme-catalyzed oxidation, 0.7 ml of 3 m$\underline{M}$ 7-methyluric acid solution and an equal volume of 4 u$\underline{M}$ peroxidase solution were mixed in a 1 cm quartz cell. The enzymatic oxidation was initiated by adding 0.7 ml of 12 m$\underline{M}$ of H_2O_2 stock solution. Typical conditions and spectral studies obtained at pH 7.5 (0.5 $\underline{M}$ NaCl plus 5 m$\underline{M}$ Na_2HPO_4) are presented in Fig. 24. Curve 1 in Fig. 24A is the spectrum of 7-methyluric acid (λ_{max} = 291, 233 and 204 nm). Initiation of the peroxidase-catalyzed oxidation causes the bands at 291 nm to decrease and shift to longer wavelength while the absorbance at 215 nm increases and the absorbance between 350-310 nm also increases. After scanning curve 4 in Fig. 24A the

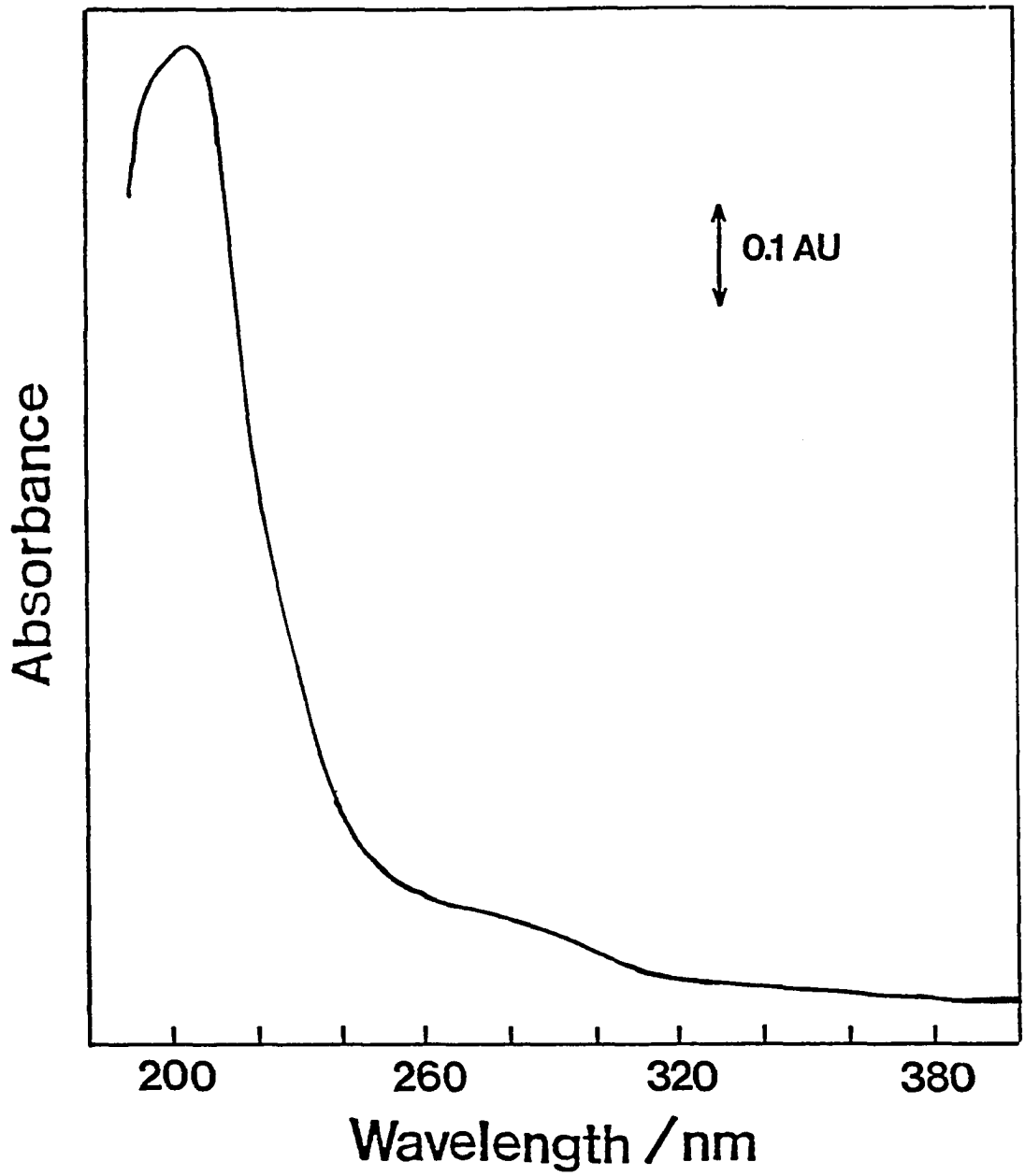

Fig. 23 U.V. spectrum of LC component F in water.

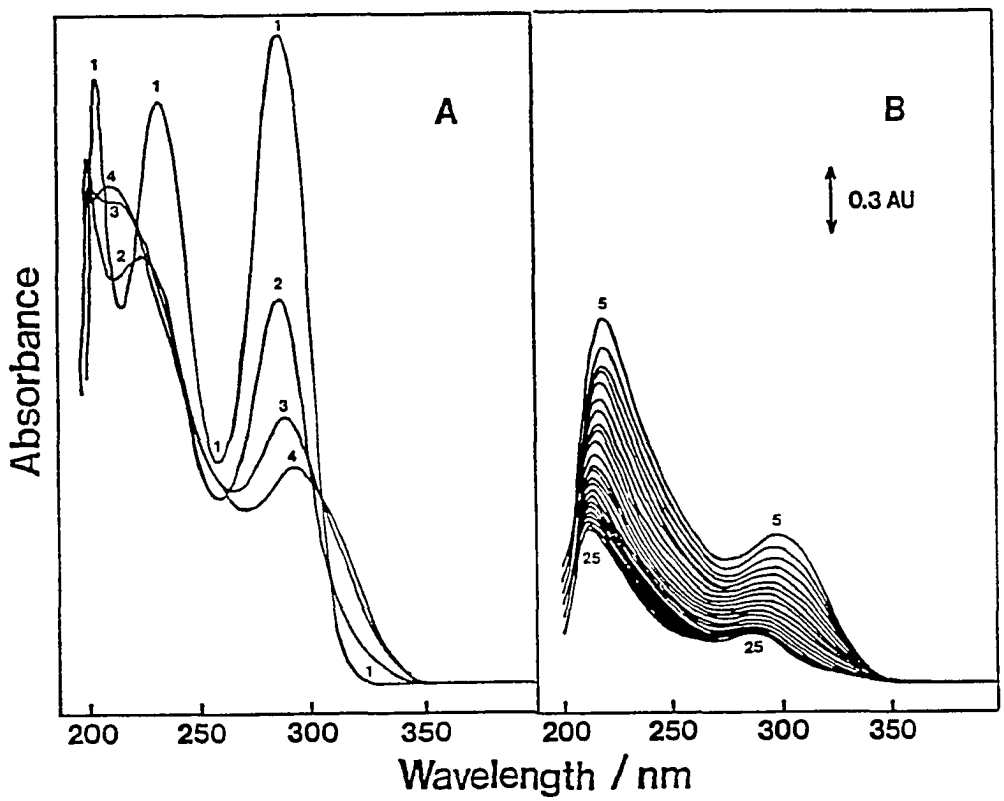

Fig. 24 Spectra taken during the course of the oxidation of 7-methyluric acid (600 uM) by H_2O_2 (1200 uM) catalyzed by the type VIII peroxidase (0.4 uM) in pH 7.5 (0.5 M NaCL plus 5 mM Na_2HPO_4). (A) Curve 1 is the initial spectrum of 7-methyluric acid and peroxidase type VIII. Curve 2 was recorded after adding H_2O_2. Curve 3 and 4 were recorded after 40 and 80 sec. (B) Curve 5 was recorded after adding catalase. Curve 25 was recorded after 20 min.

oxidation was terminated by adding catalase in the same buffer which rapidly destroys any remaining H_2O_2. The spectral changes are shown between curves 5-25 in Fig. 24B. Therefore, an intermediate species is formed as a result of the peroxidase-catalyzed oxidation of 7-methyluric acid. The spectrum of the intermediates generated in the electrochemical and peroxidase-catalyzed oxidation are very similar. Spectral changes observed during the peroxidase-catalyzed oxidation of 7-methyluric acid in pH 7.5 phosphate buffer (u = 0.1) were similar to those shown in Fig. 24 (0.5 M NaCl plus 5 mM Na_2HPO_4 adjusted to pH 7.5). The kinetics of decay of the U.V.-absorbing intermediate generated in the peroxidase-catalyzed oxidation of 7-methyluric acid were studied by monitoring the change in absorbance after the reaction had been terminated by addition of catalase. The decomposition of the intermediate species following first-order kinetics and were reported in Table 3. These values compare well with those determined for decomposition of the intermediate formed in the electrochemical oxidation reaction.

3. B. 2. Isolation and identification of enzymatic oxidation prducts

In order to trap and identify the intermediate formed in the peroxidase-catalyzed oxidation of 7-methyluric acid the reaction was carried out in 0.5 M NaCl plus 5 mM Na_2HPO_4. The reaction was allowed to proceed for 90 s or 10

Table 3

First order rate constants observed for decomposition of intermediates generated by electrochemical and peroxidase-catalyzed oxidation of 7-methyluric acid in 0.5 M NaCl plus 5 mM Na_2HPO_4 pH 7.5.

Conc.		λ(nm)	k_{obs} (s^{-1})[a]
Electrochemical oxidation			
1 mM	0.8 V	220	$1.0 \times 10^{-3} \pm 1.0 \times 10^{-5}$
		290	$1.1 \times 10^{-3} \pm 1.1 \times 10^{-5}$
		325	$1.1 \times 10^{-3} \pm 1.0 \times 10^{-5}$
Enzymatic oxidation			
1 mM	peroxidase type VIII	215	$1.3 \times 10^{-3} \pm 1.1 \times 10^{-5}$
		290	$1.4 \times 10^{-3} \pm 1.0 \times 10^{-5}$
		325	$1.1 \times 10^{-3} \pm 1.0 \times 10^{-5}$

[a] Calculated by analysis of A vs. t obtained at the wavelength noted. The average of at least three replicate measurements is reported ± standard deviation.

min to trap the intermediate or product, respectively. After this time an aliquot (2 ml) of the reaction solution was transferred to a vial maintained at - 78°C (dry ice-acetone). The frozen solution was then freeze-dried, derivatized with BSA and analyzed by GC-MS using exactly the same conditions used to analyze the intermediate generated and trapped in thin-layer spectroelectrochemi experiments. GC of a blank mixture (i.e. containing no 7-methyluric acid) carried through the same procedure gave multiple peaks. These peaks are undoubtedly due to the silylated derivatives of the degradation products of peroxidase. No attempts were made to identify these peaks. In the peroxidase-catalyzed reaction at, for example, pH 7.5, the same results were obtained as in the electrochemical study, i.e., the trapped intermediate had a molar mass of 198 g and possessed three silylatable sites. Furthermore, the intermediate species decomposed to one major product (molar mass of 172 g). The GC and GC-MS behaviors of the intermediates and products formed in the enzymatic reaction were identical to those formed in thin-layer spectroelectrochemical oxidation of 7-methyluric acid.

In order to compare the mechanism of electrochemical and enzymatic oxidation of 7-methyluric acid it was of more interest to examine the products formed in the enzymatic oxidation. However, under the conditions used above only one major product (4-methylallantoin) was obtained. It was

necessary to carry out oxidations on a large scale because the yield of the three minor products is very small (< 0.5%). Typically, 10-12 mg of 7-methyluric acid was dissolved in 30 ml of phosphate buffer (u = 0.1 M) pH 7.5 or in 0.5 M NaCl plus 5 mM Na_2HPO_4 having the same pH. Then 1.4 ml of H_2O_2 (880 mM) solution was added followed by 3-4 mg of type VIII peroxidase. The resulting initial concentrations of 7-methyluric acid, H_2O_2 and peroxidase were thus ~2 mM, 38.5 mM, 3.125 uM, respectively. The homogeneous reaction mixture was stirred at room temperature for 1 h. The spectral changes observed during the enzymatic oxidation were similar to those shown in Fig. 24. After one hour the oxidation was complete. The product solution was freeze-dried. The resulting solid was dissolved in ca. 2 ml of distilled water and injected onto a column of Sephadex G-10 using water as the eluent. Typical liquid chromatograms of product mixture formed in pH 7.5 phosphate buffer shows five liquid chromatographic peaks (A, B, C, D and E, Fig. 25). Liquid chromatographic (LC) peak A is primarily due to peroxidase. LC peak B is due to inorganic phosphate. Liquid chromatograms of the enzymatic products formed in 0.5 M NaCl plus Na_2HPO_4 at pH 7.5 (Fig. 26) were similar to those obtained when the oxidation was carried out in phosphate buffer, except that one more LC peak A' appeared between LC peaks A and B. Again LC peak A is due to the peroxidase. LC peak A' is due to chloride ion. LC peak B is due to inorganic phosphate. The remaining LC peaks C-E are essen-

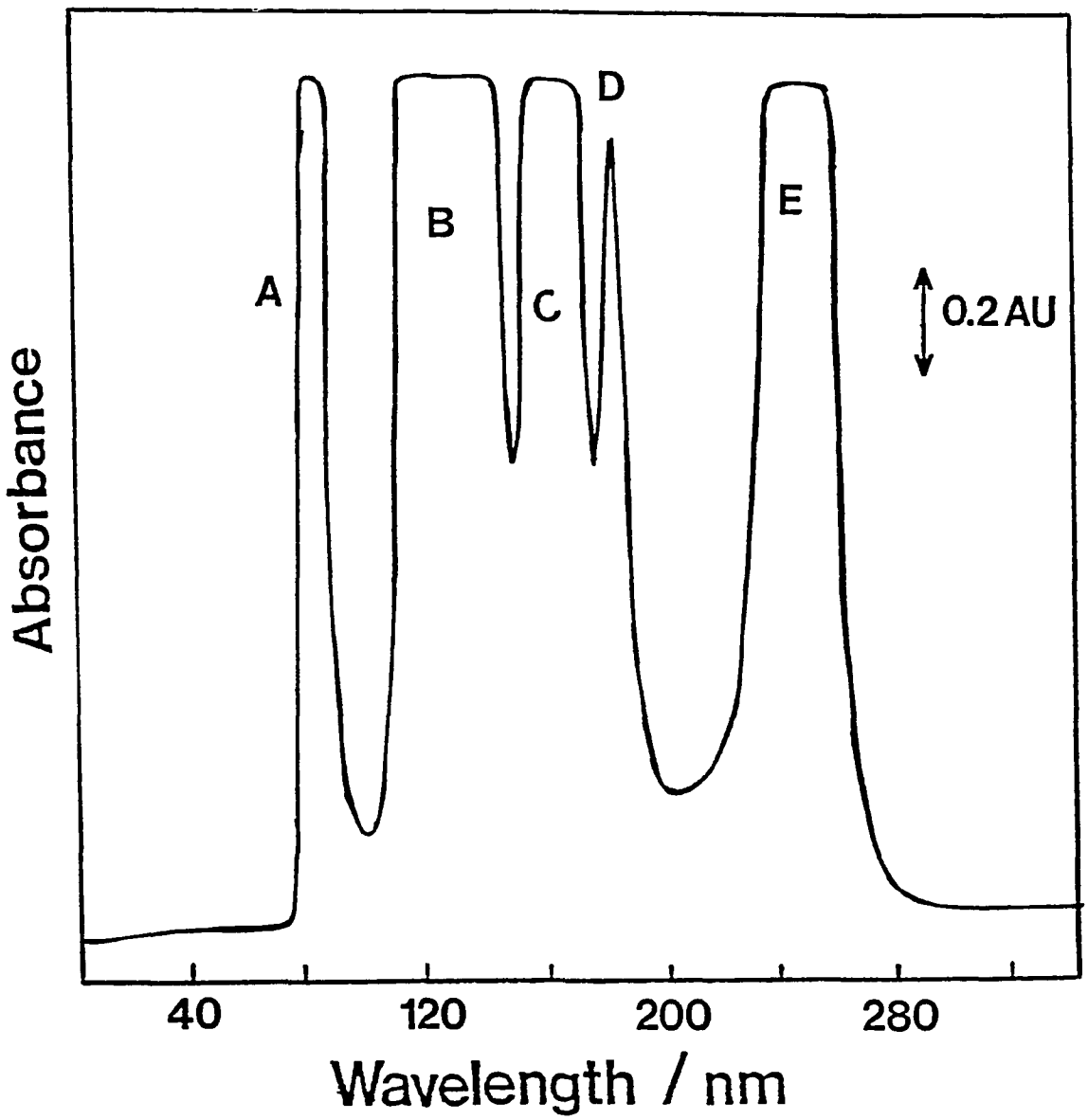

Fig. 25 Liquid chromatogram of the products formed by oxidation of 7-methyluric acid (2 mM) by H_2O_2 (38.5mM) in the presence of type VIII peroxidase (3.125 uM) in pH 7.5 phosphate buffer (u = 0.1 M). Chromatography was done on a column of Sephadex G-10 (90 x 2.5 cm) using water as the eluent (34 $ml h^{-1}$).

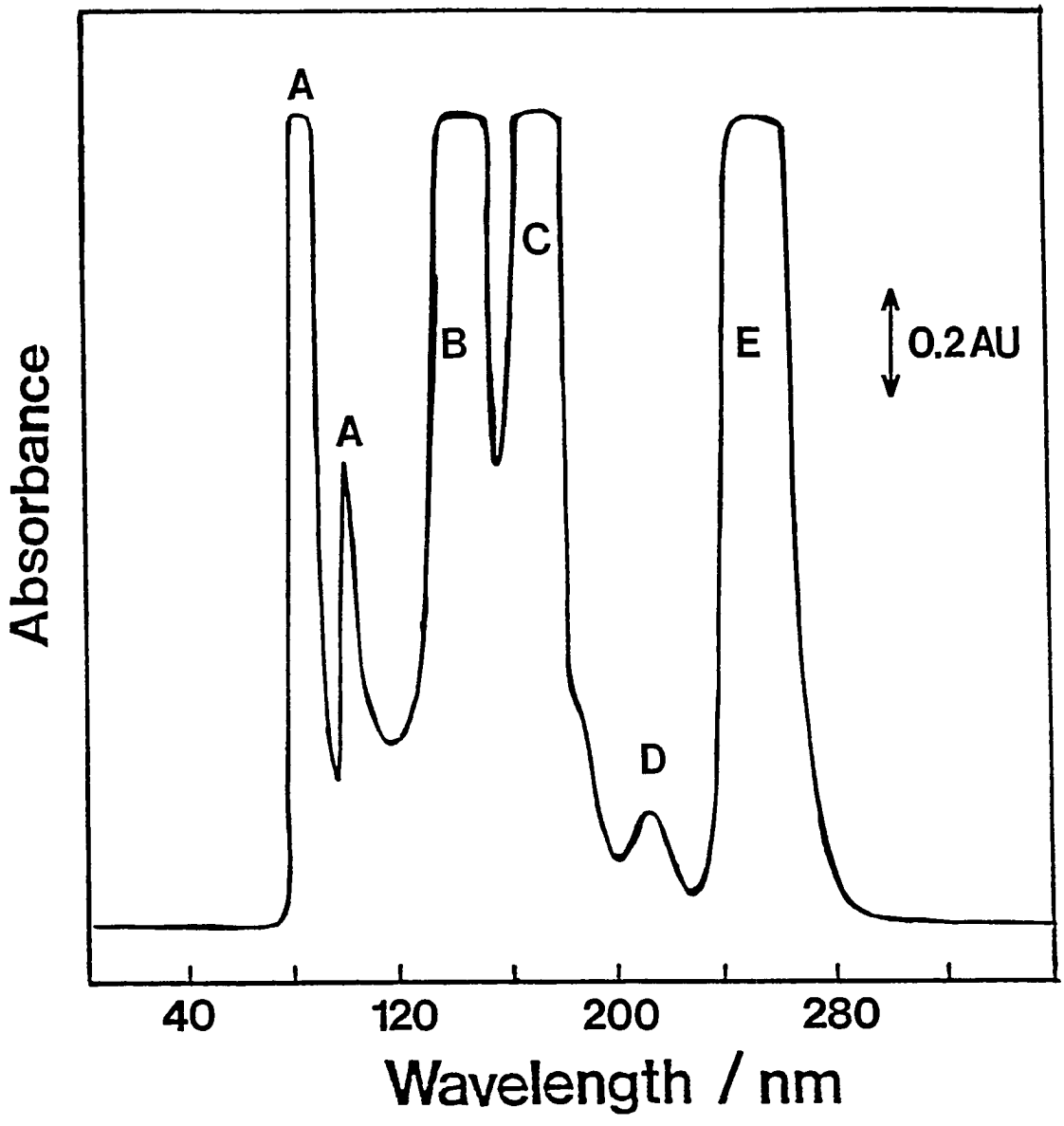

Fig. 26 Liquid chromatogram of the products formed by oxidation of 7-methyluric acid (2 mM) by H_2O_2 (38.5mM) in the presence of type VIII peroxidase (3.125 uM) in 0.5 M NaCl plus 5 mM Na_2HPO_4 at pH 7.5. Chromatography was done on a column of Sephadex G-10 (90 x 2.5 cm) using water as the eluent (34 $ml h^{-1}$).

tially the same for the products formed in both phosphate buffer and 0.5 M plus 5 mM Na_2HPO_4 at pH 7.5. The eluent corresponding to LC peaks C-E was collected and freeze-dried.

The component eluted under LC peak C was isolated after freeze-drying as a white powder. In water it showed a characteristic U.V. spectrum with λ_{max} = 207 nm. The mass spectrum on solid sample gave the following results (70 eV, 200°C), m/e (relative abundance): 173 (1.6%), 172 (M^+, 20.6%), 157 (0.4%), 156 (1.8%), 155 (26.1%), 146 (0.6%), 145 (6.5%), 144 (100%), 129 (80.5%) and 128 (41.1%). Silylation with BSTFA in acetonitrile at room temperature for 2 h gave GC peaks at t_R = 28.75 min having molar mass of 460 g (based on EI and CI mass spectrometry). These results indicate that this major product had a molar mass of 172 g. Fragmentation data obtained from MS, EI- and CI-MS indicate that this product is 4-methylallantoin. Thus, LC component C obtained from electrochemical oxidation and LC component C obtained from enzymatic oxidation are the same compound.

The product eluting under LC peak D was isolated after freeze drying as a white solid. In water this product exhibited an U.V. absorption band at 210 nm. Silylation with BSTFA in acetonitrile at room temperature for 2 h gave GC peak at t_R = 18.88 min having a molar mass of 271 g (based on EI and CI mass spectrometry). Silylation with MTBSTFA in acetonitrile at room temperature for 2 h gave GC

peak at t_R = 19.5 min having a molar mass of 355 g. These results indicate that the compound has a molar mass of 127 g and possesses 2 silylatable sites. Fragmentation data obtained from EI- and CI-MS indicate that this product is 1-methyl-2,5-diketo-4-imino-imidazole. Thus, LC component D obtained from electrochemical oxidation and LC component D obtained from enzymatic oxidation are the same compound.

After removal of the eluent by freeze-drying, the compound eluted under LC peak E was found to be a white solid. In water it showed U.V. absorption bands at $_{max}$ = 198 and 268 nm. Low resolution mass spectrometry (70 eV, 200°C) gave the following major peaks, m/e (relative abundance): 161 (2.2%), 160 (M^+, 26.1%), 145 (1.9%), 144 (9.3%), 143 (M^+-OH, 77.1%), 132 (1.6%), 131 (6.7%), 130 (M^+ - CH_3NH, 100%), 119 (1.8%), 118 (3.1%) and 117 (M^+-NHCO, 58.2%). Silylation with BSTFA in acetonitrile at room temperature for 2 h gave GC peak at t_R = 24.3 min having a molar mass of 358 g (based on EI and CI mass spectrometry). Silylation with MTBSTFA in acetonitrile at room temperature for 2 h gave a peak at t_R = 31.4 min having a molar mass of 484 g. These results indicate that the compound has a molar mass of 142 g and possesses three silylatable sites. The molar mass of this compound obtained from mass spectrometry and GC/MS is 18 g different. This can be explained that during silylation water molecule is eliminated from this compound to give a six-membered ring compound. Thus, LC component E obtained

from electrochemical oxidation and LC component E obtained from enzymatic oxidation are the same compound.

3. C. Discussion

The peak I_a electrochemical oxidation of 7-methyluric acid appears to follow the same basic reaction pathway previously described for uric acid and various other N-methyluric acid. Controlled potential coulometry indicates that oxidation peak I_a of 7-methyluric acid is a 2 e reaction. The $dE_p/d(pH)$ slope for peak I_a oxidation of 7-methyluric acid, ca. 49 mV, is close to that expected for a $2e\text{-}H^+$ irreversible electrode process (see earlier discussion). Thus, the initial peak I_a step involves a two electron, one proton electrooxidation of 7-methyluric acid (I, Fig. 27) to give the quinonoid cation II (Fig. 27). Hydration of quinonoid II then leads to tertiary alcohol III (Fig. 27). Compound III has a molar mass of 198 g and possesses three silylatable sites and is believed to be an U.V.-absorbing intermediate which may be detected by thin-layer spectroelectrochemical experiments (Figs. 5, 7, 8 and 11). Further evidence for the formation of III has been obtained by additional thin-layer spectroelectrochemical studies. For example, formation of 7-methyluric acid in a thin-layer cell followed by reduction at a potential of peak II_c leads to partial regeneration of 7-methyluric acid (Figs. 7 and 11). This observation may be rationalized by reduction of the tertiary alcohol III to a dihydro compound

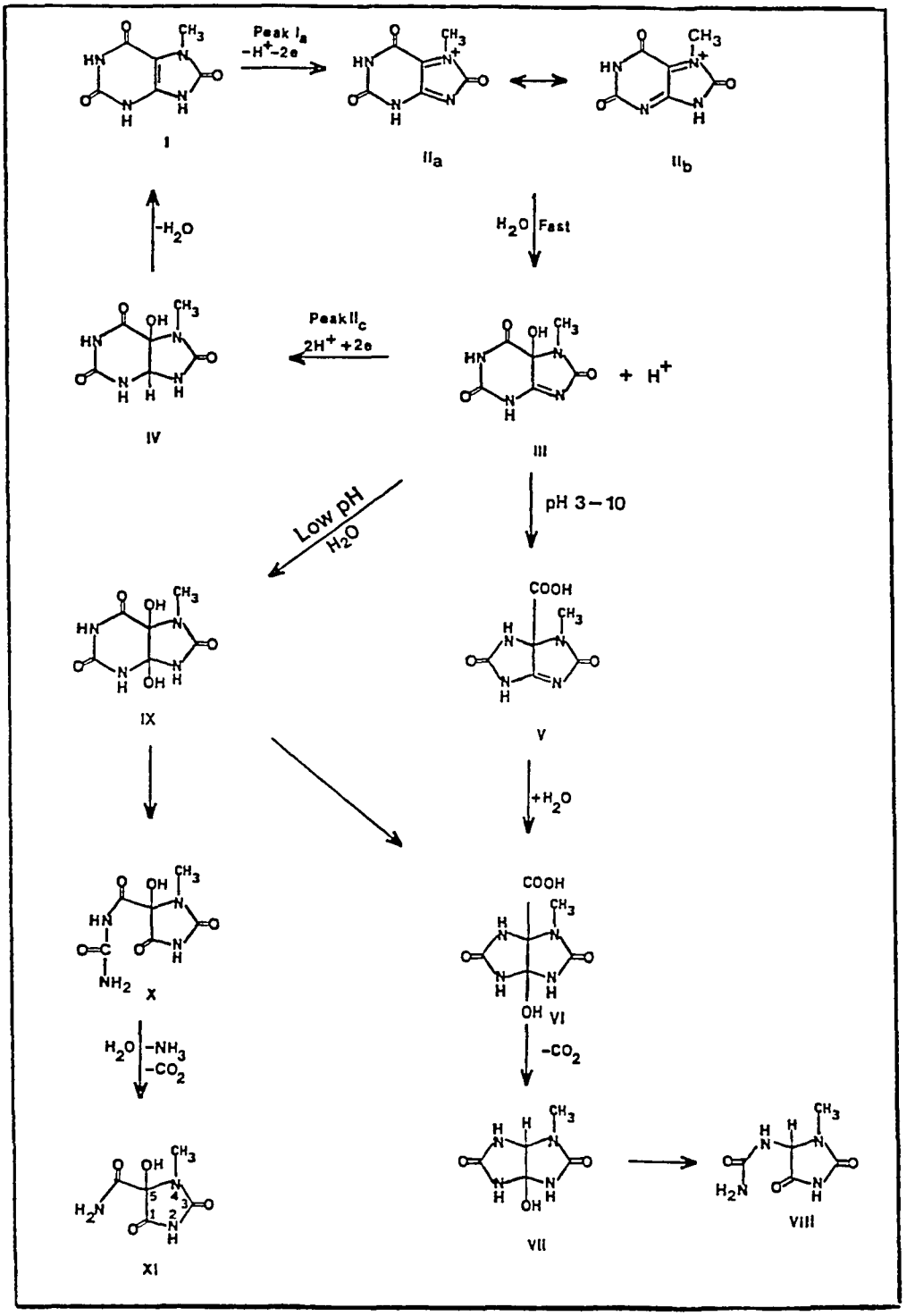

Fig. 27 Reaction scheme proposed to account for the peak I_a electrochemical oxidation reactions of 7-methyl-uric acid.

(IV, Fig. 27) in the peak II_c process followed by a rapid dehydration of IV to 7-methyluric acid (I, Fig. 27).

In order to account for the peak I_a product, 4-methylallantoin (VIII, Fig. 27), it is proposed that the tertiary alcohol intermediate (III, Fig. 27) undergoes a ring contraction leading to the carboxylic acid V (Fig. 27). This compound has the same molar mass (198 g) and number of silylatable sites (3) as the putative tertiary alcohol III and may therefore, in part, account for some of the observed thin-layer spectroelectrochemical and GC-MS behavior noted. Hydration, decarboxylation and ring opening via the pathway V ---> VI --->VII ---> VIII (Fig. 27) leads to 4-methylallantoin (VIII, Fig. 27). Additional evidence for the formation of intermediate V (Fig. 27) will be presented in the discussion of the peak II_a oxidation reaction.

At pH $\leq$ 5.0 an addition peak I_a product having molar mass of 173 g appears. This product may also be accounted for on the basic of the reaction schemes proposed for peak I_a of uric acid. Thus, with decreasing pH the tertiary alcohol III (Fig. 27) is apparently hydrated to the diol IX (Fig. 27) which undergoes ring opening, deamination and decarboxylation to give 4-methyl-5-hydroxyhydantoin-5-carboxamide (XI, Fig. 27). The latter compound has a molar mass of 173 and possesses only three of its four available sites.

Oxidation peak II_a of 7-methyluric acid could only be

observed clearly at pH $\geq$ 5.7. Coulometric n-values for peak II_a are dependent on the ionic strength of the phosphate buffer used. Thus, at a phosphate buffer ionic strength of 0.1 M the apparent n-value (n_{app}) was 2.3 $\pm$ 0.1 which increased to 3.1 $\pm$ 0.2 at an ionic strength of o.5 M then slightly decreased to 2.7 $\pm$ 0.1 at an ionic of 1.0 M (Fig. 12). Indeed, the major product of the peak II_a electrolysis was the same as was obtained from the peak I_a electrolysis (4-methylallantoin, VIII, Fig. 27). However, three minor products were formed in the peak II_a oxidation. The first minor product has a molar mass of 127 g and formula of $C_4H_5N_3O_2$. The second minor product has a molar mass of 160 g and formula of $C_4H_8N_4O_3$. The last minor product has not been identified. The peak II_a products which were isolated and characterized from 7-methyluric acid may be rationalized by a scheme shown in Fig. 28. Thus,it is proposed that the carboxylic acid V (Fig. 28) at pH $\geq$ 5.7 dissociates to form the electroactive anion XII (Fig. 28). The principal peak II_a electrode process is then a Kolbe-type reaction leading to tertiary alcohol XIII (Fig. 28), i.e., 1-hydroxy-2-methyl-2,4,6,8-tetraaza-3,7-dioxo-5-ene-bicyclo[3.3.0] octane. In order to rationalize the peak II_a product of 7-methyluric acid which has an elemental formula of $C_4H_8N_4O_3$ (molar mass = 160 g) according to mass spectrometry and $C_4H_6N_4O_2$ (molar mass = 142 g) according to GC/MS it is proposed that a hydration reaction of XIII (Fig. 28) occurs giving XVI (Fig. 28). Ring opening of the latter compound

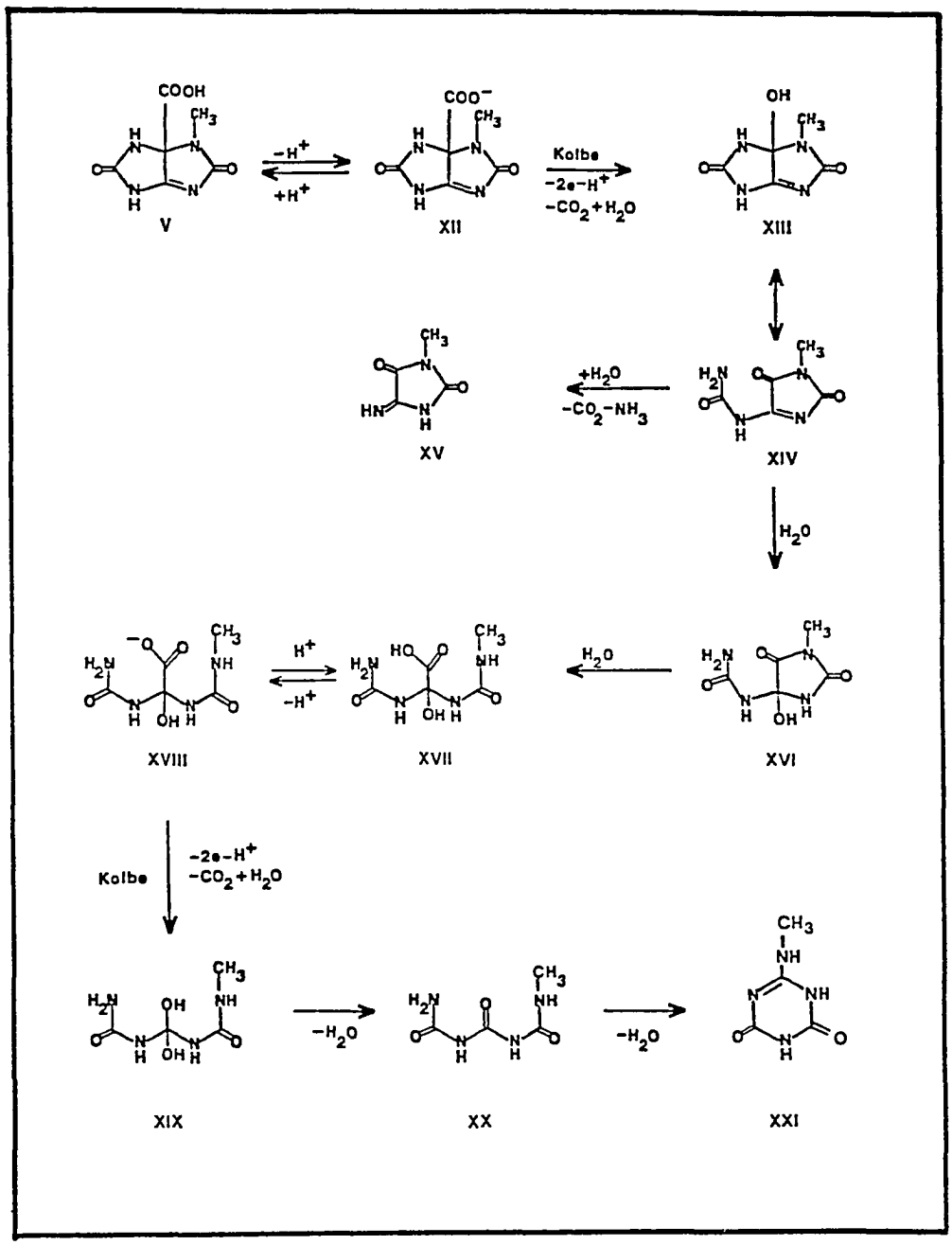

Fig. 28 Reaction scheme proposed to account for the peak II_a electrochemical oxidation reactions of 7-methyluric acid.

would lead to the carboxylic acid XVII (Fig. 28) and hence the carboxylate anion XVIII (at pH > 5.7). A second two-electron-one-proton Kolbe oxidation would lead to the urea derivative XIX which would readily give N'(1)-amido-N(3)-N-methylamido-urea (XX, Fig. 28). This compound would be dehydrated to give a six-membered ring compound XXI during silylation to account for the molar mass of 142 g obtained from GC/MS. The second peak II_a electrooxidation product of 7-methyluric acid has a molar mass of 127 g and formula of $C_4H_5N_3O_2$. Ring opening of the putative intermediate XIV (Fig. 28) followed by hydrolysis could lead to 1-methyl-2,5-diketo-4-imino-imidazole (XV, Fig. 28).

The last peak II_a electrooxidation product of 7-methyluric acid which eluted under LC peak F at this time has not been identified yet. Therefore, the scheme proposed for the electrooxidation for peak II_a of 7-methyluric acid must at this time be regarded as tentative.

The peroxidase-catalyzed oxidation of 7-methyluric acid appears to follow the same chemical pathway as the peak I_a plus peak II_a electrochemical oxidations. Thus, the same U.V.-absorbing intermediate(s) are formed in both electrochemical and enzymatic oxidation reactions. The intermediate species break down to give the same major product, 4-methylallantoin (Fig. 28). However, the peroxidase-catalyzed oxidation of 7-methyluric acid on a large scale gave two addition products which are the same as those obtained

from electrochemical oxidation at peak II_a potentials. It may be reasonably concluded that the chemical pathways followed in the enzymatic oxidation of 7-methyluric acid are the same as for peak I_a plus peak II_a electrochemical oxidation process.

CHAPTER 4

CONCLUSION

7-methyluric acid gives two voltammetry oxidation peaks (I_a and II_a) at a pyrolytic graphite electrode in low and high phosphate buffers. The peak I_a oxidation is a two-electron reaction forming a very unstable quinonoid cation that gives 4-methylallantoin (VIII, Fig. 27) as the product at pH 3.0 - 10.0. At low pH values 4-methyl-5-hydroxyhydantoin-5-carboxamide (XI, Fig. 27) is also observed as a product. The peak II_a reaction is due to Kolbe-type oxidation of the anion 1-carbohydroxy-2-methyl-2,4,6,8-tetraaza-3,7-dioxo-5-ene-bicyclo [3.3.0] octane (XII, Fig. 28, an unstable peak I_a product). The expected tertiary alcohol product (XIII, Fig. 28) of this reaction is apparently unstable and undergoes further chemical and electrooxidation reactions to give three new minor products, 1-methyl-2,5-diketo-4-N-imino-imidazole, N'(1)-amido-N(3)-N-methylamido-urea which would be dehydrated to a six-membered ring compound XXI (Fig. 28) during silylation and one unidentified compound.

It appears to be quite evident from this investigation that the enzymatic oxidation of 7-methyluric acid by H_2O_2

catalyzed by type VIII peroxidase and the electrochemical oxidation yields intermediates that are spectrally, kinetically and analytically identical. These intermediates then decompose to identical end-products. Hence, it seems reasonable to conclude that, in chemical sense, the courses of the two reaction are essentially identical.

PART III

SPECTROELECTROCHEMICAL SEARCH FOR A TERTIARY ALCOHOL INTERMEDIATE IN THE ELECTROCHEMICAL OXIDATION OF URIC ACID

CHAPTER 1

INTRODUCTION

The electrochemical[78,93-95,97,98] and enzymatic[80,96] oxidation of uric acid has been studied quite extensively by Dryhurst and coworkers. They have observed the formation of several unstable intermediate species following the initial quasi-reversible $2e\text{-}2H^+$ electrooxidation reaction. A simplified summary of the mechanisms applicable to the electrooxidation reaction in phosphate containing supporting electrolytes is presented in Figure 1.

Figure 2 shows a series of cyclic voltammograms of uric acid at pH 4.5 and 9.5 in supporting electrolytes containing low and high concentrations of phosphate. Oxidation peak I_a in Fig. 2 corresponds to the $2e\text{-}2H^+$ oxidation to give the quinonoid intermediate (IIa and IIb, Fig. 1).

In the pH range 5.0 - 7.0, at a pyrolytic graphite

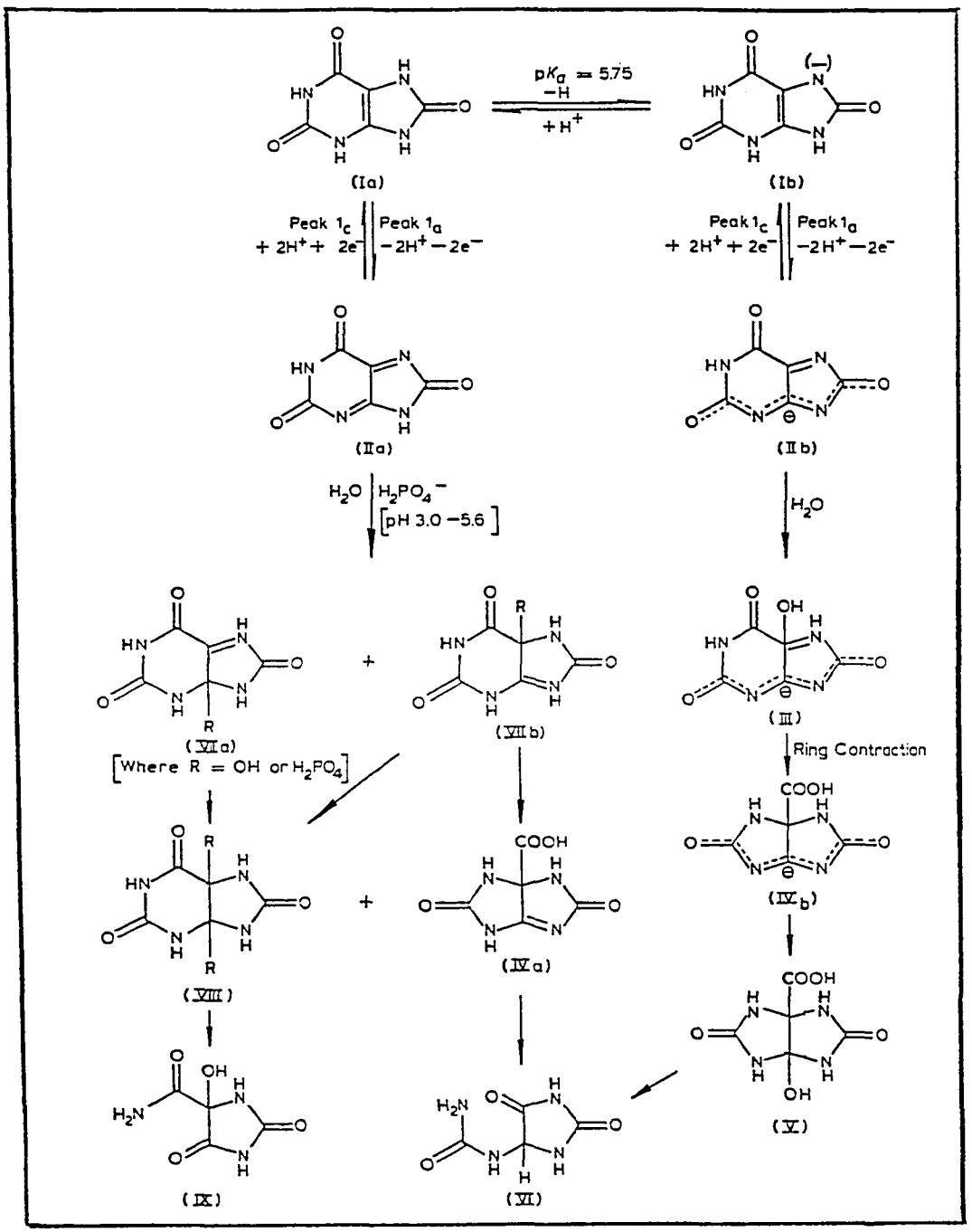

Fig. 1 A simplified reaction scheme proposed to account for the peak I_a electrochemical oxidation reactions of uric acid.

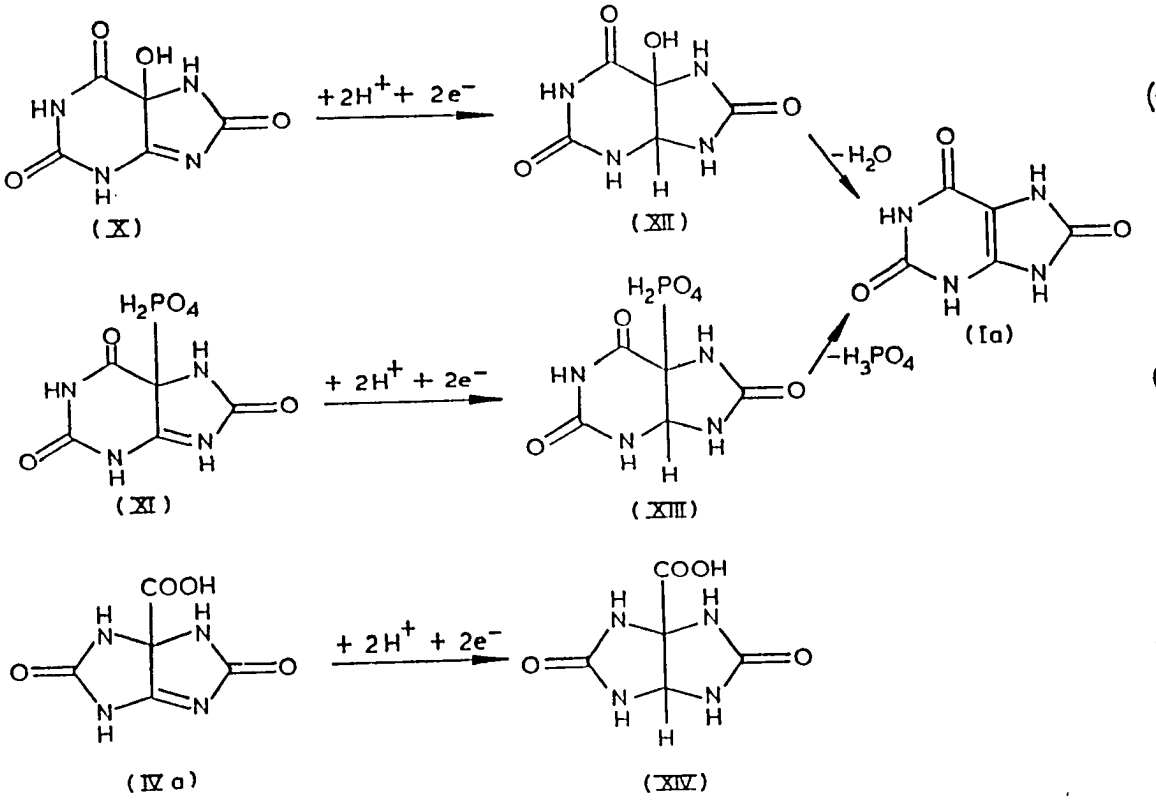
+2H+ + 2e−
-H2O
(X)
(XII)
(Ia)
(a)
H2PO4
+ 2H+ + 2e−
-H3PO4
(XI)
(XIII)
(b)
COOH
+ 2H+ + 2e−
(IV a)
(XIV)
(c)

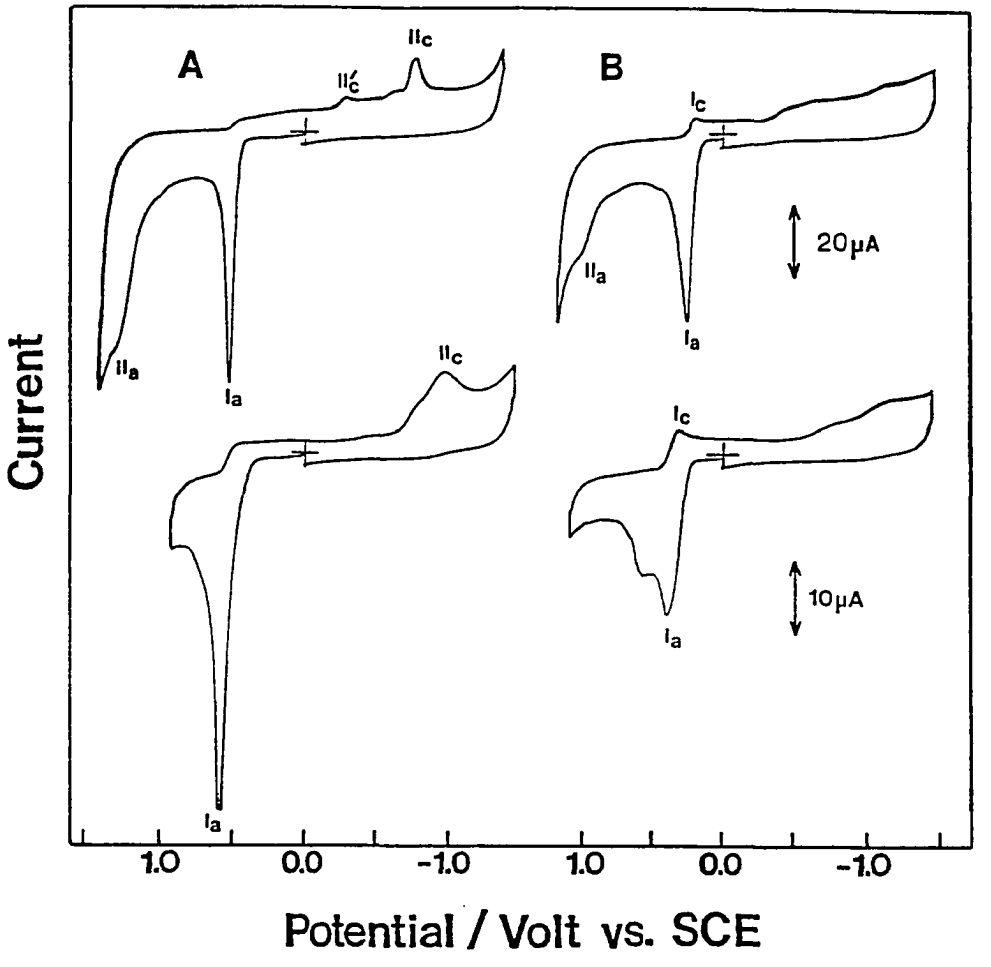

Fig. 2 Cyclic voltammograms at a pyrolytic graphite electrode of 1 mM uric acid at (A) pH 4.5 and (B) pH 9.5. Upper traces were obtained in phosphate buffers (u = 0.5 M), low traces were obtained in 0.5 M NaCl plus 5 mM Na_2HPO_4 adjusted to the required pH with HCl or NaOH. Sweep rate: 200 mVs^{-1}.

electrode (PGE), a quasi-reversible reduction peak I_c (Fig. 2) is observed which probably corresponds to reduction of the putative quinonoid back to uric acid[78]. A broad second reduction peak II_c (Fig. 2) is observed at negative potentials. It has been proposed that reduction peak II_c is due to electrochemical reduction of the tertiary alcohol intermediate (III or VIIb, R = OH, Fig. 1)[78] or possibly to electrochemical reduction of the bicyclic carboxylic acid intermediate (IVa or IVb, Fig. 1)[94].

Hence, detailed information concerning both the electrochemical oxidation and subsequent reduction reactions responsible for peak I_a and II_c are required to justify oxidation formation of putative tertiary alcohol (III, VIIa, VIIb, Fig. 1) or bicyclic carboxylic acid intermediates (VIa, VIb, Fig. 1).

Thus, a study was carried out to provide evidence to support formation of a tertiary alcohol intermediate following the electrochemical oxidation of uric acid by using thin-layer spectroelectrochemistry techniques.

CHAPTER 2

EXPERIMENTAL

2. A. CHEMICALS

Uric acid was obtained from Calbiochem-Behring (La Jolla, CA) and used without further purification. Phosphate buffers had an ionic strength of 0.5 M[68]. Other supporting electrolytes were prepared from 0.5 M NaCl plus 5 mM phosphate and the pH was adjusted by adding dilute HCl or NaOH. Other chemicals have been described in CHAPTERS 2 (PART I and II).

2. B. APPARATUS

Equipment used for electrochemical and thin-layer spectroelectrochemical studies have been described in CHAPTER 2 (PART I).

2. C. PROCEDURES

All of the procedures have been described in CHAPTERS 2 (PART I and II).

CHAPTER 3

RESULTS AND DISCUSSION

As noted in the Introduction, peak II_c observed on cyclic voltammetry of uric acid could be due to electrochemical reduction of the putative tertiary-alcohol (X, Eqn. 1a) or its phosphorylated analog (XI, Eqn. 1b) or the bicyclic carboxylic acid (IV_a, Eqn. 1c). However, in the case of compounds X and XI (Eqns. 1a and 1b) an overall $2e\text{-}2H^+$ reduction of the C=N- double bond must lead to the dihydro compounds XII and XIII (Eqns. 1a and 1b), respectively. Compound XII (Eqn. 1a) would be expected to dehydrate very readily and compound XIII (Eqn. 1b) to dephosphorylate giving uric acid (I_a, Eqn. 1)[107]. The reduction of IV_a might reasonably be expected to yield compound XIV. The chemical reaction of the later compound is not easy to predict but almost certainly would not lead to the regeneration of uric acid (I_a, Eqn. 1). Thus, it may be concluded that if electrochemical reduction of the U.V.-absorbing intermediate, generated by electrochemical oxidation of uric acid, at peak II_c potentials leads to the reappearance of uric acid then the tertiary-alcohol intermediates in the overall electrooxidation process is proved.

3. A. SPECTROELECTROCHEMICAL STUDIES IN LOW CONCENTRATIONS OF PHOSPHATE BUFFER.

Spectroelectrochemical studies of the electrooxidation of uric acid at peak I_a potentials followed by immediate reduction at peak II_c were carried out in a thin-layer cell containing an optically-transparent RVC electrode in supporting electrolytes containing 0.5 M NaCl plus 5 mM Na_2HPO_4 adjusted to pH values between pH 3.0 and 9.5. The behavior noted in a solution initially at pH 4.6 in Fig. 3 is typical of that observed for solutions initially between pH 3.0 - 6.0. Curve 1 in Fig. 3A is the initial spectrum of uric acid at pH 4.6 (λ_{max} = 283, 229 and 200 nm). Initiation of the peak I_a electrooxidation at 0.8 V causes the band at 283 nm to decrease and slightly shift to shorter wavelength while a new band grows in at 222 nm (curves 2-7, Fig. 3A). If, after scanning curve 7 in Fig. 3A the RVC electrode was open-circuited and the spectra shown in Fig. 3B were recorded. Curve 25 in Fig. 3B is the spectrum due to some residual uric acid and to the final product. However, if the U.V.-absorbing intermediate was first electrogenerated and then the RVC electrode was potentiostated at -1.4 V the spectrochemical behavior noted in Fig. 3C was observed. Thus, electroreduction of the intermediate (curve 8, Fig. 3C) causes the long wavelength to grow and to shift slightly to longer wavelength while the shorter wavelength band decreases. After 8 min the spectrum observed is identical to

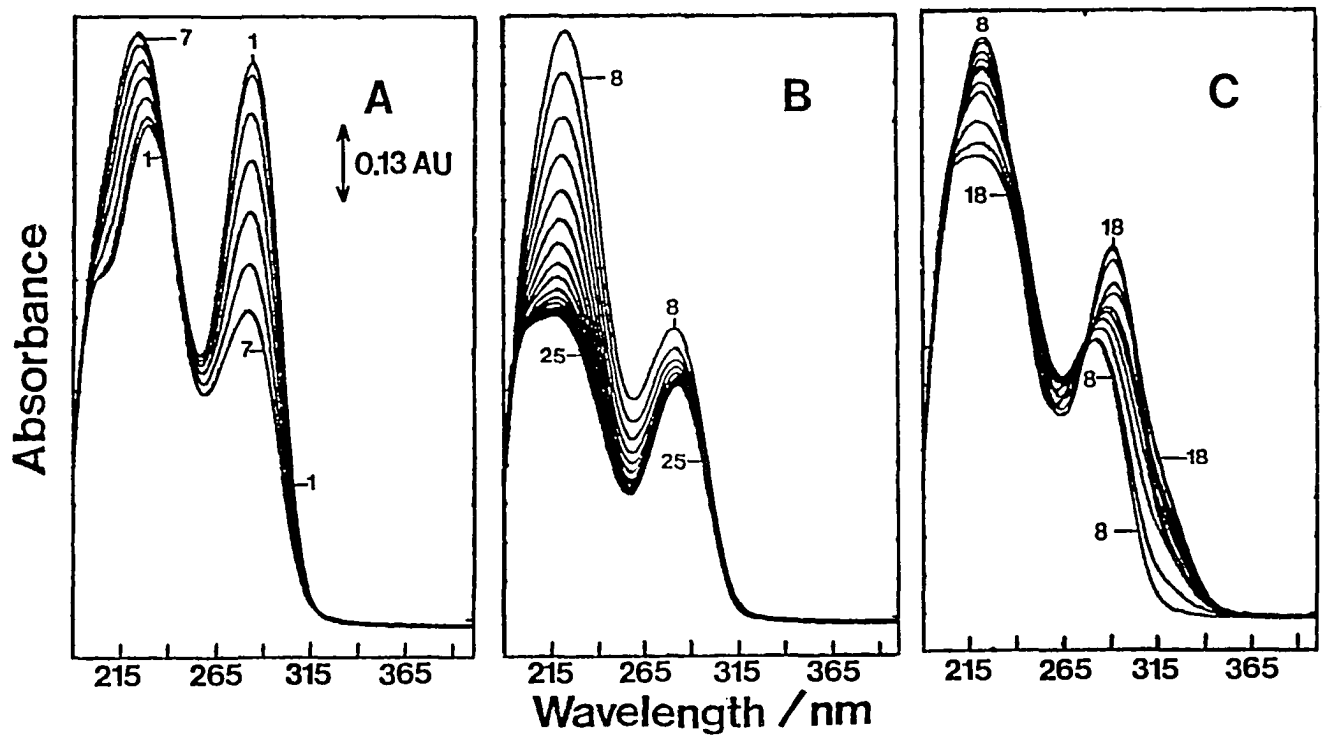

Fig. 3 (A) Spectra of 1 mM uric acid in 0.5 M NaCl plus 5 mM Na_2HPO_4 adjusted to pH 4.6 with HCl undergoing electrooxidation at 0.8 V in a thin-layer cell containing a RVC electrode. Curve 1 is the initial spectrum, curves 2-7 after initiation of the electrolysis. Each spectral sweep had a duration of 10s. (B) After scanning curve 7 in (A) the RVC electrode was open-circuited and curves 8-25 recorded. Each sweep had a duration of 20 s. (C) After sweeping curve 7 in (A) the RVC electrode was potentiostated at -1.4 V and curves 8-18 recorded. Spectra were recorded at the following times: (9) 5, (10) 10, (11) 15, (12) 20, (13) 25, (14) 75, (15) 125, (16) 225, (17) 425 and (18) 495s.

that of uric acid (curve 18, Fig. 3C).

The spectroelectrochemical behavior at pH $\geq$ 7.0 is illustrated in Fig. 4 with experiments conducted at pH 7.5. Curve 1 in Fig. 4 is the initial spectrum of uric acid (λ_{max} 287, 230 and 206 nm). Application of a potential to the RVC electrode of 0.8V causes the long wavelength band to decrease while a new band grows in at short wavelengths (ca. 221 nm) and the absorbance between about 352-302 nm also increases. After about 80s electrolysis curve 7 (Fig. 4A) may be observed which is the spectrum of intermediate species (λ_{max} = 297 and 221 nm). If, after sweeping curve 7 in Fig. 4A the RVC electrode was open-circuited, the spectrum of the intermediate species decreased (curves 8-18, Fig. 4B). Curve 18 in Fig. 4B is the spectrum due to some residual uric acid and to the final reaction product. However, if the U.V.-absorbing intermediate was first electrogenerated and then the RVC was potentiostated at -1.4V the spectroelectrochemical behavior noted in Fig. 4C was observed. Thus, electroreduction of the intermediate (curve 8, Fig. 4C, λ_{max} = 297 and 221 nm) causes the long wavelength band to grow and to shift to shorter wavelengths while the short wavelength band decreases. After about 6 min (curve 16, Fig. 4C) the spectrum observed is identical to that of uric acid.

The spectroelectrochemical behavior of uric acid at pH 9.5 is shown in Fig. 5. Figure 5A shows that upon electroly-

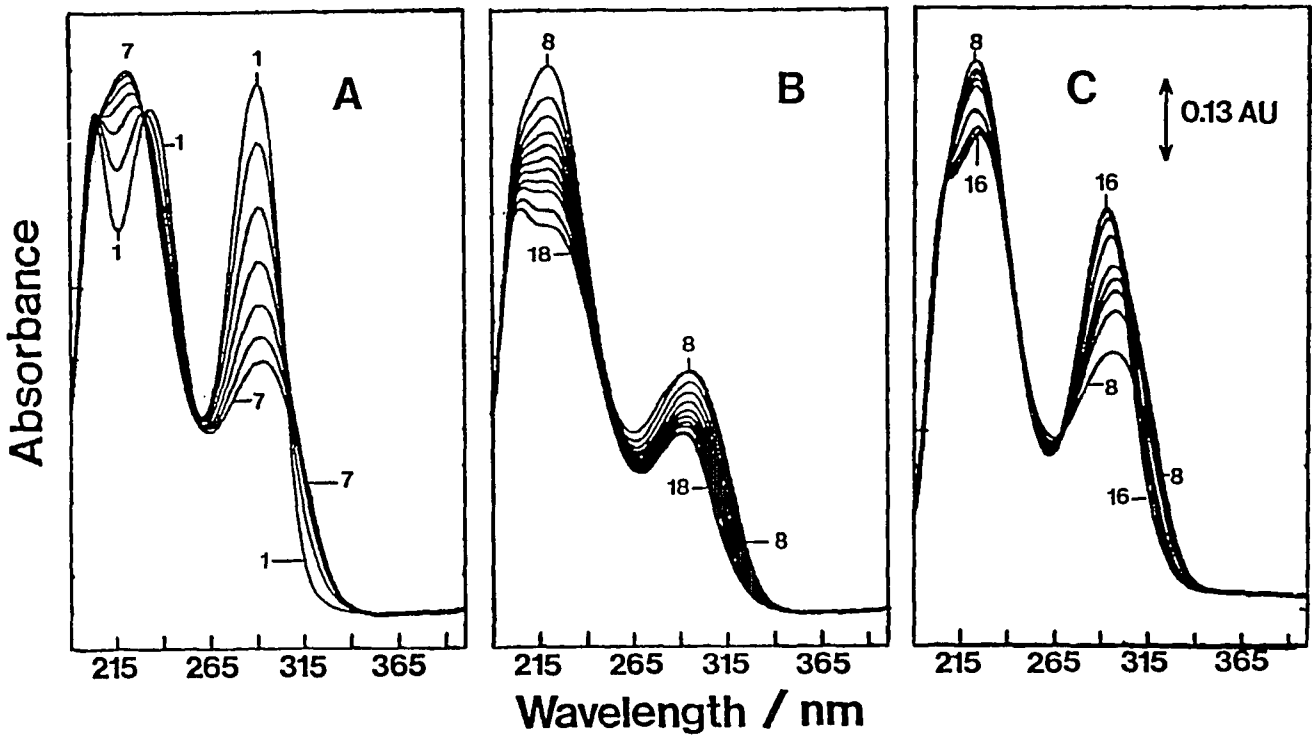

Fig. 4. (A) Spectra of 1 nM uric acid undergoing electrooxidation at 0.8 V at a RVC electrode in a thin-layer cell in 0.5 M NaCl plus 5 mM Na_2HPO_4 adjusted to pH 7.5 with NaOH. Curve 1 is the initial spectrum, curves 2-7 after initiation of the electrolysis. Each spectral sweep had a duration of 10 s. (B) After sweeping curve 7 in (A) the RVC electrode was open-circuited and curves 8-18 recorded, each sweep having a duration of 40 s. (C) After sweeping curve 7 in (A) the RVC electrode was potentiostated at -1.4 V. Spectra were recorded at the following times: (8) 5, (9) 10, (10) 15, (11) 20, (12) 30, (13) 80, (14) 180, (15) 280 and (16) 405 s.

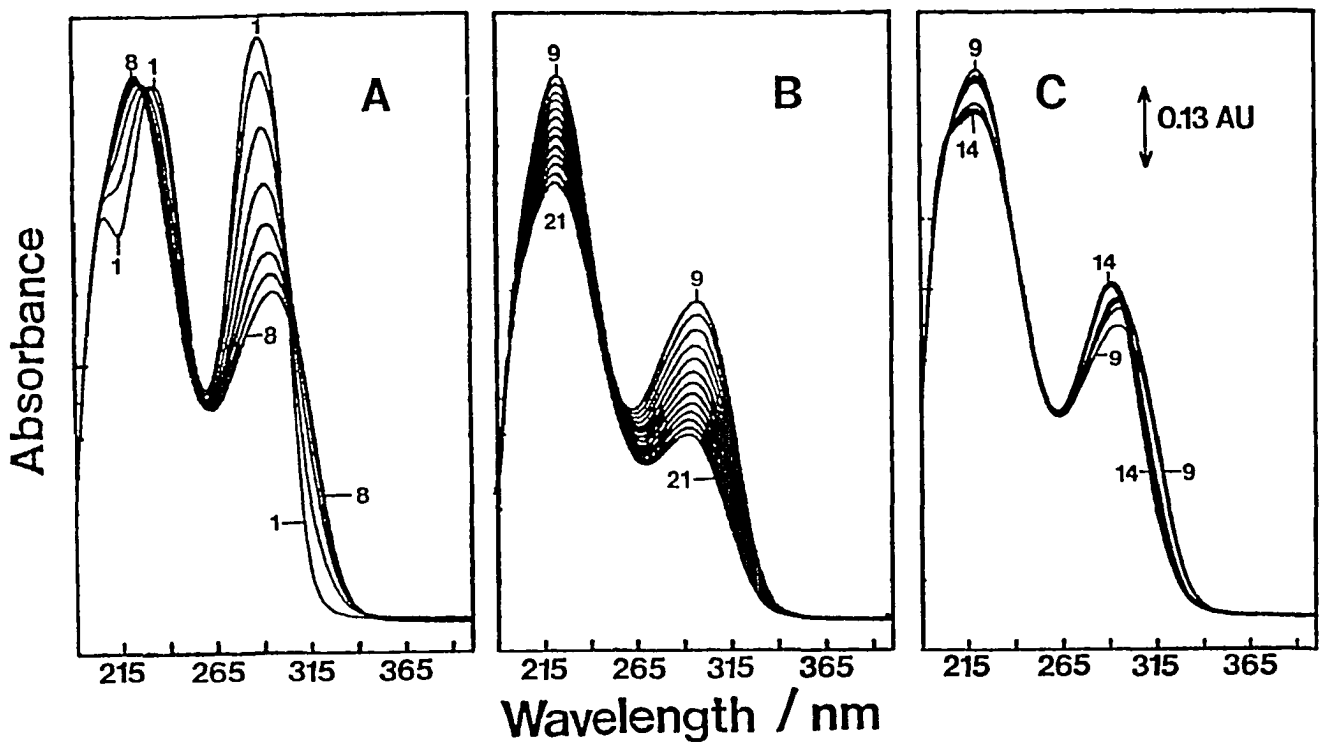

Fig. 5. (A) Spectra of 1 nM uric acid undergoing electrooxidation at 0.8 V at a RVC electrode in a thin-layer cell in 0.5 M NaCl plus 5 mM Na_2HPO_4 adjusted to pH 9.5 with NaOH. Curve 1 is the initial spectrum, curves 2-8 after initiation of the electrolysis. Each spectral sweep had a duration of 10 s. (B) After sweeping curve 8 in (A) the RVC electrode was open-circuited and curves 9-21 recorded, each sweep having a duration of 60 s. (C) After sweeping curve 8 in (A) the RVC electrode was potentiostated at -1.4 V. Spectra were recorded at the following times: (9) 10, (10) 20, (11) 30, (12) 40, (13) 160, (14) 290 s.

sis the long wavelength band of uric acid decreases and shifts to longer wavelengths whereas the shorter wavelength bands merge to give a new band at 221 nm. The open-circuit decay of the electrogenerated intermediate is shown between curves 9-21 in Fig. 5B. If the RVC electrode was potentiostated at -1.4 V (Fig. 5C) then a small but significant amount of uric acid could be formed as evidenced by curve 14 in Fig. 5C. Thus, it indicates that at this pH the tertiary alcohol intermediate is less stable than at pH 7.0 (Figs. 4C and 5C).

3. B. SPECTROELECTROCHEMICAL STUDIES IN HIGH CONCENTRATIONS OF PHOSPHATE BUFFER

The spectroelectrochemical behavior of uric acid in phosphate buffers (u = 0.5 M) between pH 3-6 may be illustrated by the results shown in Fig. 6 obtained at pH 4.3. Curve 1 in Fig. 6A is the initial spectrum of uric acid (λ_{max} = 282, 231 and 195 nm). Electrooxidation at 0.8V causes the long wavelength band to decrease and the short wavelength band to shift to shorter wavelengths and to grow. After scanning curve 6 in Fig. 6A the RVC electrode was open-circuited and the spectral behavior shown in Fig. 6B was recorded. The absorbance between 340-190 nm systematically decreases (curves 7-20, Fig. 6B). Electrogeneration of the U.V. absorbing intermediate species followed by reduction at -1.4 V gave the results shown in Fig. 6C. Thus, electroreduction of the intermediate causes the short wave-

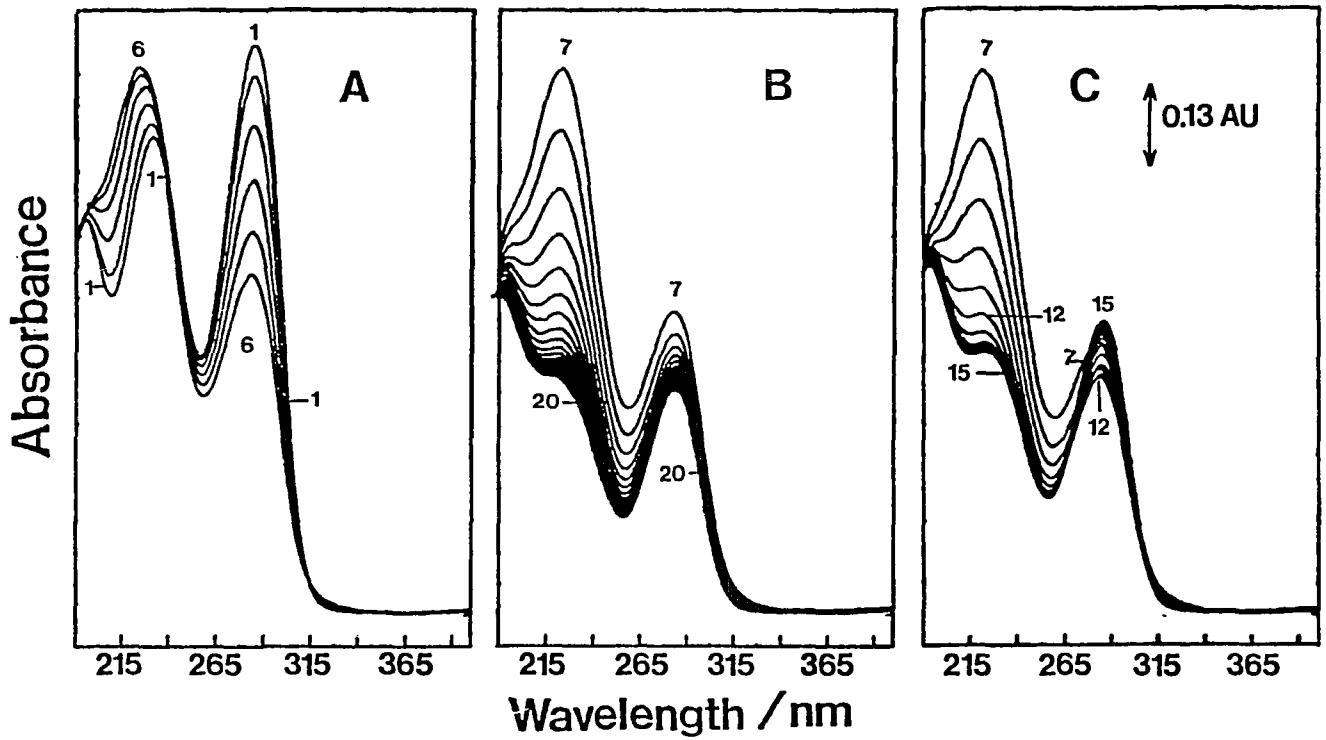

Fig. 6. (A) Spectra of 1 mM uric acid undergoing electrooxidation at 0.8 V at a RVC electrode in a thin-layer cell in phosphate buffer (u = 0.5 M) pH 4.3. Curve 1 is the initial spectrum, curves 2-6 after initiation of the electrolysis. Each spectral sweep had a duration of 5 s. (B) After sweeping curve 6 in (A) the RVC electrode was open-circuited and curves 7-20 recorded, each sweep having a duration of 20 s. (C) After sweeping curve 6 in (A) the RVC electrode was potentiostated at -1.4 V and curves 7-12 recorded. Each sweep had a duration of 20 s. Curve 15 was recorded after 6 min.

length band to decrease and to split into two bands while the longer wavelength decreases for about 80 s (curve 12, Fig. 6C) then it increases. After 6 min (curve 15, Fig. 6C) is identical to that of uric acid.

The spectroelectrochemical behavior of uric acid at pH $\geq$ 7.0 is illustrated in Fig. 7. The result is obtained at pH 9.0. Curve 1 in Fig. 7A is the initial spectrum of uric acid (λ_{max} = 289,231 and 206 nm). Upon electrolysis the long wavelength band of uric acid (λ_{max} = 289 nm) decreases and shifts to longer wavelengths whereas the short wavelength bands (λ_{max} = 231 and 206 nm) merge to give a new band at 223 nm (curves 2-10, Fig. 7A). If, after scanning curve 10 in Fig. 6A the RCV electrode was open-circuited and the spectra shown in Fig. 7B were recorded. Curve 26 in Fig. 7B is the spectrum due to some residual uric acid and to the final products. However, if the U.V.-absorbing intermediate was first electrogenerated and then the RVC electrode was potentiostated at -1.4 V the spectrochemical behavior noted in Fig. 7C was observed. Thus, the absorbance between 352-190 nm decayed with time but no uric acid was regenerated. It indicates that at high pH the tertiary alcohol intermediate is unstable.

3. B. DISCUSSION

The spectroelectrochemical results obtained in 0.5M NaCl plus 5 mM phosphate (Figs. 3 and 4) reveal, at pH

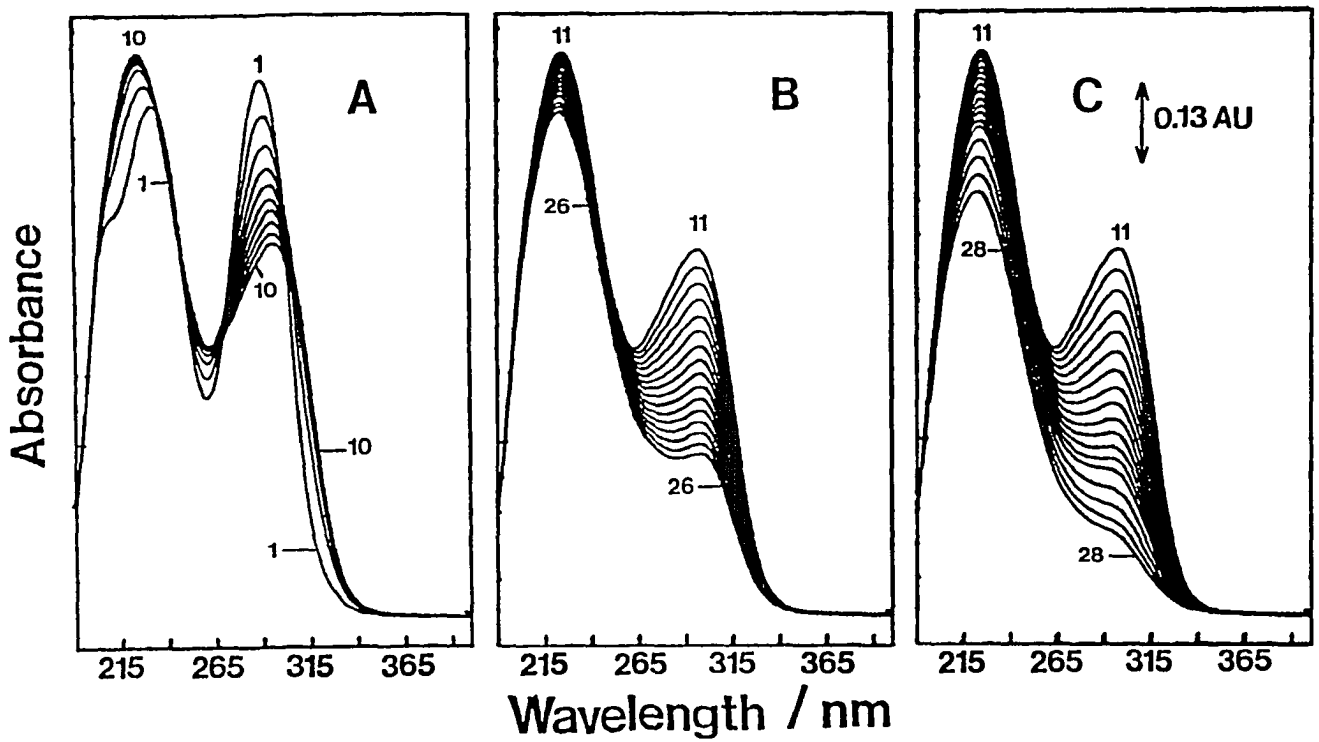

Fig.7. (A) Spectra of 1 nM uric acid undergoing electrooxidation at 0.8 V at a RVC electrode in a thin-layer cell in phosphate buffer (u = 0.5 M) pH 9.0. Curve 1 is the initial spectrum, curves 2-10 after initiation of the electrolysis. Each spectral sweep had a duration of 10 s. (B) After sweeping curve 11 in (A) the RVC electrode was open-circuited and curves 11-26 recorded, each sweep having a duration of 20 s. (C) After sweeping curve 10 in (A) the RVC electrode was potentiostated at -1.4 V and curves 11-28 recorded. Each sweep had a duration of 30 s.

values both below and above the pK_a of uric acid (5.75)[108], that electrolysis of the electrogenerated intermediate species at the RVC electrode at potentials close to or more negative than cyclic voltammetric peak II_c (Fig. 2) results in the appearance of an U.V. spectrum characteristic of uric acid. At low pH more uric acid is regenerated by electrochemical reduction of the electrogenerated intermediate (Figs. 4C and 5C) indicates that the tertiary alcohol is stable at low pH. It should be noted, however, that the cyclic voltammograms shown in Fig. 2 were obtained at a PGE whereas electrolysis in a thin-layer cell were carried out at the RVC electrode. Electrolysis in a thin-layer cell is always subject to some IR drop hence the actual potential on the RVC electrode is probably less than the applied potential. The regeneration of uric acid following electrochemical reduction of the U.V. absorbing intermediate(s) at peak II_c potential was demonstrated by comparing the GC-MS behavior of the silylated product formed upon open-circuited decay of the intermediate with that formed after reduction at peak II_c potentials. Open circuited decay of the intermediate generated at pH 7.0 and 9.5 gave GC-MS behavior characteristic of silylated allantoin. The reduced intermediate solution, however, gave a smaller amount of allantoin and a very large amount of uric acid. Thus, it is reasonable to conclude that reduction of the U.V. absorbing intermediate species generated upon electrooxidation of uric acid between pH 3.0-9.0 at potentials close to peak II_c does lead

to significant regeneration of uric acid. This clearly supports the view that cyclic voltammetric peak II_c is due to electrochemical reduction of the tertiary-alcohol (X, Eqn. 1a) to give the dihydro compound (XII, Eqn. 1a) which dehydrates to give uric acid (I_a, Eqn. 1a).

In phosphate buffers at pH < pK_a of uric acid electrooxidation of the latter compound yields an U.V. absorbing intermediate which may reduced at peak II_c potentials to regenerate a significant quantity of uric acid (Fig. 6C). However, at pH > pK_a, no uric acid is formed upon reduction of intermediate species (Fig. 7C). This indicates that the tertiary alcohol intermediate is too reactive in high concentration of phosphate to be detected. However, in high concentration of phosphate , particularly at pH > pK_a reduction of the electrogenerated U.V.-absorbing intermediate species at -1.4 V still causes the intermediate species to decay more rapidly than at open-circuited. Since electrochemical reduction of the U.V.-absorbing intermediate species at - 1.4 V does not result in formation of uric acid it must be concluded that more than one U.V.-absorbing and reducible species is present following the electrooxidation reaction. The more readily reducible species apparently does not give rise to uric acid whereas the species reduced at more potentials does give uric acid. Previous kinetic studies[93] have implicated tertiary-alcohol (X) and BCA (IV_a) as being intermediate. However, BCA and its precusor tertiary-alco-

hol have exactly the same molecular weight, molecular formula and possess four silylatable positions. Thus, it is possible that a mixture of tertiary-alcohol and BCA are in fact detected and trapped. These would be expected to exhibit very similar U.V-Visible and mass spectra. It may be concluded, therefore, that the tertiary-alcohol (X, Eqn. 1a) is the intermediate reduced at more negative potential and BCA (IV_a, Eqn. 1c) the species reduced at more positive potential.

CHAPTER 4

CONCLUSION

Thin-layer spectroelectrochemical studies of the electrochemical oxidation of uric acid between pH 3.0-9.0 clearly reveal that the $2e\text{-}2H^+$ oxidation reaction results in formation of U.V.-absorbing intermediate species. In low phosphate buffer at all pH's studied the U.V.-absorbing intermediate species may be partially electrochemically reduced to regenerate uric acid. The amount of regenerated uric acid is more at low pH (Figs. 4 and 5). However, in high phosphate buffer only at pH < pK_a of uric acid the regeneration of uric acid by electrochemical reduction of U.V.-absorbing intermediates is observed. This behavior provides some compelling evidence that a tertiary alcohol (X, Eqn. 1a) is one of the U.V.-absorbing intermediates. It also indicates that the tertiary alcohol (X, Eqn. 1a) is more stable in low phosphate buffer and at low pH. It is necessary to reduce the U.V.-absorbing intermediate at peak II_c potential to observe the regeneration of uric acid. Thus, it indicates that reduction peak II_c is due to the tertiary alcohol intermediate (X, Eqn. 1a). It may be tentatively concluded that the bicyclic carboxylic acid IV_a

(Eqn. 1a) is one of the other electrochemically reducible U.V.-absorbing intermediates.

CHAPTER 5

REFERENCES

1. W. A. Remers, in Indoles, W. J. Houlilian (ed.), Part I, Wiley-Interscience, New York, 1972, pp. 1-226.

2. W. C. Rose, Physiol. Rev., 18, 109 (1938).

3. F. Kogl, A. J. Haagen-Smit and H. Erxleben, Z. Physiol. Chem., 214, 241 (1933).

4. H. G. Baumgarten, A. Bjorklund, L. Lachenmeyer, A. Nobin and U. Stenevi, Acta. Physiol. Scand. Suppl., 373, 1 (1971).

5. H. G. Baumgarten, K. D. Evetts, R. B. Holman, L. L. Iversen, M. Vogt and G. Wilson, J. Neurochem., 19, 1587 (1972).

6. H. G. Baumgarten, M. Goethert, A. F. Holstein and H. G. Schlossberger, Z. Zellforsch., 128, 115 (1972).

7. A. Bjorklund, A. Nobin and U. Stenevi, Brain Res., 53, 117 (1973).

8. A. Bjorklund, A. Nobin and U. Stenevi, Z. Zellforsch, 145, 479 (1973).

9. A. Saner, L. Pieri., J. Moran, M. DaPrada and A. Pletscher, Brain Res., 76, 109 (1975).

10. H. G. Baumgarten and L. Lachenmeyer, Z. Zellforsch., 135, 399 (1972).

11. A. B. Lerner, J. D. Case and R. V. Heinzelman, J. Amer. Chem. Soc., 81, 6084 (1959).

12. R. H. Heacock, in Advances in Heterocyclic Chemistry, Vol. 9 (A. R. Katritzky, ed.), Academic Press, New York, 1965, p.1.

13. W. C. Sumpter and F. M. Miller, in The Chemistry of Heterocyclic Compounds, A. Weissberger (ed.), Vol. 8, Interscience Publishers, New York, 1954.

14. Cerighelli, Compt. Rend., 179, 1193 (1924).

15. Sack, Pharm. Weekblad, 48, 307 (1911).

16. Hesse and Zeitschel, J. Prakt. Chem., [2] 66, 481 (1902).

17. Herter, J. Biol. Chem., 5, 489 (1909).

18. Weissgerber, Ber., 43, 3520 (1910).

19. Boes, Pharm. Ztg., 47, 131 (1902).

20. G. Dryhurst, in Electrochemistry of Biological Molecules, Academic Press, New York, 1977, pp. 1-5.

21. R. S. Nicholson and I. Shain, Anal. Chem., 36, 706 (1964).

22. Neumeister, Z. Biol., 26, 329 (1890).

23. Hopkins and Cole, J. Physiol., 27, 418 (1901); J. Chem. Soc., I, 82, 193 (1902).

24. Willock and Hopkins, J. Physiol., 35, 88 (1906-1907).

25. V. du Vigneaud, R. R. Sealock and C. V. Etten, J. Biol. Chem., 98, 565 (1932).

26. D. W. Woolley, in The Biochemical Bases of Psychoses, Wiley-Interscience, New York, 1962.

27. A. Meister, in Biochemistry of Amino Acids, Academic Press, New York, 1965.

28. R. R. Brown and J. M. Price, J. Biol. Chem., 219, 985 (1956).

29. R. Kido, T. Noguchi and Y. Matsumara, Biochim. Biophys. Acta, 141, 270 (1967).

30. J. E. Leklem, J. Woodford and R. R. Brown, Comp. Biochem. Physiol., 31, 95 (1969).

31. H. S. Mason, Adv. Enzymol., 19, 79 (1957).

32. Y. Kotake and T. Masayama, Hoppe-Seyler's Z. Physiol. Chem., 243, 237 (1936).

33. W. E. Knox and A. H. Mehler, J. Biol. Chem., 187, 419 (1950).

34. O. Hayaishi, S. Rothberg, A. H. Mehler, and Y. Saito, J. Biol. Chem., 229, 889 (1957).

35. T. Tanaka and W. E. Knox, J. Biol. Chem., 234, 1162 (1959).

36. C. A. Elvehjem, R. J. Madden, F. M. Strong and D. W. Wooley, J. Am. Chem. Soc., 59, 1767 (1937).

37. C. Heidelberger, M. E. Gullberg, A. F. Morgan and S. Lepkovsky, J. Biol. Chem., 175, 471 (1948).

38. C. Heidelberg, E. P. Abraham and S. Lepkovsky, J. Biol. Chem.,179, 151 (1949).

39. P. Feigelson, J. N. Williams and C. A. Elvehjem, J. Biol. Chem., 193, 737 (1951).

40. C. E. Dalgliesh, Quart. Revs., 5, 227 (1951).

41. P. L. Julian, E. W. Meyer and H. C. Printy, in Heterocyclic Compounds, R. C. Elderfield (ed.), Vol. 3, pp. 63, 182 (1952).

42. M. Kotake, T. Sakan and T. Miwa, J. Am. Chem. Soc., 72, 5085 (1950).

43. T. Sakan and O. Hayaishi, J. Biol. Chem., 186, 177 (1950).

44. M. Mason, and C. P. Berg, J. Biol. Chem., 188, 783 (1951).

45. C. E. Dalgliesh, W. E. Knox and A. Neuberger, Nature, 168, 20 (1951).

46. A. H. Mehler and W. E. Knox, J. Biol. Chem., 187, 431 (1950).

47. B. Witkop, Ann., 558, 98 (1947).

48. B. witkop, Ann., 556, 103 (1944).

49. B. Witkop and J. Fiedler, Ann., 558, 91 (1947).

50. B. Witkop, J. Am. Chem. Soc., 72, 1428 (1950); 72, 2331 (1950).

51. B.Witkop and J. B. Patrick, J. Am. Chem. Soc., 73, 713 (1951); 73, 2196 (1951).

52. M. Nakagawa, T. Kanedo, Y. Hoshikawa and T. Hino, J. Am. Chem. Soc., 96, 624 (1974).

53. M. Nakagawa, K. Yoshikawa and T. Hino, J. Am. Chem. Soc., 97, 6496 (1975).

54. M. Nakagawa, H. Okajima and T. Hino, J. Am. Chem. Soc., 98, 635 (1976).

55. M. Nakagawa, H. Okjima and T. Hino, J. Am. Chem. Soc., 99, 4424 (1977).

56. M. Nakagawa, H. Watanabe, S. Kodala, H. Okajima, T. Hino, J. L. Flippen, and B. Witkop, Proc. Nat. Acad. Sci. U.S.A., 74, 4730 (1977).

57. I. Saito, T. Matsura, M. Nakagawa and T. Hino, Acc. Chem. Res., 10, 346 (1977).

58. S. Yamamoto and O. Hayaishi, J. Biol. Chem., 242, 5260 (1967).

59. N. C. Chen, R. K. Gholson and N. Raica, Biochim. Biophys. Acta, 343, 167 (1974).

60. R. B. Frydman, M. L. Tomaro and B. Frydman, Biochem. Biophys. Acta, 284, 63 (1972).

61. K. Takai, H. Ushiro, Y. Noda, S. Narumiya, T. Tokuyama and O. Hayaishi, J. Biol. Chem., 252, 2648 (1977).

62. H. Ushiro, K. Takai, Y. Noda, S. Narumiya, T. Tokuyama and O. Hayaishi, J. Biol. Chem., 253, 9002 (1978).

63. Y. Noda, K. Takai, T. Tokuyama, S. Narumiya, H. Ushiro and O. Hayaishi, J. Biol. Chem., 252, 4413 (1977).

64. R. J. Sundberg, in The Chemistry of Idoles, Academic Press, New York, 1970.

65. Y. Takayama, Bull. Soc. Chem. Japan, 8, 213 (1933).

66. V. Brabec and V. Mornstein, Biophys. Chem., 12, 159 (1980).

67. B. Malfoy and J. A. Reynaud, J. Electroanal. Chem., 114, 213 (1980).

68. G. D. Christian and W. C. Purdy, J. Electroanal.

69. W. E. Savige, Austr. J. Chem., 28, 2275 (1975).

70. T. W. Findley, D. Swern, and J. T. Scanlan, J. Amer. Chem. Soc., 67, 412 (1945).

71. W. E. Savige and A. Fontana, Int. J. Peptide Protein Res., 15, 285 (1980).

72. G.Dryhurst,M. Rosen, and P. J. Elving, Anal. Chim. Acta, 42, 143 (1968).

73. D. L. McAllister and G. Dryhurst, Anal. Chim. Acta, 64, 121 (1973).

74. L. Meites, in Polarographic Techniques, 2nd ed., Wiley, New York, p. 441, 1965.

75. G. Dryhurst, Talanta, 19, 769 (1972).

76. G. Dryhurst, Anal. Chim. Acta, 57, 137 (1971).

77. G.Dryhurst and P. J. Elving, J. Electrochem. Soc., 115, 1014 (1968).

78. J. L. Owens, H. A. Marsh, and G. Dryhurst, J. Electroanal. Chem., 91, 231 (1978).

79. V. E. Norvell and G. Mamantov, Anal. Chem., 49, 1470 (1977).

80. R. N. Goyal, A. B. Toth, G. Dryhurst and N. T. Nguyen, Bioelectrochem. Bioenerg., 9, 39 (1982).

81. J. P. Greenstein and Winitz, in Chemistry of the Amino Acids, Vol. I, John Wiley, New York, 1961.

82. R. C. Amstrong, Biochim. Biophys. Acta, 158, 174 (1968).

83. G. Dryhurst, in Electrochemistry of Biological Molecules, Academic Press, New York, p. 15 , 1977.

84. A. J. Bard and L. R. Faulkner, in Electrochemical Methods, John Wiley and Sons, New York, p. 223, 1980.

85. R. H. Wopschall and I. Shain, Anal. Chem., 39, 1514 (1967).

86. R. N. Adams, in Electrochemistry at Solid Electrodes, Marcel Dekker, New York, p. 136, 1969.

87. R. W. Murray, W. R. Heineman, and G. W. O'Dom, Anal. Chem., 39, 1666 (1967).

88. W. R. Heineman, Anal. Chem., 50, 390A (1978).

89. R. L. Hinman and C. Bauman, J. Org. Chem., 29, 2431 (1964).

90. R. L. Hinman and J. Lang, Biochem., 4, 144 (1965).

91. A. Ek, H. Kissman, J. B. Patrick and B. Witkop, Experientia, 8, 36 (1952).

92. A. I. Scott, in Interpretation of the Ultraviolet Spectra of Nature Products, Pergamon, New York, p. 172, 1964.

93. R. N. Goyal, A. B. Toth and G. Dryhurst, J. Electroanal. Chem., 131, 181 (1982).

94. A. B. Toth, R. N. Goyal, M. Z. Wrona, T. Lacava, N. T. Nguyen and G. Dryhurst, Bioelectrochem. Bioenerg., 8, 413 (1981).

95. A. B. Toth and G. Dryhurst, J. Electroanal. Chem., 122, 205 (1981).

96. H. A. Marsh and G. Dryhurst, J. Electroanal. Chem., 95, 81 (1979).

97. G. Dryhurst, J. Electrochem. Soc., 119, 1559 (1972).

98. R. N. Goyal, N. T. Nguyen and G. Dryhurst, Bioelectrochem. Bioenerg., 9, 273 (1982).

99. M. Z. Wrona and G. Dryhurst, Biochim. Biophys. Acta, 570, 371 (1979).

100. M. Z. Wrona, J. L. Owens and G. Druhurst, J. Electroanal. Chem., 105, 295 (1979).

101. R. N. Goyal, M. Z. Wrona and G. Dryhurst, Bioelectrochem. Bioenerg., 7, 433 (1980).

102. T. R. Chen and G. Dryhurst, J. Electroanal. Chem., 144, 191 (1983).

103. T. R. Chen and G. Dryhurst, J. Electroanal. Chem., 154, 107 (1983).

104. T. R. Chen and G. Dryhurst, Bioelectrochem. Bioenerg., 11, 75 (1983).

105. T. R. Chen and G. Dryhurst, J. Electroanal. Chem., 177, 149 (1984).

106. R.N.Goyal, A. B. Toth and G. Dryhurst, J. Electroanal. Chem., 133, 287 (1982).

107. A.T. Nielsen and W. J. Houlihan in Organic Reactions, Vol. 16, R. Adams, A. H. Blatt, V. Boekelheide, T. L. Cairns, D. J. Cram and H. O. House (Eds.), John Wiley and Sons, New York, 1968, pp. 1-439.

108. F. Bergman and S. Dikstein, J. Amer. Chem. Soc., 77, 691 (1955).